

**SYNERGISTIC ANTICANCER POTENTIAL OF ISOLATED
PHYTOCONSTITUENTS FROM *EUPHORBIA*
PULCHERRIMA AND *RICINUS COMMUNIS*
(EUPHORBIACEAE) AGAINST BREAST CANCER**

Thesis Submitted For the Award of the Degree of

DOCTOR OF PHILOSOPHY
in
Pharmaceutical Chemistry

By

Shinde Prashali Gorakh

Registration number : 42000196

Supervised By

Dr. Gurdeep Singh (26222)

Professor

Department of Pharmaceutical Chemistry

Lovely Professional University, Punjab

Co-Supervised by

Dr. Deepak Kardile

Assistant Professor

Department of Pharmaceutical Chemistry

Savitribai Phule University, Pune



LOVELY PROFESSIONAL UNIVERSITY
PUNJAB
2025

DECLARATION

I, hereby declared that the presented work in the thesis entitled “**Synergistic anticancer potential of isolated phytoconstituents from *Euphorbia pulcherrima* and *Ricinus communis* (Euphorbiaceae) against breast cancer**” in fulfilment of degree of **Doctor of Philosophy (Ph.D.)** is outcome of research work carried out by me under the supervision of **Dr. Gurdeep Singh**, working as Professor, in the Department of Pharmaceutical Chemistry, School of Pharmaceutical Sciences, Lovely Professional University, Punjab, India. In keeping with general practice of reporting scientific observations, due acknowledgements have been made whenever work described here has been based on findings of other investigator. This work has not been submitted in part or full to any other University or Institute for the award of any degree.

(Signature of Scholar)

Name of the scholar : **Shinde Prashali Gorakh**

Registration No.: 42000196

Department/school: Department of Pharmaceutical Chemistry

School of Pharmaceutical Sciences

Lovely Professional University,

Punjab, India

CERTIFICATE

This is to certify that the work reported in the Ph.D. thesis entitled “**Synergistic anticancer potential of isolated phytoconstituents from *Euphorbia pulcherrima* and *Ricinus communis* (Euphorbiaceae) against breast cancer**” submitted in fulfillment of the requirement for the award of degree of **Doctor of Philosophy (Ph.D.)** in the department of **Pharmaceutical Chemistry**, School of Pharmaceutical Sciences, Lovely Professional University, Punjab, India is a research work carried out by **Shinde Prashali Gorakh** Registration No. **42000196** is bonafide record of her original work carried out under my supervision and that no part of thesis has been submitted for any other degree, diploma or equivalent course.

(Signature of Supervisor)

Dr. Gurdeep Singh

Professor

School of Pharmaceutical Sciences

Department of Pharmaceutical Chemistry

Lovely Professional University, Punjab

(Signature of Co-Supervisor)

Dr. Deepak Kardile

Assistant Professor

Raigad Dnyanpeeth's College of

Pharmacy, Bhore, Pune

Department of Pharmaceutical Chemistry

Savitribai Phule University, Pune

ABSTRACT

Generally, *Euphorbia pulcherrima* is considered a native Mexican and Central American flowering plant. Initially discovered by Europeans, this shrub is primarily used for Christmas decorations. It was initially cultivated for its antipyretic properties and to produce red dye by Mesoamerican civilizations. In Ayurveda medicine in India utilized the seeds, leaves, and roots of *Ricinus communis*. This research aims to evaluate the synergistic anticancer potential of isolated phytoconstituents from *Euphorbia pulcherrima* and *Ricinus communis* (Euphorbiaceae) against breast cancer. A comprehensive database search using PubMed, ScienceDirect, Scopus, Medline, and EBSCO documented the phytochemical and pharmacological significance of these plants. The authentication and initial pharmacognostic assessment of the crude drugs were conducted to quantitatively investigate *Euphorbia pulcherrima* and *Ricinus communis*. The extraction of both plant parts was carried out using Soxhlet extraction procedures with petroleum ether as the solvent. Furthermore, the process of extracting and purifying phytoconstituents from *Euphorbia pulcherrima* and *Ricinus communis* was conducted. Specifically, thin-layer chromatography (TLC) and column chromatography were employed to isolate the phytoconstituents. The isolated phytoconstituents were further confirmed using spectroscopic techniques, including ultraviolet (UV), Infrared (IR), nuclear magnetic resonance (NMR), and MASS spectroscopy. The data provided conclusive evidence that Beta-sitosterol from *Euphorbia pulcherrima* and stigmasterol from *Ricinus communis* were successfully extracted. The quantification of Beta-sitosterol and stigmasterol in petroleum ether extracts was carried out using high-performance thin-layer chromatography (HPTLC). An *in silico* study utilizing molecular docking tools was employed to predict the interaction between the protein and its ligand, aiding in the screening of active compounds to determine their pharmacological impact. The potential benefits of selected phytoconstituents in treating breast cancer were investigated using *in silico* methods. For the study utilized the Protein Data Bank (PDB) ID: 3HB5 and included nine ligands sourced from plants, selected based on their phytochemical literatures. Schrödinger and AutoDock Vina were the specific software packages employed for molecular docking. Additionally, a molecular dynamics (MD) simulation study was conducted, where the root-mean-square deviation (RMSD) and root-mean-square fluctuation (RMSF) values were computed from 1000 trajectories generated during a 100-nanosecond simulation period.

This research study focuses on evaluating the antioxidant capabilities of aqueous, ethanol, and petroleum ether extracts of *Euphorbia pulcherrima* and *Ricinus communis* using various *in vitro* methods, including the DPPH (2,2-diphenyl-1-picrylhydrazyl) assay, ferric reducing antioxidant Power (FRAP) assay, total antioxidant capacity (TAC) assay, and total phenolic content (TPC) assay. Furthermore, the antioxidant capacity of Beta-sitosterol and stigmasterol was assessed using the DPPH and superoxide dismutase assay (SOD). This research focuses on the pharmacological evaluation of the synergistic effect of Beta-sitosterol and stigmasterol on breast cancer cell lines. The MCF-7 and MDA-MB-231 cell lines were utilized to investigate the impact of individual components and their combined effect in a 1:1 ratio using the MTT and SRB assays. The Bliss independence model was employed to assess synergism. In conclusion, the investigation revealed that both Beta-sitosterol and stigmasterol exhibit significant anticancer potential. Moreover, when combined in a 1:1 ratio, these compounds demonstrate a synergistic effect, enhancing their anticancer efficacy. To explore further potential derivatives and their simulated interactions with PDB ID: 3HB5, a total of ten hypothetical derivatives of Beta-sitosterol and stigmasterol were designed and synthesized *in silico*. These compounds were generated by integrating maleic anhydride, phthalic anhydride, adipic acid, malonic acid, citric acid, and other modifiers using ChemSketch. The resulting CES ester derivatives were then evaluated using *in silico* molecular docking with AutoDock Vina. Among all the compounds, the CES derivatives of Beta-sitosterol and stigmasterol, modified using maleic anhydride, exhibited the highest binding affinity, with scores of -18.4 kcal/mol and -18.6 kcal/mol, respectively. The CES derivative of Beta-sitosterol and stigmasterol were subsequently synthesized using maleic anhydride, and spectroscopic methods were employed for characterization. To enhance the polarity of the derivative, the CES was further treated with polyethylene glycol (PEG) of different molecular weights (4000, 6000, and 8000). The resulting CES-PEG conjugates were characterized by analysing their melting points, solubility, and FTIR spectroscopic profiles. Further physicochemical properties and pharmacokinetic parameters of the most active derivatives CES and hydrophilic derivatives of Beta-sitosterol and stigmasterol were calculated using *in silico* studies (SwissADME software).

ACKNOWLEDGEMENT

Though only my name appears on the cover of this dissertation, a several great people have contributed in it. I owe my gratitude to all those people who have made this dissertation possible and because of whom my **DOCTOR OF PHILOSOPHY (Ph.D.)** experience has been one that I will cherish forever. I express my deep sense of gratitude towards **School of Pharmaceutical Sciences, Lovely Professional University, Punjab** for providing healthy and supportive environment for carrying out my research. At the heart of every event, lies a cause, a reason and a motivating force or an inspiration. To a student, in whatever walk of life he may be, this inspiration is always there through a guide, a mentor. It gives me a deep seated pleasure to express my sense of gratitude to my guide, **Dr. Gurdeep Singh** Professor (Department of Pharmaceutical Chemistry) School of Pharmaceutical Sciences, Lovely Professional University, Punjab. I am short of words to thank for their unlimited patience and the affection bestowed upon me during my entire research work. Every event, small or big in nature, is itself a creation. I express my gratitude to my coguide **Dr. Deepak Kardile**, Assistant Professor (Department of Pharmaceutical Chemistry) Raigad Dnyanpeeth's College of Pharmacy, Bhore, Pune for their unparalleled, constant encouragement, constructive criticism and excellent guidance. I am also indebted to the Professors of Lovely Professional University **Dr. Deepshikha**, **Dr. Charnajeet Kaur**, **Dr. Gurvinder Singh**, **Dr. Bhoopinder Kapoor** and other office staff with whom I have interacted during the course of my Ph.D. studies.

I specially thank to **Shikshan Prasarak Mandal's** College of Pharmacy, Akulj for valuable active guidance and constant support during project work.

I am highly indebted to our **Golden team** **Dr. Neha Kajale, Drug Inspector Mrs. Raziya Sayyad**, **Dr. Swapnil Nazarkar**, **Dr. Samrat Khedkar**, **Dr. Reshma Pawar**, **Ms. Aishwarya Phutane**, **Ms. Shubhangi Kharat**, **Mrs. Nutan Dhudhal**, **Mr. Swapnil Rajeghadage**, **Mr. Pravin Dupade**, **Mr. Mahesh Mitkal** for their guidance as well as friendly support while I am in trouble for completing the work. I kindly express vote of thanks to **Dr. Sandeep Patil**, **Dr. Ashpak Tamboli**, **Dr. Jawed Md. Yakoob**, **Dr. Prafulla Choudhary** for helping me to carry out the experimental work at their place and providing me all the necessary material required for my research work with nice guidance for smooth running of my project work. I also my

special thanks to my student **Dr. Kiran Lokhande** (Post-Doctoral fellow , Computation Genomic Laboratory , Shiv Nadar Institution of Eminence , Greater Noida, Delhi - NCR, India. Helping in MD simulation and docking study.

Last but not least, I would like to express my heartfelt gratitude to my "**Bharaka Guru**", **Dr. Snehal Uttam Kashid**. Words are insufficient to express her unwavering support and guidance in every situation. I have learned invaluable lessons from her. I am also deeply thankful to all my colleagues from the College of Pharmacy, Akhuj, for their support and motivation. I extend my sincere thanks to all the Non-Teaching Staff and my students, including Vishal Narsale, Harshad Patil (final year), and Siddhant Basate, Rehan Shaikh, Aditya Kulkarni, and Bhounmik Bakliwal (second year), who assisted me during my project work.

I appreciate my best friends, **Mohini, Rutuja, Smita** and many more for moral support. I wish to express my gratitude towards my support system my **Family**. I am indebted infinitely to care support and trust being shown by my loving Parents **Mrs. Sushila Shinde (Aai) and Mr. Gorakh Shinde (Dada)** and my mother-in-law **Mrs. Saraswati Dhas (Aai) and my father-in-law Mr. Sayaji Dhas (Aaba) and my all family members**, who are the actual driving force that enabled me to complete my PhD work in time .

I would like to express my heartfelt thanks to the strongest pillar and luckiest person in my life, my lovely brother, **the late Dr. Prashant Gorakh Shinde**. He was my lucky charm, but unfortunately, he is no longer with me to see the completion of my Ph.D. His absence is a deeply sorrowful moment in my life. I will always cherish the memories of his unwavering moral support and constant encouragement. His reassuring words, "**ALL IS WELL**" will forever be etched in my mind.

Last but not least, I would like to express my heartfelt gratitude to my rock, my dear husband, **Mr. Madhav Dhas**. Without his unwavering support, this journey would have been impossible. He helped me overcome countless difficulties and challenges throughout my studies. I also want to thank my little bundle of joy, my lovely son **Vedant (Kanuli)**, for being my constant source of motivation. He even accompanied me to my ETP presentation, showing immense care and concern. His innocent words, "**Mummy, load nahi leneka**" (**Mummy, don't worry**), still resonate in my heart.

I am overwhelmed with gratitude and have no words to express my thanks, but my heart remains full of appreciation for the favors received from every person.

Ms. Shinde Prashali Gorakh

LIST OF CONTENTS

Chapter No.	Title	Page No.
1	Introduction	1-9
2	Literature review	10-38
3	Hypothesis and plan of work	39
4	Aim and objectives	40-43
5	Materials and methods	44-60
6	Results and discussion	61-148
7	Summary and conclusion	149-153
8	Bibliography	154-171

LIST OF TABLES

Table No.	Title	Page No.
5.1	HPTLC specification for isolated Beta-sitosterol	47
5.2	HPTLC specification for isolated Stigmasterol	47
6.1	Preliminary phytochemical analysis of <i>Euphorbia pulcherrima</i> leaves powder in different extracts	61
6.2	Preliminary phytochemical analysis of <i>Ricinus communis</i> seeds powder in different extracts.	62
6.3	Physical evaluation of <i>Euphorbia pulcherrima</i> leaves powder	62
6.4	Physical evaluation of <i>Ricinus communis</i> seeds powder	63
6.5	Extractive value determination of <i>Euphorbia pulcherrima</i> leaves powder	63
6.6	Extractive value determination of <i>Ricinus communis</i> seeds powder	63
6.7	FTIR interpretation of Beta-sitosterol	67
6.8	FTIR interpretation of Stigmasterol	73
6.9	Quantification of Beta-sitosterol using HPTLC	80
6.10	Quantification of Stigmasterol using HPTLC	82
6.11	Binding pockets and area of PDB ID: 3HB5	82
6.12	Selected ligands for molecular docking study	83
6.13	Molecular interaction analysis of selected ligand against PDB ID: 3HB5	84
6.14	RMSD values for complexes formed with PDB ID: 3HB5	87
6.15	RMSF values for complexes formed with PDB ID: 3HB5	88
6.16	List of selected ligands for molecular docking against PDB ID: 3HB5	89
6.17	2D and 3D interaction of ligand against PDB ID:3HB5	90
6.18	Binding affinities of ligand against PDB ID: 3HB5	93
6.19	Amino acid residues and bond interaction of protein and ligand	94
6.20	Anti-oxidant properties of <i>Euphorbia pulcherrima</i> in different extracts	95

6.21	Anti-oxidant properties of <i>Ricinus communis</i> in different extracts	97
6.22	<i>In vitro</i> Anti-Oxidant properties of Beta-sitosterol and Stigmasterol (DPPH)	101
6.23	<i>In vitro</i> antioxidant study by SOD assay of Beta-sitosterol and Stigmasterol	101
6.24	MTT assay cell viability of isolated phytoconstituents on MCF-7	103
6.25	Summary of MTT assay percent inhibition against MCF-7	104
6.26	MTT assay cell viability of isolated phytoconstituents on MBA-MB-231	105
6.27	Summary of MTT assay percent inhibition against MBA-MB-231	106
6.28	SRB assay cell viability of isolated phytoconstituents on MCF-7	107
6.29	Summary of SRB assay percent inhibition against MCF-7	109
6.30	SRB assay cell viability of isolated phytoconstituents on MDA-MB-231	110
6.31	Summary of SRB assay percent inhibition against MDA-MB-231	113
6.32	Bliss independence expected and observed effect (MTT assay MCF-7)	114
6.33	Bliss independence expected and observed effect(MTT assay MDA-MB-231)	115
6.34	Bliss independence expected and observed effect (SRB assay MCF-7)	117
6.35	Bliss independence expected and observed effect (SRB assay MDA-MB-231)	118
6.36	Binding affinities of Beta-sitosterol derivatives (CES)	120
6.37	2D and 3D interaction of Beta-sitosterol derivatives	120
6.38	Amino acid residues and bond interaction of Beta-sitosterol derivatives	121
6.39	Binding affinities of Stigmasterol derivatives (CES)	122
6.40	2D and 3D interaction of Stigmasterol derivatives	122
6.41	Amino acid residues and bond interaction of Stigmasterol derivatives	123
6.42	FTIR interpretation of Beta-sitosterol CES derivative	125
6.43	FTIR interpretation of Stigmasterol CES derivative	128
6.44	Physical evaluation of hydrophilic derivatives of Beta-sitosterol	129

6.45	Physical evaluation of hydrophilic derivatives of Stigmasterol	131
6.46	Canonical smiles of Beta-sitosterol CES derivatives	133
6.47	<i>In silico</i> physicochemical properties of Beta-sitosterol CES derivatives	133
6.48	<i>In silico</i> lipophilic and hydrophilic properties of Beta-sitosterol CES derivatives	134
6.49	<i>In silico</i> pharmacokinetic profiling of Beta-sitosterol CES derivatives	134
6.50	Canonical Smiles of Stigmasterol CES derivatives	135
6.51	<i>In silico</i> physicochemical properties of Stigmasterol CES derivatives	135
6.52	<i>In silico</i> lipophilic and hydrophilic properties of Stigmasterol CES derivatives	136
6.53	<i>In silico</i> pharmacokinetic profiling of Stigmasterol CES derivatives	136
6.54	Canonical smiles of hydrophilic Beta-sitosterol derivatives	137
6.55	<i>In silico</i> physicochemical properties of hydrophilic Beta-sitosterol derivatives	137
6.56	<i>In silico</i> lipophilic and hydrophilic properties of Beta-sitosterol derivatives	138
6.57	<i>In silico</i> pharmacokinetic profiling of hydrophilic Beta-sitosterol derivatives	138
6.58	Canonical smiles of hydrophilic Stigmasterol derivatives	138
6.59	<i>In silico</i> physicochemical properties of hydrophilic Stigmasterol derivatives	139
6.60	<i>In silico</i> lipophilic and hydrophilic properties of hydrophilic Stigmasterol derivatives	139
6.61	<i>In silico</i> pharmacokinetic profiling of hydrophilic Stigmasterol derivatives	140

LIST OF FIGURES

Figure No.	Title	Page No.
1.1	General classification of cancer depending upon types of cell	3
1.2	Cancer cell cycle and its phases	4
1.3	Extrinsic and Intrinsic pathways of apoptosis	5
1.4	Stages of breast cancer	6
1.5	Histopathological classification of breast cancer	7
1.6	Conventional and novel treatments for breast cancer	7
2.1	<i>Euphorbia pulcherrima</i> plant	10
2.2	<i>Euphorbia pulcherrima</i> leaves	10
2.3	Chemical constituents of <i>Euphorbia pulcherrima</i> leaves	12
2.4	<i>Ricinus communis</i> plant	18
2.5	<i>Ricinus communis</i> seeds	18
2.6	Chemical constituents of <i>Ricinus communis</i> seeds	19
5.1	The 3D structure of the Estradiol 17-beta-dehydrogenase - 1 - Enzyme with PDB ID:3HB5	49
5.2	The selected binding site residues of Estradiol 17-beta-dehydrogenase -1- Enzyme	50
5.3	Synthetic scheme for Beta-sitosterol and Stigmasterol derivatives	56
6.1	UV visible spectrum of standard Beta-sitosterol	65
6.2	UV visible Spectrum of isolated Beta-sitosterol	66
6.3	FTIR spectrum of standard Beta-sitosterol	66
6.4	FTIR spectrum of isolated Beta-sitosterol	67
6.5	¹ H NMR of standard Beta-sitosterol	68
6.6	¹³ C NMR of the standard Beta-sitosterol	68

6.7	¹ H NMR of isolated Beta-sitosterol	69
6.8	¹³ C NMR of isolated Beta-sitosterol	70
6.9	MASS spectrum of standard Beta-sitosterol	70
6.10	MASS spectrum of isolated Beta-sitosterol	71
6.11	UV visible spectrum of standard Stigmasterol	71
6.12	UV-Visible spectrum of the isolated Stigmasterol	72
6.13	FTIR spectrum of standard Stigmasterol	72
6.14	FTIR spectrum of isolated Stigmasterol	73
6.15	¹ H NMR of standard Stigmasterol	74
6.16	¹³ C NMR of standard Stigmasterol	74
6.17	¹ H NMR of isolated stigmasterol	75
6.18	¹³ C NMR of the isolated Stigmasterol	75
6.19	MASS spectrum of the standard Stigmasterol	76
6.20	MASS spectrum of isolated Stigmasterol	77
6.21	HPTLC of extract <i>Euphorbia pulchirima</i>	78
6.22	HPTLC of standard Beta-sitosterol	78
6.23	Overlay graph of <i>Euphorbia pulchirrima</i> extract and standard Beta-sitosterol	79
6.24	Spectrum scan of <i>Euphorbia pulchirrima</i> extract and standard	79
6.25	HPTLC of <i>Ricinus communis</i> extract	80
6.26	HPTLC of standard Stigmasterol	81
6.27	Overlay graph of <i>Ricinus communis</i> extract and standard Stigmasterol	81
6.28	Spectrum scan of <i>Ricinus communis</i> extract and standard	82
6.29	Intermolecular interaction between <i>Euphorbia pulcherrima</i> and <i>Ricinus communis</i> phytoconstituents with PDB ID 3HB5	85
6.30	2D and 3D docked pose interaction between <i>Euphorbia pulcherrima</i> leaves and <i>Ricinus communis</i> seed phytoconstituents with PDB ID 3HB5	86
6.31	Root Mean Square Deviation plot for Estradiol 17-beta dehydrogenase 1 enzyme	87
6.32	Root Mean Square Fluctuation plot for Estradiol 17-beta dehydrogenase 1 enzyme	88
6.33	<i>In vitro</i> antioxidant activity of aqueous extract of <i>Euphorbia pulcherrima</i>	96
6.34	<i>In vitro</i> antioxidant activity of ethanolic extract of <i>Euphorbia pulcherrima</i> (DPPH)	96

6.35	<i>In vitro</i> antioxidant activity of ethereal extract of <i>Euphorbia pulcherrima</i> (DPPH)	97
6.36	<i>In vitro</i> antioxidant activity of <i>Ricinus communis</i> aqueous extract (DPPH)	98
6.37	<i>In vitro</i> Antioxidant activity of ethanolic extract of <i>Ricinus communis</i> (DPPH)	98
6.38	<i>In vitro</i> Antioxidant activity of ethereal extract of <i>Ricinus communis</i> (DPPH)	99
6.39	<i>In vitro</i> Antioxidant activity of ascorbic acid (DPPH)	99
6.40	Comparative data of antioxidant activity of <i>Euphorbia pulcherrima</i>	100
6.41	Comparative data of antioxidant activity of <i>Ricinus communis</i>	100
6.42	Antioxidant potential of isolated phytoconstituents	102
6.43	Comparative data of MTT assay (MCF-7 cell line)	104
6.44	Comparative data of MTT assay (MDA-MB-231 cell line)	107
6.45	Comparative data of SRB method (MCF-7 cell line)	110
6.46	Comparative data of SRB method (MDA-MB-231 cell line)	113
6.47	Bliss independence for synergism (MTT assay using MCF-7 cell line)	113
6.48	Concentration dependent dose response (MTT assay using MCF-7)	114
6.49	Bliss independence for synergism (MTT assay using MDA-MB-231)	115
6.50	Concentration dependent dose response (MTT assay using MDA-MB-231)	116
6.51	Bliss independence for synergism (SRB assay using MCF-7)	116
6.52	Concentration dependent dose response (SRB assay using MCF-7)	117
6.53	Bliss independence for synergism (SRB assay using MDA-MB-231)	118
6.54	Concentration dependent dose response (SRB assay using MDA-MB-231)	119
6.55	Synthetic scheme for Beta-sitosterol derivative using Maleic anhydride	125
6.56	FTIR spectrum of Beta-sitosterol CES derivative	125
6.57	MASS spectrum CES derivative of Beta-sitosterol	126
6.58	Synthetic scheme for stigmasterol derivative using Maleic anhydride	127
6.59	FTIR spectrum of Stigmasterol CES derivative	127
6.60	MASS spectrum of Stigmasterol CES derivative	128
6.61	FTIR spectrum of hydrophilic derivative of Beta-sitosterol (PEG-4000)	129
6.62	FTIR spectrum of hydrophilic derivative of Beta-sitosterol (PEG-6000)	130
6.63	FTIR spectrum of hydrophilic derivative of Beta-sitosterol (PEG-8000)	130

6.64	FTIR spectrum of hydrophilic derivative of Stigmasterol (PEG-4000)	131
6.65	FTIR spectrum of hydrophilic derivative of Stigmasterol (PEG-6000)	132
6.66	FTIR spectrum of hydrophilic derivative of Stigmasterol (PEG-8000)	132

ABBREVIATIONS

US	United States
WHO	World Health Organization
BSI	Botanical Survey of India
2D	Two dimensional
3D	Three dimensional
IARC	International Agency for Research on Cancer
CNS	Central Nervous System
DNA	Deoxyribonucleic Acid
ER	Estrogen Receptar
Bcl-xL	B-cell lymphoma-extra large
AIDS	Acquired immunodeficiency syndrome
BC	Breast Cancer
MTT	(3-[4,5-dimethylthiazol-2-yl]-2,5 diphenyl tetrazolium bromide)
μ M	Micrometre
SGC	Stomach cancer cells
NCI-H460 cells	Non-small cell lung cancer
ROS	Reactive oxygen species
LDH	Lactate dehydrogenase
TB	Tuberculosis
SD	Standard deviation
mRNA	Messenger Ribonucleic acid
ATP	Adenosine triphosphate
MAPK	Mitogen-activated protein kinase
mg	Milligram

gm	Gram
kg	Kilogram
p-ERK	Phosphorylated extracellular signal-regulated kinase
c-fos	Proto-oncogene c-Fos
c-jun	Proto-oncogene
ERK-2	Extracellular signal-regulated kinase 2
Fe-NTA	Ferric nitrilotriacetate
GEMBS	Genome bisulfites sequencing
MIA-PaCa2	MIA PaCa-2 is an epithelial cell line
BXPC-3	BxPC-3 is a cell line isolated from the pancreas tissue
μM/L	Micromoles per liter
PCNA	Proliferating cell nuclear antigen
COLO320 DM	Caucasian colon adenocarcinoma
PCNA	Proliferating cell nuclear antigen
b.w.	Body weight
PI-3K	Phosphatidylinositol-3 kinase
%	Percentage
PCR	Polymerase chain reaction
EC	Endometrial cancer
MCF-7	Michigan Cancer Foundation-7
IGF1R	Insulin like growth factor 1 receptor
mTOR	Mammalian target of rapamycin
CSC	Cancer Stem Cells
OC	Ovarian cancer
ROS	Reactive oxygen species
ml	Milliliter

HepG-2	Hepatoblastoma cell line -2
PD-L1	Programmed death-ligand 1
GC	Gastric cancer
JAK	Janus kinase
STAT	Signal transducer and activator of transcription
GES-1	Guiana extended-spectrum
PC3	Prostate Cancer-3
IC ₅₀	Inhibitory concentration at 50%
HIV	Human immunodeficiency virus
MIC	Minimum inhibitory concentration
DPPH	2,2-diphenyl-1-picrylhydrazyl
MDA-MB-231	M D Anderson metastatic breast cancer
SGOT	Serum glutamic oxaloacetic transaminase
SGPT	Serum glutamic pyruvic transaminase
MES	Maximal electroshock seizures
PTZ	Pentylentetrazole
TNBC	Triple-negative breast cancer
HER	Human epidermal receptor
CI	Combination index
SSRI	Selective serotonin reuptake inhibitor
FIC	Fractional inhibitory concentration
MICs	Minimum inhibitory concentrations
ADAM	A disintegrin and metalloproteinase
CCK8	Cell counting kit 8
PTX	Paclitaxel

VEGFR-2	Vascular endothelial growth factor receptor 2
ROS	Reactive oxygen species
Bcl2	B-cell lymphoma 2
VEGF-A	Vascular endothelial growth factor A
NF-kB	Nuclear Factor Kappa B
Ki-67	Antigen Kiel 67
DMBA	Dimethylbenz anthracene
TLC	Thin layer chromatography
UV	Ultraviolet
IR	Infrared
NMR	Nuclear magnetic resonance
HPTLC	High performance thin layer chromatography
FRAP	Ferric reducing antioxidant property
HCL	Hydrochloric acid
BSI	Botanical Survey of India
Rf	Retention factor
FTIR	Fourier transform Infrared Spectroscopy
μl	Microliter
nm	Nanometer
mm	Milimeter
RCSB	Research collaboratory for structural bioinformatics
PDB	Protein data bank
OPLS	Optimized potentials for liquid simulations
MD	Molecular dynamic
NPT	Nuclear non proliferation treaty
RMSD	Root Mean Square Deviation

RMSF	Root Mean Square Deviation
DHT	Dihydrotestosterone
TAC	Total antioxidant capacity
OD	Optical density
pH	Potential of Hydrogen
GAE	Gallic acid equivalence
H ₂ SO ₄	Sulfuric acid
DMSO	Dimethyl sulfoxide
NaOH	Sodium hydroxide
PBS	Phosphate buffered saline
CO ₂	Carbon dioxide
DCE	Dichloroethane
PEG	Polyethylene glycol
DCC	1,3-dicyclohexylcarbamide
DAMP	4-dimrthylaminopyridine
SD	Standard deviation
cm	Centimeter
MHz	Megahertz
CDCl ₃	Deuterated chloroform
δ	Delta
ppm	Parts per million
Kcal/mol	Kilocalorie per mole
SOD	Superoxide dismutase assay
SRB	Sulforhodamine B
COX	Cyclooxygenase

LIST OF APPENDICES

Sr. No.	Title
1	Authentication letter of <i>Euphorbia pulcherrima</i>
2	Authentication letter of <i>Ricinus communis</i>
3	Laboratory certificate

CHAPTER - 1

INTRODUCTION

1. INTRODUCTION

1.1 Cancer

Cancer is a major global public health concern. According to reports, it ranks second in the US in terms of cause of death (1). One of the most characteristic of cancer is the rapid growth of aberrant cells that can invade and spread to other parts of the body (2). Cancer-related risks accumulate; the incidence of cancer rises with age. A person's overall risk of illness increases since cellular repair processes become less effective with age. Developing countries need to improve cancer care, according to the WHO (3). Cancer is a complicated illness that involves several different time- and space-dependent alterations in cell physiology, eventually resulting in malignant tumors (4). Neoplasia is the biological endpoint of this disease. The main reason contributing to the disease and death of the majority of cancer patients is tumor cell invasion of nearby distant organs, tissues, or metastasis (5). The International Agency for Research on Cancer (IARC) has too determined numerous additional causes of cancer, including wood dust, plants, sunlight, tobacco, drugs, hormones, alcohol, parasites, fungi, bacteria, and salted seafood (6). Some well-known reasons for cancer growth include aging, prolonged sun exposure, smoking, radioactivity material exposure, hormonal drugs, chemicals, and viruses (7). Globally, 2.3 million women were diagnosed with breast cancer in 2022 (8).

Role of Herbal drug and their phytoconstituents

1) Turmeric (*Curcuma longa*): Curcumin, a polyphenol in turmeric, it inhibits key signaling pathways implicated in cancer development. Inhibits NF- κ B signaling pathway, reducing inflammation and cancer cell proliferation. Induces apoptosis and inhibits angiogenesis.

Potential use: Anti-inflammatory, antioxidant, anti-cancer (breast, colon, prostate, pancreatic cancers).

2) Green Tea (*Camellia sinensis*): Catechins, particularly EGCG, inhibits cancer cell growth, induces apoptosis, and blocks angiogenesis by targeting multiple

signaling pathways (PI3K/Akt, MAPK/ERK).

Potential use: Anti-cancer (breast, prostate, colorectal, lung cancers), antioxidant, anti-inflammatory.

3) Ginger (*Zingiber officinale*): Anti-inflammatory effects by inhibiting COX-2 and NF- κ B pathways. Induces apoptosis and inhibits cancer cell growth.

Potential use: Anti-nausea, anti-inflammatory, anti-cancer (colorectal, breast, ovarian cancers) Ginger extracts have anti-inflammatory and antioxidant properties.

4) Ginseng (*Panax ginseng*): Ginsenosides, they increase natural killer cell activity and induce apoptosis in cancer cells. Modulates immune response, inhibits cancer cell growth, and induces apoptosis by targeting PI3K/Akt and MAPK pathways.

Potential use: Anti-cancer (lung, breast, prostate cancers), adaptogenic, anti-fatigue . Ginseng may enhance chemotherapy efficacy and reduce side effects.

5) Ashwagandha (*Withania somnifera*): Withaferin A, a steroidal lactone, induces apoptosis and inhibits angiogenesis in cancer cells. It may sensitize cancer cells to chemotherapy.

6) Boswellia (*Frankincense*): Boswellic acids have anti-inflammatory properties, inhibiting enzymes involved in inflammation 5-LOX enzyme and NF- κ B signaling pathway. Induces apoptosis and inhibits cancer cell growth and tumor growth. They induce apoptosis and block angiogenesis in cancer cells.

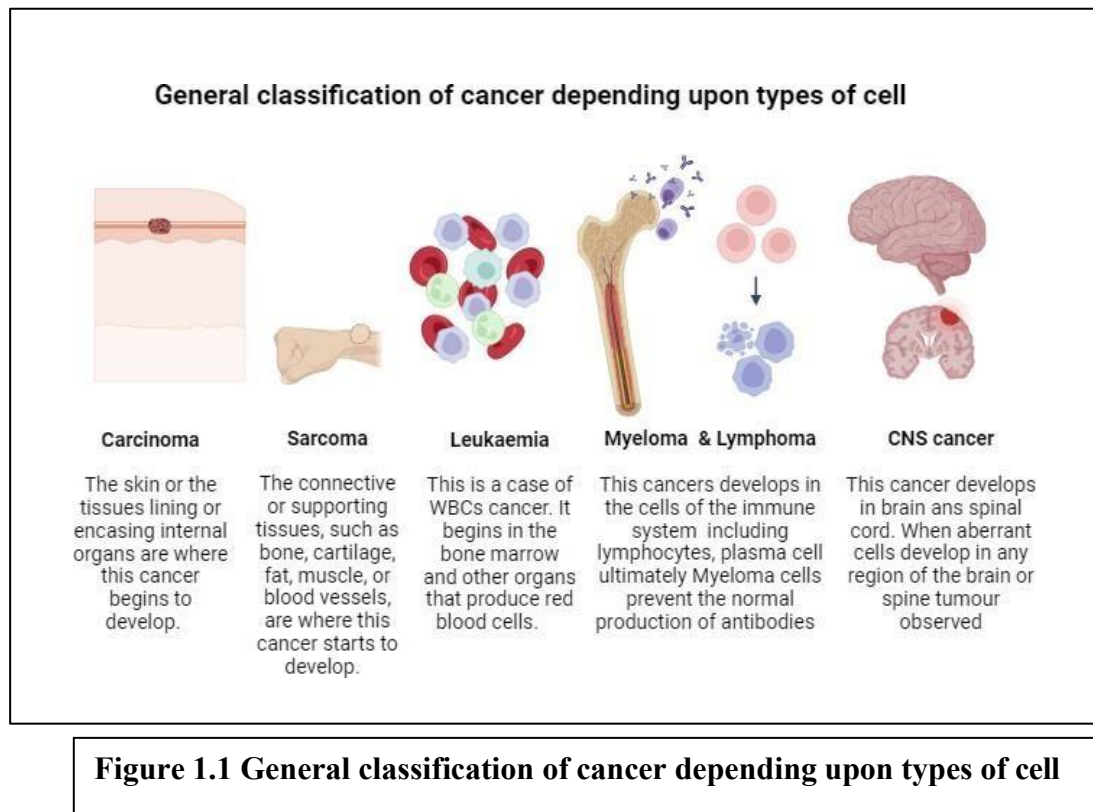
Potential use: Anti-inflammatory, anti-cancer (brain, breast, colon cancers).

7) Milk Thistle (*Silybum marianum*): Silymarin prevents liver damage from chemotherapy and radiotherapy, induces apoptosis, and hinders cancer cell growth. Antioxidant and anti-inflammatory effects, inhibiting cancer cell growth and inducing apoptosis by targeting PI3K/Akt and MAPK pathways.

Potential use: Liver protection, anti-cancer (liver, prostate, skin cancers) (31,33-36).

1.2 Types of Cancer

In the field of cancer pathology, distinguishing between benign and malignant tumors is crucial. Benign tumors don't spread to other parts of the body, malignant tumors have the ability to infiltrate adjacent healthy tissue and travel throughout the blood stream. Furthermore, malignant tumors can change healthy cells into cancerous ones (9). Cancers can be classified into five major categories based on the type of cell they originate from, which accounts for approximately 90% of all cancers. These categories include carcinoma, sarcoma, leukemia, central nervous system (CNS) cancer, lymphoma, and myeloma, as in Figure 1.1



Furthermore, there are over 100 different forms of cancer. Accordant to the WHO, the most common cancers in men are liver, colorectal, prostate, lung , and stomach cancers, while in women, the most common cancers are lung, thyroid, breast, colorectal, cervica, and other types .

1.3 Mechanism of cancer

Malignant cell and normal cells both are same order to divide. The cancer cell cycle is a well configured series of biological processes that are controlled by chemical signals generated by genes. Cell division and growth are induced by some genes, known as proto-oncogenes. Cell cycle progress is restricted by another genes, known as tumor suppressor genes. While some cancer cells are not susceptible to density dependent inhibition, normal cells exhibit when it comes to cell proliferation. The normal cell (eukaryotic cell) cycle and its phases were described in below Figure (1.2). Cancer cell often remain rising to high cell densities globally reproducing their uncontrolled, spread, multiplication *in vivo* instead of reacting the pointers that induce regular cells to end proliferation and goes into G₀ phase .

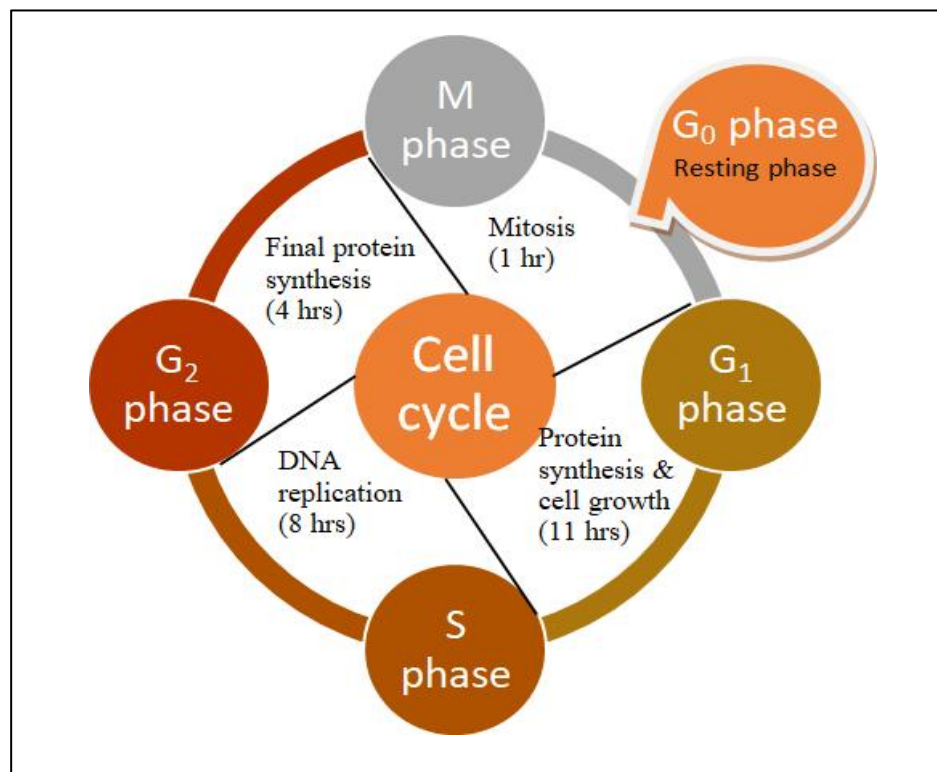


Figure 1.2 Cancer cell cycle and its phases

There are at least two major signaling pathways that induce apoptosis, the intrinsic and extrinsic mechanisms. Extrinsic apoptosis is triggered by exogenous signals from other cells. When external circumstances indicate that a cell must die, the extrinsic pathway of apoptosis is initiated. In contrast, intrinsic apoptosis is a self initiated process, often triggered by cellular stress, such as DNA damage, which activates the apoptotic pathway and initiates the intrinsic mechanism of apoptosis. Cysteine proteases, known as caspases, are activated by signals in both pathways of apoptosis. The caspases then proceed in a proteolytic cascade to dismantle and eliminate the dying cell (10).

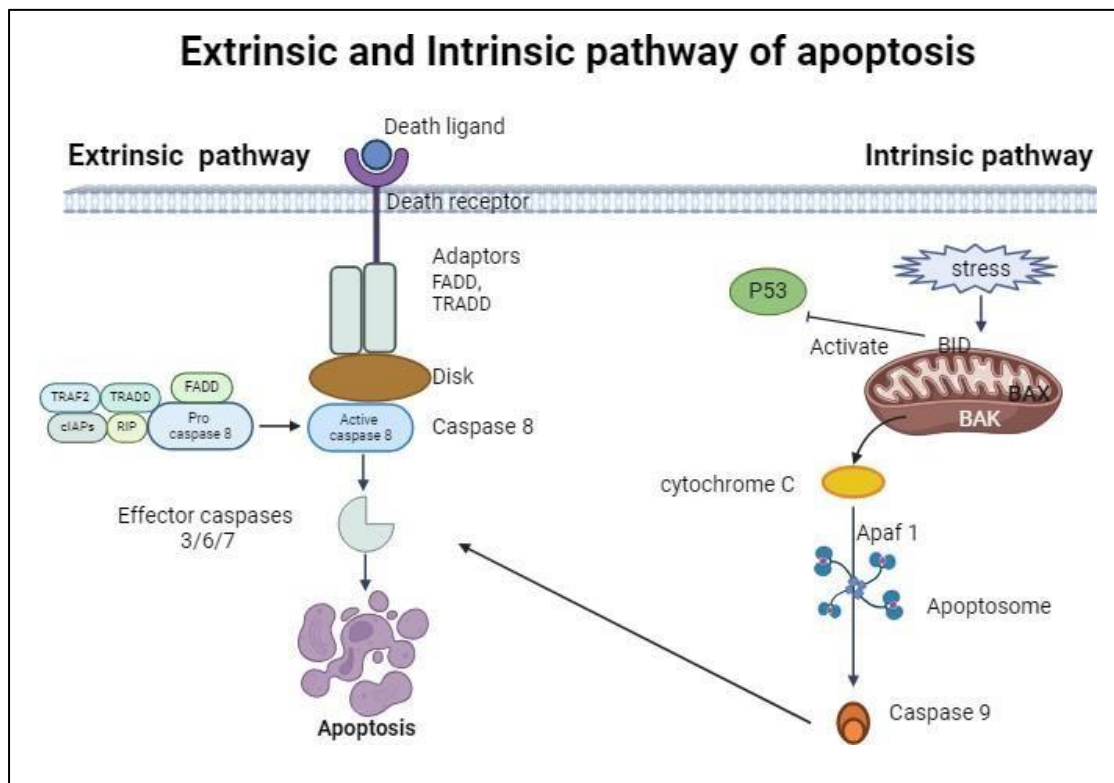


Figure 1.3 Extrinsic and Intrinsic pathways of apoptosis

1.4 Breast cancer

According to the World Health Organization (WHO), breast cancer accounted for

670,000 fatalities worldwide in 2022, affecting women in 157 of the 185 countries globally (8). Globally, breast cancer is the least popular malignant tumor to be diagnosed in women. Furthermore, with one in ten new cases identified in women, breast cancer ranks as the second least common reason of cancer related deaths worldwide. Breast cancer also affects less than 1 percent of men. A major factor in the death rate from breast cancer is changing life styles (11-12). Treatment for breast cancer typically involves immunotherapy, chemotherapy, surgery, and radiation depending on the stage and type of tumor. Advances in various therapy techniques have significantly improved overall survival rates and patient reported outcomes (12).

Stages of cancer

Breast cancer stage is based on tumor size, metastasis, nodal involvement, and specific biomarkers such as the ERBB2 receptor, progesterone receptor, and estrogen protein. The breast cancer stages are summarized below in Figure 1.4

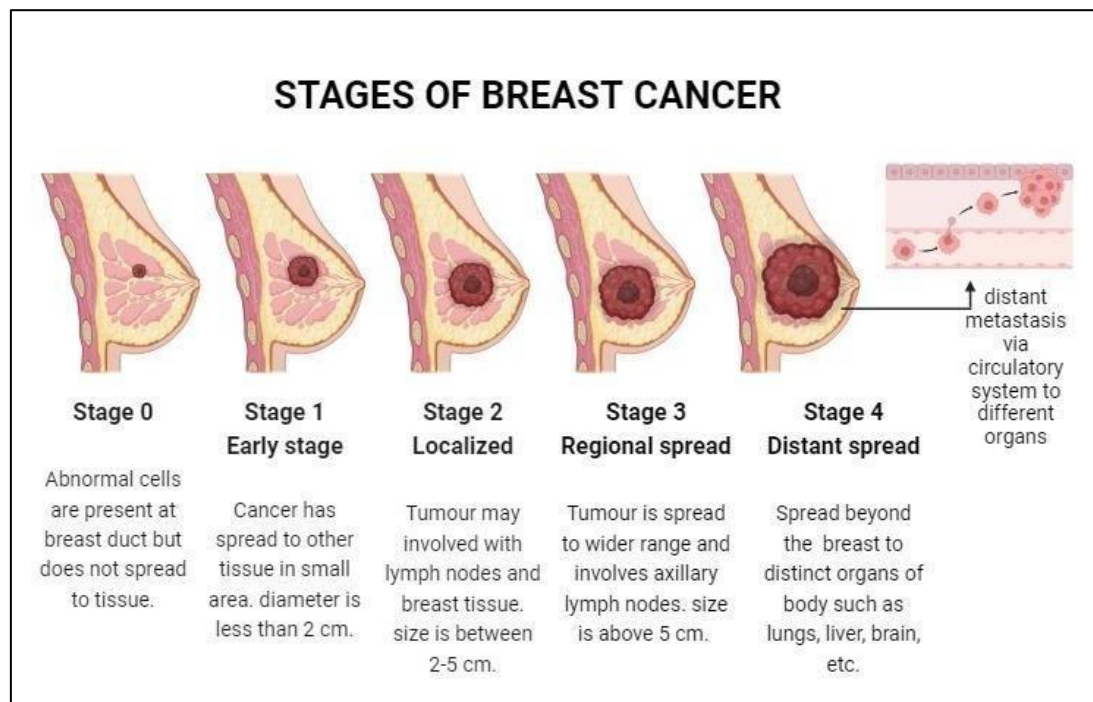


Figure 1.4 Stages of breast cancer

1.4.1 Histopathological classification of breast Cancer

In terms of histopathology, breast cancer can be broadly classified into two groups non-invasive (*in situ*) carcinoma and invasive carcinoma. Inflammatory breast cancer and angiosarcoma of the breast are typically the most aggressive types of cancer, whereas phyllodes tumors, ductile carcinoma in situ and lobular carcinoma in situ typically progress more slowly (13).

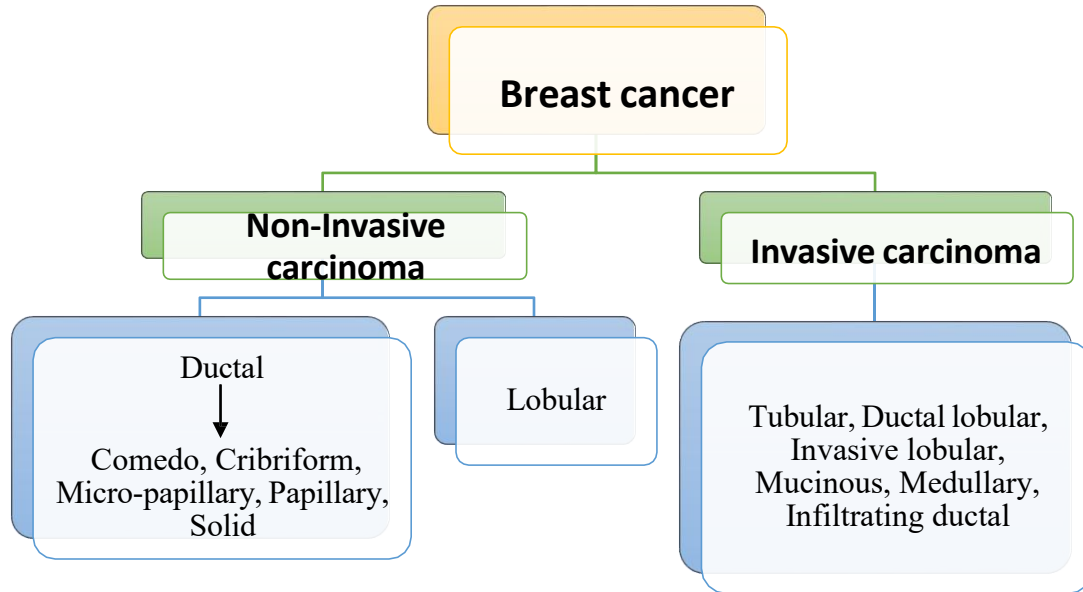


Figure 1.5 Histopathological classification of breast cancer

1.4.2 Treatment for breast cancer

Patients with breast cancer receive both local and systemic treatments. Local treatments, such as radiation therapy and surgery, focus on removing the tumor. Additionally, systemic treatments, including immunotherapy, targeted therapy, hormone therapy, and chemotherapy, may also be used (13-14).

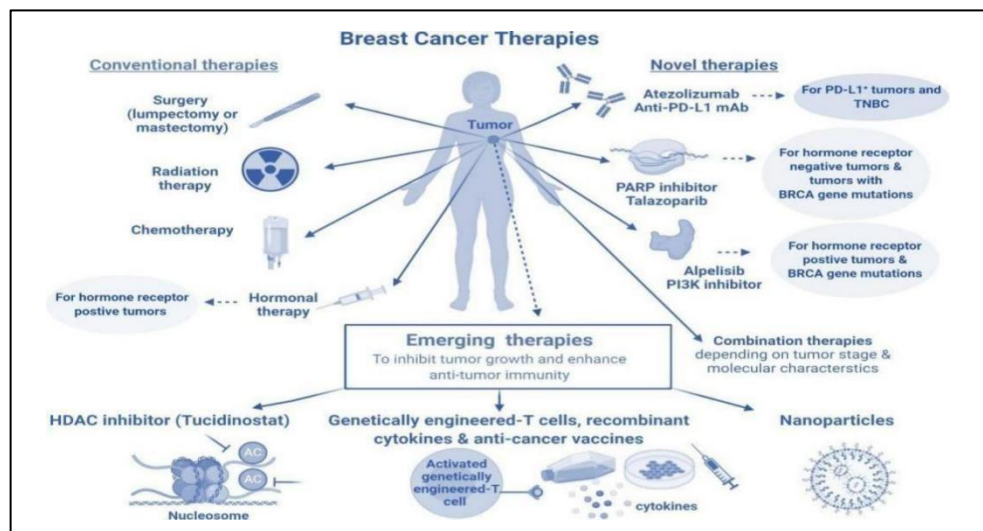


Figure 1.6 Conventional and novel treatments for breast cancer

1.5 Plant sterols and breast cancer

The United States has a threefold higher age adjusted incidence of cancer than Asian nations, and immigrants are more likely to develop the disease. This suggests that lifestyle and nutrition play crucial roles. Plant based foods may help lower the risk of cancer (15). Certain compounds not synthesized by the body are introduced through diet, primarily found in lipid rich plants, such as vegetable oils and nuts. Although there are various types of plant sterols, the three most common ones in the diet are campesterol, stigmasterol, and beta-sitosterol (16). The amount of plant sterols in the diet may be a nutritional element influencing the disease's distribution. Estrogen is a well established modulator of breast cell development. Overexpression of the ESR1 gene is required for the proliferative effects of estradiol in breast cancer cells (15). Consuming beta-sitosterol has been shown to increase the likelihood of having an estrogen receptor positive profile compared to an estrogen receptor negative profile (17). Bcl-xL and Bcl-2 expression is markedly reduced by stigmasterol (18).

1.6 Plant sterols and antioxidant potential

Antioxidants are compounds that prevent oxidation and serve as protective agents, shielding the body from the harmful effects of free radicals, which are natural chemical reactions that occur in the body. The DNA of healthy cells is changed when free radicals harm them, which encourages the development of cancer. Antioxidants are abundant in fruits and vegetables. The idea of using antioxidant interventions to prevent cancer was developed (19). Some research suggests that plant sterols, such as stigmasterol, beta-sitosterol, campesterol exhibit antioxidant effects (20).

1.7 *In vitro* cell line breast cancer study

Cancer cell lines have been extensively utilized in research and have proven to be a valuable tool in the genomic approach. Their characterization also indicates that they are an excellent model for studying the molecular processes underlying cancer (21). The development of current anticancer medications, the testing of novel treatments,

and the replacement of transplantable animal tumors in chemotherapeutic testing have all been facilitated by using cell models (22). The characterization and screening of cancer therapies, and the study of cancer progression, propagation, deregulation, and apoptosis all rely on the use of proper *in vitro* models (23). As the results of studies on different cancer cell lines are typically translated to *in vivo* settings, many biomedical researchers have recognized the value of employing human tumors as models for drug testing and translational research (22-24).

1.8 Synergism in breast cancer

Combinations of drugs have been used to treat various conditions, including chronic disorders like AIDS, asthma, and cancer. This approach takes advantage of the fact that different molecular pathways contributing to a given disease are susceptible to the actions of individual drugs, thereby increasing treatment effectiveness, slowing the development of drug resistance and reducing cytotoxicity (25). The primary goal of combining two or more medications is to produce positive effects by providing stronger evidence of the benefits of the combination compared to each medication taken alone. Demonstrating that a drug combination offers greater advantages than either medicine alone is crucial for optimizing the effectiveness of the therapeutic combination (26). Numerous theoretical and experimental studies have characterized the interaction effects of drug combinations as primarily antagonistic or synergistic, representing less or more effect than expected (27).

CHAPTER – 2

LITERATURE

REVIEW

2. REVIEW OF LITERATURE

2.1 *Euphorbia pulcherrima*

2.1.1 Description

Euphorbia pulcherrima, (Euphorbiaceae) also known as poinsettia or Christmas flower, is a member of the genus *Euphorbia*, which is the third largest genus of flowering plants (28). The Euphorbiaceae family, also known as the spurge family, is the largest flowering family among the Anthophyta. This family comprises 300 genera and 5,000 species worldwide. Members of this family are a vital and abundant source of bioactive natural products (29). Plants can be found throughout Asia, Nepal, and the Pacific coast of North America, as well as in Mexico and Guatemala. *Euphorbia pulcherrima* is a popular Christmas plant, cultivated for its scarlet, leafy bracts. Although certain species of the Euphorbiaceae family that produce latex can be hazardous, this plant is generally benign. Spurges are recognized for their uses as houseplants and ornamental plants (30).

2.1.1.1 Biological source

The dried leaves of *Euphorbia pulcherrima* Willd are utilized which belongs to the family Euphorbiaceae (31).

2.1.1.2 *Euphorbia pulcherrima* features

Euphorbia pulcherrima grows to a height of 0.6-4 meters (2-13 feet) as small tree. The dark green, dentate leaves of the plant range in length from 6 to 16 cm (2.4 to 6.3 in). The bracts are typically flaming red, pink, pale green, or white, and are sometimes confused with flower petals, but they are actually modified leaves (32).



Figure 2.1 *Euphorbia pulcherrima* plant



Figure 2.2 *Euphorbia pulcherrima* leaves

***Euphorbia pulcherrima* leaves (Morphology)**

Shape : Broadly ovate with smooth edges (entire leaf margin) or pointed lobes

Size : 6 to 16 cm.

Colour : Darkgreen

Odour : Sweet

2.1.1.3 Taxonomic classification

Kingdom : Plantae

SubKingdom : Viridiplantae

Phylum : Tracheophyta

Class : Magnoliopsida

Sub class : Rosidae

Division : Tracheophyta

Super division : Embryophyta

Order: Euphorbiales

Family : Euphorbiaceae

Genus : Euphorbia

Species : *Euphorbia pulcherrima* (33 to 36).

2.1.1.4 Vernacular names

Sanskrit : Arkapushpa

Marathi : Ratnaphool

Hindi : Lalpatta

English : Christmas Flower, Mexican Flame Tree, Poinsettia

Punjabi : Christmas Flower

Nepali : Lalupate

Bengali : Lalpata

2.1.2 Phytochemistry

Fixed oils :

Palmitic acid, Linolenic acid, Heptadecenoic acid, Eicosenoic acid, Stearic acid, Tetracosanoic, and Docosanoic acid (34).

Terpenoids :

Eupulcherol A, Euphorimaoid A, Euphorimaoid B, Ellagitannins, Ealactomannans,

Furanoditerpenoids, Pulcherrimins, and Diterpene dibenzoates (35-37).

Flavonoids :

Spinacetin, Patuletin (38), Rutin (37, 39).

Phenolic acids :

Gallic, Syringic, Chlorogenic, P-coumaric, Vanillic, Caffeic, P-hydroxybenzoic and Ferulic (39).

Amino acids :

Glycine, Valine, Alanine , Isoleucine, Serine, Threonine, Glutamic acid, Glutamine, Lysine, Histidine, Cystine, Aspartic acid, Arginine, Leucine, Phenylalanine and Proline (40).

Sterol :

Cycloartenol, 3-Amyrin acetate and Germanicol acetate (41). Beta-amyrin, Germanicol, Pseudo - taraxasterol, Puobucol , Octaeicosanol , and Beta-Sitosterol (42).

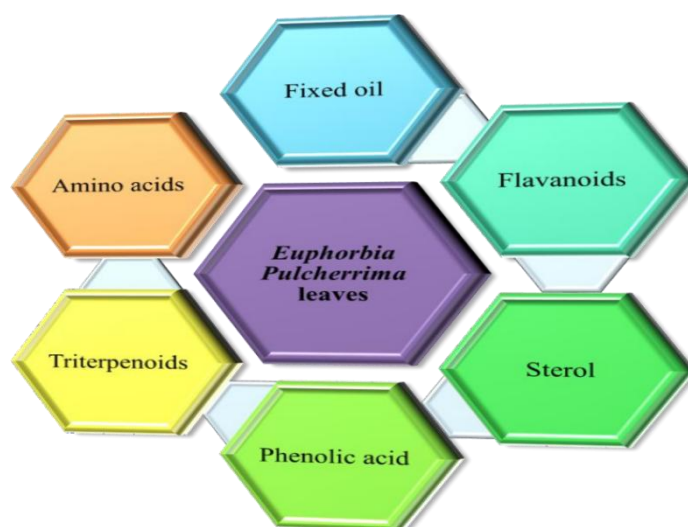
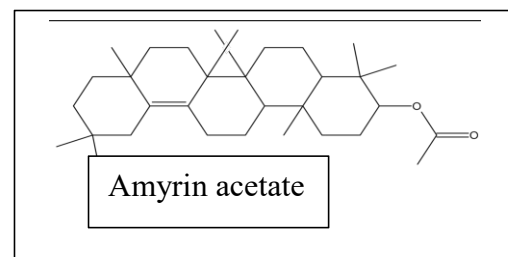
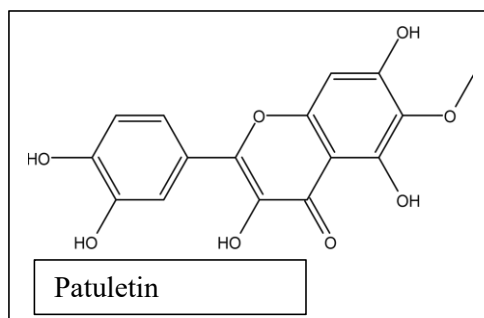
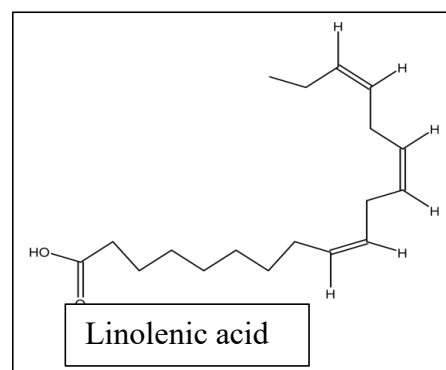
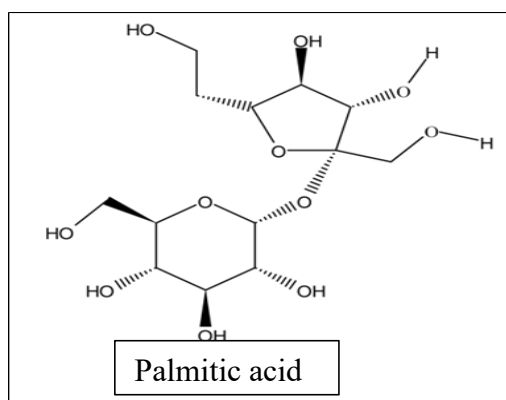
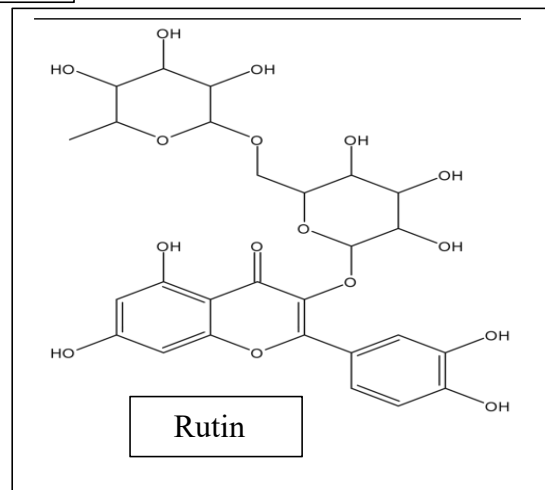
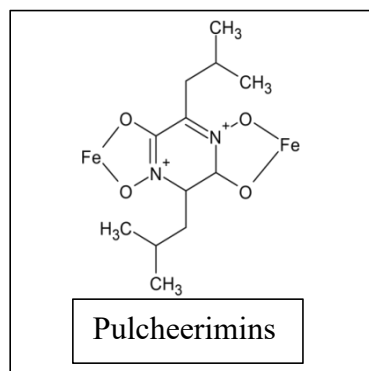
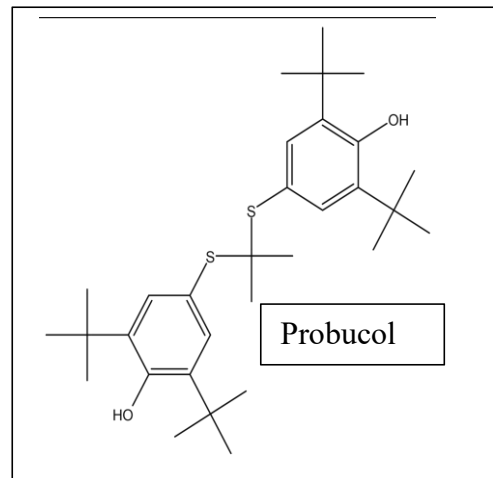
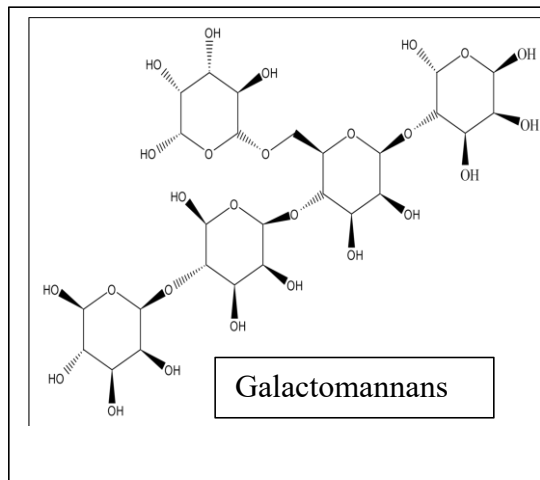
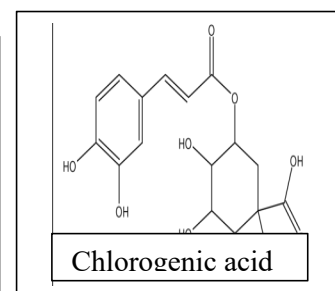
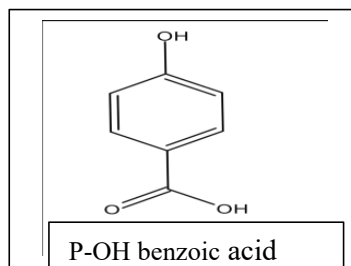
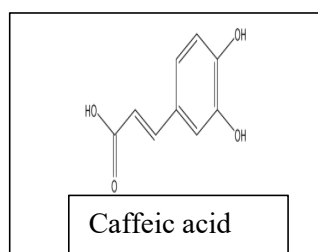
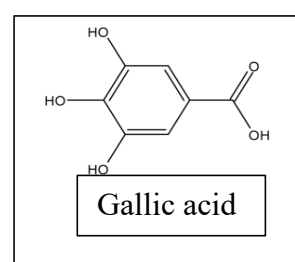
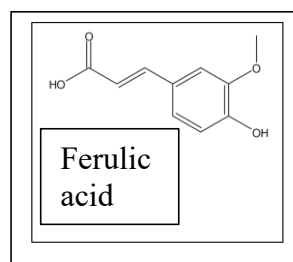
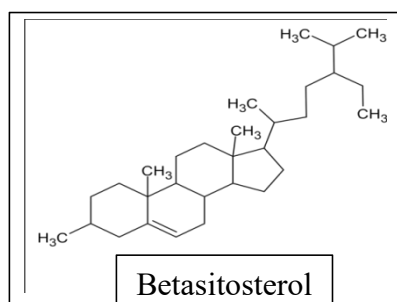
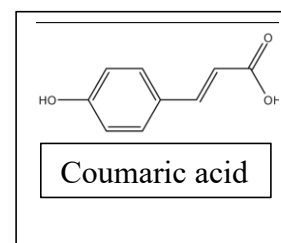
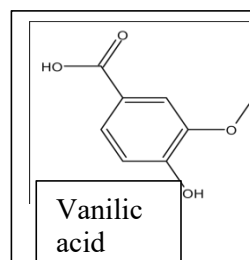
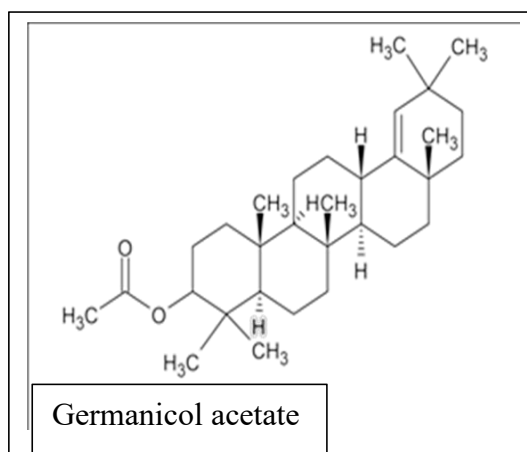
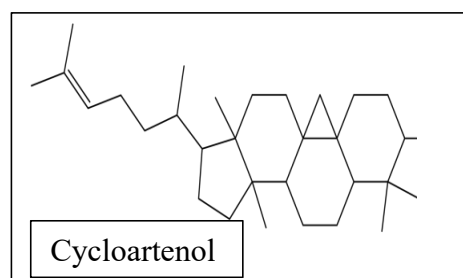
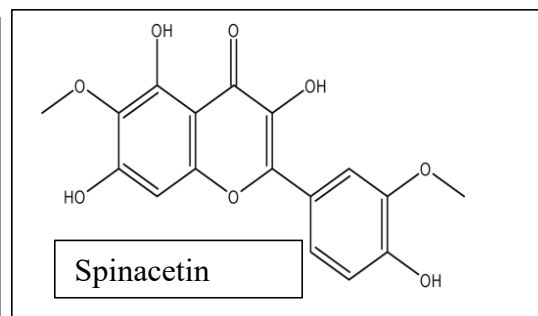
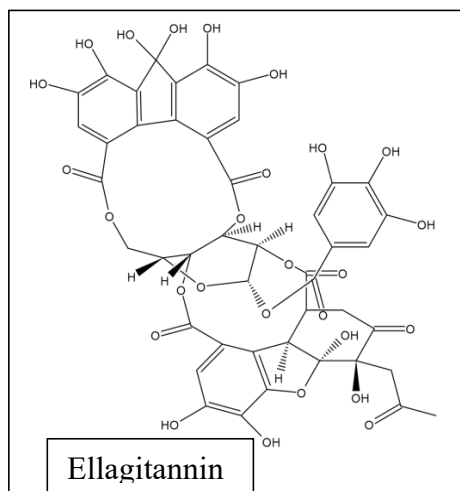
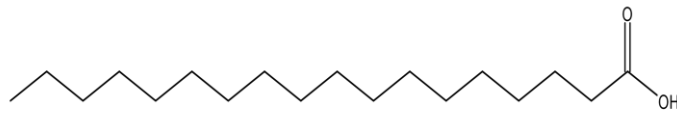


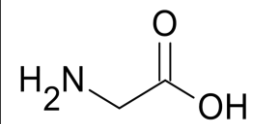
Figure 2.3 Chemical constituents of *Euphorbia pulcherrima* leaves



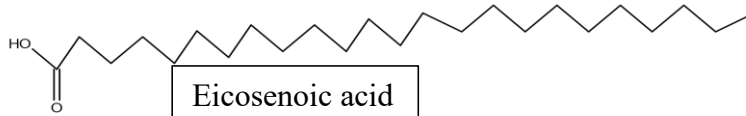




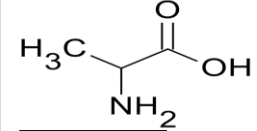
Stearic acid



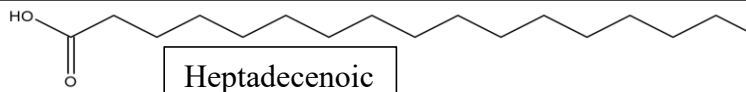
Glycine



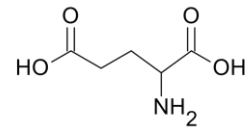
Eicosenoic acid



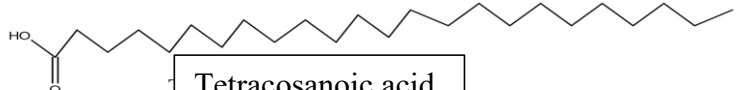
Alanine



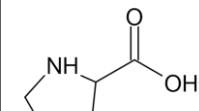
Heptadecenoic



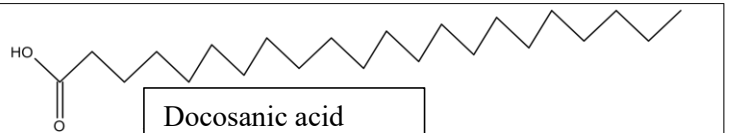
Glutamic acid



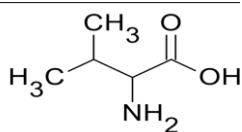
Tetracosanoic acid



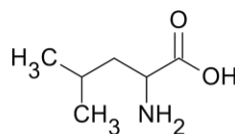
Proline



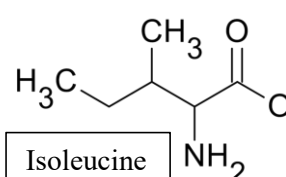
Docosanoic acid



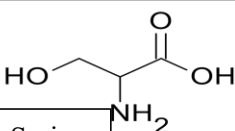
Valine



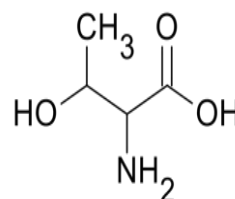
Leucine



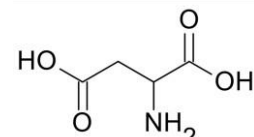
Isoleucine



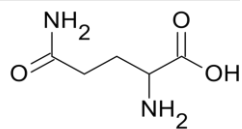
Serine



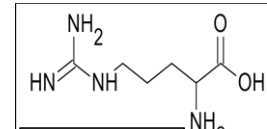
Threonine



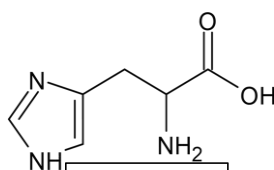
Aspartic acid



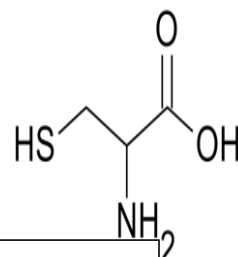
Glutamine



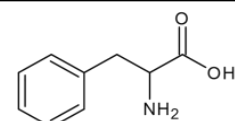
Arginine



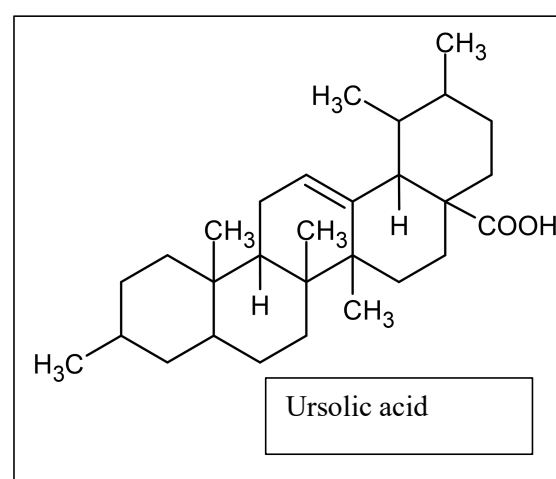
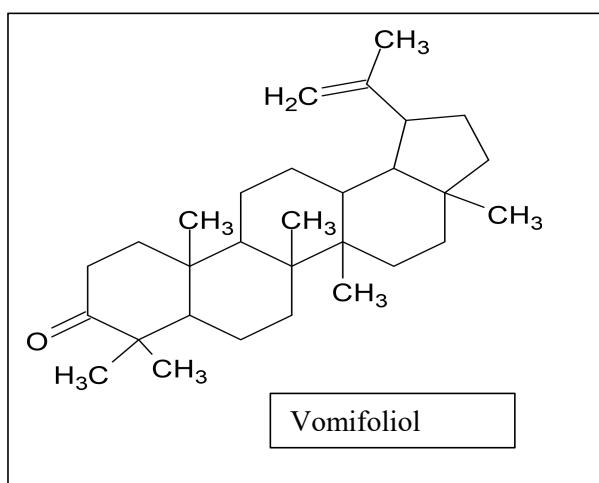
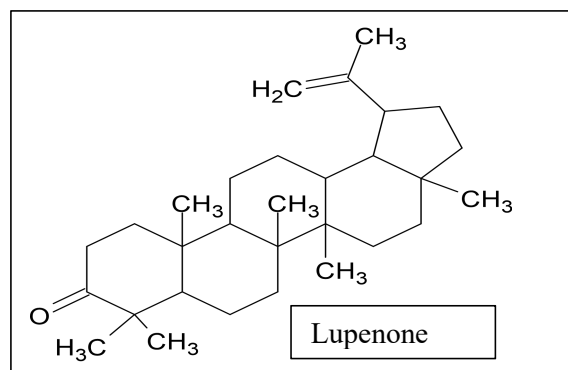
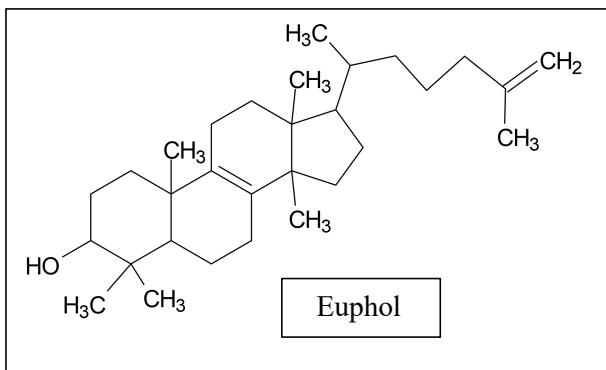
Histidine



Cysteine



Phenylalanine



Many species of *Euphorbia* are used to treat skin and subcutaneous cellular tissue diseases. They are also used to cure a variety of skin conditions, including dermatitis, nodules, warts, sores, carbuncles, boils, psoriasis, ulcers, sunburn, eczema, inflammation, and respiratory system illnesses. Several studies have highlighted the purgative and emetic properties of *Euphorbia* species, including their use as an astringent (42). Various species are used to treat several diseases, such as microbial illnesses, cellular tissue ailments, injuries, endocrine and nutritional diseases, pregnancy or birth disorders, inflammatory infections, digestive issues, blood syndromes, body pain, inflammatory infections, body and skin irritations, and genitourinary syndromes (43). The plant was used by the Aztecs to make red dye. Poinsettias are a common Christmas decoration in companies, homes, and churches worldwide (44). Certain components of *Euphorbia pulcherrima* are utilised in traditional medicine to heal disorders like constipation, skin disorders, and to encourage nursing mothers to secrete more milk. *Euphorbia pulcherrima* has also been demonstrated to have a numbers of

biological activities both *in vitro* and *in vivo*, such as hypnotic, antipyretic, analgesic, anti-inflammatory, and neuroleptic qualities (45). Additionally, it possesses anti-arthritic, antimicrobial, antidiabetic, anti-eczema, antispasmodic and antitussive properties (46). It is used in traditional Chinese medicine to decrease osteoclastogenesis, cure fractures, excessive bleeding, bruising, and hypermenorrhea (47).

2.2 *Ricinus communis* seed

2.2.1 Description

Ricinus communis (Euphorbiaceae) also known as castor bean or castor (48). The optimal temperature for castor plant growth is around 20°C to 25°C. Temperatures below 12°C and above 38°C can adversely affect growth and yield. The seeds are categorized by their shape, which can be oval, ovoid, elongated, or square. Seed color varies from red to black, grey, brownish-yellow, brown, and white, with patterns ranging from finely dotted to broad splotches (49-50). The utilization of herbal medicine has become increasingly popular not only in India but also worldwide, making it a fascinating area of interest (51).

2.2.1.1 Biological source

These are dried seeds of *Ricinus communis* belongs to the family Euphorbiaceae.

2.1.1.2 *Ricinus communis* seed features

The fruit is a greenish to reddish purple, spiny capsule with large, oval, shiny seeds featuring brownish mottling. Native to India, East Africa, and the south east Mediterranean Basin, castor is extensively cultivated as an ornamental plant in tropical regions. Castor bean seeds are available in various cultivars with differing oil contents (45–55%). The residue remaining after castor oil extraction is known as castor bean pomace, which hold approximately 36% protein. Additionally, castor bean pomace hold the highly poisonous and heat sensitive ricin and albumin, as well as a potent allergen protein fraction that is more heat resistant (52).



Figure 2.4 *Ricinus communis* plant



Figure 2.5 *Ricinus communis* seeds

2.1.1.3 *Ricinus communis* seed (Morphology)

Shape : Oval, elliptical

Size : 1 to 2 cm

Colour : Reddish purple, greenish, red with mottled with black, brown, gray, white .

2.1.1.2 Taxonomic Classification (51, 53).

Kingdom : Plantae

Family : Euphorbiaceae

Domain : Eukaryota

Phylum : Spermatophyta

Subphylum : Angiospermae

Class : Dicotyledonae

Sub class : Rosidae

Division : Magnoliophyta

Order : Euphorbiales

Genus : *Ricinus*

Species : *communis*

2.1.1.4 Vernacular Names

Common name : Palm of Christ

Marathi : Errandi

Hindi : Arand, errand

English : Castor bean

Sanskrit : Vatari, Rrubu, Urubu.

Assam : Eda

Punjabi : Diveli

Bengali : Verenda

Gujrat : Erando

Kashmiri : Aran, Banangir.

Kanada : Haralu, Gida.

Malyalam : Avanakku (54-55).

2.2.2 Phytochemistry

Ricinus communis contained alkaloids, saponins, steroids, glycosides, flavonoids.

Glycosides : Stearic Acid, Isoricinoleic, Dihydroxy Stearic Acids, Ricinoleic, and Crystalline Ricinine.

Alkaloid : Ricin

Fatty acids : Stearic, Palmitic, Oleic Acid, Ricinoleic Acid, Hexadecenoic Oleic , Dihydroxy stearic Acids , Arachidic , Linoleic, and Ricinoleic .

Triglycerides : Ricinolein.

Steroids : Stigmasterol, Ergost-5-en-3-Ol, Probucol , Flucosterol. Also Contains 1,8 Cineole , α -Thujone, α -Pinene, Camphor, Camphene and Lupeol (56).

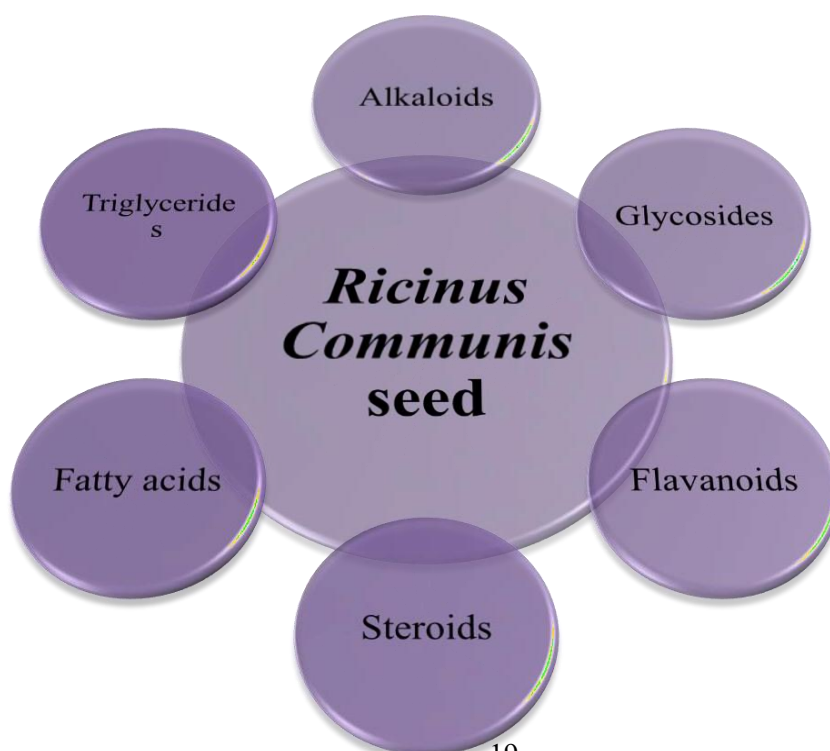
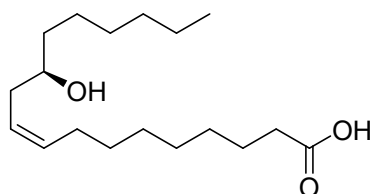
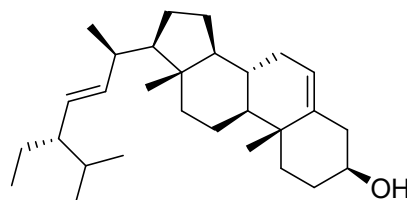


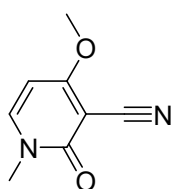
Figure 2.6 Chemical constituents of *Ricinus communis* seeds



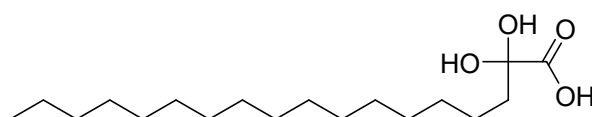
Ricinolic acid



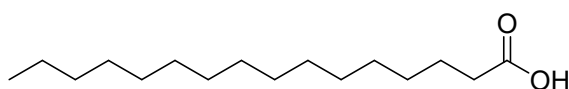
Stigmasterol



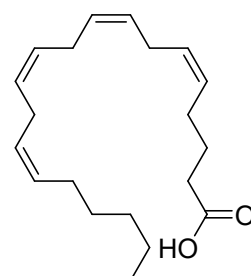
Recinine



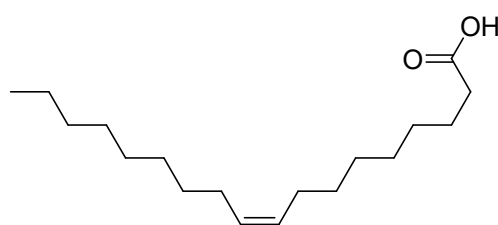
Dihydroxysteic acid



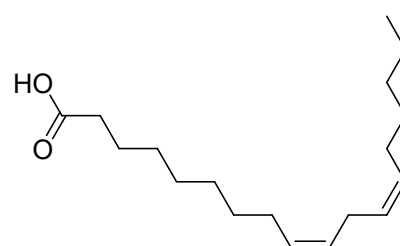
Palmitic acid



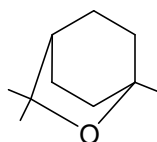
Arachidonic acid



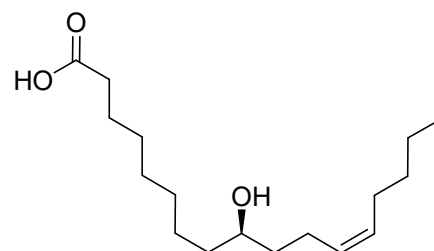
Oleic acid



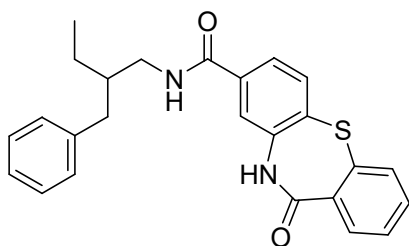
Linoleic acid



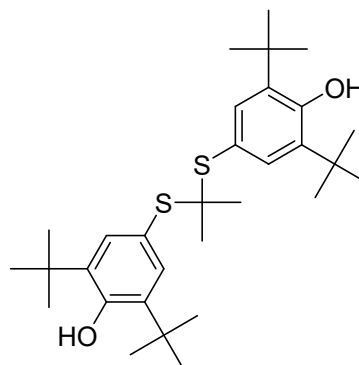
1,8 -cineole



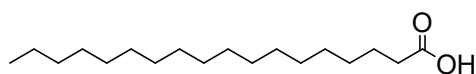
Lsoricinoleic Acid



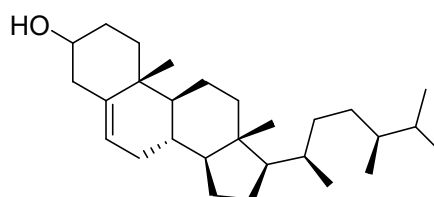
Ricin



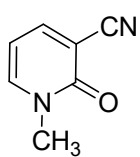
Probucol



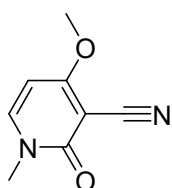
Stearic acid



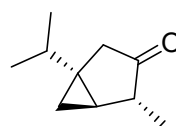
Ergost-5-en-3-ol



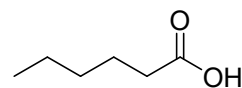
Rcinidine



Ricinine



Thujone



Hexanoic acid

2.2.3 Ethnomedical uses

The *Ricinus communis* plant has several applications, with all its parts, including roots, seeds, bark, flowers, fruits, leaves, and stem, being utilized. Castor oil has been utilized worldwide in traditional medicine for various diseases since ancient times. The plant's seeds were found in Egyptian tombs dating back to around 4000 BC. Historical records indicate that castor oil was used in Egypt to treat eye irritations. Greek explorers, such as Herodotus, documented the use of castor seed oil as an ointment and light source. By 2000 BC, castor seed oil was recorded in Indian folk medicine as a laxative and for lighting purposes. Folk medicine has revealed that *Ricinus communis* seeds and oil have been used for centuries in China for internal and external applications, like dressings, inducing labor pain during pregnancy, and treating constipation (57). The seeds have also been reported to possess various pharmacological activities, including anticancer, laxative, antiasthmatic, antifungal, anti-diabetic, anti-inflammatory, antimicrobial, antioxidant, uterine-contracting, molluscicidal, antiulcer, wound-healing, bone regeneration, cytotoxic, anti-arthritis, and hepatoprotective properties, as well as antidandruff, insecticidal, and antimalarial effects (58). Castor or ricinus oil can be obtained by removing the seed coat. This oil has been used as a laxative, cathartic, and rheumatic treatment. Due to its ability to hold water and cleanse the large intestine, the oil is considered one of the safest purgatives for mild to moderate constipation. Historically, it also used to treat different conditions, including tumors, gout, piles, corns, moles, warts, breast indurations, inflammations, cysts, and paralysis (59). The oil has also been used to treat several skin conditions, like psoriasis, eczema, as well as eye diseases like conjunctivitis and styes (60). Additionally, oral administration of the oil during pregnancy, alone or in combination with quinine sulfate, has been reported to induce labor in certain women (61).

2.1.4. Anticancer activity of Beta-sitosterolStomach cancer:

Beta-sitosterol, campesterol and stigmasterol are the typical plant sterols found in food, but in varying concentrations. Phytosterols and their derivatives offer protection against a variety of chronic disorders, including inflammation, arteriosclerosis, cancer and ulcers. The anticancer potential of Beta-sitosterol was

assessed using several assay methods, such as MTT assay, lactate dehydrogenase, clone creation, ethidium bromide leakage assay, acridine orange double staining, and others. Apoptosis, cytotoxicity, and proliferation in human stomach cancer cells (SGC-7901) were assessed by these assays. The findings, which varied according to time and dosage, showed that Beta-sitosterol suppresses stomach cancer cells (SGC-7901) growth and cytotoxicity in a concentration dependent way (8, 16, 32, 64 μ M). Additionally, beta-sitosterol showed higher activation of pro-caspase-3, DNA damage, reduction of bcl-2 expression, and morphological changes (62).

Lung cancer :

Beta-sitosterol has also been found to be effective against lung cancer. The molecular mechanism underlying its action has been reported to involve the inhibition of Trx/TrxR1 protein expression, leading to increased apoptotic cell death and ROS accumulation in NCI-H460 and A549 cells. Lactate dehydrogenase leakage data show that Beta-sitosterol is effective against human lung cancer cells. Several studies have also investigated its effects on A549 cells at various doses and time points. The MTT assay results revealed that Beta-sitosterol significantly impacted A549 cell growth at different concentrations and time intervals, with growth suppression observed at the 72 hour mark, and an IC_{50} value of 24.7 μ M. Furthermore, the lactate dehydrogenase leakage assessment results demonstrated that the release of LDH following Beta-sitosterol treatment in A549 cells was concentration dependent (63).

Prostate cancer :

The most prevalent malignancy among men is prostate cancer. Beta-sitosterol is used to treat various conditions, including prostatic hyperplasia, hair loss, tuberculosis, cervical cancer, and heart disease. Prostate cancers can be classified into four categories: neuroendocrine tumors, small cell carcinomas, transitional cell carcinomas, and sarcomas. The effect of Beta-sitosterol extract on viable cells, BCL-2, Bcl-xL mRNA, and Mcl-1 mRNA expression was evaluated in PC3 cells. Beta-sitosterol was tested at varying concentrations (25 μ M, 50 μ M, and 100 μ M) in relation to the PC-3 cell line and Bcl-xL expression in mRNA. The efficacy of

Beta-sitosterol significantly increased with concentration and showed maximum activity at 100 μ M (64).

Renal cell cancer :

In US Renal cell carcinoma is the eighth leading cause of cancer related death and has an yearly frequency of more than 270,000 new cases (65). A crucial aspect in the progression of human renal cell cancer is the modification of mitogen-activated protein kinases (MAPKs). The development and start of renal cell carcinoma are significantly influenced by changes in the MAPK and endothelial growth factor receptor systems. This study demonstrated that inhibiting Fe-NTA facilitated the maintenance of endothelial growth factor receptor signaling. Beta-sitosterol regulates extracellular signal-regulated kinase activity, thereby preventing tumor growth and maintenance. Beta-sitosterol interacts with the ATP-binding site and inhibits ERK-2, according to molecular docking studies conducted after rats were pretreated with carcinogens at a dose of 20 mg/kg body weight. This study shows that Beta-sitosterol inhibits oncogenic MAPK signaling, cell proliferation, angiogenesis, and induces apoptotic actions to prevent kidney carcinogenesis caused by N-diethylnitrosamine and ferric nitrilotriacetate (66).

Pancreatic cancer :

Pancreatic cancer is characterized by metastasis and invasive growth, making it one of the deadliest types with only a five percent chance of survival (67). Cancer and AIDS are the two most common disorders treated using combination therapies (68-69). To evaluate the synergistic, additive or antagonistic effects of combined therapy. Gemcitabine and Beta-sitosterol were tested on MIA-PaCa2 and BXPC-3 cells. According to the combination index (CI) values, this combination worked in concert to prevent the growth of MIA-PaCa2 and BXPC-3 cells. When treated with different concentrations of Gemcitabine and Beta-sitosterol, the CI values for MIA-PaCa2 and BXPC-3 cells were 0.665 and 0.316, respectively (70).

Lung cancer :

In both economically developed and developing nations, breast cancer in women and lung cancer in men are the most common cancers diagnosed and the primary cause of cancer-related deaths for each sex. Lung cancer accounted for 13% of all cases and 18% of cancer related fatalities (71,72). To determine the effectiveness of

Beta-sitosterol, three distinct human cancer cell lines were tested MDA-MB-231 for breast adenocarcinoma, A549 for lung epithelial carcinoma, and A431 for skin epidermoid carcinoma. Beta-sitosterol, at concentrations between 30 and 90 μ M, had no discernible effects on apoptosis and proliferation of A431 cells after 48 and 72 hours. In contrast, comparable Beta-sitosterol treatments reduced A549 cell proliferation up to 13% ($p < 0.05$) after 48 hours and 14% ($p \leq 0.05-0.0001$) after 72 hours. MDA-MB-231 cell growth was markedly inhibited by Beta-sitosterol in a dose-dependent manner., with results showing 31-63% inhibition ($p < 0.0001$) after 48 hours and 40-50% inhibition ($p \leq 0.0001$) after 72 hours (73).

Colon cancer :

A pathological level of ongoing oxidative stress, which damages DNA, causes mutations in genes linked to cancer, and promotes cell cycle death and regeneration, is often the underlying cause of colon cancer (74). In the present study, Beta-sitosterol demonstrated dose-dependent growth inhibition in colon cancer using COLO 320 DM cells. These findings demonstrated that Beta-sitosterol can inhibit the buildup of proliferating cell nuclear antigen (PCNA) in the colon, hence preventing 1,2-dimethylhydrazine (DMH) induced carcinogenesis. It was discovered that doses of 10–20 mg/kg body weight of Beta-sitosterol were effective against cancer in male Wistar rats that had been injected with 1,2-dimethylhydrazine (20 mg/kg body weight) and treated with Beta-sitosterol for 16 weeks (75).

Ovarian cancer :

In females, ovarian cancer is challenging to identify because there are no visible symptoms in the early stages (76). Beta-sitosterol, stimulated the ER mitochondrial axis, inhibiting cell proliferation and decreasing the PI3K/MAPK signal transduction. Specifically, Beta-sitosterol enhanced ovarian cancer cell mortality when combined with paclitaxel or cisplatin. Beta-sitosterol showed synergistic anti-cancer benefits when combined with regular anti-cancer medications for ES2 and OV90 ovarian cancer cells at concentrations of 10, 25, and 50 μ g/mL, resulting in 243%, 568%, and 1100% increases in cell mortality, respectively. Similarly, at concentrations of 5, 10, and 50 μ g/mL of Beta-sitosterol, cell mortality increased by 310%, 790%, and 1000%, respectively (77).

Cervical cancer :

Cervical carcinoma is one of the most common malignant tumors in women and has a high death rate. With a 52% five-year survival rate, it ranks second in terms of mortality rates among all malignant tumors found in females. Every year, more than 10,000 new instances of cervical cancer are reported in the US. When Caski and HeLa cells were exposed to 20 $\mu\text{mol/l}$ of Beta-sitosterol, scanning and transmission electron microscopy showed that the cells' expression of multiply cell nuclear antigen (PCNA) reduced, which exerted an inhibitory influence on cell proliferation. Western blot and real-time PCR techniques were used to quantify variations in mRNA and protein expression, respectively (78).

Breast cancer :

Beta-sitosterol is one of the most rich naturally occurring phytosterols in plants. Which is applied in several fields such as medicine, agriculture, and chemical industries, due to its unique biological and physicochemical properties. In addition, Beta-sitosterol exerts an anti-tumor effect on multiple cancerous tumors such as breast, gastric, lung, kidney, pancreatic, prostate, and other cancers. Various mechanisms of Beta-sitosterol included, apoptosis or programmed cell death is controlled by diverse signaling pathways involving various regulatory proteins. p53 is a tumor-suppressive protein that strictly regulates cell growth by promoting apoptosis and DNA repair under specific conditions. Mutated p53 can lead to abnormal cell proliferation and tumor development due to loss of function, Beta-sitosterol treatment led to a significant decrease in the expression of cyclin-D1, Bcl-2, and vascular endothelial growth factor (VEGF) along with a substantial increase in the expression of caspase, with high concentration dose arrested human breast cancer T47D cells in the G_0/G_1 phase because it augmented the proportion of cells in the G_0/G_1 phase while reducing their proportion in the S phase, consequently decreasing proliferation index and suppressing cell proliferation, also blocked the MAPK pathway by inhibiting the ATP binding site and acting as a competitive inhibitor of ATP to prevent the activation of ERK1/2 and Proliferating cell nuclear antigen (PCNA) is an important protein that affects tumor cell proliferation and is involved in diverse DNA metabolic processes, such as DNA

replication and repair, chromatin organization and transcription, and condensation of sister chromatids (170).

2.2.4 Anticancer activity of Stigmasterol

Breast cancer :

Plant sterol stigmasterol has been shown through molecular docking studies and *in vivo* and *in vitro* methods to have a variety of pharmacological prospects, including anti-osteoarthritic, antitumor, immunomodulatory, cytotoxic, antiparasitic, antifungal, anti-diabetic, antibacterial, antimutagenic, antioxidant, neuroprotective, and anti-inflammatory effects (79, 80). Using isolated stigmasterol as a starting point, various processes such as oxidation, acetylation, epoxidation, epoxide ring opening, and dihydroxylation were carried out to produce derivatives. Stigmasterol can incisively target Bcl-2 and Bcl-xl by down regulating these genes, cutting off key signal transmission required for the growth and proliferation of cancer cells, it induces apoptosis or programmed cell death is controlled by diverse signaling pathways involving various regulatory proteins. The synthesized derivatives of stigmasterol were evaluated for cytotoxicity in vitro using the resazurin assay against three different cancer cell lines. Triple-negative breast cancer (HCC70) with EC₅₀ values ranging from 67.73 to 44.54 μ M, hormone receptor positive breast cancer (MCF-12A) with EC₅₀ values of 30.18 to 51.79 μ M, and non-tumorigenic mammary epithelial cells (MCF-7) with EC₅₀ values ranging from 42.85 to 22.94 μ M (81).

Endometrial cancer :

Endometrial cancer (EC) is a common gynecological cancer found in women worldwide. Stigmasterol, a naturally occurring phytosterol with anti-cancer properties, is found in seeds and vegetable oils. Through the inhibition of the IGF1R/AKT/mTOR and Wnt/ β -catenin pathways, it has a number of beneficial effects on human health, such as anti-angiogenic, hypoglycemic, chemopreventive, anti-inflammatory, and antioxidant qualities. At 20 and 40 μ M, stigmasterol can reduce the potential of cancer stem cells (CSCs), cell migration, and proliferation. Furthermore, it has the ability to suppress the expression of markers linked to the epithelial mesenchymal transition (EMT), such as ZEB1 and SNAI1, as well as

markers linked to CSCs, such as OCT4, c-MYC, and NANOG (82).

Ovarian cancer :

A prevalent malignant tumor among women is ovarian cancer (OC), often diagnosed at advanced stages due to its gradual onset and uncommon symptoms. Stigmasterol has been shown to possess antineoplastic properties against different malignancies (83). However, there hasn't been any prior reporting of its anticancer effects on ovarian cancer (84). Stigmasterol prevents the migration of ovarian cancer cells and induces calcium overload, reactive oxygen species (ROS) generation, and cell death in OV90 and ES2 cells. Also stigmasterol promotes cell death in a dose-dependent manner via activating the ER-mitochondrial axis. Significant inhibition was seen upon treatment with stigmasterol at doses of 0, 5, 10, and 20 $\mu\text{g/mL}$. Notably, in OV-90 and ES2 cells, the treatment of stigmasterol (20 $\mu\text{g/mL}$) reduced tumor volume by 60.1% and 72.8%, respectively (85).

Hepatic cancer :

Currently, there is no cure for liver cancer, and treatment options are limited to immunotherapy, chemotherapy, radiation, surgery, and monoclonal antibody therapy. Due to its remarkable biological activities, stigmasterol has garnered significant attention. It has demonstrated the ability to decrease cholesterol levels, as well as exhibit anti-inflammatory, anti-cancer, antioxidant, and anti-osteoarthritis properties. Notably, numerous clinical trials have shown that stigmasterol has few or no negative effects, even at higher doses, confirming its potential medical value (86). Similarly, stigmasterol and other plant sterols have demonstrated remarkable anticancer effects in various cancer cell lines through their diverse possible modes of action. Hepatocarcinoma (HepG2) cells are susceptible to the inductive action of stigmasterol on apoptosis. At doses of 5, 10, and 20 μM , stigmasterol exhibited dose-dependent toxicity on HepG2 cells, with corresponding toxicities of approximately 40%, 43%, and 54% (87).

Skin cancer :

Skin tumors frequently develop on regions of the body that acquire prolonged sun exposure, such as the ear, mouth, face, and back of the hands. However, malignant melanomas can arise in areas not exposed to the sun. Development skin cancer is higher in individuals who have experienced long term sun exposure (88).

Stigmasterol has been shown to have anti-melanoma qualities through downregulating PD-L1 expression and producing antioxidant effects. Using the melanoma cell lines B16F10 and A375, it was shown that oxidative stress is crucial to melanogenesis and the development of melanoma. As demonstrated by cell viability experiments, stigmasterol caused apoptosis at the same concentration and markedly decreased cell viability at doses more than 20 µg/mL (89).

Gastric cancer :

Most prevalent forms of cancer is gastric cancer. It has been demonstrated that stigmasterol inhibits the growth of SNU-1 stomach cancer cells. The JAK/STAT pathway is a key signaling mechanism that plays a crucial role in the growth and carcinogenesis of various cancer types. In SNU-1 gastric cancer cells, Stigmasterol inhibits the JAK/STAT pathway at concentrations of 0, 7.5, 15, and 30 µM in a concentration-dependent manner. This inhibition decreases SNU-1 cell viability, with a lesser effect on GES-1 cell viability. Additionally, stigmasterol induces apoptosis in a concentration dependent manner (90).

Prostate cancer :

Steroids have been demonstrated to effectively inhibit human cancer cells, providing a number of advantages such as preventing leukemia and malignancies of the neck, breast, head, and lung. As well as multiple myeloma, melanoma, ovarian, and kidney cancers. Additionally, they exhibit anti-proliferative properties against PC3 and human prostate cancer cells. The expression of various apoptosis related proteins, including p53, IAP, Bax, and Bcl-2, is altered in prostate cancer PC3 cells, disrupting normal apoptotic pathways and rendering the cells resistant to apoptosis. Therefore, enhancing the apoptotic process may be a key strategy for treating prostate cancer in humans and inhibiting PC3 cells. This study demonstrated that stigmasterol exhibits inhibitory effects against PC3, MCF-7, K562, and DU145 human cancer cells, with IC₅₀ values of 18.28, 22.73, 11.14, and 21.43 µM, respectively, in a dose-dependent manner (91).

2.1.5 Other Pharmacological activity of *Euphorbia Pulcherrima*

Anticonvulsant activity :

The Euphorbiaceae family includes *Euphorbia pulcherrima*, a plant whose leaves

and flowers have been utilised as an herbal remedy for various diseases, including skin disorders, to enhance milk production in nursing mothers, and as a mild laxative. Several *Euphorbia* species are reported to possess beneficial properties, such as antipyretic, central depressive, central analgesic, and sedative effects (92-93). This study investigated the anticonvulsant properties of *Euphorbia pulcherrima* crude dried milky extracts using the Electroshock Seizure (MES) test. In conclusion, this study used animal models to assess the effects of three different doses (250, 500, and 1000 mg/kg) of crude dried extracts of *Euphorbia pulcherrima* on the central nervous system. The results indicate that the crude dry extracts also exhibit antinociceptive, and anticonvulsant properties (94).

Antimicrobial activity:

Euphorbia pulcherrima has the potential to be used as a chemotherapeutic plant due to its rich chemical composition, which includes tannins, resins, steroids, glycosides, alkaloids, reducing sugars, and saponins (95). The antibacterial properties of ethanolic and aqueous extracts of the flower, leaf, stem, and entire plant of *Euphorbia pulcherrima* were evaluated using agar disc diffusion and macro broth dilution procedures against bacteria and fungi. *Salmonella typhi* and *Escherichia coli* showed high sensitivity to both aqueous and ethanolic extracts, as well as the whole plant, but not to the flower extract. The fungal exhibited sensitivity with *Aspergillus niger* showing high sensitivity to the leaf aqueous extract. *Candida albicans* displayed a low level of sensitivity (96).

Antibacterial activity :

Phytochemical analysis of *Euphorbia pulcherrima* has discovered the presence of various compounds, like, flavonoids, terpenoids, alkaloids, steroids, and reducing sugars. The antibacterial properties of *Euphorbia pulcherrima* were evaluated in several solvent fractions, including methanol, n-hexane, chloroform, and ethyl acetate. The n-hexane fraction exhibited zones of inhibition of 10, 12, 16, and 10 mm against *Salmonella typhimurium*, *Staphylococcus epidermidis*, *Bacillus stearothermophilus*, and *Klebsiella pneumoniae*, respectively. The chloroform fraction showed zones of inhibition of 18, 16, 14, and 12 mm against these bacterial strains. The ethyl acetate fraction demonstrated moderate antibacterial activity with a zone of inhibition of 12 mm. The methanolic extract and ethyl

acetate fraction of the plant exhibited mild antibacterial properties, particularly against *S. typhimurium*, *B. stearothermophilus*, *K. pneumoniae* and *S. epidermidis*. This study found that the plant extract exhibits dose dependent antibacterial activity. The ethanolic plant extract had the highest efficacy against both Gram positive (*Staphylococcus aureus*) and Gram negative (*Escherichia coli*) bacteria using the Cup plate method, with a stronger effect (97).

Antifungal activity :

Euphorbia pulcherrima has been found to exhibit antifungal effects against various types of fungi. The acetone extract of *Euphorbia pulcherrima* leaves was shown to suppress the growth of *Aspergillus fumigatus*. The findings showed that the extract had a concentration-dependent effect on the fungus development and shape. Specifically, the extract inhibited fungal growth and the degree of inhibition increased directly with the extract's concentration. Furthermore, the alcoholic extract of *Euphorbia pulcherrima* inflorescence also suppressed the development and morphology of the test fungus, with this effect being directly proportional to the extract's concentration (98).

1.2.5 Other Pharmacological activity of *Ricinus communis*

Antibacterial activity :

Ricinus communis, ordinarily known as castor oil, is a soft woody perennial shrub (99). Castor oil and products have numerous industrial applications, including the manufacture of lubricants, cosmetics, and polymers. *Ricinus communis* has also been found to possess potent purgative, laxative, hepatoprotective, anti-HIV, anti-inflammatory, and antioxidant properties (100-103). *Pseudomonas aeruginosa* is significantly inhibited by the seed protein of *Ricinus communis* with a minimum inhibitory concentration (MIC of 250 µg/ml), *Staphylococcus aureus* (MIC 125 µg/ml), and *Escherichia coli* (MIC: 62.5 µg/ml) (104).

Anti-oxidant activity :

Ricinus communis typically contains flavonoids, which possess potent antioxidant properties. Flavonoids are polyphenolic compounds with a broad range of beneficial biochemical and antioxidant properties, found in fruits, vegetables, and certain beverages. The development of human cancer is considered to be significantly influenced by free radicals. Antioxidant properties of the plant extracts and pure

compounds were evaluated using the DPPH method. The benzene extract exhibited the highest level of antioxidant activity, with an IC_{50} value of $36.19 \pm 2.332 \mu\text{g/ml}$, followed by the 50% methanol extract, with an IC_{50} value of $34.40 \pm 5.98 \mu\text{g/ml}$. Antioxidant activity was also demonstrated by the methanolic extract, with an IC_{50} value of $64.18 \pm 3.20 \mu\text{g/ml}$, and the chloroform extract, with an IC_{50} value of $66.17 \pm 6.30 \mu\text{g/ml}$. The antioxidant activity of the aqueous extract was lower, with an IC_{50} value of $106.14 \pm 4.33 \mu\text{g/ml}$ (105).

Anticancer activity :

Globally, breast cancer is a leading cause of death among women (106). Traditionally, various parts of the *Ricinus communis* plant have been used to treat a range of ailments, including warts, constipation, paralysis, pain, and gastritis (107-108). This study demonstrated that the fruit extract of *Ricinus communis* exhibits anti-breast cancer activity against MCF-7 and MDA-MB-231 cells. Notably, MDA-MB-231 cells showed the highest percentage of invasion inhibition (81%) compared to MCF-7 cells. The study also found that *Ricinus communis* fruit extract induced dose and time-dependent cytotoxicity in these cells (109).

Anti-diabetic activity :

Abnormally high serum lipid levels associated with diabetes mellitus are typically linked to an increased risk of cardiac disease. Flavonoids present in *Ricinus communis* have been found to possess hypoglycemic properties (110). The 50% ethanolic extract of *Ricinus communis* roots exhibited significant hypoglycemic activity in normal and diabetic rats. Administration of the *Ricinus communis* root extract outcome in substantial reductions in elevated levels of all biochemical parameters (111).

Antifertility activity :

Steroids and alkaloids are present in the methanolic extract of *Ricinus communis* seeds. Phytosterols are steroidal substances that may be responsible for the antifertility properties of the methanolic extract of *Ricinus communis* seeds. Results display that treatment of male rats with ethanol extracts of *Ricinus communis* resulted in antifertility effects, changes in sperm count, movement pattern, and morphology. Additionally, declines in fructose and testosterone levels indicated reduced reproductive function (112).

Anticonvulsant activity :

Epilepsy is a common chronic neurological condition defined by recurrent unprovoked seizures (113). Ricinine, phytoconstituent isolated from *Ricinus communis* seeds, and the ethanolic extract of the seeds, demonstrated anticonvulsant efficacy in mice with maximal electroshock seizures (MES) induced convulsions (114). Using pentylenetetrazole (PTZ) induced seizures in albino mice and the MES model in albino rats, the anticonvulsant qualities of *Ricinus communis* were examined. Both MES and PTZ-induced seizures were inhibited by the ethanolic extract of *Ricinus communis* in a dose-dependent manner (115).

Antiulcer activity :

The oil that extracted from the seeds of *Ricinus communis* has anti ulcer properties at 500 mg/kg and 1000 mg/kg body weight. However, the higher dose of 1000 mg/kg body weight was much efficacious in preventing ulceration in rats induced by ethanol, pylorus ligation, and aspirin. According to the findings, the oil's cytoprotective action, which strengthening the stomach mucosa and heightens mucosal defense, is responsible for its anti ulcer properties.(116).

Wound healing activity :

The wound healing effects of castor oil are attributed to its component that inhibits lipid peroxidation, thereby providing antioxidant action. To assess castor oil capacity to cure wounds, the excision wound model was utilized assessing parameters such as the percentage of closed scar sites, scar area, and epithelialization time. The astringent and antibacterial properties of castor oil constituents, including tannins, flavonoids, triterpenoids and sesquiterpenes, facilitate wound healing and accelerate epithelial formation. This study demonstrates that castor oil treatment in the excision wound model reduced scar area and epithelialization time, thereby promoting wound healing (117).

1.1.6 Betasitosterol**Synergistic Effect****Breast C ancer : (Beta-sitosterol and Quercetin)**

Breast cancer is the prime cause of death in women. Triple negative breast cancer

(TNBC), which is defined by the deficiency of the receptor like progesterone or estrogen and the human epidermal growth factor receptor (HER2), may be identified in 20–50% of women with breast cancer (118–119). Triple negative breast cancer (TNBC) has few available treatments, nevertheless. Interestingly, it was discovered that beta-sitosterol and quercetin had synergistic cytotoxicity. The comet assay and Western blot analysis were used to examine the effects on DNA damage and repair mechanisms. In both *in vitro* and *in vivo* shown that the plant not only caused DNA damage but also specifically hindered the processes that repair and repair cross links and double strand breaks that come from the homologous recombination process (120).

Pancreatic Cancer : (Beta-sitosterol and Gemcitabine)

Beta-sitosterol, a significant bioactive component found in plants, has demonstrated strong anti-tumor effects on numerous human cancer cells. However, reports on its efficacy against pancreatic cancer cells have been scarce. Gemcitabine is a first line treatment for pancreatic cancer. in MIA PaCa-2 and BXPc-3 cells, Beta-sitosterol and Gemcitabine demonstrated a significant synergistic impact. For 48 hours, cells were exposed to several doses of Gemcitabine (0, 12.5, 25, 50, 100 $\mu\text{M/L}$) and Beta-sitosterol (0, 62.5, 125, 250, and 500 $\mu\text{M/L}$), either separately or in combination. The combination demonstrated a greater suppression of cell growth than either treatment alone. Synergistic effects were measured using the combination index, $\text{CI}=1$ indicates an additive impact, $\text{CI} > 1$ indicates antagonism, while $\text{CI} < 1$ indicates synergy. The MTT experiment revealed that the combination synergistically suppressed the growth of pancreatic cancer cells. The greatest synergistic effect was indicated by the CI values of 0.316 for BXPc-3 cells and 0.665 for MIA PaCa-2 cells (121). Overall survival has been somewhat improved by combination therapies, such as Gemcitabine and Erlotinib (122).

Lung cancer : (Beta- sitosterol and Daucosterol)

The most common cause of death in both industrialized and developing nations is lung cancer. About 85% of deaths from lung cancer are caused by two major risk factors smoking and exposure to environmental pollutants (123). Beta-sitosterol, a phytosterol derived from the therapeutic plant *Grewia tiliaefolia* . Both alone and in combination, phytosterols specifically, daucosterol and Beta-sitosterol significantly

slowed the development of A549 cells. Using the MTT assay, the effects of Beta-sitosterol and Daucosterol were assessed and contrasted with those of the common medication cisplatin. Both Daucosterol and Beta-sitosterol significantly suppressed the growth of A549 cells in a time and dose dependent manner. Interestingly, compared to beta-sitosterol and cisplatin, daucosterol had stronger anti-cancer properties. Additionally, A549 cells demonstrated increased antitumor activity when Beta-sitosterol and Daucosterol (1:1) were combined (124).

Anxiolytic activity : (Beta- sitosterol and Fluoxetine)

Conditions related to stress, and anxiety are commonly observed in both developed and developing countries. Pharmacological regulation of hormone and neurotransmitter systems plays a crucial role in current therapy options for anxiety- and stress-related disorders (125). Phytosterols, including Beta-sitosterol, possess neuroprotective and antioxidative properties, which can influence various biological processes (126). According to a study, Beta-sitosterol causes synergistic effects when combined with fluoxetine, a selective serotonin reuptake inhibitor, and shows immediate anxiolytic efficacy. Mice given either Beta-sitosterol (100 mg/kg), Fluoxetine (20 mg/kg), or combination of Beta-sitosterol (20 mg/kg) and Fluoxetine (5 mg/kg) were able to eat at the same rate as the control group. These findings imply that Beta-sitosterol combination treatments could be advantageous at modest dosages (127).

1.2.6 Stigmasterol

2.3 Synergistic Effect

Antibacterial : (Stigmasterol and Ampicillin)

Stigmasterol, a typical steroid derivative found in plants, is commonly added to food due to its cholesterol lowering properties and has also demonstrated anticancer effects in a variety of cell lines (128). However, its potential role as an adjuvant to antibiotics remains unknown. Multidrug-resistant bacteria, antibiotics are often used in combination with non-antibiotic adjuvants. Adjuvants are substances that, when administered alone, does not exhibit antibiotic activity but, when combined with antibiotics, enhance the microbicidal effect (129). The results of the disc diffusion assay showed that the combination of stigmasterol and ampicillin (1 µg/disc each)

exhibited a higher zone of inhibition against various bacteria compared to individual treatments. Notably, *Streptococcus pyogenes* exhibited a higher combined effect compared to other Gram positive and Gram negative bacteria. The minimum inhibitory concentrations (MICs) for ampicillin were >200 µg/ml for most bacteria and 100 µg/ml for *Escherichia coli*, indicating high ampicillin resistance. In contrast, the MICs for the combination therapy ranged from 3.13 to 6.25 µg/ml, indicating a significant reduction in bacterial growth when stigmasterol and ampicillin were used together (130).

Breast cancer : (Stigmasterol and Barasertib)

Breast cancer severely affects both women and men, with the treatment choice depending on the exact nature and phase of the illness, the patient's overall condition, and available choices, including targeted therapy, radiation therapy, and chemotherapy. The prognosis for breast cancer is poor, and the incidence is high. Cuproptosis, a novel form of cellular death characterized by disruption of the cell's copper metabolism, is an important regulator of carcinogenesis and tumor growth (131). Stigmasterol, obtained from *Curcuma longa L.* may target the prognostic model's gene ADAM9. A combination therapy of barasertib and stigmasterol demonstrated significant synergistic effects on breast cancer (BRCA) cells. This study compared the combination of barasertib and stigmasterol with three other drugs. AZD-9496 and XAV-939 cell showed that the IC₅₀ values obtained using the CCK8 test in MCF-7 cells were 0.812, 1.76, and 5.53, respectively, at concentrations ranging from 5 to 30 µM, with a synergistic effect (132).

Liver cancer : (Stigmasterol and Paclitaxel)

There is a full incidence of liver cancer (HepG2) in Asia, Europe, and the US, highlighting the need for novel adjuvants or medications to counteract toxicity and treatment resistance (133). Paclitaxel (PTX), which is effective against a range of cancer cells both *in vitro* and *in vivo*, has been utilized in medical applications for ovarian cancer, melanoma, non-small cell lung cancer, metastatic breast cancer, and other malignancies (134) . In both liver malignant cells (HepG2) and normal liver cells (AML12), the effects of Paclitaxel and Stigmasterol combination on apoptosis and cell survival were investigated. The findings demonstrated that, at 500 and 1000 µg/ml, stigmasterol blocked the JAK/STAT, Akt/mTOR, and VEGFR-2 signaling

pathways, created reactive oxygen species (ROS), stopped the G₁ phase, and caused apoptosis via the caspase pathway in a dose-dependent manner. With IC₅₀ values of 464.44 µg/ml for HepG2 and 1056.44 µg/ml for AML12, the combination of Stigmasterol and Paclitaxel (1:1 ratio) demonstrated the strongest anticancer effects on HepG2 cells. These values differed from those obtained when the medicines were employed separately (135).

Breast cancer : (Stigmasterol and Sorafenib)

Breast cancer is not only the least prevalent disease in women worldwide, but it is also a leading cause of mortality. Sorafenib, an anti-angiogenic multi kinase receptor inhibitor, is used to treat various cancers. It has been demonstrated that the phytosterol stigmasterol has anticancer effects on human breast cancer cells, particularly MCF-7 and MDA-MB-231 cells. The effects of stigmasterol were evaluated at concentrations of 35, 70, 140, and 560 µM, while sorafenib was tested at concentrations of 3, 6, 12, 24, and 48 µM. Notably, the maximum concentration of stigmasterol achieved only 70% cell growth inhibition, indicating minimal suppression of cell growth and making it impossible to calculate the IC₅₀ value. However, when stigmasterol and sorafenib were combined, caspase-3 activity was elevated, while VEGFR-2, NF-κB, VEGF-A, Bcl-2, and Ki-67 levels were decreased. This combination therapy demonstrated significant potency in the treatment of breast cancer, inhibiting angiogenesis and promoting apoptosis signaling (136).

Skin cancer : (Stigmasterol and Palmatine)

Phytochemicals, derived from plants, have significant medicinal properties. Synergistic action occurs when two medications are taken simultaneously, resulting in combined effects that exceed the effects of taking them individually. Therefore, evidence-based phytotherapy is a viable treatment option for various human ailments, including cancer and low to mild-grade illnesses (137). In this study, palmatine and stigmasterol, which were isolated from *Tinospora cordifolia* and *Azadirachta indica*, respectively, in equal proportions at doses of 100 mg/kg and 200 mg/kg body weight, were measured for their synergistic chemopreventive effects. The combined drug sample demonstrated a synergistic effect on skin carcinogenesis induced by croton oil and DMBA (7, 12-dimethylbenz anthracene)

in animals fed a standard diet. DMBA was applied to the animals' shaved areas, and dosages of 100 mg/kg and 200 mg/kg body weight of the combined drug sample were given orally to the animals. After a 16-week experiment, with weekly examinations, the outcome showed that oral administration of the combined drug sample increased the average latency period, weight, and reduced the number of papillomas. Skin papillomas can be suppressed through dietary interventions, depending on the dose (138).

CHAPTER - 3

HYPOTHESIS

3. HYPOTHESIS

Cancer remains the major reason of death worldwide and is a grave medical concern. As our perceptive of the molecular mechanisms underlying cancer development has grown, numerous anticancer drugs have been created. However, chemically synthesized drugs have not significantly developed the general survival rate in recent years. Therefore, novel strategies and advanced chemo prevention medications are needed to enhance the efficacy of current cancer treatments. Natural substances called phytochemicals, which are present in plants, are essential for the creation of novel medications and the treatment of cancer. Natural drugs, derived from plants, animals, or microorganisms, may offer comparable or superior efficacy and safety profiles compared to synthetic drugs in treating various diseases, due to their complex biochemical composition and evolutionary conserved mechanisms of action. Natural products have evolved over millions of years to interact with biological systems, potentially resulting in more effective and safer interactions with human biology, have a lower risk of adverse effects due to their natural origin and the body's ability to metabolize and eliminate them. It can target multiple pathways and mechanisms, potentially addressing the complexity of diseases like cancer, diabetes, and neurodegenerative disorders. Phytochemicals include vinca alkaloids such as vinblastine, vincristine, and podophyllotoxin analogs. These compounds often work by controlling molecular pathways linked to cancer development and spread, immune system regulation, cell cycle arrest, apoptosis, proliferation inhibition, antioxidant status enhancement, and carcinogen deactivation. This discussion aims to explore the current understanding of the pharmacological efficacy and specific molecular targets of active compounds present in natural products. Current trends and unmet needs in the development of anticancer medications based on phytochemicals are also examined. I hope to broaden the field of phytochemical research to investigate their potential for druggability and scientific validity. There are still numerous unsolved questions about the safety and effectiveness of taking herbal medicines, even with increased funding for research into herbal medicine. Synergistic interactions between combination ingredients can reduce the required doses, potentially decreasing the risk of adverse reactions. Combinations of drugs are commonly used to treat infections, tumors, pain, and various other illnesses. However, demonstrating synergism is challenging, requiring proof that the combined effect exceeds the estimated potencies of individual drugs.

CHAPTER - 4

AIM AND OBJECTIVES

4. AIM AND OBJECTIVES

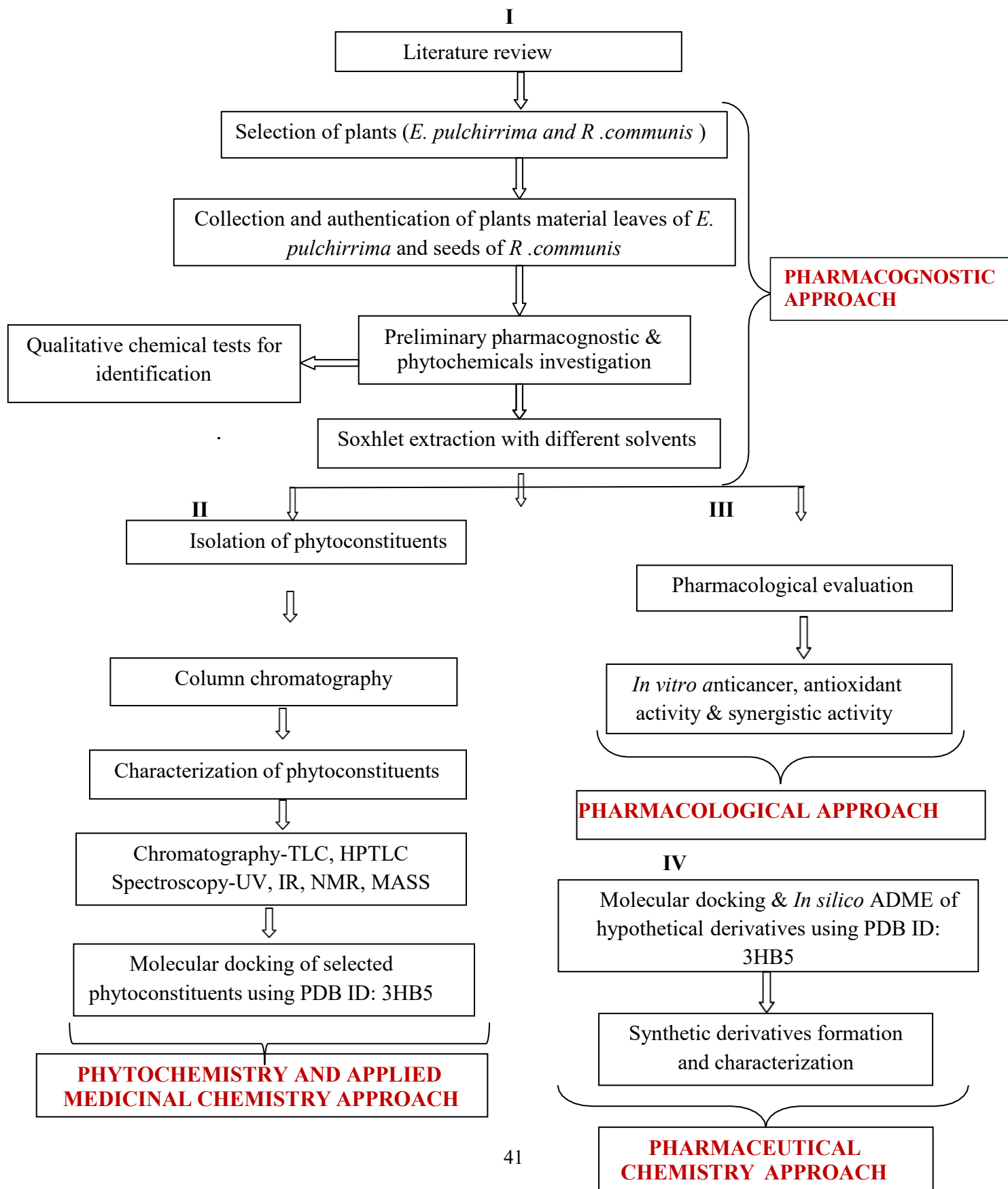
Aim

Synergistic anticancer potential of isolated phytoconstituents from *Euphorbia pulcherrima* and *Ricinus communis* (Euphorbiaceae) against breast cancer.

Objectives

- Selection, collection and authentication of plants.
- Pharmacognostic and preliminary phytochemical investigation of plants.
- Isolation and characterization of phytoconstituents.
- Screening of phytoconstituents for its *in vitro* antioxidant activity.
- Screening of phytoconstituents for its *in vitro* (breast) anticancer activity.
- Investigation of synergistic effect of isolated phytoconstituents.

PLAN OF WORK-



The proposed topic is divided into 4 phases

Phase-I : Pharmacognostic approach

Phase-II : Phytochemistry and applied medicinal chemistry approach

Phase-III : Pharmacological approach

Phase-IV: Pharmaceutical chemistry approach

Phase-I: Pharmacognostic approach

- Review of literature on *Euphorbia pulcherrima* (leaves) and *Ricinus communis* (seeds).
- Identification, procurement, and authentication of *Euphorbia pulcherrima* (leaves) and *Ricinus communis* (seeds).
- Phytochemical and physicochemical study of leaves and seeds powder.
- Extraction of *Euphorbia pulcherrima* leaves and *Ricinus communis* seeds powder using the Soxhlet extraction method.

Phase-II : Phytochemistry & applied medicinal chemistry approach

- Phytochemical study of the extract to identify potential phytoconstituents.
- Isolation of phytoconstituents, such as Beta-sitosterol from *Euphorbia pulcherrima* (leaves) and stigmasterol from *Ricinus communis* (seeds), using TLC followed by column chromatography.
- Spectroscopic and chromatographic characterization of isolated phytoconstituents using UV, IR, NMR, HPTLC, MASS, and comparison with standard markers .

Phase-III : Pharmacological approach

- Estimation of antioxidant potential of isolated phytoconstituents using various *in vitro* methods (DPPH, FRAP, etc.).

- *In vitro* anticancer activity of Beta-sitosterol and stigmasterol on cancer cell lines .
- using methods such as MTT assay and Sulforhodamine B assay.
- *In vitro* synergistic effect of isolated Beta-sitosterol and stigmasterol.

Phase-IV : Pharmaceutical chemistry approach

- The hypothetical derivatives of Beta-sitosterol and stigmasterol were screened using different acids such as adipic acid, citric acid, malonic acid, maleic anhydride, and phthalic anhydride.
- Molecular docking against PDB ID: 3HB5 and *In silico* physicochemical studies were carried out on these hypothetical derivatives (CES).
- Hydrophilic derivatives of Beta-sitosterol and stigmasterol were synthesized using polyethylene glycol (PEG) of different molecular weights.
- Melting point, solubility, and spectroscopic methods were used to characterize the produced compounds.
- *In silico* studies were conducted on the synthesized derivatives to confirm their physicochemical properties.

CHAPTER - 5

MATERIALS AND

METHODS

5. MATERIALS AND METHODS

5.1 Part-I : Pharmacognostic approach

Materials :

Instruments : Bunsen burner, Water bath , Hot air oven (Bio Techniques India), Hot plate, Heating mental (Lab hosp), Muffle furnace (Bio Technics India), Soxhlet apparatus etc.

Chemicals : Fehlings A and B solution, benedicts reagent, wagner's reagent, mayer's reagent, hager's reagent, dragendorff's reagent, α naphthol solution, sulphuric acid, hydrochloric acid, acetic acid, glacial acetic acid, ruthenium red, sudan Red III, picric acid, potassium chloride solution, sodium hydroxide , tannic acid , ninhydrin solution, phloroglucinol solution, ferric chloride solution, copper sulphate solution , chloroform, ethanol, ether, ammonia, methanol and distilled water etc.

Method :

5.1.1 Procurement and authentication of plants

The leaves of *Euphorbia pulcherrima* and seeds of *Ricinus communis* were collected from the Nature Garden Akulj. The Botanical Survey of India (BSI), Pune, verified the fully grown leaves and seeds of these plants, which are cultivated in the rural areas of the Solapur district.

5.1.2 Phytochemical evaluation of leaves and seeds powder

Qualitative chemical tests were carried out for estimation of primary and secondary metabolites, glycosides, phenol, steroids, terpenoids, tannins, amino acids, saponins, alkaloids etc., using test procedure as mentioned in the official books (139-141).

5.1.3 Physicochemical evaluation of powder of leaves and seeds

Numerous physical drug evaluations were conducted in accordance with the procedure described in the official books. These included chemical drug evaluations, loss on drying, total ash values, extractive values in alcohol, water, petroleum ether, foreign organic matter, and water soluble and acid insoluble ash values (139–141).

5.1.4 Extraction by soxhlet extractor

The solid sample is placed on a thimble-shaped filter paper, positioned into Soxhlet

extractor, and the device is assembled. The solvent is added to the solvent reservoir flask and mounted onto a heating mantle. After heating, the condensed vapors of the solvent come in contact with the sample powder, and the soluble part of the powder gets mixed with the solvent for extraction. When the solvent surface exceeds the maximum height of the siphon, the solvent containing the extract is siphoned back. The flask is repeated, extracting a portion of the material each time so that the solid material is constantly used as a pure solvent and the extracted material is concentrated in the flask. For extraction 100 g of powder was placed into the thimble and placed in the soxhlet chamber and 500 ml of selected solvents. After completed the extraction process, the solvent and extractor were placed on water bath to evaporate the solvent. The leaves and seeds powder were gradually extracted using water, ethanol, and petroleum ether. A rotary vacuum evaporator was used to dry each extract, followed by stored in the dark area until analysis (142).

Part II : Phytochemistry and applied medicinal chemistry approach

5.2.1 Thin layer chromatography

5.2.1.1 Thin layer chromatography of *Euphorbia pulcherrima*

Hexane and ethyl acetate in the ratios of 9:1, 4:1, 7:3, and 3:2 were among the solvent systems used for thin layer chromatography of the ether extract of powdered *Euphorbia pulcherrima* leaves using a standard precoated silica gel G TLC plates and 1: 1. and petroleum ether, ethyl acetate, acetonitrile in 8.2:1.8:0.1 at varying concentrations ratio to identify the solvent system which gave the greatest separation of compounds and extract's components separated by using petroleum ether : ethylacetate : acetonitrile and the slides were viewed under a UV light and R_f value was calculated.

5.2.1.2 Thin layer chromatography of *Ricinus communis*

A standard precoated silica gel G TLC plate was used to expose the petroleum ether extract of *Ricinus communis* seed powder for TLC in order to determine which solvent system resulted in the best separation of compounds with solvent systems like petroleum ether, ethyl acetate, acetonitrile in 8.2:1.8:0.1 ratios at different conc. and extract components separated by using petroleum ether : ethyl acetate : acetonitrile and the slides were viewed under a UV light & R_f value calculated.

Column chromatography :

5.2.1.3 Column chromatography of *Euphorbia pulcherrima*

A glass column (30 cm x 3 cm) filled with column silica was used to separate the ether extract of *Euphorbia pulcherrima* leaves. For this separation 4 gm. of extract was used with a solvent system consisting of petroleum ether, ethyl acetate, and acetonitrile in an 8.2:1.8:0.1 ratio. The polarity of the system was gradually increased for column chromatography. Twenty-five eluents were collected at regular intervals after Thin Layer Chromatography (TLC) analysis, and similar compounds were pooled together based on the TLC results.

5.2.1.4 Column chromatography of *Ricinus communis*

The ether extract of *Ricinus communis* seed was separated using a glass column (30 cm x 3 cm) packed with column silica. For this separation, 4 gm. of extract was used with a solvent system consisting of petroleum ether, ethyl acetate, and acetonitrile in an 8.2:1.8:0.1 ratio. The polarity of the system was gradually increased for column chromatography. Following Thin layer chromatography (TLC) analysis, twenty five eluents were collected at intermissions and analogous constituents were pooled together afterward TLC.

5.2.2 Characterization of isolated phytoconstituents

FTIR (Bruker), NMR, MASS, and UV visible spectroscopy were used to analyze the isolated phytoconstituents.

5.2.3 Quantification of isolated phytoconstituents

5.2.3.1 Quantification of Beta-sitosterol from *Euphorbia pulcherrima* extract

Quantification of isolated phytoconstituents were carried out using HPTLC. The specification for HPTLC given below in Table 5.1

Table 5.1 HPTLC specification for isolated Beta-sitosterol

Parameter	Specification for isolated Beta-sitosterol
Mobile phase	acetonitrile: petroleum ether:ethyl acetate (01:1.8:8.2)
Stationary phase	TLC silica gel 60F254
Size of plate	20 × 100
Slit dimension	6 × 0.45 mm micro
Application volume (std)	7µl
Application volume (extract)	15µl
Derivatization agent	Anisaldehyde solution
Detection wavelength (nm)	540
Scanning speed	20 mm/s

Preparation of standard: 5 mg. of standard Beta-sitosterol powder were weigh and dissolved in 1ml ethanol. Sonicated it and diluted with 5 ml with ethanol.

Preparation of sample : 5 mg. of *Euphorbia pulchirima* leaves extract were weight and dissolved in 1 ml ethanol. Sonicated it and diluted with 5 ml with ethanol

5.2.3.2 Quantification of stigmasterol from *Ricinus communis* seeds extract

Quantification of isolated phytoconstituents were carried out using HPTLC the specification for HPTLC were given in Table 5.2.

Table. 5.2 HPTLC specification for isolated stigmasterol

Parameter	Specification for isolated stigmasterol
Mobile phase	acetonitrile: petroleum ether: ethyl acetate (0.1 :1.8: 8.2)
Stationary phase	TLC silica gel 60F254

Size of plate	20 × 100
Slit dimension	6 × 0.45 mm micro
Application volume (std.)	5µl
Application volume (extract)	10µl
Derivatization agent	Anisaldehyde solution
Detection wavelength (nm)	540
Scanning speed	20 mm/s

Preparation of Standard : 5 mg. of standard stigmasterol powder were weighed and dissolved in 1ml ethanol. Sonicated it and diluted with 5 ml with ethanol.

Preparation of Sample : 5 mg. of *Ricinus communis* seeds extract were weighed and dissolved in 1 ml ethanol. Sonicated it and diluted with 5 ml with ethanol.

5.2.4 Molecular docking

5.2.4.1 Protein structure retrieval and preparation :

With PDB ID 3HB5, the x-ray crystal structure of the estradiol 17 beta-dehydrogenase 1 enzyme was accessible through the RCSB PDB database at 2 Å resolution (143). (Figure 5.1) After downloading the structure in pdb file format, we performed *in silico* protein structure preparation using protein preparation wizard (144). of Schrodinger software. The process included hydrogenation, adjustment of protonation states, side-chain sampling, and energy minimization. The prepared structure was then validated for quality, and the final output was saved for subsequent molecular docking and simulation analyses.

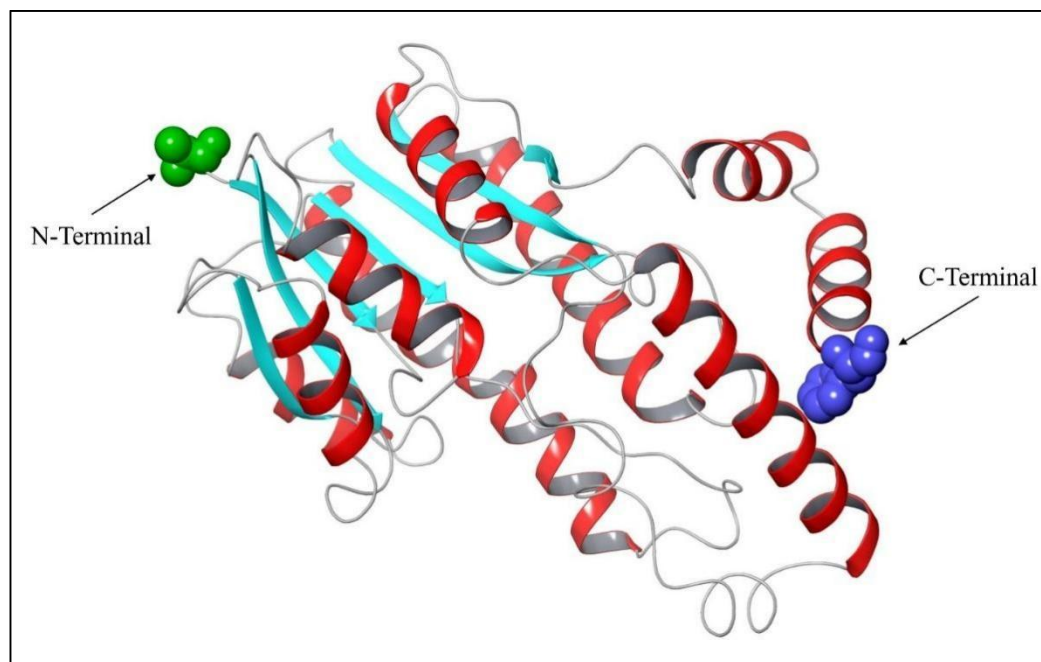


Figure 5.1 The 3D structure of the Estradiol 17- beta-dehydrogenase- 1 - Enzyme with PDB ID:3HB5

5.2.4.2 Ligand structure retrieval and preparation

The 2D structures of *Euphorbia pulcherrima* and *Ricinus communis* phytoconstituents, including rutin, kaempferol-3-O-Glucoside, stigmasterol, beta-sitosterol, and germanicol were received from the PubChem database. To convert these 2D structures into 3D structures, the Open Babel program was employed (145). Subsequently, the obtained 3D structures underwent energy minimization using the Maestro software, employing the OPLS-2005 force field (146). This process aimed to achieve energetically minimized structures for further utilization in molecular docking studies.

5.2.4.3 Binding site definition and molecular docking study

Binding cavity of the Estradiol 17-beta-Dehydrogenase- 1- Enzyme is defined using FlexX software (147-148). As, the crystal structure of 17-beta-Dehydrogenase 1 enzyme is available in complex with the inhibitor i.e., 17beta-HSD type 1: a lead compound, so we have defined binding site by taking this compound as reference for binding site information using FlexX software. In FlexX when we prompt co-crystal ligand for reference ligand to define the binding site it automatically selects the binding site residue which are involved within the 6.5 position of the co-crystal ligand. For 17-beta-dehydrogenase 1 enzyme we have selected amino acid residues viz. Ser12, Gly13, Gly15, Gly92, Lue93, Thr140, Tyr155, Lys159, Cys185, Val188 and Phe192 etc. (Figure 5.2).

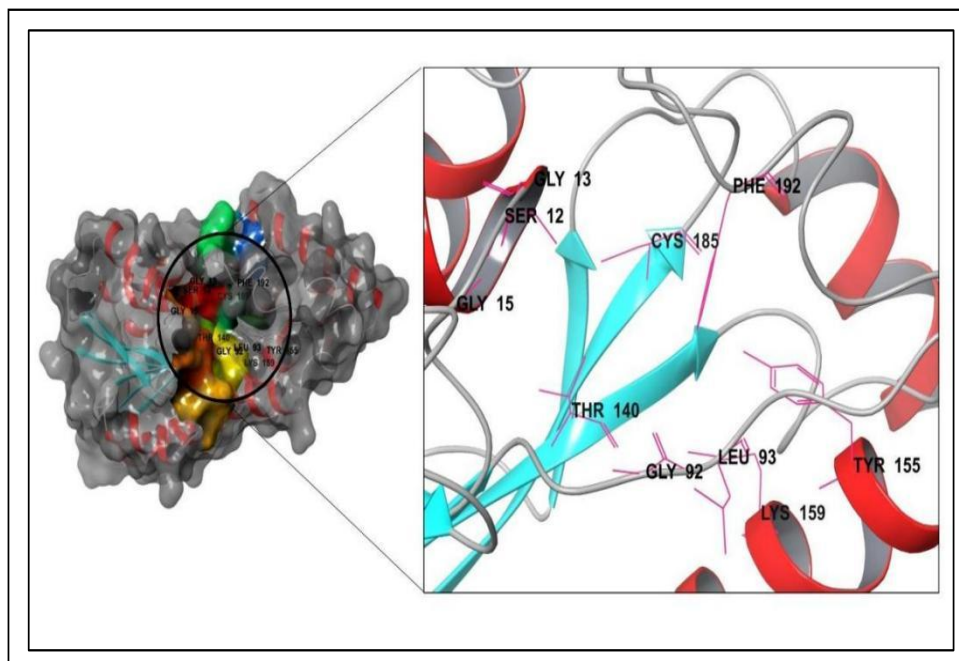


Figure 5.2 The selected binding site residues of Estradiol 17-beta-dehydrogenase 1 Enzyme

After defining the binding site for estradiol 17-beta-dehydrogenase 1 enzyme, the prepared and energetically minimized ligand were subjected for molecular docking and binding affinity prediction using FlexX and Hyde software, respectively(149). After

the docking and binding affinity prediction we have visualized the intermolecular interactions and subsequently performed the molecular dynamic simulation studies to realise the binding stability of docked ligands within the binding cavity if the enzyme (150).

5.2.4.4 Molecular dynamic simulation

In this investigation, molecular dynamics simulations were conducted using the Desmond software (151). To explore the dynamic behavior of the complex system involving the Estradiol 17-beta-Dehydrogenase 1 enzyme and five phytoconstituents like rutin, kaempferol-3-O-Glucoside, tigmasterol, beta-sitosterol, and germanicol. The simulations were executed under physiological conditions at 300K temperature, 1.01325 bar pressure, and within a cubic box of 10 Å. To accurately capture intermolecular interactions, the OPLS-2005 force field was employed, and solvation was achieved using TIP3P water molecules. The system underwent an initial energy minimization to rectify steric clashes, followed by a gradual release of constraints for system relaxation. Equilibration stages (NVT and NPT) were implemented to adjust temperature and pressure through thermostats and barostats. Subsequently, production MD simulations were performed for 100 ns, with energy recorded at 1.2 ps intervals, and trajectories saved every 100 ps (152-154). The simulations, conducted independently five times, aimed to scrutinize the stability and dynamics of the complex formed between the Estradiol 17- beta-Dehydrogenase -1- enzyme and the five phytoconstituents. Analysis of resulting trajectories utilized Desmond's tools, focusing on parameters such as RMSD and RMSF to offer insights into the system's behavior. This comprehensive approach contributes to understanding of the molecular dynamics exhibited by the studied complex.

5.2.5. Molecular docking study using autodock vina

5.2.5.1 Selection of protein

The protein 3BH5, was selected depends upon mechanism of action. It is a novel inhibitor of 17β-hydroxysteroid dehydrogenase type 1 (17β-HSD1), which plays a important role in regulating the growth of breast cancer cells (BCC). The 17β-HSD1

enzyme promotes BCC growth through its dual action on estradiol synthesis and dihydrotestosterone (DHT) production. Inhibition of 17 β -HSD1 by 3BH5 has been shown to exert an anti-proliferative effect.

5.2.5.2 Selection of ligand

Ligand selected from *Euphorbia pulcherrima* were Beta-sitosterol (CID-22284), Germanicol acetate (CID-14167342), Germanicol (CID-122857), Rutin (CID-5280805), Kaempferol- 3-O-glucoside (CID-5282102) while ligand selected from *Ricinus communis* were Ricinine (CID-10666), Stigmasterol (CID-5280794), Probucol (CID-4912) and Ricinolic acid (CID643684).

5.2.5.3 Molecular docking

The chosen ligands were molecularly docked against the protein target (PDB ID: 3BH5) using Open Babel, Biovia Discovery Studio 2022, and AutoDock Vina 1.1.2. The RCSB Protein Data Bank (<https://www.rcsb.org>) provided the protein structure, while PubChem (<https://pubchem.ncbi.nlm.nih.gov>) provided the ligand structures.

5.3 Part -III: Pharmacological approach

5.3.1 In vitro antioxidant activity

5.3.1.1 In vitro antioxidant activity of extracts

For the evaluation of *in vivo* antioxidant properties of petroleum ether, aqueous, and ethanolic extracts of *Euphorbia pulcherrima* and *Ricinus communis*, various methods were employed, such as ferric reducing antioxidant property (FRAP), DPPH (2,2-diphenyl-1-picrylhydrazyl) assay, total antioxidant capacity (TAC), and total phenolic content (TPC) .

5.3.1.1.1 DPPH radical scavenging activity

To assess *Euphorbia pulcherrima* capacity to scavenge free radicals, The optical density (OD) at 517 meters was measured using a device known as a Shimadzu UV Mini-1240 UV Vis spectrophotometer. The blank was methanol (155).

5.3.1.1.2 Ferric reducing antioxidant power (FRAP)

The following method was used to calculate the ferric reducing antioxidant power (FRAP) 500 μ L of the sample and 120 μ L of phosphate buffer solutin (pH 7) were

combined in a 1000 mL volumetric flask. The phosphate buffer was made by combining 61.5 mL of 1 M dibasic potassium phosphate, 38.1 mL of 1M monobasic potassium phosphate, and water. After homogenization, 220 μ L of 1% potassium ferrocyanide was added and it was 20 minutes incubated at 50°C. After that, 10 μ L of 0.1% ferric chloride, 12 μ L of 10% trichloroacetic acid, and distilled water were added. Measured the absorbance at 734 nm. using gallic acid as the standard (156).

5.3.1.1.3 Total phenolic content assay

In this experiment, 0.2 milliliters of the sample and 0.2 milliliters of a 10% Folin-Ciocalteu solution were mixed together, and kept in a dark setting for few minutes. Add 1 mL of a 15% sodium carbonate solution, and the agitated for four to five minutes. After that, incubated for 30 minutes at ambient temperature, out of direct sunlight. At 760 nm, the absorbance was determined with a UV visible spectrophotometer. A total of three duplicate readings were obtained. Using an equation established from a reference curve created with varying amounts of gallic acid, the total phenolic content of *Euphorbia pulcherrima* was represented as gallic acid equivalent (GAE) (157).

5.3.1.1.4 Total anti-oxidant capacity

In this process, 100 mg of the sample was combined with 3 mL of a reagent solution containing 4 mM ammonium molybdate, 28 mM sodium phosphate, and 0.6 M H₂SO₄ and incubated at 95°C for 90 minutes. The absorbance was measured at 695 nm. The results were expressed as milligrams per gram (mg/g) of total antioxidant capacity, with ascorbic acid (0.1 mg/mL in distilled water) serving as the reference standard (158).

5.3.1.1.5 Activity of superoxide scavenging

0.6 mL of the extract, 0.2 mL of NBT (1 mg/mL solution in DMSO), and 2 mL of alkaline DMSO (5 mM NaOH in 1 mL DMSO and 0.1 mL H₂O) made up the reaction mixture for this method. The total volume of the reaction was 2.8 mL. At 560 nm, the absorbance was determined with a spectrophotometer. A colorful diformazan chemical was the result of the reaction. Pure DMSO made up the blank (159).

5.3.1.2 *In vitro* antioxidant activity of isolated phytoconstituents

5.3.1.2.1 DPPH assay of Beta-sitosterol and stigmasterol

100 µL of isolated phytoconstituents sample solution (1 mg/mL) and 100 µL of a 0.1% methanolic DPPH solution were applied to a microtiter plate. The plate was then incubated for 30 minutes in the dark, the samples discoloration was noted a shift from purple to yellow or pale pink, respectively, indicated robust and weak antioxidant activity. An ELISA plate reader was used to quantify the absorbance at 490 nm (160).

5.3.1.2.2 SOD activity of Beta-sitosterol and stigmasterol

The reaction mixture for SOD activity, which included 0.6 ml of the isolated phytoconstituensts sample solution, 0.2 ml of NBT (1 mg/ml of solution in DMSO), and the DMSO standard, was measured for absorbance at 560 nm using a spectrophotometer. To reach a final volume of 2.8 ml, 2 ml of alkaline DMSO was added. For calculating radical scavenging activity following formula used (161).

$$\% \text{ Scavenging} = (A \text{ control} - A \text{ sample}) / A \text{ control} \times 100$$

5.3.2 *In-vitro* anticancer cell line study of isolated phytoconstituents

5.3.2.1 MTT assay of isolated pytoconstituents

The MDA-MB-231 and MCF-7 cell lines were employed to screen for anticancer potential *in vitro*. Cell viability was assessed using the MTT test incubated for 24 hours at 37°C in culture media with a cell concentration of 1×10^4 cells/ml. Tissue culture grade microplates with 96 wells were seeded with 70 µl of 10^4 cells per well in 100 µl of culture media and 100 µl of Beta-sitosterol, stigmasterol, and their combination compounds (6.10, 12.5, 25, 50, and 100 µg/ml) in each microplate. Control wells were used to cultivate the cell line and DMSO (0.2% in PBS). To find out the percentage of living cells and the survival rate of control cells following the maintenance of culture and controls. Cell cultures were cultured for 24 hours at 37°C with 5% CO₂ in a Thermo Scientific BB150 CO₂ incubator. After the incubation period, the medium was fully withdrawn and add 20 µl of MTT reagent (5 mg/min PBS). For four hours, the cell was cultured at 37°C in a CO₂ incubator. To see if formazan crystals had formed, the wells were inspected under a microscope. Only living cells were capable to change the

yellowish MTT into a dark colored formazan . After adding 200µl of DMSO and waiting 10 minutes, incubate at 37°C (covered with aluminum foil). Three duplicate samples were examined using an Elisa microplate reader to measure absorbance at 570 nm (162-163).

5.3.2.2 SRB assay of isolated phytoconstituents

Cell lines MCF-7 and MDA-MB-231 were selected for assessing their potential as *in vitro* anticancer agents. The SRB assay was used to evaluate the cells cytotoxicity. After counting the cells, the cell suspension concentration was changed. In a 96-well microplate, add 100 µl of cell suspension to each well using repeated dilutions, held for a whole day in a CO₂ incubator with 5% CO₂. Remove the old media and add 100 µl of fresh media to each well, including the background measurement wells, if a media change is necessary. 10 µl of medium containing various (6.25, 12.5, 25, 50, 100 µg/ml) of the Beta-sitosterol and stigmasterol and its combination compounds to each well. Incubated set period of 24 hrs in a CO₂ incubator and then added 10 µl solution of SRB to each well in a 96 well microplate. Kept in a CO₂ incubator 5% CO₂ for 1 to 4 hours. Measured the absorbance with the help of microplate reader at 450 nm (164).

5.3.2.3 Bliss independence for synergism

It is common practice to employ the bliss independence model for the analysis of medication combination data. When demonstrating antagonism, additivity, and synergy in medication combinations (165).

Bliss formula

$$CI = EA+EB-EAEB/EAB$$

$$EAB = EA+EB (1-EA) ,$$

Where,

EA-Effect of Beta-sitosterol

EB-Effect of stigmasterol

CI-Combination index

While the Synergistic effect indicated as $CI < 1$, antagonism as $CI > 1$ and additive effect as $CI = 1$ (165).

5.4 Part -IV: Pharmaceutical chemistry approach

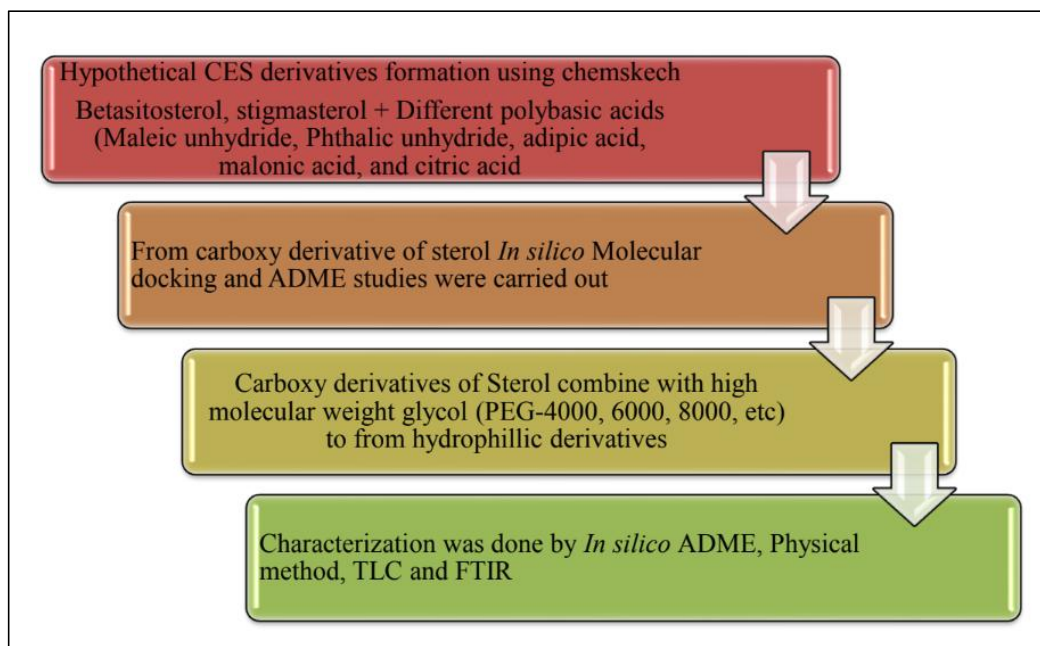


Figure 5.3 Synthetic scheme for Beta-sitosterol and stigmasterol derivatives

5.4.1 Molecular docking study of CES derivatives of Beta-sitosterol and stigmasterol

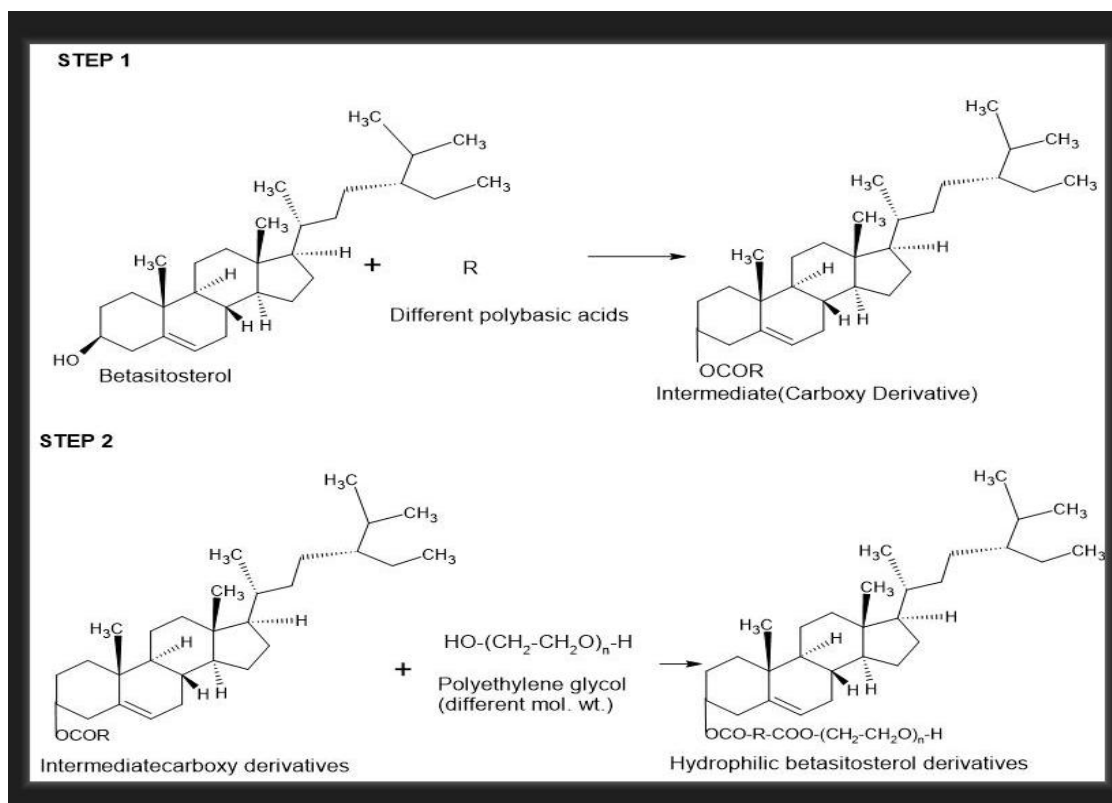
The *in silico* pharmacological potential of synthetic derivatives was screened using AutoDock Vina, Biovia Discovery Studio, and Open Babel software. Five hypothetical derivatives each of Beta-sitosterol and stigmasterol were synthesized using ChemSketch. Various acids, including maleic anhydride, phthalic anhydride, adipic acid, citric acid, and malonic acid, were incorporated into Beta-sitosterol and stigmasterol. The binding affinities of these synthetic derivatives were evaluated against the 3BH5 protein. The derivatives with the highest binding affinity, namely the CES derivatives of Beta-sitosterol and stigmasterol, were selected for further synthetic derivative formation.

5.4.2 Synthesis of CES by using maleic anhydride with Beta-sitosterol and stigmasterol

Step I : Preparation of carboxy ethylene sterol of Beta-sitoste rol and stigmasterol

50 gm of Beta-sitosterol / stigmasterol and 24.1 g maleic anhydride were dissolved in 250 ml of DCE (Dichloroethane). Then mixture was heated for 2 hrs. at 80°C after addition of 16.7 ml triethanolamine. After conformation of reaction completion via TLC the solvent was evaporated from reaction mixture. The collected solid residue was dissolved in 500 ml ethanol. Add 11 ml of concentrated HCL dropwise. Then add 500 ml water and filter , white precipitate was collected and dried . The recrystallization of was carried by using hexane. And the characterization were done by using spectroscopic methods.

I) Mechanism reaction between sterol and acid



The reaction mechanism between an acid anhydride and a sterol is a nucleophilic acyl substitution, also known as an esterification or acylation reaction. The sterol's hydroxyl (-OH) group acts as a nucleophile, attacking one of the anhydride's electrophilic carbonyl groups. This results in the formation of a sterol ester and a carboxylic acid.

Mechanism steps :

- 1) Nucleophilic attack :** The oxygen atom of the sterol's hydroxyl group, which has lone pairs of electrons, attacks a carbonyl carbon of the anhydride. This breaks the pi (π) bond of the carbonyl, pushing the electrons onto the carbonyl oxygen and forming a tetrahedral intermediate.
- 2) Elimination :** The negatively charged oxygen of the tetrahedral intermediate reforms the carbon oxygen double bond. This eliminates a carboxylate ion RCOO^- as a leaving group, which is a resonance stabilized carboxylic acid.
- 3) Proton transfer :** The resulting protonated sterol ester is deprotonated, while the carboxylate leaving group is protonated to form a carboxylic acid. If a base like pyridine is used as a solvent, it can perform the deprotonation.
- 4) Formation of products :** The final products are the sterol ester and the carboxylic acid.

5.4.3. *In silico* ADME of CES derivatives

The physicochemical and pharmacokinetic parameters of CES derivatives were estimated using SwissADME software. (*In silico* studies)

5.4.4. Characterization of CES derivative of Beta-sitosterol and stigmasterol

Characterization of CES derivative of Beta-sitosterol and stigmasterol was performed using TLC, FTIR, and MASS spectroscopy (Bruker).

5.4.5 Hydrophilic derivatives formation of CES Beta-sitosterol and CES stigmasterol

II) Mechanism reaction between carboxy ethylene sterol and polyethylene glycol :-

The reaction between carboxy ethylene sterol and polyethylene glycol would involve an

esterification reaction between the carboxylic acid group of the sterol and the hydroxyl end groups of the polyethylene glycol (PEG). The specific mechanism depends on the reaction conditions, such as the use of catalysts or activating agents.

Reagents : A common combination is dicyclohexylcarbodiimide (DCC) and 4-dimethylaminopyridine (DMAP)

Mechanism steps :

- 1) The coupling reagent activates the carboxylic acid group of the sterol, creating a more reactive intermediate.
- 2) The hydroxyl group of the PEG performs a nucleophilic attack on the activated carboxylic acid.
- 3) The leaving group from the activated sterol and a proton from the PEG's hydroxyl group are released.
- 4) This reaction forms a stable ester linkage between the sterol and the PEG molecule. (166).

Step II: Preparation of hydrophilic derivatives of Beta-sitosterol and stigmasterol

The reaction mixture were prepared 15.0 gm of Polyethylene glycol (PEG) of molecular weight 4000, 6000, 8000 were mixed with 2.7 gm of DCC (1,3-dicyclohexyl carbodiimide) and add 0.1 gm DMAP (4-dimethylaminopyridine) were dissolved in 100 mL of methylene chloride at room temperature. Then 7.7 gm of intermediate (step - I end product) dissolved in 25ml methylene chloride. This mixture were added drop wise into reaction mixture at 30°C. Filter and evaporate the filtrate and recrystallize using isopropyl alcohol (166).

5.4.6. Characterization of hydrophilic derivatives of Beta-sitosterol and stigmasterol

Synthesized hydrophilic derivatives by using PEG 4000, 6000, 8000 characterized by melting point, solubility, and FTIR.

5.4.7. *In silico* physicochemical study of hydrophilic derivatives

The physicochemical parameters of the hydrophilic derivatives of Beta-sitosterol and stigmasterol were estimated using SwissADME (*In silico* studies).

Above all advanced techniques used that researchers can accelerate discovery and development of new therapeutic agents, improve understanding of biological systems, and ultimately develop more effective treatments for various diseases. These advanced techniques are used in various fields, particularly in pharmaceutical research, cancer research, and biomedical sciences. Technique likes , chromatography helps separate and purify complex mixtures of compounds, allowing researchers to isolate and analyze specific molecules. Chromatography enables the quantification of specific compounds in a mixture, which is crucial for pharmaceutical development and quality control and identification of compounds. Assay can be adapted for high throughput screening, enabling rapid testing of large numbers of compounds. Bliss model helps researchers identify optimal combination therapies and predict potential interactions between compounds. By leveraging various spectral techniques, researchers can gain valuable insights into the structure, properties, and behavior of molecules, ultimately driving advances in fields like chemistry, biology, and materials science. Docking software facilitates rational drug design by predicting optimal binding modes and interactions between compounds and protein targets. Techniques for combining synthetic drugs with chemical compounds to create a new hybrid molecule with improved efficacy and reduced side effects. The combination of synthetic drugs with other compounds can affect their absorption, distribution, metabolism, and excretion (ADME) properties. So by exploring these techniques and approaches, researchers can develop more effective and targeted therapies for various diseases.

CHAPTER - 6

RESULT AND DISCUSSION

6. RESULT AND DISCUSSION

6.1 Part I: Pharmacognostic approach

6.1.1 Authentication of leaves and seeds

Leaves of *Euphorbia pulcherrima* and seeds of *Ricinus communis* were authenticated at the Botanical Survey of India (BSI), No.BSI/WRC/Iden.Cer./2022/0802220002464 No.BSI/WRC/ Iden. Cer/ 2022/2901220010676 (2) Pune. Their certificates were attached in annexure I and II respectively.

6.1.2 Phytochemical evaluation of leaves and seeds

6.1.2.1 Preliminary phytochemical analysis of *Euphorbia pulcherrima* leaves powder in different extracts.

Ethanol, water, and petroleum ether extracts of *Euphorbia pulcherrima* leaves powder were used for phytochemical analysis. Different extracts found various secondary metabolites are listed in Table 6.1. The petroleum ether and ethanolic extract showed maximum presence of phytochemicals, while in aqueous extract only showed presence of saponins, amino acids, and glycosides .

Table 6.1 Preliminary phytochemical analysis of *Euphorbia pulcherrima* leaves powder in different extracts

Phytochemicals	Ethanol extract	Petroleum ether extract	Aqueous extract
Steroids	+	+	-
Tannins and phenol	+	+	-
Terpenoids	+	+	-
Amino acids	+	+	+
Saponin	+	+	+
Glycosides	+	+	+
Flavonoids	+	+	-
Alkaloids	+	+	-

(+ Presence & - Absence)

6.1.2.2 Preliminary phytochemical analysis of *Ricinus communis* seeds powder in different extracts.

Ethanol, water, and petroleum ether extracts of *Ricinus communis* seeds powder were used for phytochemical analysis. Different extracts found various secondary metabolites are listed in Table 6.2. The petroleum ether and ethanolic extract showed maximum presence of phytochemicals, while in aqueous extract only showed presence of saponins, amino acids, and glycosides. Using the chemical tests listed in official books, the phytochemical screening of seed powder was completed.

Table 6.2 Preliminary phytochemical analysis of *Ricinus communis* seeds powder in different extracts.

Phytochemicals	Ethanol extract	Petroleum ether extract	Aqueous extract
Steroids	+	+	-
Amino acids	+	+	+
Terpenoids	+	+	-
Flavonoids	+	+	-
Alkaloids	+	+	-
Phenol and tannins	+	+	-
Saponins	+	+	+
Glycosides	+	+	+

(+ presence & - absence)

6.1.3 Physical evaluation of leaves and seeds powder

The physical evaluations of powder, *Euphorbia pulcherrima* leaves and *Ricinus communis* seed were carried out as per the Ayurvedic pharmacopoeia and finding were within limit.

Table 6.3 Physical evaluation of *Euphorbia pulcherrima* leaves powder

Parameters	Mean %	Standard deviation	Mean±SD
Foreign matter	0.0	0.0	0.00
Total ash value	3	0.5	3.00 ± 0.5

Acid in-soluble ash value	1	0.50	1.00 ± 0.50
Water soluble ash value	0.9	0.10	0.90 ± 0.10
Loss on drying	0.27	0.5	0.27 ± 0.5

Table 6.4 Physical evaluation of *Ricinus communis* seeds powder

Parameters	Mean	Standard deviation	Mean \pm SD
Foreign matter	00	00	00
Total ash value	7	0.5	7.00 ± 0.5
Acid in-soluble ash value	6	0.55	6.00 ± 0.55
Water soluble ash value	2	0.20	2.00 ± 0.20
Loss on drying	1	0.2	1.0 ± 0.2

Table 6.5 Extractive value determination of *Euphorbia pulcherrima* leaves powder

Extractive value	Mean %	Standard deviation	Mean \pm SD
Alcohol soluble	4	0.20	4.0 ± 0.20
Water soluble	6.9	0.11	6.9 ± 0.11
Petroleum ether soluble	4.4	0.11	4.4 ± 0.69

Table 6.6 Extractive value determination of *Ricinus communis* seeds powder

Extractive value	Mean %	Standard deviation	Mean \pm SD
Alcohol soluble	2.4	0.20	2.4 ± 0.20
Water soluble	8.0	0.20	8.0 ± 0.20
Petroleum ether soluble	3.8	0.87	3.8 ± 0.87

6.1.4 Extraction by soxhlet extractor

A soxhlet extractor was used to progressively extract 100 g of *Euphorbia pulcherrima* leaves powder using ethanol, water, and petroleum ether. The highest extract yield was obtained using petroleum ether with a percentage yield of 5.3%. The same procedure was followed for the extraction of seeds powder of *Ricinus communis* resulting in a percentage yield of 4% .

6.2 Part -II: Phytochemistry and applied medicinal chemistry approach

6.2.1 Thin Layer Chromatography

6.2.1.1 Thin Layer Chromatography of *Euphorbia Pulcherrima* leaves powder (ether extract)

Standard precoated silica gel G TLC plates were used to perform thin layer chromatography (TLC) on the petroleum ether extract of *Euphorbia pulcherrima* leaves. Petroleum ether, ethyl acetate, and acetonitrile at a ratio of 8.2:1.8:0.1, as well as hexane and ethyl acetate in ratios of 9:1, 4:1, 7:3, 3:2, and 1:1, were used to separate the extract's constituent parts. The plates were then examined under a UV lamp. Accordingly, the R_f values were calculated.

6.2.1.2 Thin Layer Chromatography of *Ricinus communis* seeds powder (ether extract)

Using a conventional precoated silica gel G TLC plate, the petroleum ether extract of *Ricinus communis* seed powder was exposed for thin layer chromatography. Petroleum ether, ethyl acetate, and acetonitrile in 8.2:1.8:0.1 ratios were among the solvent systems used to separate the extract's constituent parts. The slides were examined under a UV lamp, and the R_f value were calculated.

6.2.2 Column chromatography

6.2.2.1 Column chromatography of *Euphorbia Pulcherrima* leaves powder (ether extract)

To separate the ether extract of *Euphorbia pulcherrima* leaves, a glass column (30 cm x 3 cm) filled with column silica was used. Petroleum ether, ethyl acetate, and acetonitrile in an 8.2:1.8:0 solvent system were combined with 4 grams of ether extract for this separation. The polarity of the mixture was then gradually increased in order to fit it for column chromatography. Following thin-layer chromatography (TLC), At regular intervals, 25 eluents were collected, and following TLC examination, similar compounds were pooled.

6.2.2.2 Column chromatography of *Ricinus communis* seeds powder ether extract

The ether extract of *Ricinus communis* seeds were separated using a glass column (30 cm x 3 cm) packed with column silica. For this purpose, 4 gm of extract were used with a solvent system consisting of petroleum ether, ethyl acetate, and acetonitrile in an 8.2:1.8:0.1 ratio. This system were then adapted for column chromatography by gradually increasing the polarity. Following thin layer chromatography (TLC), At regular intervals, 25 eluents were collected, and following TLC examination, similar compounds were pooled.

6.2.3 Characterization of isolated phytoconstituents

The isolated Beta-sitosterol and stigmasterol were compared with standard Beta-sitosterol and stigmasterol. The findings suggested that the isolated compounds showed the significant spectroscopic characteristics as compared with standard compounds.

6.2.3.1 Characterization of *Euphorbia pulchirima*

UV visible spectroscopy, FTIR (Bruker), NMR and MASS spectroscopy.

UV visible spectroscopy of Beta - sitosterol

The isolated Beta-sitosterol showed an absorption maximum at a wavelength of 208 nm, which is within the expected range for standard Beta-sitosterol (200-210 nm). A possible wavelength shift of 2 nm from the standard value may be due to the presence of traces of the mobile phase.

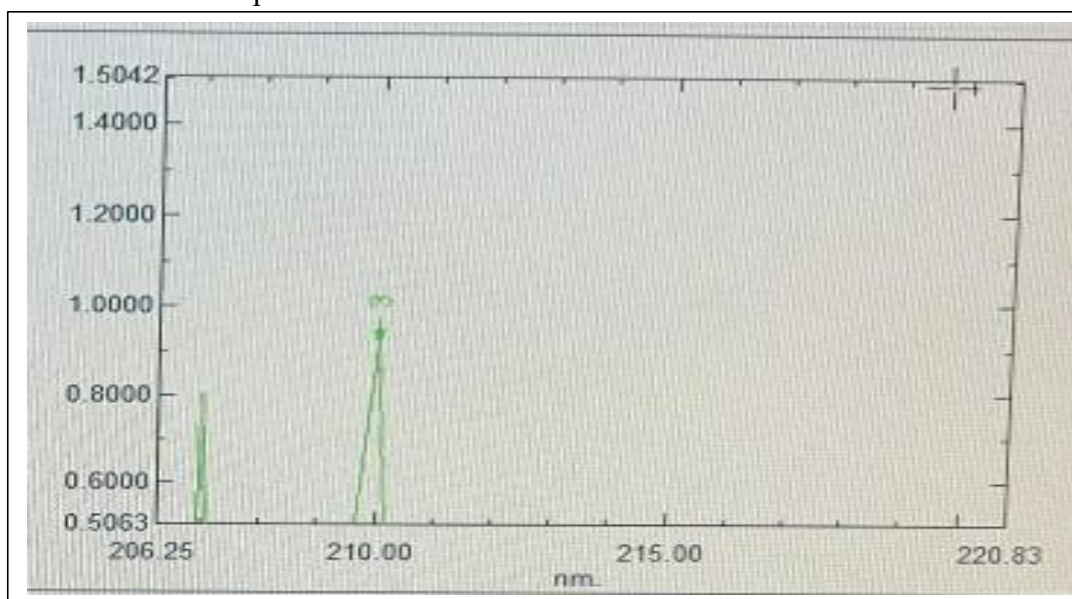


Figure 6.1 UV visible spectrum of standard Beta-sitosterol

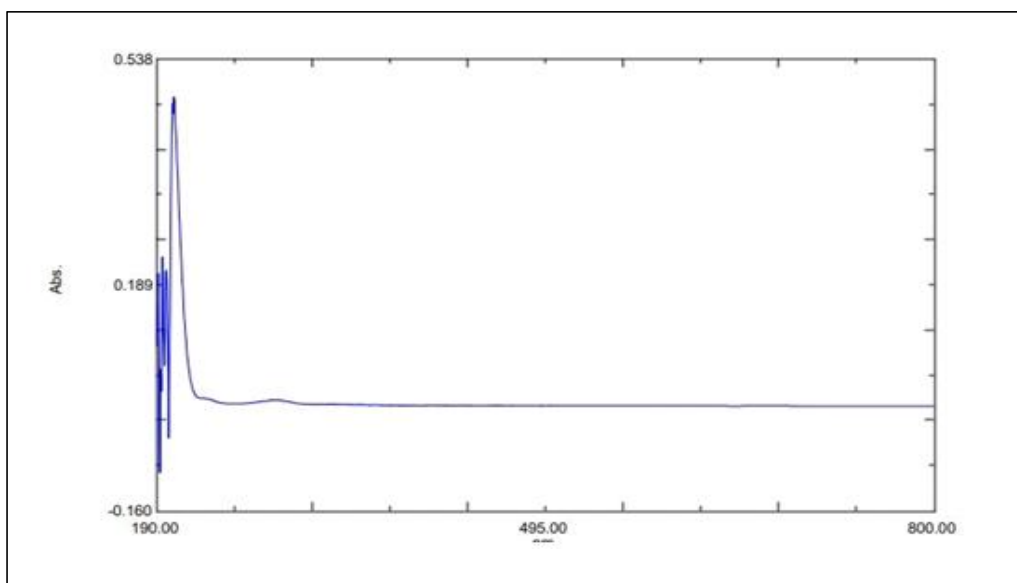


Figure 6.2 UV visible Spectrum of isolated Beta-sitosterol

FTIR Spectrum of Beta - sitosterol

Chemical bonds in molecules are detected by FTIR, with a scanning range of 4000–400cm⁻¹.

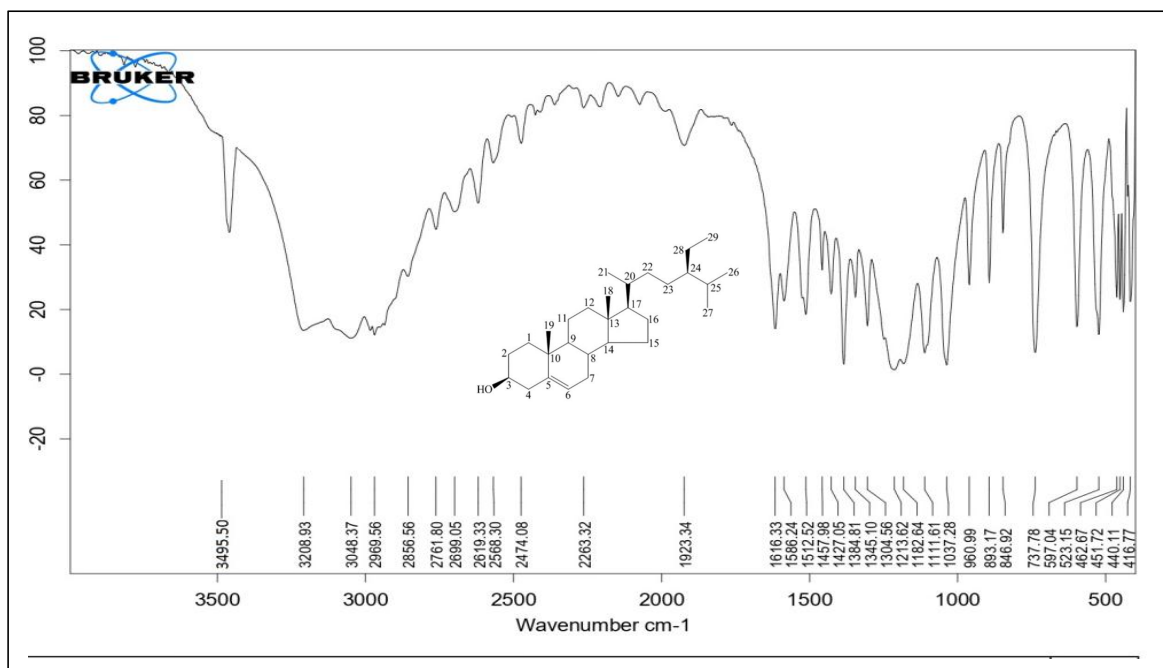


Figure 6.3 FTIR spectrum of standard Beta-sitosterol

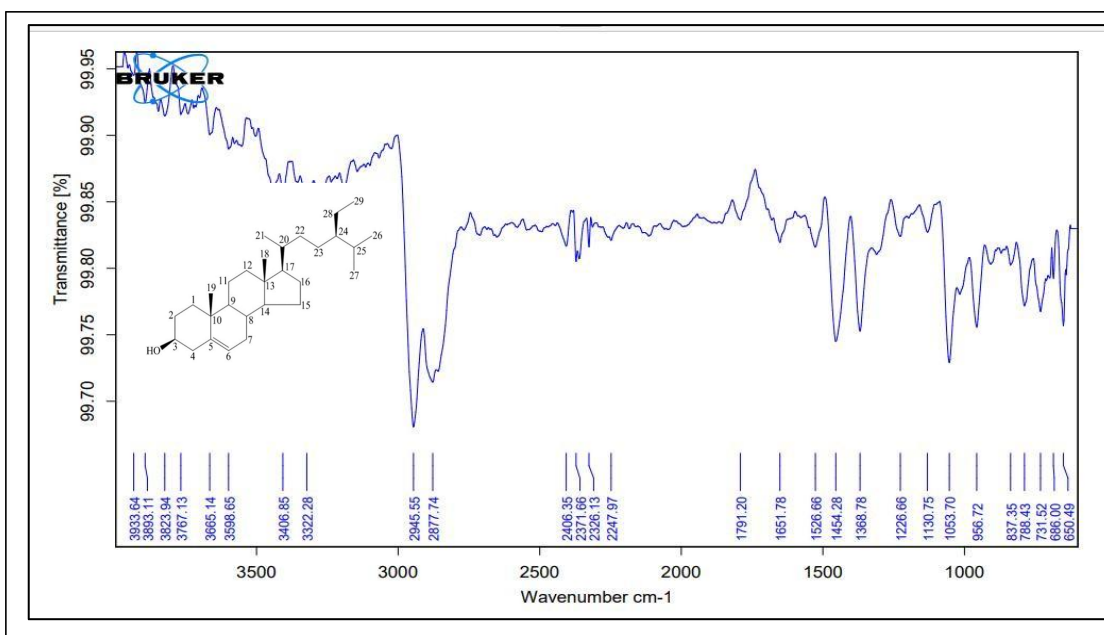


Figure 6.4 FTIR spectrum of isolated Beta-sitosterol

Table 6.7 FTIR interpretation of Beta-sitosterol

Standard Beta-sitosterol Bands (cm ⁻¹)	Isolated Beta-sitosterol Bands (cm ⁻¹)	Std.Value (cm ⁻¹)	Interpretation
3495.50	3406.85, 3598.65, 3665.14	3400-3700	Stretching vibration for OH
2856.56	2877.74	2850-2975	Stretching vibration for CH alkane
2969.56	2945.55	3020-3100	Stretching vibration for CH alkene
1616.33	1651.78	1640-1680	Stretching vibration for C=C
1457.98	1454.28	1395-1440	Bending vibration for OH
1384.81	1368.78	1365-1372	Bending vibration for isopropyl
1037.28, 1111.61, 1213.62	1053.70	1000-1300	Bending vibration for C-O of alcohol
1384.	1368.78	1375- 1450	Bending vibration for CH ₃

NMR Spectrum

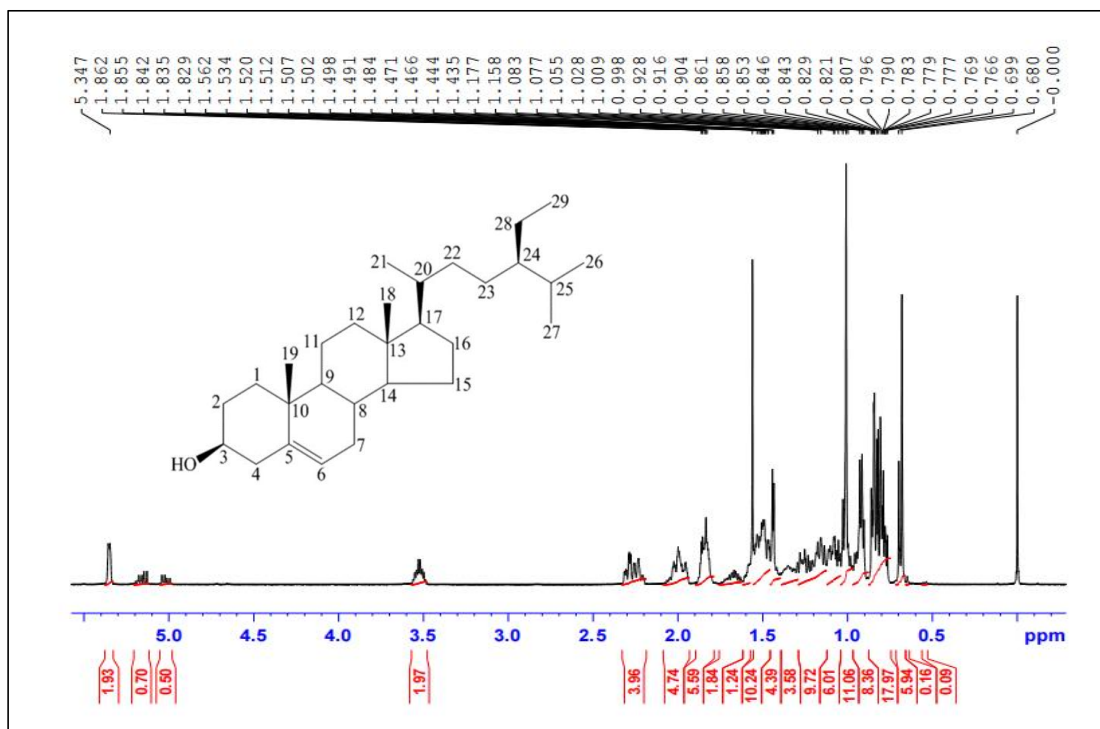


Figure 6.5 ¹H NMR of standard Beta-sitosterol

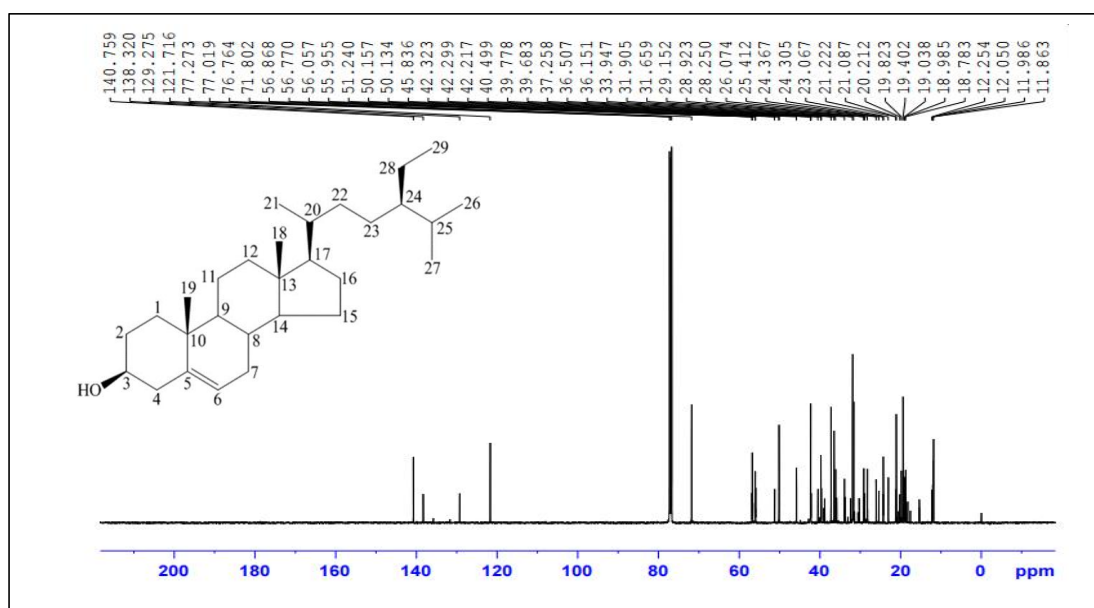


Figure 6.6 ¹³C NMR of the standard Beta-sitosterol

NMR Interpretation of the standard Beta-sitosterol

¹H NMR (400 MHz, CDCl₃, δ, ppm) : 5.34 (dd, *J* = 5.2 Hz, 1H, CH=CH), 3.53 (m,

¹H, O-CH), 2.17-2.33 (m, 4H, Allylic 2-CH₂), 1.94-2.07 (m, 8H, 4-CH₂), 1.75-1.82 (m, 2H), 1.56-1.65 (m, 14H), 0.8-1.34 (m, 20H).

¹³C-NMR (100 MHz, CDCl₃, δ [ppm]): 72 (C₁), 32 (C₂), 36.15 (C₃), 37.25 (C₄), 51.24 (C₅), 32 (C₆), 57 (C₇), 40.4 (C₈), 56.05 (C₉), 29.15 (C₁₀), 24.30 (C₁₁), 141 (C₁₂), 122 (C₁₃), 34 (C₁₄), 21.08 (C₁₅), 42.21 (C₁₆), 19.4 (C₁₇), 12.2 (C₁₈), 18.7 (C₁₉), 34 (C₂₀), 26 (C₂₁), 46 (C₂₂), 29,15 (C₂₃), 19.04 (C₂₄), 19 (C₂₅), 20.21 (C₂₆), 19.8 (C₂₇), 23.06 (C₂₈), 12.05 (C₂₉).

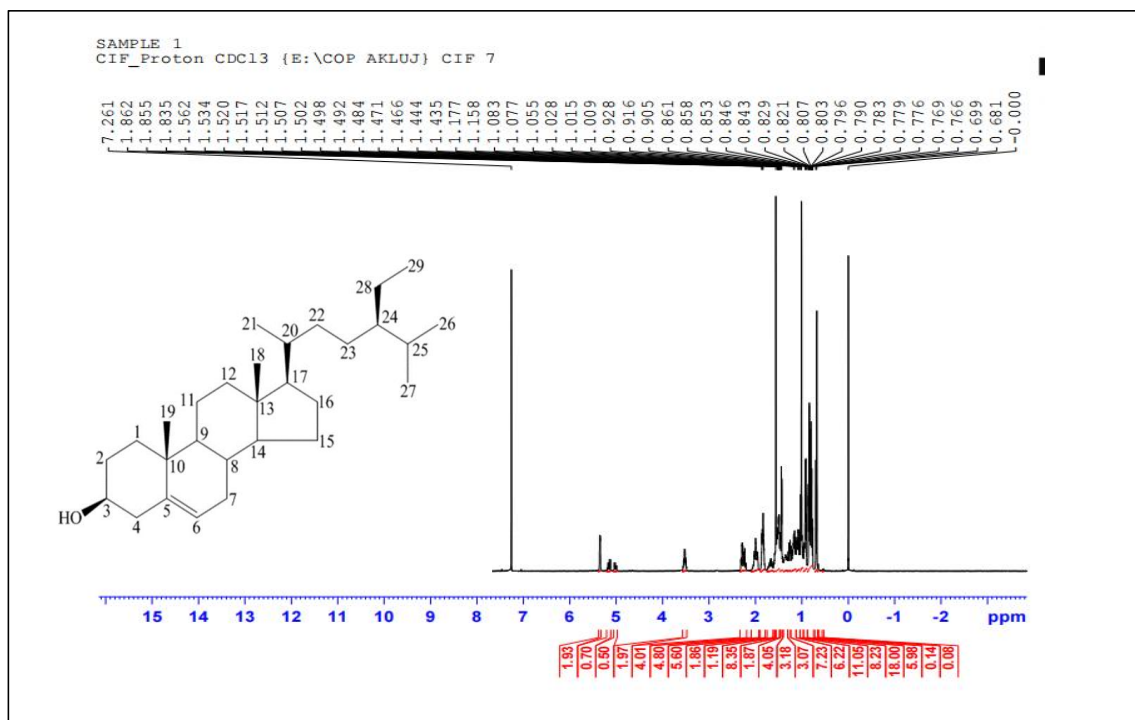


Figure 6.7 ¹H NMR of isolated Beta-sitosterol

NMR Interpretation of the isolated Beta-sitosterol

¹H NMR (400 MHz, CDCl₃, δ, ppm) : 5.35 (dd, *J* = 5.2 Hz, 1H, CH=CH), 3.53 (m, 1H, O-CH), 2.17-2.33 (m, 4H, Allylic 2-CH₂), 1.94-2.07 (m, 8H, 4-CH₂), 1.75-1.82 (m, 2H), 1.56-1.65 (m, 14H), 0.8-1.34 (m, 20H).

¹³C NMR (100 MHz, CDCl₃, δ [ppm]): 72 (C₁), 32.41 (C₂), 36.14 (C₃), 37.2 (C₄), 51.23 (C₅), 32.41 (C₆), 57 (C₇), 40.51 (C₈), 56.02 (C₉), 29.11 (C₁₀), 24.29 (C₁₁), 141 (C₁₂), 122 (C₁₃), 34 (C₁₄), 21.07 (C₁₅), 42.19 (C₁₆), 19.4 (C₁₇), 12.2 (C₁₈), 18.7 (C₁₉), 34 (C₂₀), 26 (C₂₁), 46 (C₂₂), 29,15 (C₂₃), 19.40 (C₂₄), 20 (C₂₅), 20.21 (C₂₆), 19.8 (C₂₇), 23.04 (C₂₈), 12.04 (C₂₉).

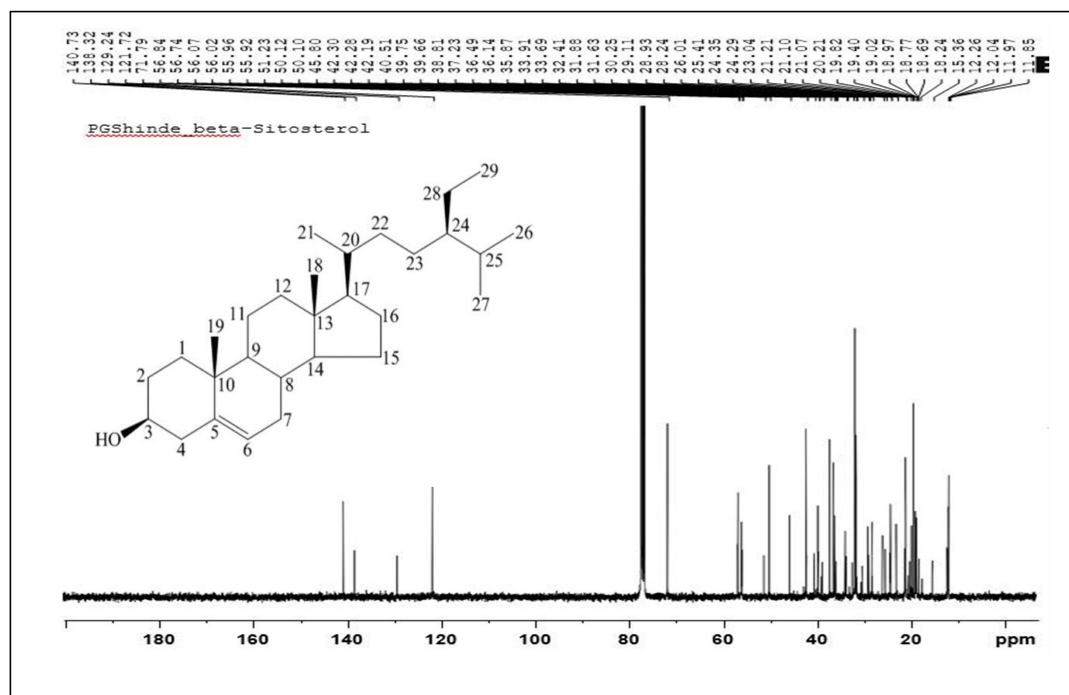


Figure 6.8 ^{13}C NMR of isolated Beta-sitosterol

MASS spectrum of Beta-sitosterol

Standard Beta-sitosterol ($\text{C}_{29}\text{H}_{50}\text{O}$) fragmentation patterns usually include a molecular ion peak at m/z 414, and other characteristic fragments related to ring cleavage at 397, 350, 283, 195, 150, and 122.

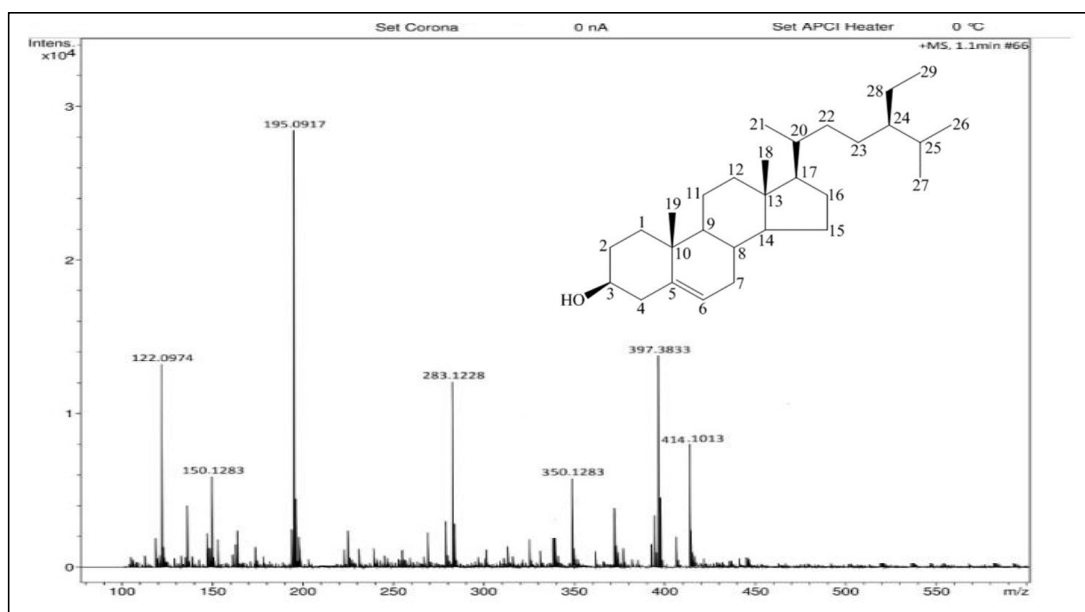


Figure 6.9 MASS spectrum of standard Beta-sitosterol

In isolated Beta-sitosterol ($C_{29}H_{50}O$), the fragmentation pattern usually includes a molecular ion peak at m/z 415. and other characteristic fragments related to ring cleavage, 395, 371, 338, 283, 195, 150, and 122.

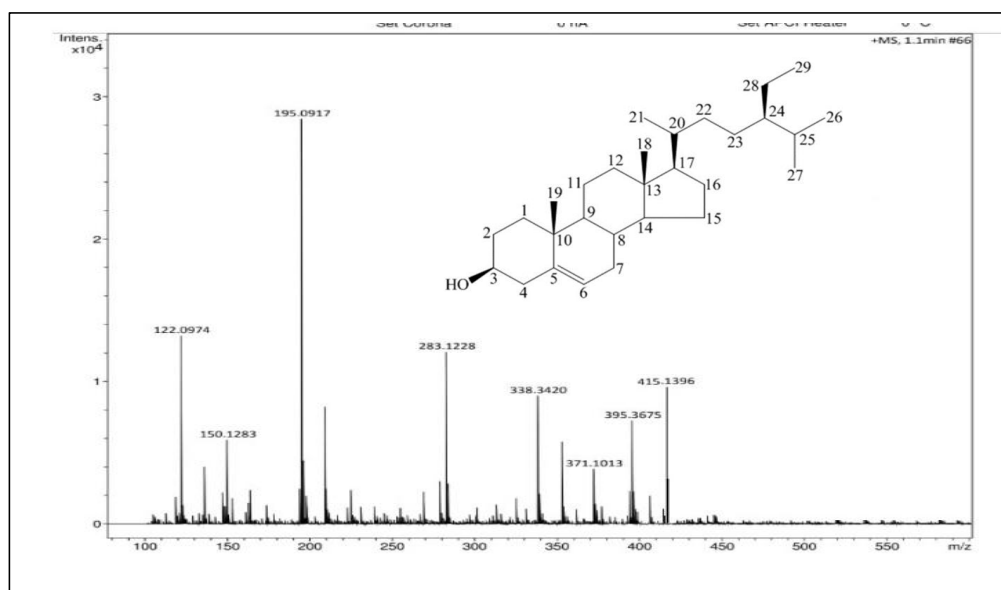


Figure 6.10 MASS spectrum of isolated Beta-sitosterol

6.2.3.2 Characterization of *Ricinus communis*

UV visible spectroscopy of Stigmasterol

The isolated Stigmasterol showed an absorption maximum at a wavelength of 248 nm, which is within the expected range for standard Stigmasterol (251 nm). A possible wavelength shift of 2-5 nm from the standard value may be due to the presence of traces of the mobile phase.

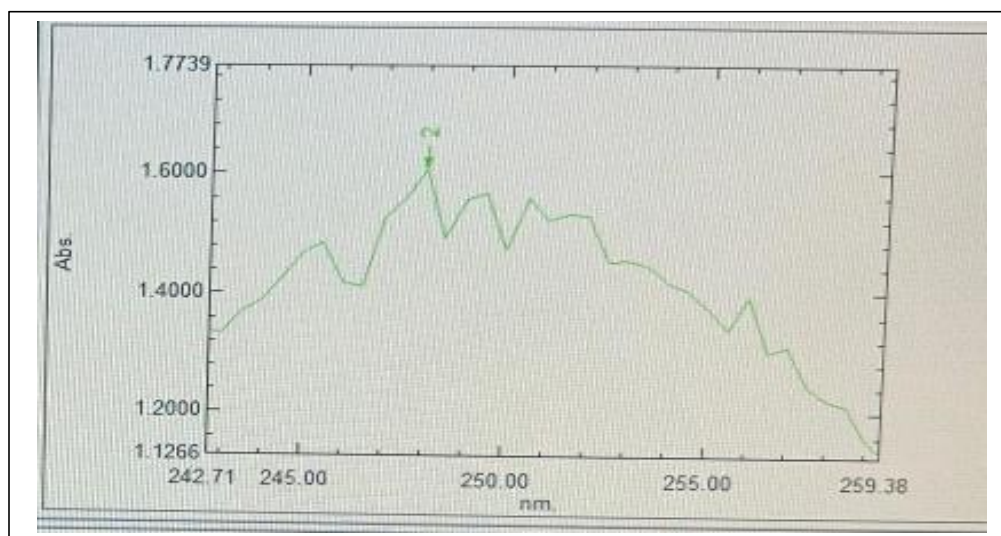


Figure 6.11 UV visible spectrum of standard Stigmasterol

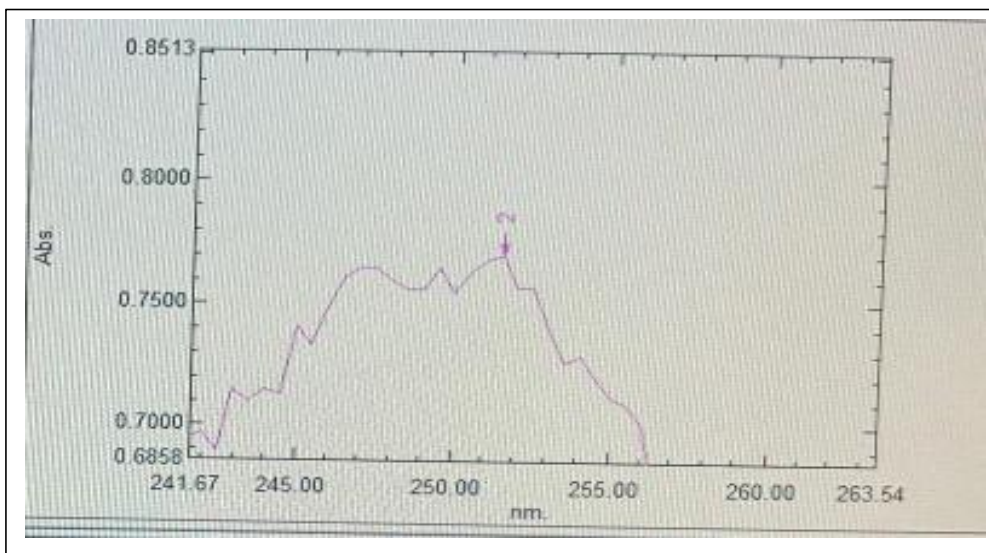


Figure 6.12 UV visible spectrum of the isolated Stigmasterol

FTIR spectrum of Stigmasterol

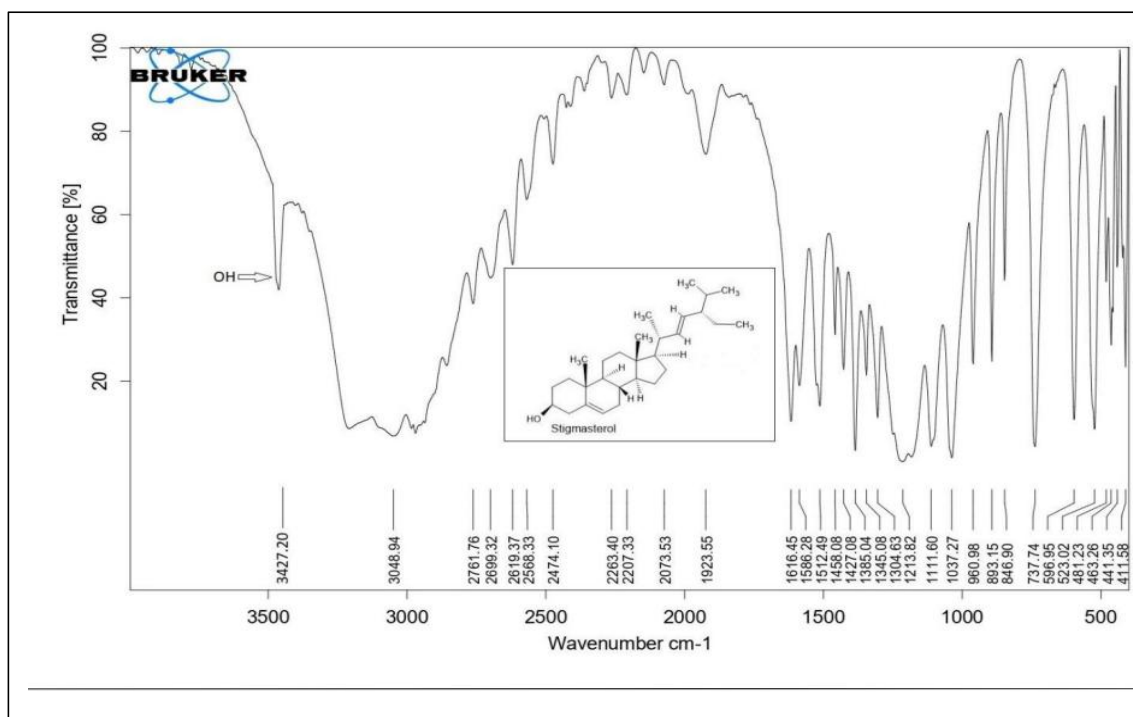


Figure 6.13 FTIR spectrum of standard Stigmasterol

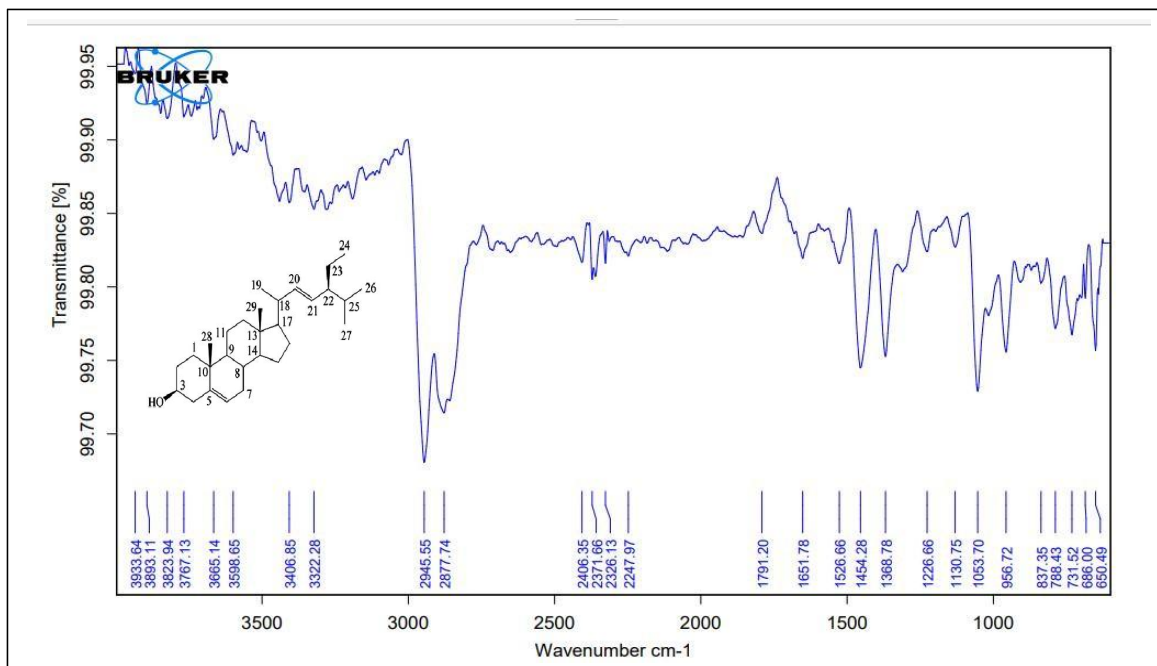


Figure 6.14 FTIR spectrum of isolated Stigmasterol

FTIR interpretation of Stigmasterol

Table 6.8 FTIR interpretation of stigmasterol

Standard Stigmasterol bands (cm ⁻¹)	Isolated Stigmasterol bands (cm ⁻¹)	Std.value (cm ⁻¹)	Interpretation
3427.20	3406.85 3598.65, 3665.14,	3400-3700	Stretching vibration for OH
	2945.55 2877.74	2850-2975	Stretching vibration for CH aliphatic
3048.94	2945.55	3020-3100	Stretching vibration for CH alkene
1616.45	1651.78	1640-1680	Stretching vibration for C=C
1427.08	1454.28	1395-1440	Bending vibration for OH
1385.04	1368.78	1365-1372	Bending vibration for isopropyl
1037.27,1111.60	1053.70	1000-1300	Bending vibration for C-O of alcohol
1458.08	1368.78	1375-1450	Bending vibration for CH ₃

NMR spectrum of Stigmasterol

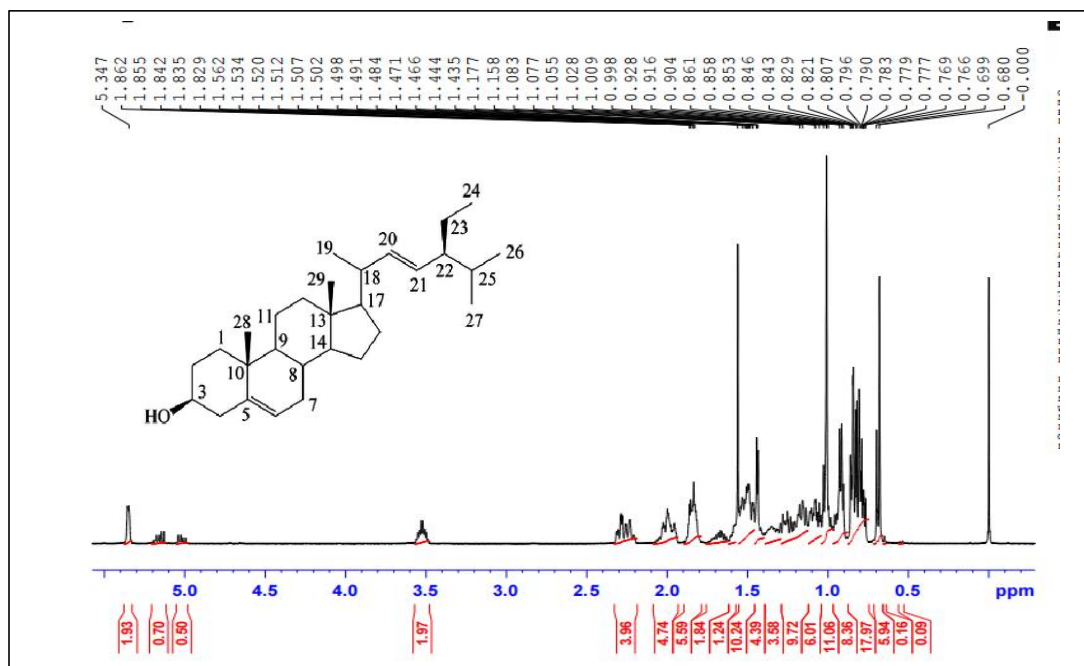


Figure 6.15 ¹H NMR of standard Stigmasterol

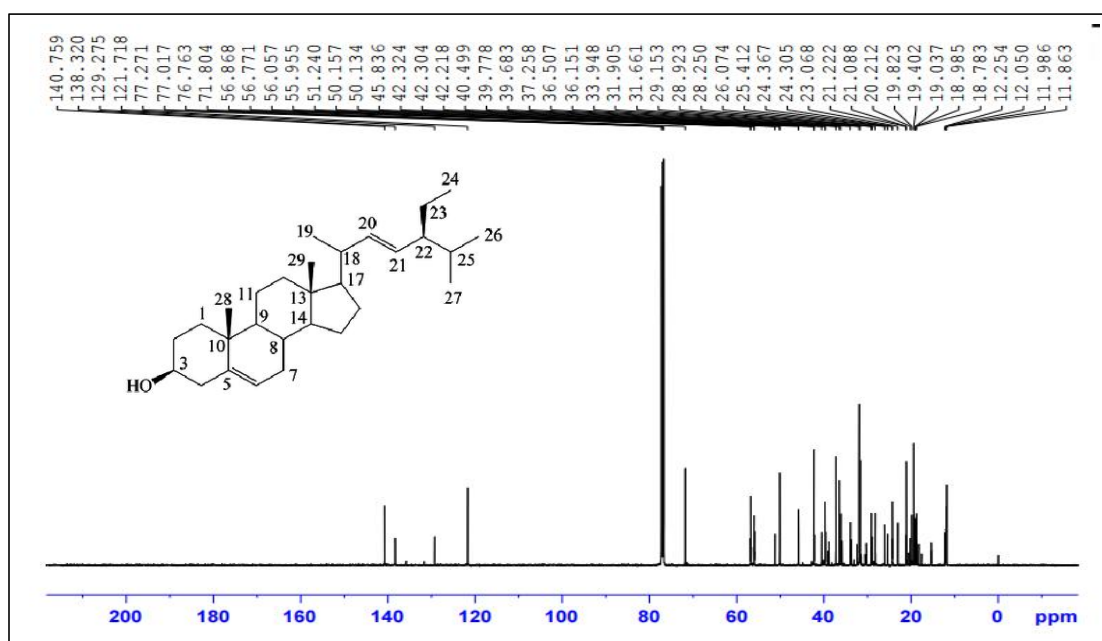


Figure 6.16 ¹³C NMR of standard Stigmasterol

NMR Interpretation of the Stigmasterol

¹H NMR (400 MHz, CDCl₃, δ , ppm): 5.34 (dd, J = 5.2 Hz, 1H, CH=CH), 5.16 (dd,

$J = 8.4, 6.8$ Hz, 1H, CH=CH), 5.05 (dd, $J = 8.4, 6.8$ Hz, 1H, CH=CH), 3.55 (m, 1H, O-CH), 2.20-2.35 (m, 2H, Allylic -CH₂), 1.90-2.10 (m, 4H, Allylic -CH₂ & -CH), 1.80- 1.88 (m, 2H), 1.54-1.68 (m, 2H), 1.43-1.52 (m, 12H), 0.8-1.38 (m, 22H)

¹³C-NMR (100 MHz, CDCl₃, δ [ppm]): 72 (C₁), 32 (C₂), 36.15 (C₃), 37.25 (C₄), 51.24 (C₅), 32 (C₆), 56.05 (C₇), 40.49 (C₈), 57 (C₉), 29.1 (C₁₀), 24.30 (C₁₁), 141 (C₁₂), 122 (C₁₃), 34 (C₁₄), 21.08 (C₁₅), 42.21 (C₁₆), 19.4 (C₁₇), 12.2 (C₁₈), 18.7 (C₁₉), 31.06 (C₂₀), 26 (C₂₁), 46 (C₂₂), 29.15 (C₂₃), 19.40 (C₂₄), 20 (C₂₅), 20.21 (C₂₆), 19.8 (C₂₇), 23.06 (C₂₈), 12.05 (C₂₉).

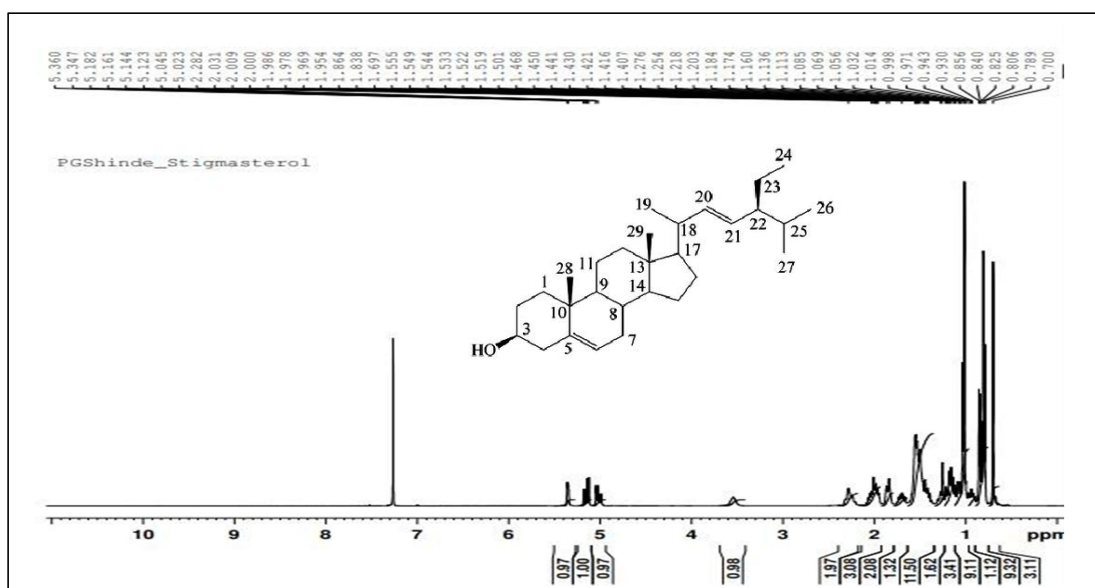


Figure 6.17 ¹H NMR of isolated Stigmasterol

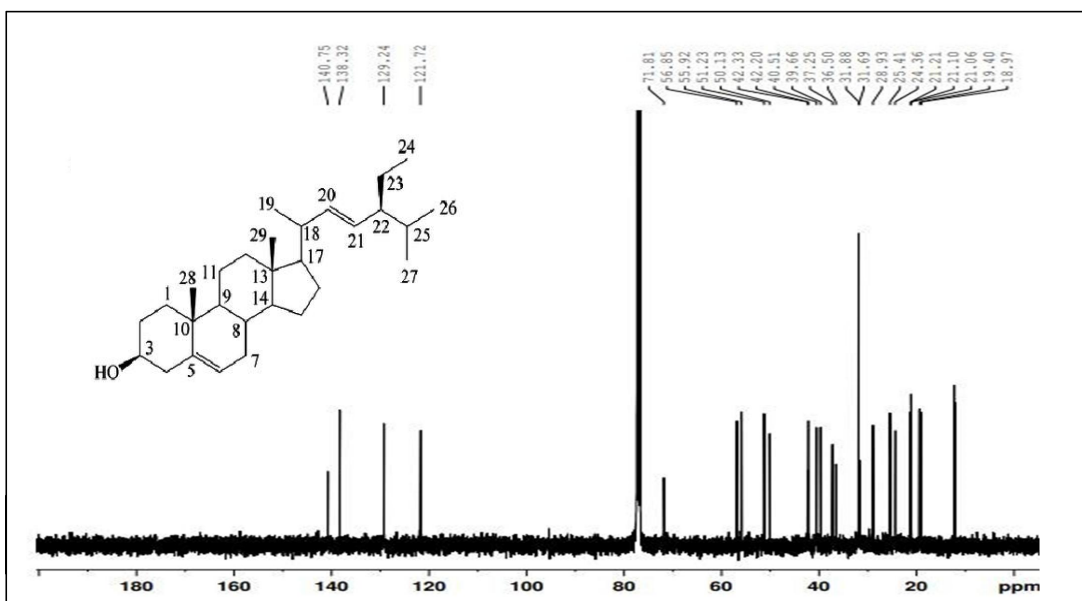


Figure 6.18 ^{13}C NMR of the isolated Stigmasterol

NMR Interpretation of the Stigmasterol

^1H NMR (400 MHz, CDCl_3 , δ , ppm): 5.36 (dd, $J = 5.2$ Hz, 1H, $\text{CH}=\text{CH}$), 5.16 (dd, $J = 8.4$, 6.8 Hz, 1H, $\text{CH}=\text{CH}$), 5.05 (dd, $J = 8.4$, 6.8 Hz, 1H, $\text{CH}=\text{CH}$), 3.55 (m, 1H, O-CH), 2.20-2.35 (m, 2H, Allylic $-\text{CH}_2$), 1.90-2.10 (m, 4H, Allylic $-\text{CH}_2$ & $-\text{CH}$), 1.80-1.88 (m, 2H), 1.54-1.68 (m, 2H), 1.43-1.52 (m, 12H), 0.8-1.38 (m, 22H)

^{13}C NMR (100 MHz, CDCl_3 , δ [ppm]): 72 (C_1), 32 (C_2), 36.50 (C_3), 37.25 (C_4), 51.23 (C_5), 32 (C_6), 57 (C_7), 40.51 (C_8), 56.02 (C_9), 29 (C_{10}), 24.36 (C_{11}), 141 (C_{12}), 122 (C_{13}), 40 (C_{14}), 21.10 (C_{15}), 42.20 (C_{16}), 19.4 (C_{17}), 12.2 (C_{18}), 19 (C_{19}), 34 (C_{20}), 26 (C_{21}), 42.33 (C_{22}), 29 (C_{23}), 21.21 (C_{24}), 20 (C_{25}), 21.06 (C_{26}), 19 (C_{27}), 24.36 (C_{28}), 19 (C_{29}).

MASS spectrum of Stigmasterol

Standard stigmasterol ($\text{C}_{29}\text{H}_{48}\text{O}$) usually exhibits a fragmentation pattern with a molecular ion peak at m/z 412. and other characteristic fragments related to ring cleavage at 395, 371, 338, 279, 195, 150, and 122.

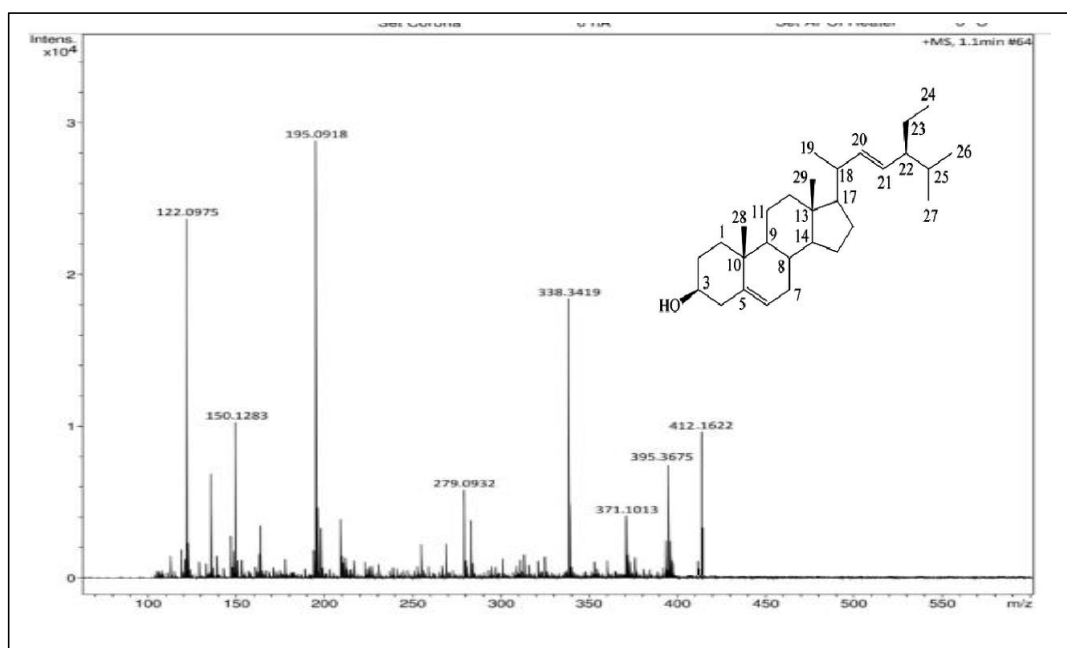


Figure 6.19 MASS spectrum of the standard Stigmasterol

Fragmentation pattern of isolated Stigmasterol ($\text{C}_{29}\text{H}_{48}\text{O}$) typically involves a

molecular ion peak at m/z 413 and other characteristic fragments related to ring cleavage at 397, 338, 283, 279, 195, 150, and 122.

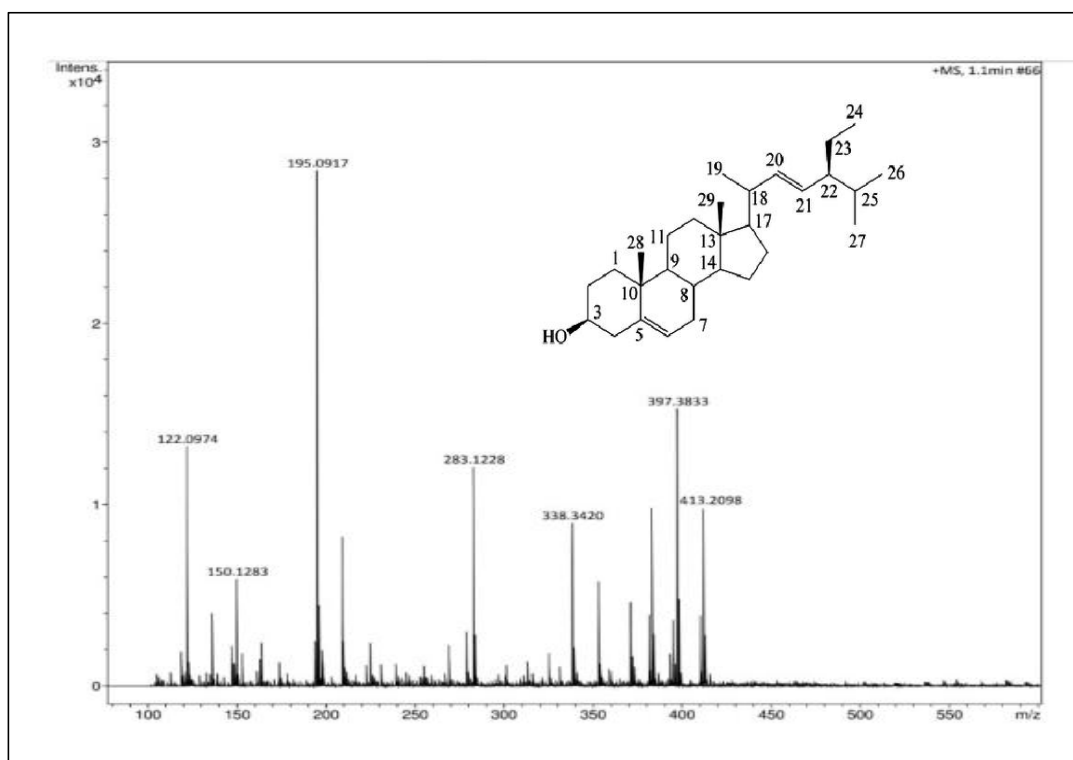


Figure 6.20 MASS spectrum of isolated Stigmasterol

6.2.4 Quantification of isolated phytoconstituents

6.2.4.1 Quantification of Beta-sitosterol from *Euphorbia pulchirima* leaves extract

HPTLC of Beta- sitosterol

Preparation of standard: 5 mg. of standard Beta-sitosterol powder were weighed and dissolved in 1 ml ethanol. Sonicated it and diluted with 5 ml with ethanol.

Preparation of sample : 5 mg. of *Euphorbia pulchirima* leaves extract were weighed and dissolved in 1 ml ethanol. Sonicated it and diluted with 5 ml with ethanol .

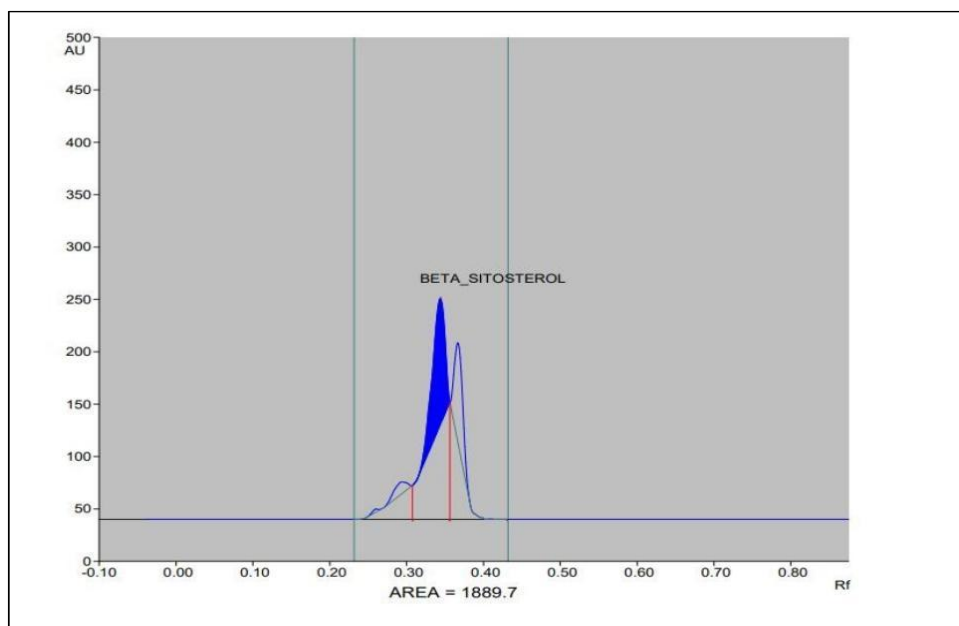


Figure 6.21 HPTLC of extract *Euphorbia pulchirima*

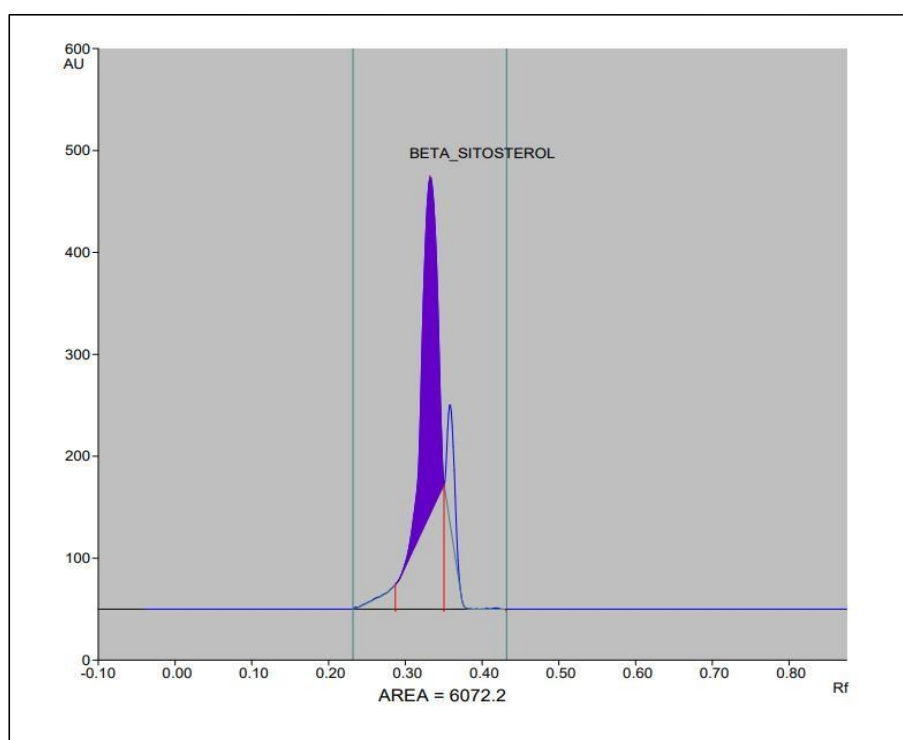


Figure 6.22 HPTLC of standard Beta-sitosterol

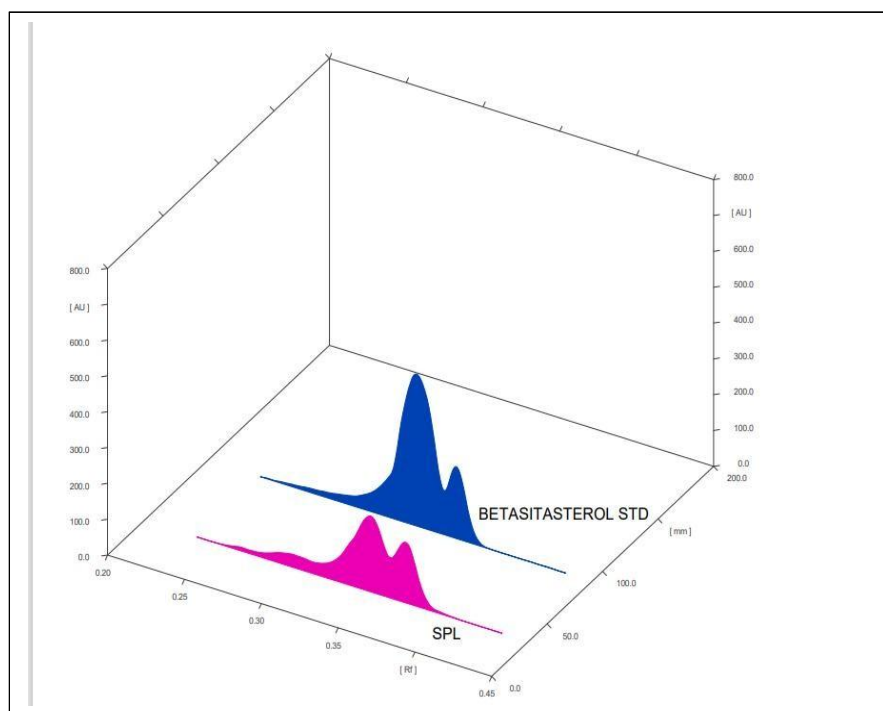


Figure 6.23 Overlay graph of *Euphorbia pulcherrima* extract and standard Beta-sitosterol

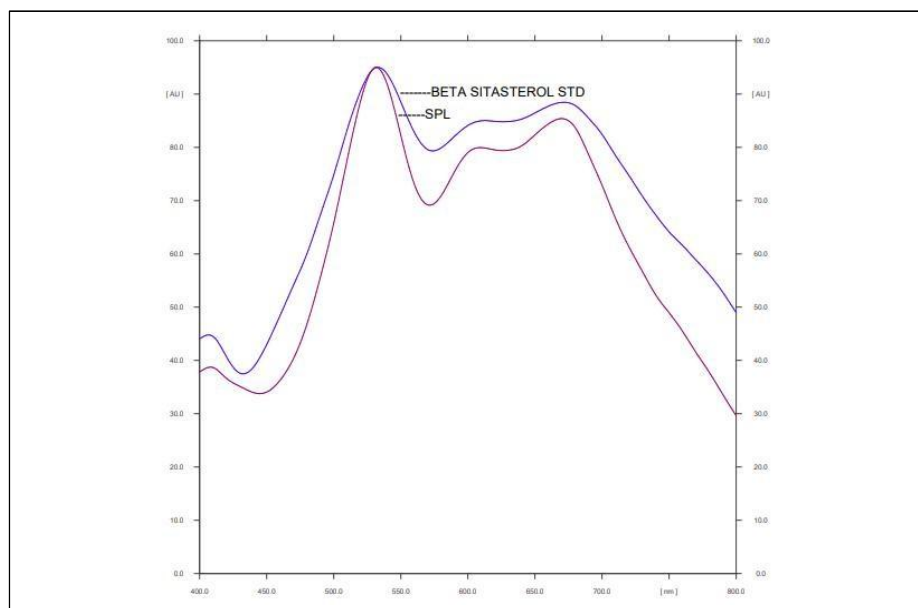


Figure 6.24 Spectrum scan of *Euphorbia pulcherrima* extract and standard

Table 6.9 Quantification of Beta-sitosterol using HPTLC

Sr. No	Name of sample	Rf value	Area	% concentration
1	Extract	0.36	1889.7	14.31
2	Beta-sitosterol	0.35	6072.2	100

6.2.4.2 Quantification of Stigmasterol from *Ricinus communis* seeds extract

HPTLC of Stigmasterol

Preparation of standard: 55.30 mg. of standard stigmasterol powder were weighed and dissolved in 1ml ethanol. Sonicated it and diluted with 5 ml with ethanol.

Preparation of sample : 10.4 mg of *Ricinus communis* seeds extract were weighed and dissolved in 1 ml ethanol. Sonicated it and diluted with 5 ml with ethanol

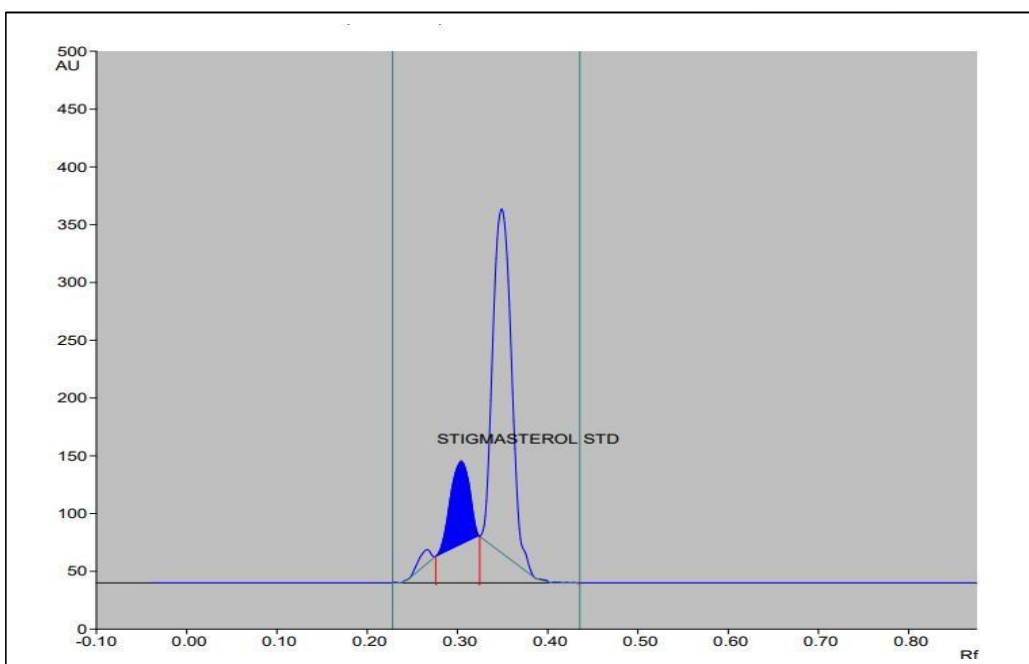


Figure 6.25 HPTLC of *Ricinus communis* extract

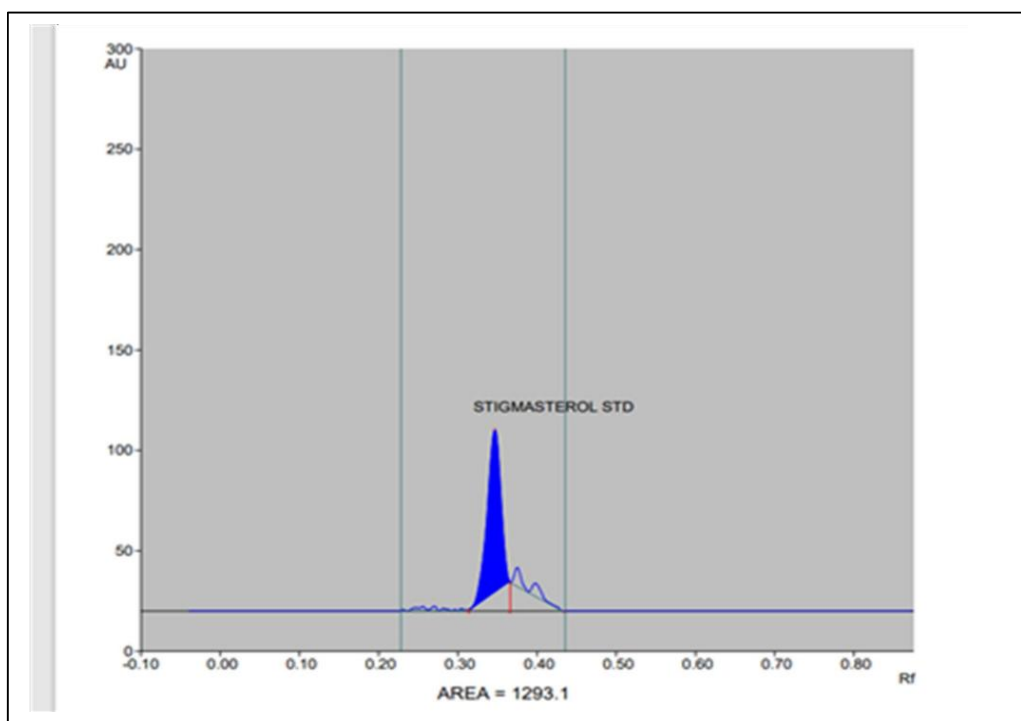


Figure 6.26 HPTLC of standard Stigmasterol

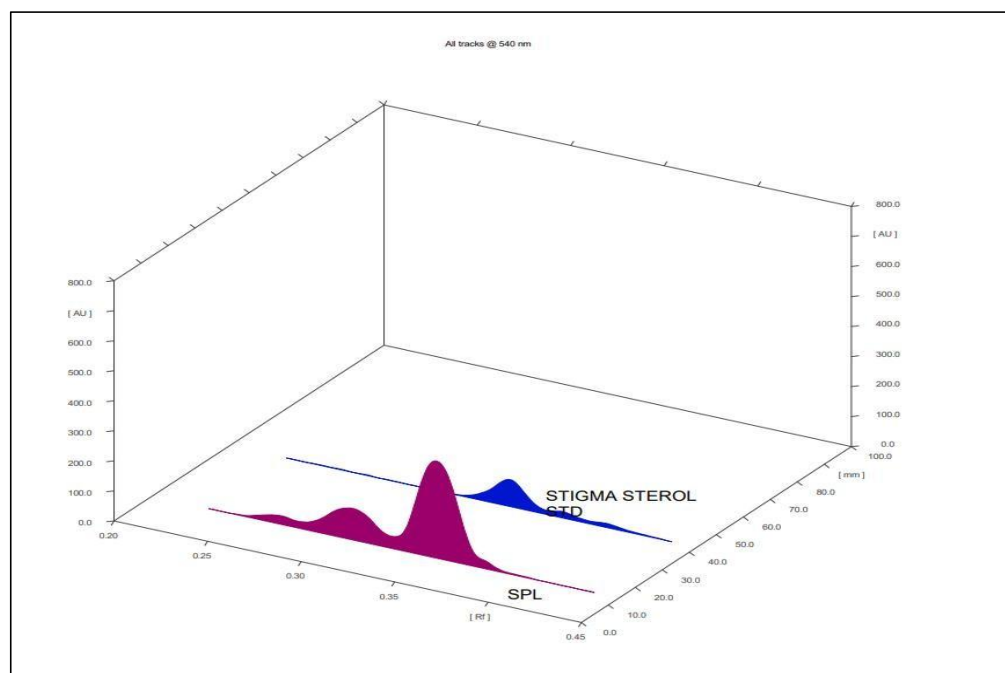


Figure 6.27 Overlay graph of *Ricinus communis* extract and standard Stigmasterol

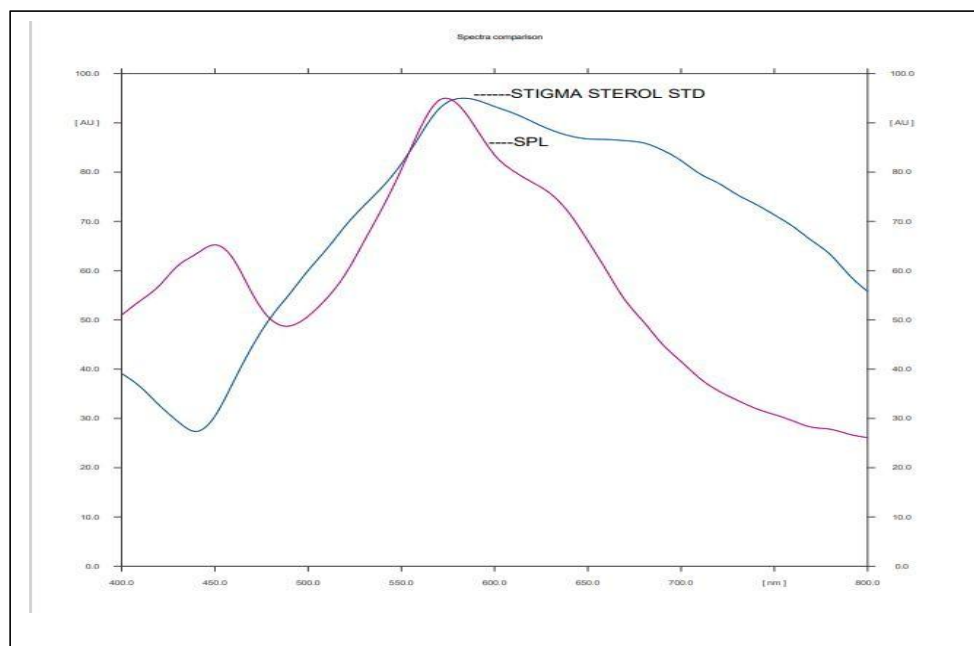


Figure 6.28 Spectrum scan of *Ricinus communis* extract and standard

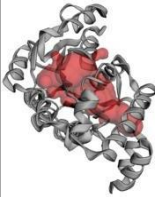
Table 6.10 Quantification of Stigmasterol using HPTLC

Sr. no	Name of sample	Rf value	Area	% concentration
1	Extract	0.33	1433.5	28.24
2	Stigmasterol	0.37	1293.1	100

6.2.5 Molecular dynamic simulation

6.2.5.1 Protein structure retrieval and preparation

Table 6.11 Binding pockets and area of PDB ID: 3HB5

PDB ID	Name of Protein	Binding Pocket	Area (SA) Å ²	Volume (SA) Å ³
3HB5	Estradiol 17-beta-dehydrogenase 1 enzyme		848.653	515.659

6.2.5.2 Ligand structure retrieval and preparation

Table 6.12 Selected ligands for molecular docking study

Name of ligand	Pub.Chem CID.	Molecular formula	Molecular wt (g/mol)	Canonical smiles
Rutin	5280805	C ₂₇ H ₃₀ O ₁₆	610.5	<chem>CC1C(C(C(C(O1)OCC2C(C(C(C(O2)OC3=C(OC4=CC(=CC(=C4C3=O)O)O)C5=CC(=C(C=C5)O)O)O)O)O)O)O</chem>
Kaempferol 1,3-O- Glucoside	5282 102	C ₂₁ H ₂₀ O ₁₁	448.4	<chem>C1=CC(=CC=C1C2=C(C(=O)C3=C(C=C(C=C3O2)O)O)OC4C(C(C(C(O4)CO)O)O)O)O</chem>
Stigmasterol	5280794	C ₂₉ H ₄₈ O	412.7	<chem>CCC(C=CC(C)C1CCC2C1(CCC3C2CC=C4C3(CCC(C4)O)C)C)C(C)C</chem>
Beta-sitosterol	222284	C ₂₉ H ₅₀ O	414.7	<chem>CCC(CCC(C)C1CCC2C1(CCC3C2CC=C4C3(CCC(C4)O)C)C)C(C)C</chem>
Germanicol	122857	C ₃₀ H ₅₀ O	426.7	<chem>CC1(CCC2(CCC3(C(C2=C1)CCC4C3(CCC5C4(CCC(C5(C)C)O)C)C)C)C)C</chem>

Binding site definition and molecular docking study

Intermolecular interaction analysis

The molecular docking results provided in Table 6.13 gives valuable insights into the interactions between the Estradiol 17-beta-dehydrogenase 1 enzyme and different compounds, highlighting their potential as ligands. The compound, Rutin stands out with a robust docking score of -18.61 Kcal/mol, indicating a strong potential for

binding (Figure 6.19) (a) and (b). Rutin produce Hydrogen bonds with Ser142, Asn152, and Val188 at bond distances of with 1.34 Å, 1.12 Å, and 1.69 Å, respectively. It also involves in three aromatic hydrogen bonds with Phe226 at bond distances of 2.77 Å, 3.42 Å, 3.43 Å. In comparison, Kaempferol-3-O-Glucoside exhibits a slightly lower docking score of -14.79 Kcal/mol. Its binding affinity range (4771073.042 to 474034315.5 nm) indicates a potential variation in binding strength, with Pi-Pi stacking with Tyr155 at bond distance of 5.39 Å and an aromatic hydrogen bond with Phe192 (3.47 Å) contributing to its binding profile (Figure 6.29) (c) and (d).

Table. 6.13. Molecular interaction analysis of selected ligand against PDB ID: 3HB5

Name of ligands	Docking score (Kcal/mol)	Binding affinity (Range in nm)	Interacting residues	Interaction type	Bond distance (Å)
Rutin	-18.61	0	Ser142	HBond	1.34
			Asn152	HBond	1.12
			Val188	HBond	1.69
			His221	HBond	3.21
			Phe226	Ar-HBond	2.77, 3.42, 3.43
Kaempferol-3-O-Glucoside	-14.79	4771073.042 to 474034315.5	Cys185	HBond	2.01
			Tyr155	Pi-Pi Stacking	5.39
			Phe192	Ar-HBond	3.47
Stigmasterol	-8.21	21.984 to 2184.311	His221	Ar-HBond	3.05
Beta-sitosterol	-7.26	3.472 to 345.020	No Interactions		
Germanicol	-3.12	15785.265 to 1568359.421	No Interactions		

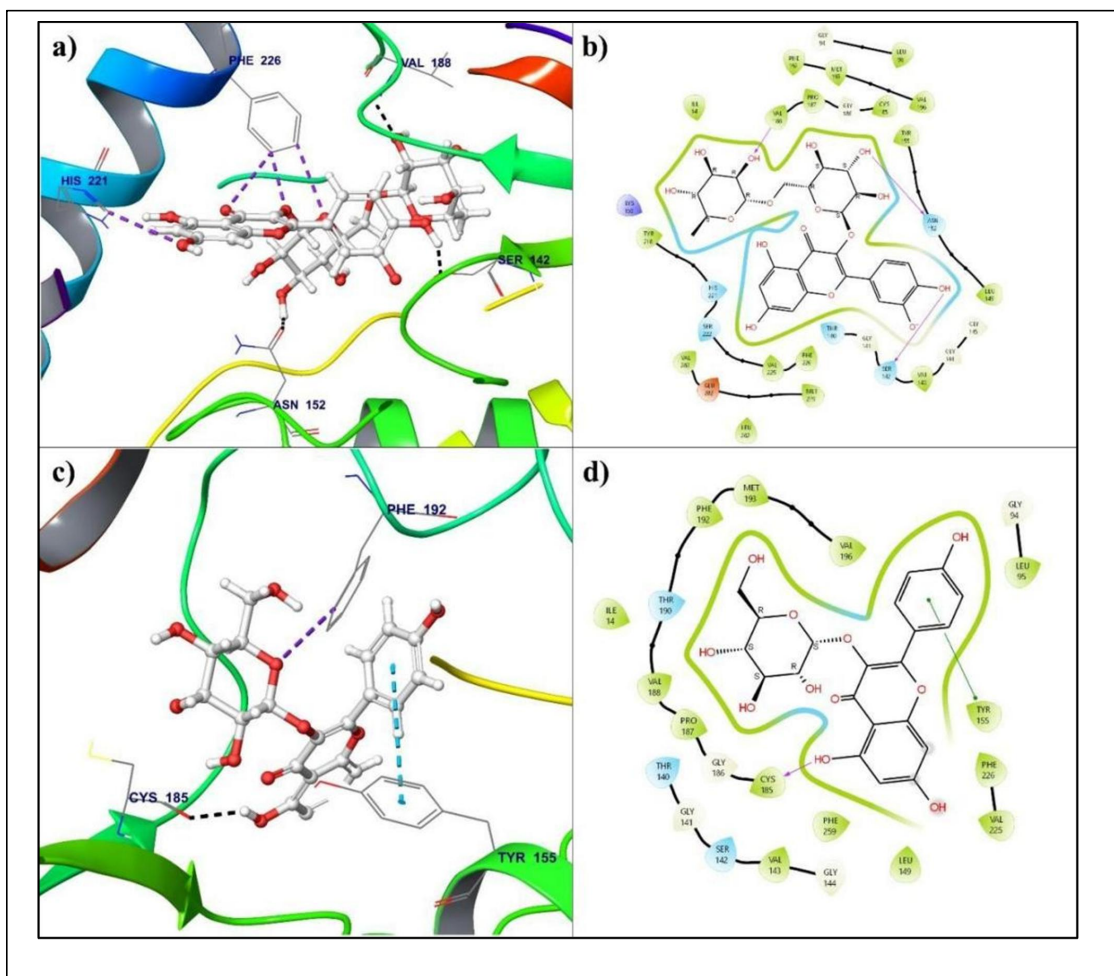


Figure 6.29 Intermolecular interaction between *Euphorbia pulcherrima* and *Ricinus communis* phytoconstituents with PDB ID 3HB5

(a) The 3D docked pose and interaction of Rutin with enzyme; (b) The 2D interaction of Rutin with enzyme (c) The 3D docked pose and interaction of Kaempferol-3-O-Glucoside with enzyme (d) The 2D interaction of Kaempferol-3-O-Glucoside with enzyme. Stigmasterol with -8.21 Kcal/mol docking score and a binding affinity range of 21.984 to 2184.311 nm, forms an aromatic hydrogen bond with His221 at bond distances of 3.05 Å (Figure 6.30) (a) and (b). Although the docking score of Stigmasterol is lower than Rutin, the interaction with a key residue suggests a specific and potentially effective binding mode and it also shows the strong binding affinity. On the other hand, Beta-sitosterol and Germanicol exhibit less favorable results.

Beta-sitosterol docking score is -7.26 Kcal/mol, with a binding affinity range of 3.472 to 345.020 nm, and no specific interactions mentioned (c) and (d). Germanicol docking score of -3.12 Kcal/mol and a wide binding affinity range (15785.265 to 1568359.421 nm), also lacks specific interactions (Figure 6.30) (e) and (f). These findings may indicate weaker binding affinities or steric clashes, limiting their potential as effective ligands.

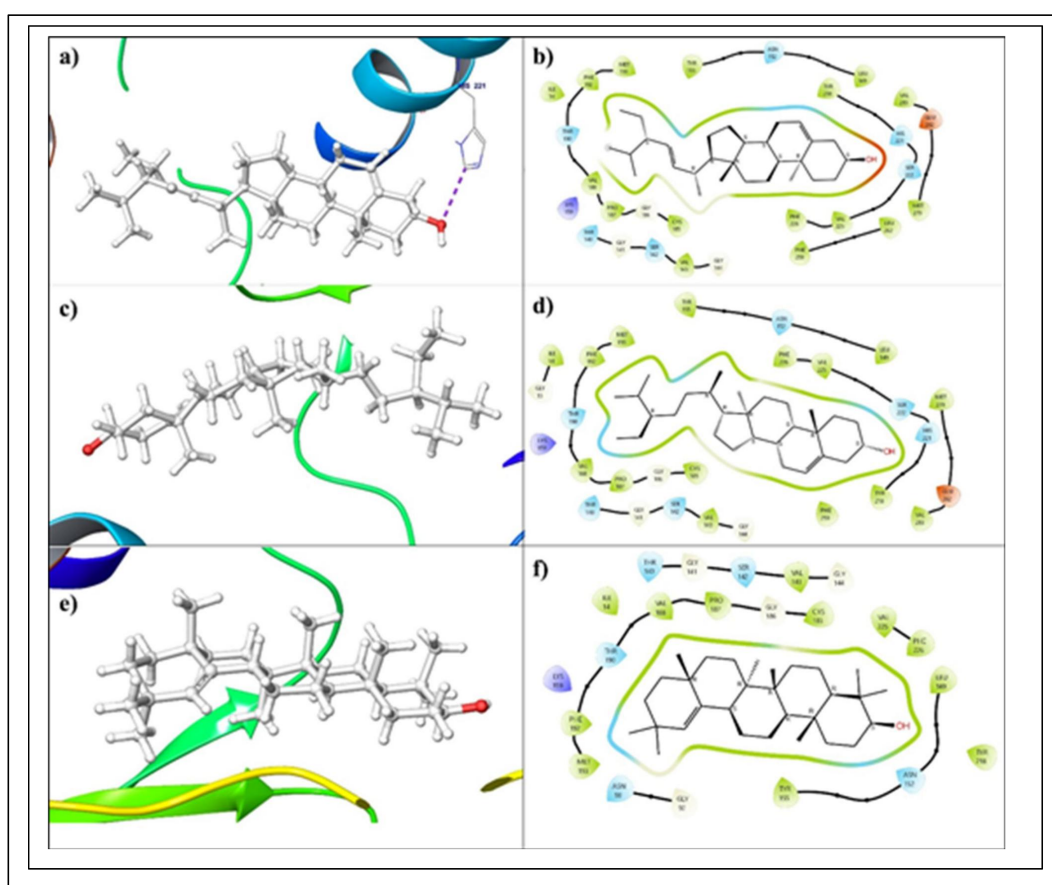


Figure 6.30 2D and 3D docked pose interaction between *Euphorbia pulcherrima* leaves and *Ricinus communis* seed phytoconstituents with PDB ID 3HB5

(a) The 3D docked pose and interaction of Stigmasterol with Enzyme; (b) The 2D interaction of Stigmasterol with Enzyme (c) The 3D docked pose and interaction of Beta-sitosterol with enzyme (d) The 2D interaction of Beta-sitosterol with enzyme (e) The 3D docked pose and interaction of Germanicol with enzyme (f) The 2D interaction of Germanicol with enzyme.

6.2.5.3 Molecular dynamic simulation

Dynamic behavior of Estradiol 17-beta dehydrogenase -1 - enzyme and ligand binding stability by MD simulation:

From the MD simulation results, the RMSD values calculated from 1000 trajectories generated during 100 nanoseconds of MD simulations for different complexes involving the compounds Rutin, Kaempferol-3-O-Glucoside, Stigmasterol, Beta-sitosterol, and Germanicol with Estradiol 17 beta-dehydrogenase 1- enzyme (PDB ID : 3HB5) (Figure 6.31) and detail information in table given below.

Table 6.14. RMSD values for complexes formed with PDB ID: 3HB5

Ligand with 3HB5 complex	RMSD (Å)	standard deviation (Å)	Structural fluctuation
Rutin complex	3.43	0.39	Moderate level
Kaempferol-3-O-Glucoside complex	3.28	0.24	Less level
Stigmasterol complex	4.08	0.48	Moderate level
Beta-sitosterol complex	3.61	0.48	Moderate level
Germanicol complex	3.31	0.32	Less level

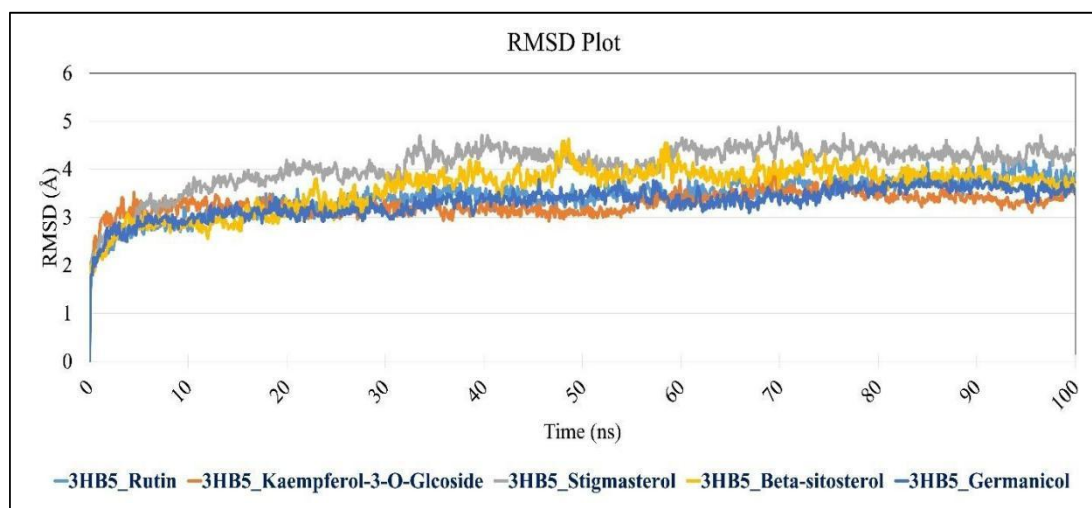


Figure 6.31 Root Mean Square Deviation plot for Estradiol 17-beta-dehydrogenase 1 enzyme

Also, we have calculated the RMSF values for Estradiol 17 β -dehydrogenase 1 enzyme when it binds with the phytoconstituents. The Figure 6.32 depict information on the RMSF calculated from 1000 trajectories generated during 100 nanoseconds of MD simulations for different complexes involving Rutin, Kaempferol-3-O-Glucoside, Stigmasterol, Beta-sitosterol, and Germanicol.

Table. 6.15. RMSF values for complexes formed with PDB ID: 3HB5

Ligand with 3HB5 complex	RMSF (Å)	standard deviation (Å)	Structural fluctuation
Rutin complex	1.53	0.77	Moderate level
Kaempferol-3-O-Glucoside complex	1.62	0.63	Less level
Stigmasterol complex	1.81	0.85	Extent level
Beta-sitosterol complex	1.75	0.73	Moderate level
Germanicol complex	1.57	0.60	Moderate level

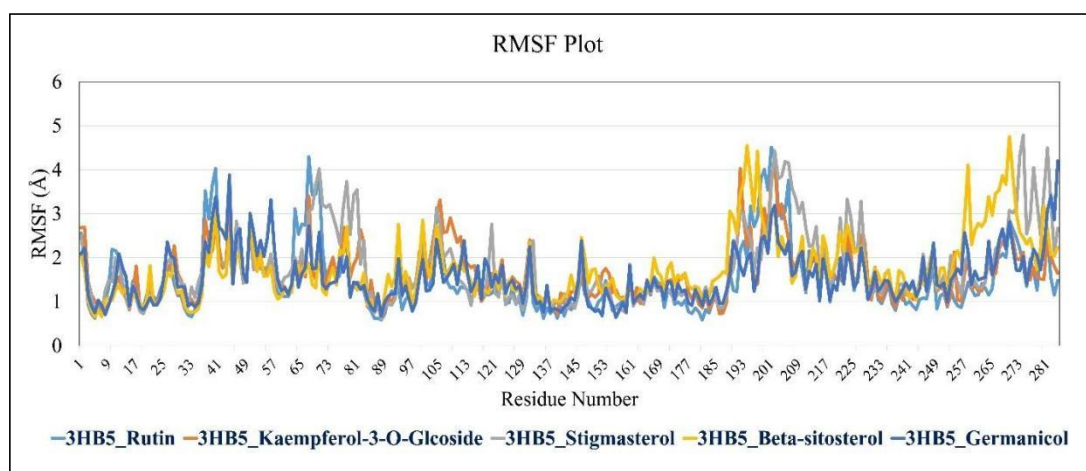


Figure 6.32 Root Mean Square Fluctuation plot for Estradiol 17- β -dehydrogenase 1 enzyme

Comparing the complexes, Kaempferol-3-O-Glucoside and Germanicol show slightly lower average RMSF values, indicating relatively stable binding configurations. Stigmasterol exhibits the highest average RMSF, suggesting more dynamic behavior during the simulations. Rutin and Beta-sitosterol fall within a moderate range of

RMSF values. The RMSF values provide insights into the flexibility of different complexes during MD simulations. Kaempferol-3-O-Glucoside and Germanicol complexes demonstrate relatively stable binding configurations, while Stigmasterol exhibits higher flexibility. Rutin and Beta-sitosterol fall within a moderate range.

6.2.6 Molecular docking study using autodock vina

Isolated phytoconstituents were characterized using different chromatographic and spectroscopic techniques and their pharmacological potential was screened by using *In silico* approach.

6.2.6.1 Selection of protein

The protein was selected based upon its mechanism of action and its details were described in Table 6.16.

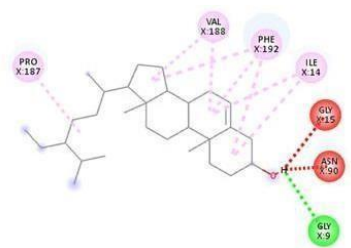
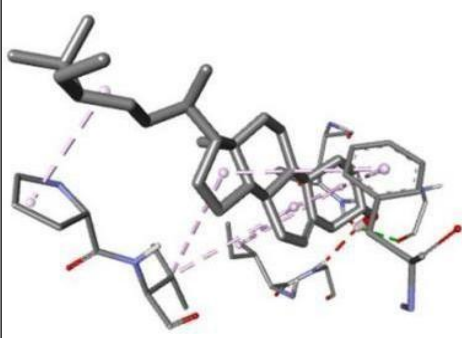
6.2.6.2 Selection of ligand

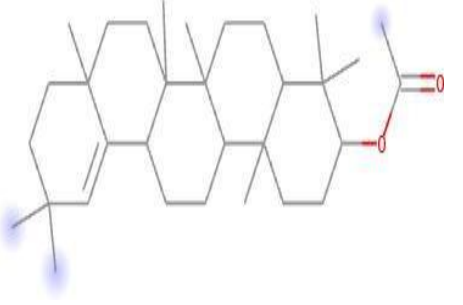
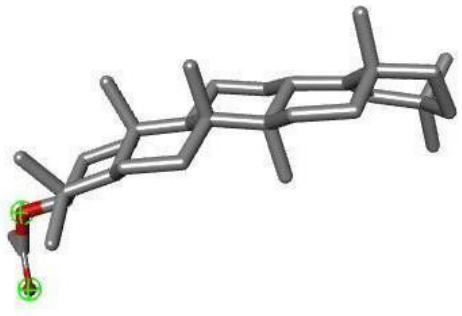
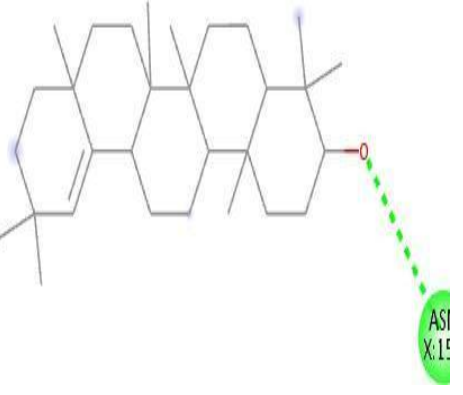
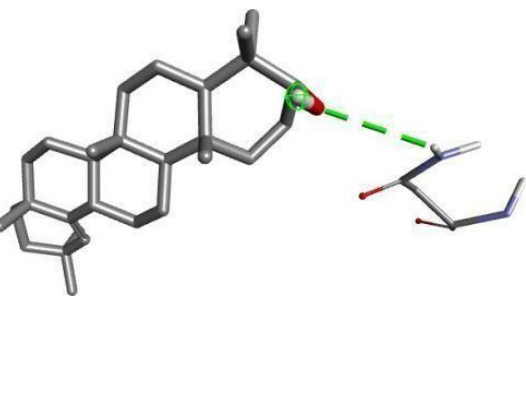
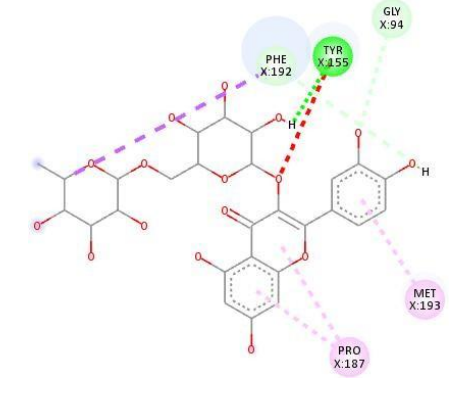
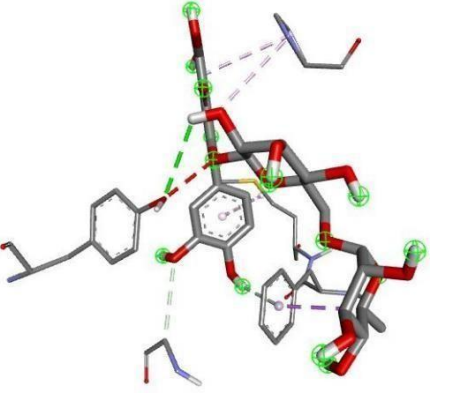
The detail information about selected ligand was given below

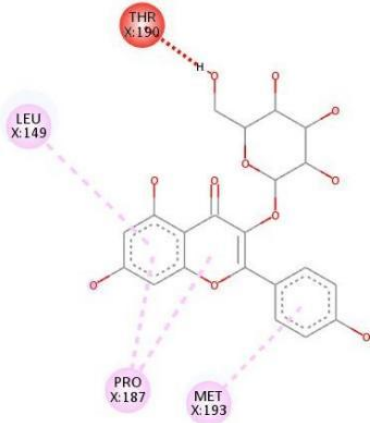
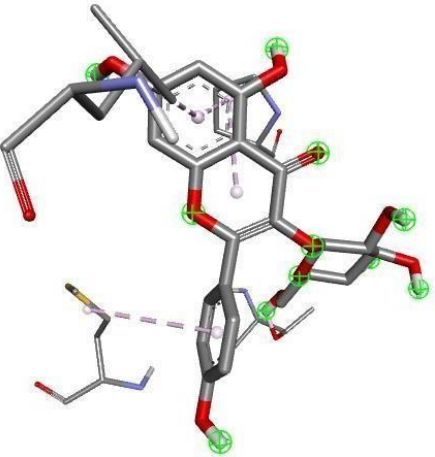
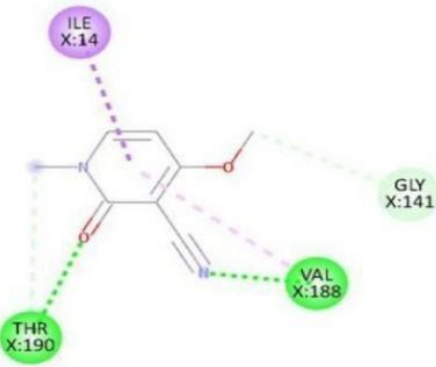
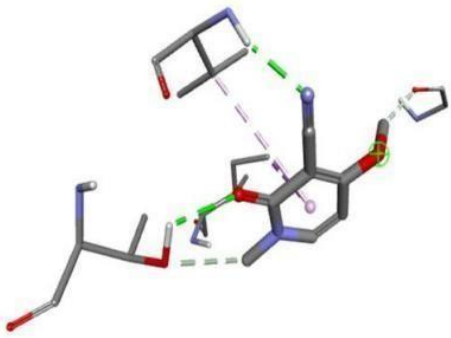
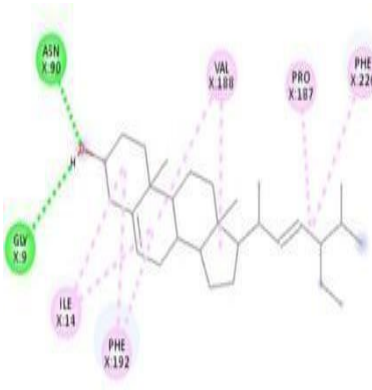
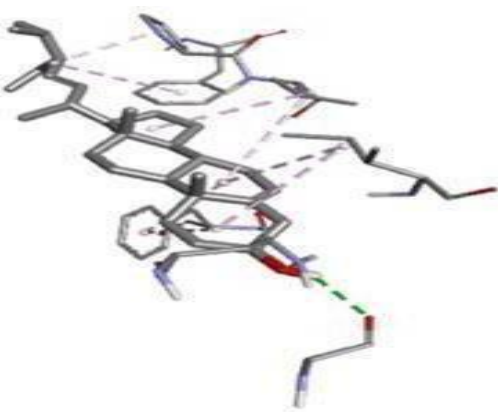
Table 6.16 List of selected ligands for molecular docking against PDB ID: 3HB5				
Name of ligands	Pub. Chem CID	Molecular formula	Mol. wt (g/mol)	Canonical smiles
Beta sitosterol	222284	C ₂₉ H ₅₀ O	414.7	<chem>CCC(CCC(C)C1CCC2C1(CCC3C2CC=C4C3(CCC(C4)O)C)C)C(C)C</chem>
Germanicol acetate	14167342	C ₃₂ H ₅₂ O ₂	468.8	<chem>CC(=O)OC1CCC2(C3CCC4C5=CC(CCC5(CCC4(C3(CCC2C1(C)C)C)C)C)C)C</chem>
Germanicol	122857	C ₃₀ H ₅₀ O	426.7	<chem>CC1(CCC2(CCC3(C(C2=C1)C)CC4C3(CCC5C4(CCC(C5(C)C)O)C)C)C)C</chem>
Rutin	5280805	C ₂₇ H ₃₀ O ₁₆	610.5	<chem>CC1C(C(C(C(O1)OCC2C(C(C(C(O2)OC3=C(OC4=CC(=CC(=C4C3=O)O)O)C5=CC(=C(C=C5)O)O)O)O)O)O)O</chem>

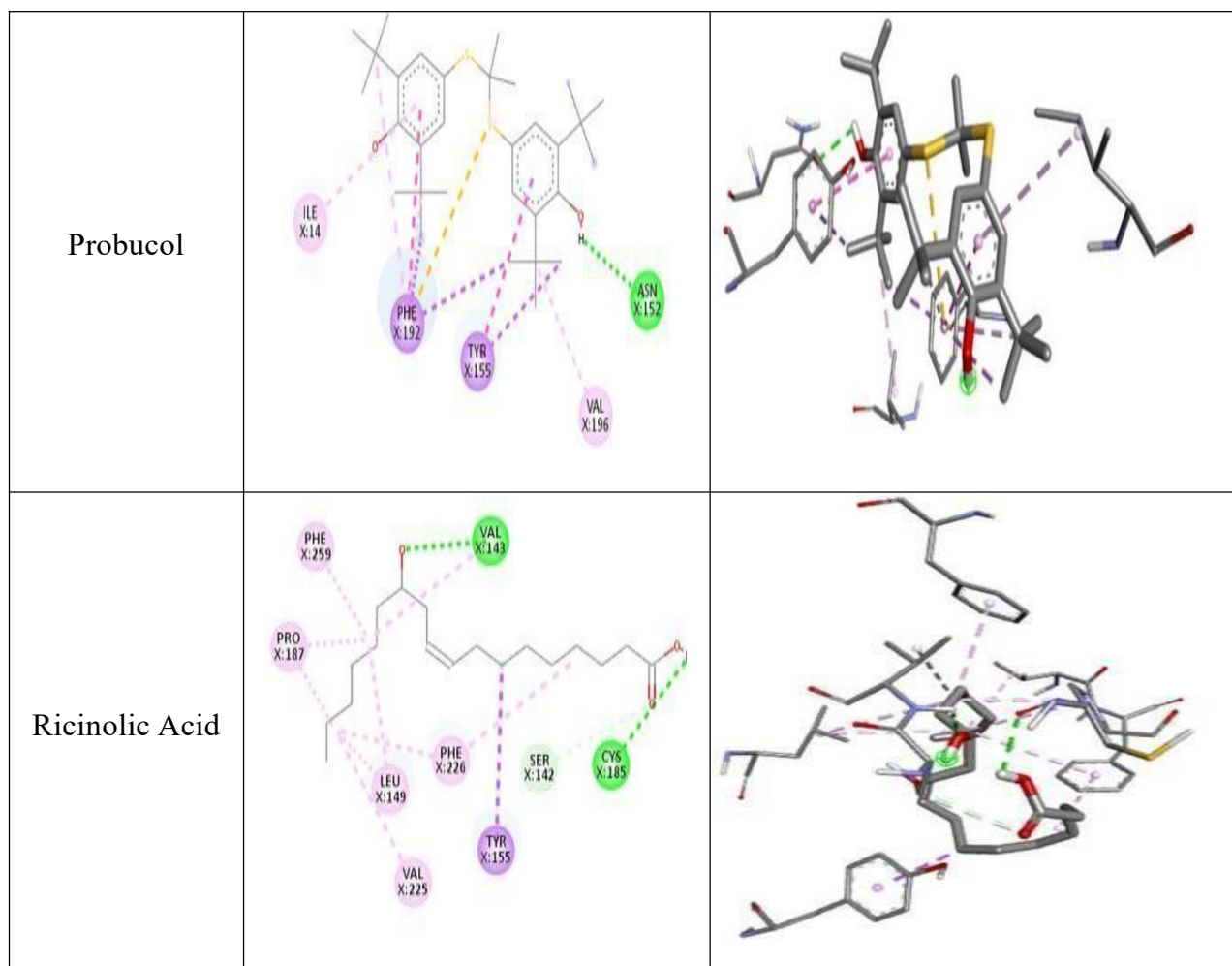
Kaempferol-3 O-Glucoside	5282102	C ₂₁ H ₂₀ O ₁₁	448.4	<chem>C1=CC(=CC=C1C2=C(C(=O)C3=C(C(=C(C=C3O2)O)O)OC4C(C(C(C(O4)CO)O)O)O)O</chem>
Ricine	10666	C ₈ H ₈ N ₂ O ₂	164.16	<chem>CN1C=CC(=C(C1=O)C#N)OC</chem>
Stigmasterol	5280794	C ₂₉ H ₄₈ O	412.7	<chem>CCC(C=CC(C)C1CCC2C1(CC3C2CC=C4C3(CCC(C4)O)C)C)C(C)C</chem>
Probucol	4912	C ₃₁ H ₄₈ O ₂ S ₂	516.8	<chem>CC(C)(C)C1=CC(=CC(=C1O)C(C)(C)C)SC(C)(C)SC2=CC(=C(C(=C2)C(C)(C)C)O)C(C)(C)C</chem>
Ricinolic acid	643684	C ₁₈ H ₃₄ O ₃	298.5	<chem>CCCCCCCC(CC=CCCCCCCCC(=O)O)O</chem>

Table 6.17 2D and 3D interaction of ligand against PDB ID:3HB5

Name of ligand	2D interaction	3D interaction
Beta-sitosterol		

<p>Germanicol acetate</p>		
<p>Germanicol</p>		
<p>Rutin</p>		

<p>Kaempferol-3-o-glucoside</p>		
<p>Ricinine</p>		
<p>Stigmasterol</p>		



Molecular docking

Table 6.18 Binding affinities of ligand against PDB ID: 3HB5

Name of ligands	Outligand mode (Binding affinity kcal/mol)								
	01	02	03	04	05	06	07	08	09
Beta-sitosterol	-9.5	-9.1	-9.1	-8.3	-8.3	-8.2	-7.8	-7.4	-7.2
Germanicol acetate	-9.1	-6.9	-6.7	-6.4	-	-	-	-	-
Germanicol	-7.6	-7.3	-	-	-	-	-	-	-
Rutin	-8.7	-8.3	-8.0	-7.7	-7.7	-7.7	-7.6	-7.6	-7.4

Kaempferol-3-O-glucoside	-9.2	-8.2	-7.8	-7.7	-7.5	-7.4	-7.1	-7.1	-6.6
Ricinine	-5.5	-5.5	-5.4	-5.4	-5.3	-5.2	-5.2	-5.2	-5.2
Stigmasterol	-9.3	-9.2	-9.1	-8.6	-8.6	-8.1	-7.9	-7.7	-7.5
Probucol	-9.8	-9.8	-9.8	-9.8	-9.7	-9.7	-9.7	-9.6	-9.0
Ricinolic acid	-6.4	-6.1	-6.1	-6.1	-6.0	-6.4	-5.9	-5.9	-5.9

Table 6. 19 Amino acid residues and bond interaction of protein and ligand

Name of ligands	Binding energy (Kcal/mol)	Bond	Amino acid residues
Beta-sitosterol	-9.5	Hydrogen bond Hydrophobic	GLY, ILE14, PRO187, VAL188, ILE14 PHE192
Germanicol acetate	-9.1	No interaction	Nil
Germanicol	-7.6	Hydrogen Bond	ASN152, HD22
Rutin	-8.7	Hydrogen Bond Hydrophobic	TYR155, GLY94, PHE192, PRO187, MET193
Kaempferol-3-O-Glucoside	-9.2	Hydrophobic	187, LEU149, MET193
Ricinine	-5.5	Hydrogen Bond Hydrophobic	VAL188, THR190, HG1 , THR190, GLY141 ILE14, VAL188

Stigmasterol	-9.3	Hydrogen Bond Hydrophobic	ASN90, HD22 ,GLY9, ILE14, PRO187, VAL188, VAL188, ILE14
Probucol	-9.8	Hydrogen Bond Hydrophobic	ASN152, TYR155, PHE192
Ricinolic acid	-6.4	Hydrogen Bond Hydrophobic	ASN152 PHE192

6.3 Part -III: Pharmacological approach

6.3.1 *In vitro* antioxidant activity

6.3.1.1 *In vitro* antioxidant activity of extracts

In vitro antioxidant potential was assessed utilizing a range of techniques, such as the DPPH assay, ferric reducing antioxidant property, total antioxidant capacity, and total phenolic content, on aqueous, ethanolic, and petroleum ether extracts of powdered *Euphorbia pulcherrima* leaves. The results are displayed in Table 6.20.

Table 6.20 Anti-oxidant properties of *Euphorbia pulcherrima* in different extracts

Sr.No	Extract of <i>Euphorbia pulcherrima</i> leaves	DPPH (% inhibition)	FRAP (mg /g)	Total anti-oxidant capacity (mg AA/g)	Total phenolic content (mg GA/g)
1.	Aqueous	56.21± 0.10	0.50± 0.015	52.25 ± 0.15	1.70 ± 0.15
2.	Ethanol	74. 20± 0.10	0.77± 0.10	79.85 ± 0.02	2.65 ± 0.10
3.	Petroleum ether	86.10± 0.15	0.80 ± 0.15	90.75 ± 0.10	3.85 ± 0.15
4	Ascorbic acid (Std.)	89.35± 0.548	0.88± 0.010	94.00± 0.177	4.35± 0.487

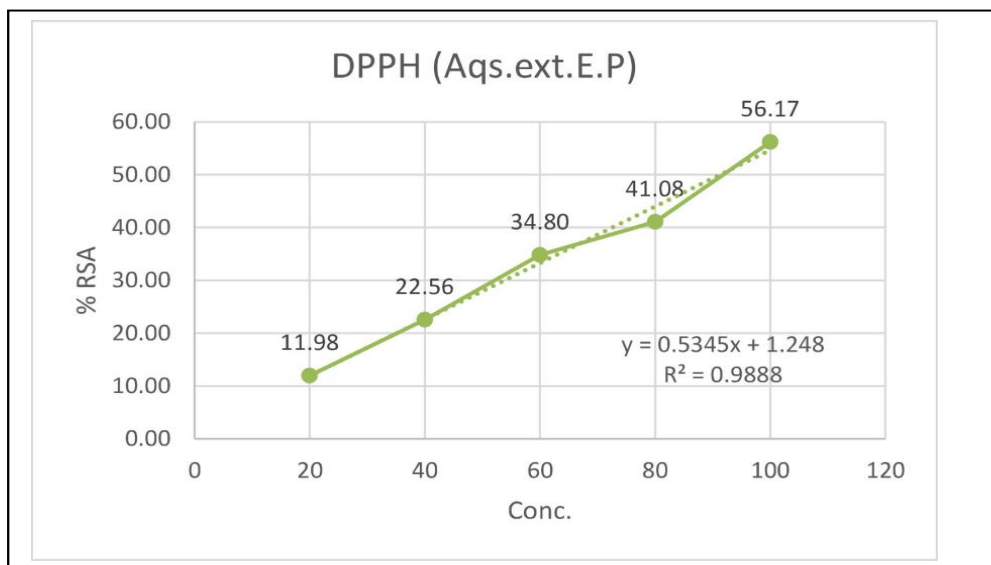


Figure 6.33 *In vitro* antioxidant activity of aqueous extract of *Euphorbia pulcherrima*

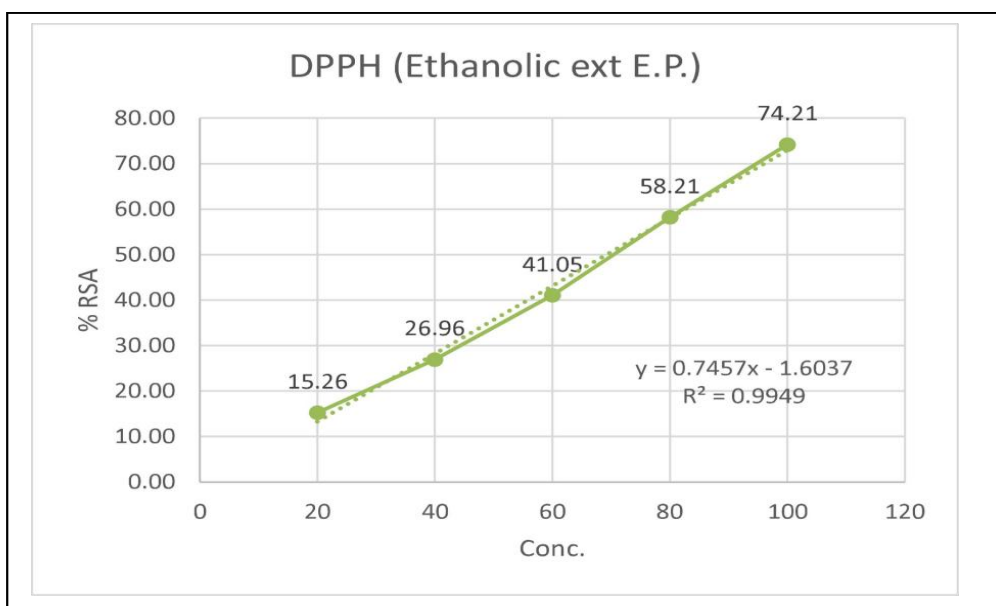


Figure 6.34 *In vitro* antioxidant activity of ethanolic extract of *Euphorbia pulcherrima* (DPPH)

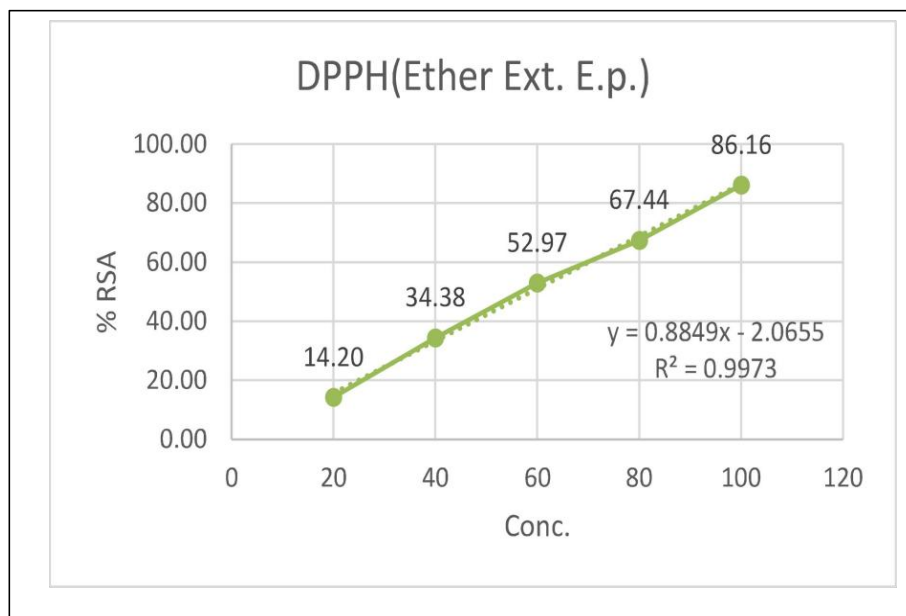


Figure 6.35 *In vitro* antioxidant activity of etheral extract of *Euphorbia pulcherrima* (DPPH)

Table 6.21 Anti-oxidant properties of *Ricinus communis* in different extracts

Sr. No	Extract of <i>Ricinus communis</i>	DPPH (% inhibition)	FRAP (mg/g)	Total anti-oxidant content (mgAA/g)	Total phenolic content (mg GA/g)
1.	Aqueous	52.81± 0.015	0.57± 0.010	56.5 ± 0.10	1.60 ± 0.015
2.	Ethanol	71. 10± 0.15	0.72± 0.10	78.5 ± 0.01	2.95 ± 0.015
3.	Petroleum ether	88.50± 0.10	0.84 ±0.015	92.5 ± 0.05	3.95 ± 0.10
4	Ascorbic acid (Std.)	89.35± 0.548	0.88± 0.010	94.00± 0.177	4.35± 0.487

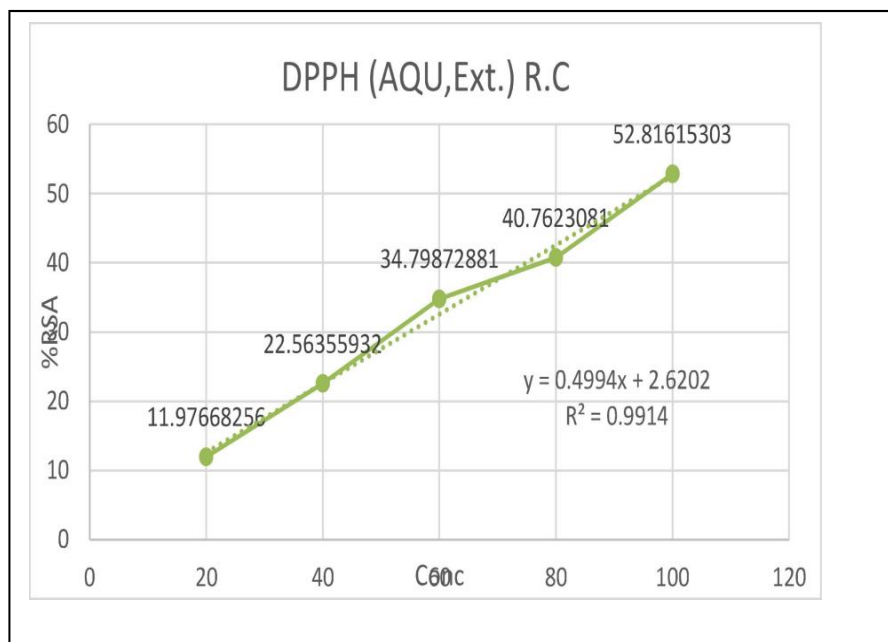


Figure 6.36 *In vitro* antioxidant activity of *Ricinus communis* aqueous extract (DPPH)

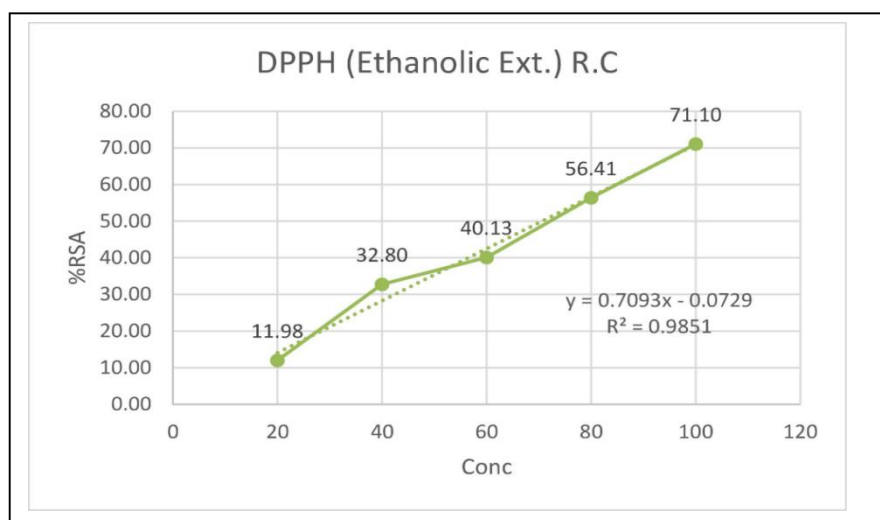


Figure 6.37 *In vitro* Antioxidant activity of ethanolic extract of *Ricinus communis* (DPPH)

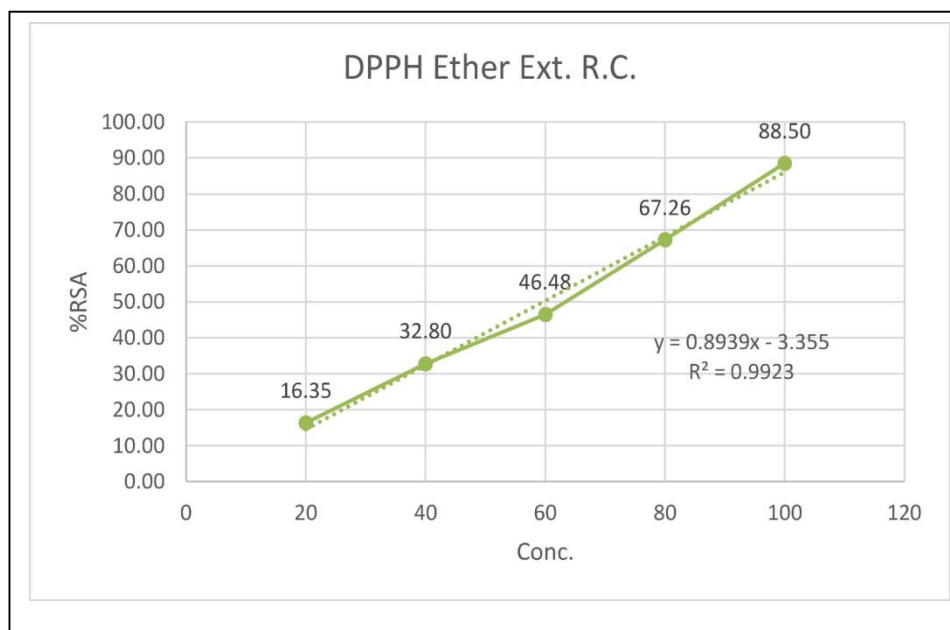


Figure 6.38 *In vitro* Antioxidant activity of ethereal extract of *Ricinus communis* (DPPH)

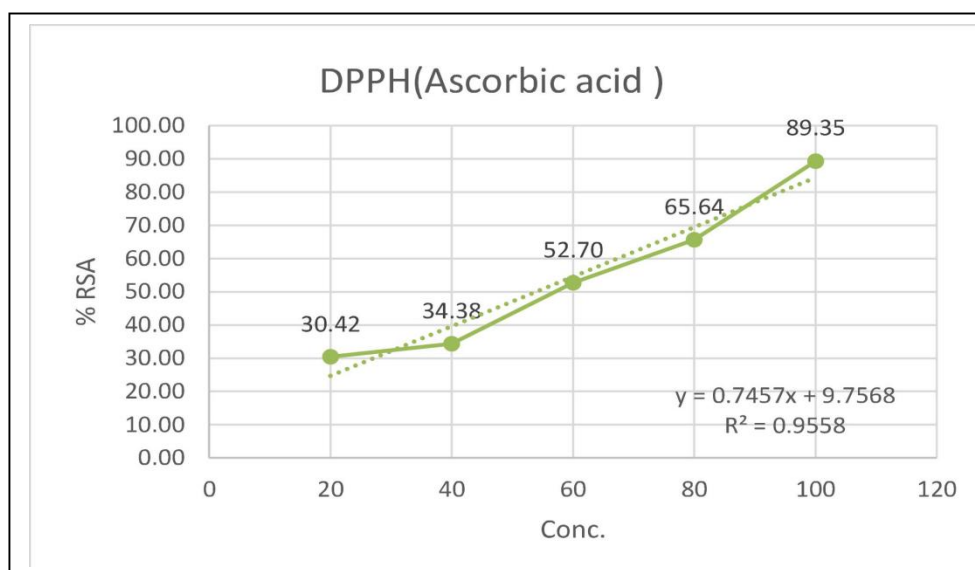


Figure 6.39 *In vitro* Antioxidant activity of ascorbic acid (DPPH)

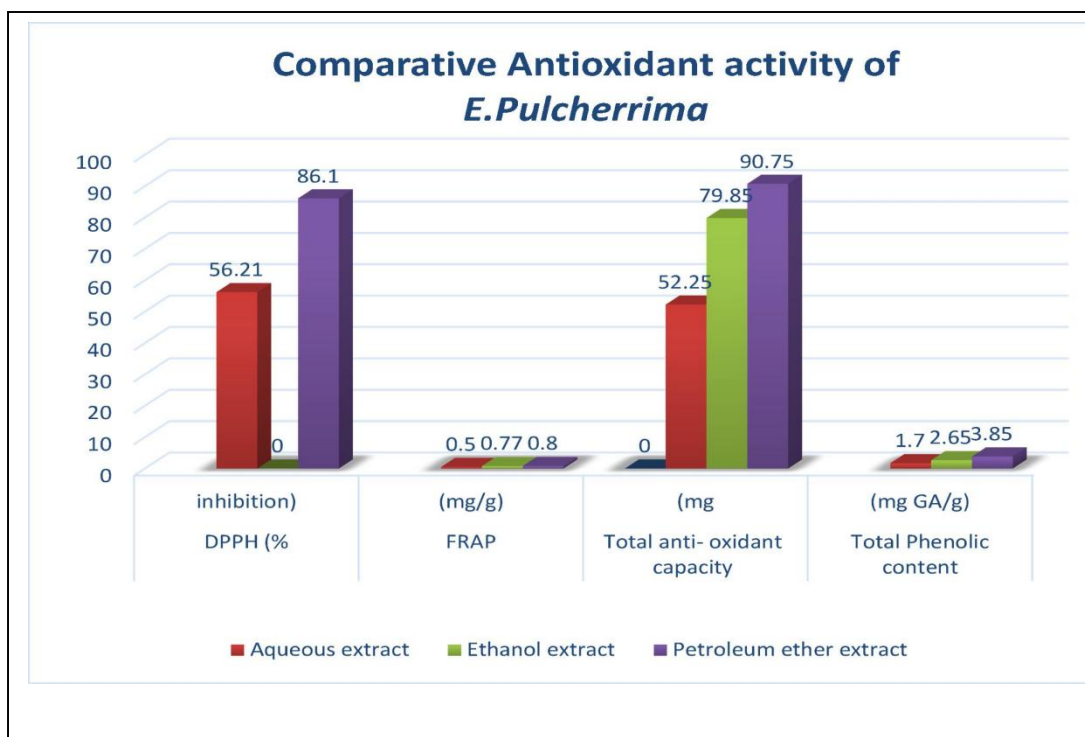


Figure 6.40 Comparative data of antioxidant activity of *Euphorbia pulcherrima*

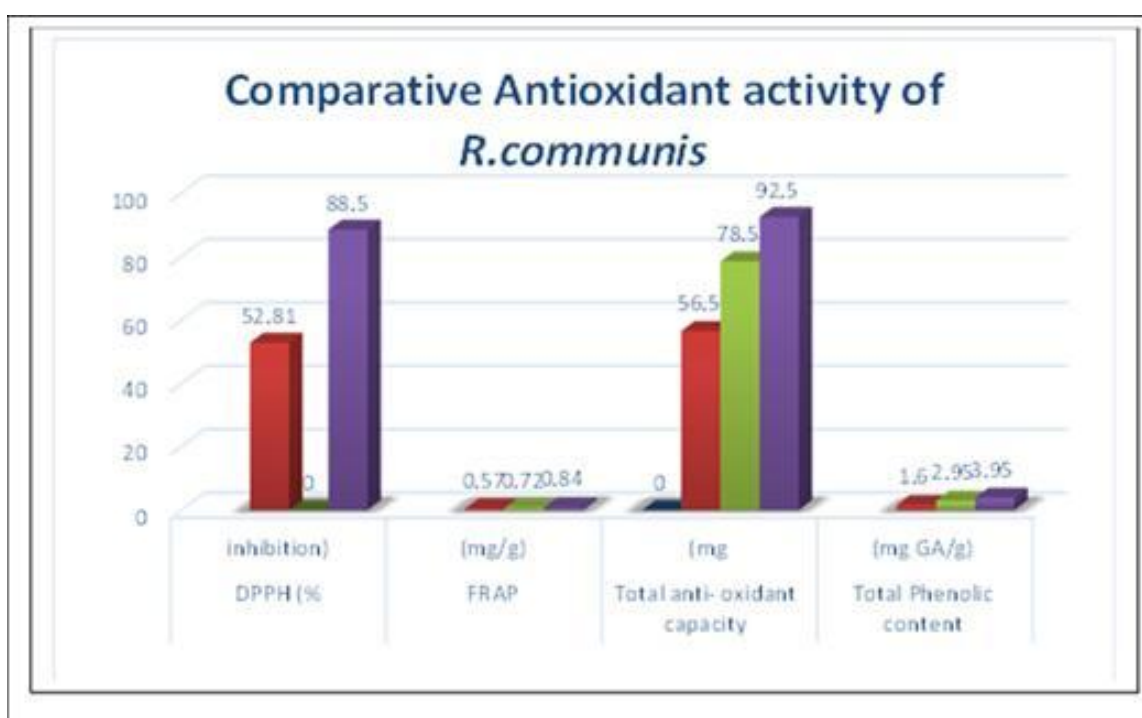


Figure 6.41 Comparative data of antioxidant activity of *Ricinus communis*

6.3.1.2 *In vitro* antioxidant activity of Beta-sitosterol and Stigmasterol (DPPH)

Table 6.22 *In vitro* Anti-Oxidant properties of Beta-sitosterol and Stigmasterol (DPPH)

Sr. no.	Sample (1mg/ml)	Absorbance	Mean	Percentage of radical scavenging activity (DPPH)
1	Control	1.689	1.858	-
		1.888		
		1.999		
2	Standard (Ascorbic acid)	0.789	0.781	57.96
		0.814		
		0.740		
3	Beta-sitosterol	1.404	1.405	24.38
		1.399		
		1.414		
4	Stigmasterol	1.423	1.444	22.28
		1.404		
		1.507		

From the *in vitro* antioxidant DPPH assay, it was clear that both the phytoconstituents possess good antioxidant potential.

6.3.1.3 *In vitro* antioxidant activity of Beta-sitosterol (SOD)

Table. 6.23 *In vitro* antioxidant study by SOD assay of Beta-sitosterol and Stigmasterol

Sr. no.	Sample (1mg/ml)	Absorbance	Mean	Percentage of radical scavenging
1	Control	0.711	0.770	-
		0.789		
		0.810		

2	Standard (Ascorbic acid)	0.098	0.102	86.75
		0.101		
		0.108		
3	Beta-sitosterol	0.280	0.264	65.71
		0.309		
		0.290		
4	Stigmasterol	0.280	0.293	61.94
		0.309		
		0.290		

From the *In vitro* antioxidant Superoxide scavenging activity it was clear that both the phytoconstituents possess good antioxidant potential.

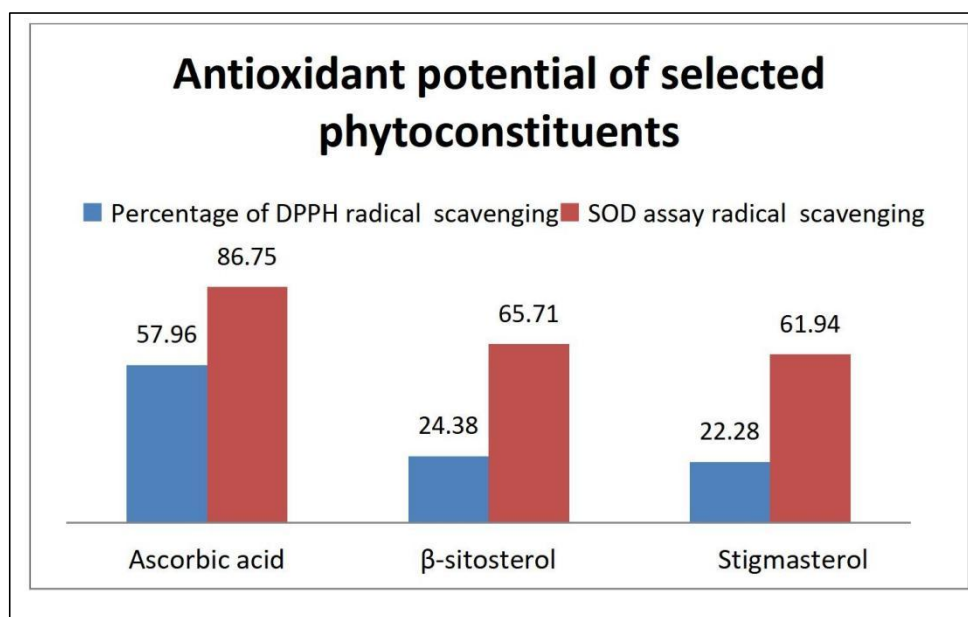


Figure 6.42 Antioxidant potential of isolated phytoconstituents

6.3.2 *In vitro* Anti-cancer cell line study of isolated phytoconstituents

The isolated Beta-sitosterol, stigmasterol, and its combination (50%) were screened against MCF-7 cell line specifically for breast cancer.

6.3.2.1 MTT assay of isolated phytoconstituents

6.3.2.1.1 MTT assay of isolated phytoconstituents using MCF-7 cell line

Table 6.24 MTT assay cell viability of isolated phytoconstituents on MCF-7

Isolated phytoconstituents	Concentration (µg/ml)	O D	Mean	% Inhibition
Control	---	0.899 0.891 0.837	0.875	-----
Beta-sitosterol	6.12	0.415 0.401 0.4	0.4053	53.68
	12.5	0.347 0.31 0.289	0.3153	63.96
	25	0.277 0.265 0.247	0.2630	69.94
	50	0.215 0.217 0.201	0.2110	75.89
	100	0.219 0.198 0.178	0.1983	77.33
Sigmasterol	6.12	0.715 0.712 0.719	0.7153	18.25
	12.5	0.617 0.638 0.604	0.6197	29.18
	25	0.542 0.476 0.546	0.5213	40.42
	50	0.409 0.423 0.412	0.4147	52.61
	100	0.367 0.345 0.323	0.3450	60.57
Combination of	6.12	0.514 0.512 0.509	0.5117	41.52

Beta-sitosterol + Sigmasterol	12.5	0.415 0.467 0.435	0.4390	49.83
	25	0.212 0.201 0.196	0.2030	76.80
	50	0.105 0.117 0.125	0.1157	86.78
	100	0.078 0.093 0.1	0.0903	89.67

Table. 6.25 Summary of MTT assay percent inhibition against MCF-7

Concentration (µg/ml)	Beta-sitosterol (% Inhibition)	Stigmasterol (% Inhibition)	Combination (% Inhibition)
6.12	53.68 ± 0.021	18.25 ± 0.080	41.52 ± 0.480
12.5	63.96 ± 0.355	29.18 ± 0.166	49.83 ± 0.040
25	69.94 ± 0.137	40.42 ± 0.061	76.80 ± 0.286
50	75.89 ± 0.100	52.61 ± 0.426	86.78 ± 0.820
100	77.33 ± 0.075	60.57 ± 0.126	89.67 ± 0.880

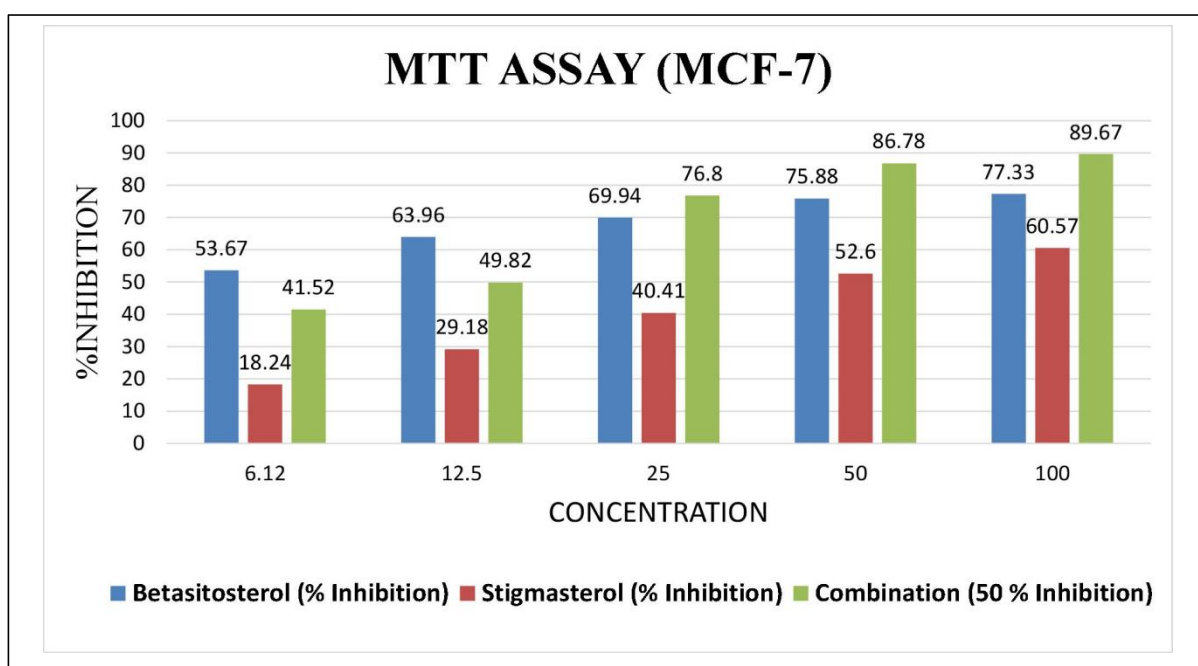


Figure 6.43 Comparative data of MTT assay (MCF-7 cell line)

6.3.2.1.2 MTT assay of isolated constituents using MBA-MB-231 cell line

Table. 6.26 MTT assay cell viability of isolated phytoconstituents on MBA-MB-231

Isolated phytoconstituents	Concentration (µg/ml)	OD	Mean	% Inhibition
Control	-	0.855 0.843 0.837	0.845	-
Beta- sitosterol	6.1	0.415 0.41 0.402	0.409	51.60
	12.5	0.348 0.302 0.322	0.324	61.66
	25	0.25 0.275 0.243	0.256	69.70
	50	0.205 0.218 0.211	0.2113333	74.99
	100	0.217 0.203 0.193	0.2043333	75.82
Sigmasterol	6.1	0.755 0.761 0.742	0.7526667	10.93
	12.5	0.633 0.64 0.639	0.6373333	24.58
	25	0.574 0.512 0.564	0.5500000	34.91
	50	0.402 0.399 0.412	0.4043333	52.15
	100	0.316 0.325 0.317	0.3193333	62.21

Combination of Beta-sitosterol + Stigmasterol	6.1	0.502 0.499 0.491	0.4973333	41.14
	12.5	0.478 0.467 0.462	0.4690000	44.50
	25	0.199 0.195 0.187	0.4043333	77.15
	50	0.118 0.102 0.122	0.1140000	86.51
	100	0.089 0.089 0.099	0.0923333	89.07

Table. 6.27 Summary of MTT assay Percent inhibition against MDA-MB-231

Concentration ($\mu\text{g/ml}$)	Beta-sitosterol (% Inhibition)	Stigmasterol (% Inhibition)	Combination (% Inhibition)
6.12	51.59 \pm 0.095	10.93 \pm 0.216	41.14 \pm 0.064
12.5	61.66 \pm 0.284	24.58 \pm 0.221	44.50 \pm 0.680
25	69.70 \pm 0.174	34.91 \pm 0.055	77.15 \pm 0.485
50	74.99 \pm 0.461	52.15 \pm 0.062	86.51 \pm 0.165
100	75.82 \pm 0.080	62.21 \pm 0.118	89.07 \pm 0.627

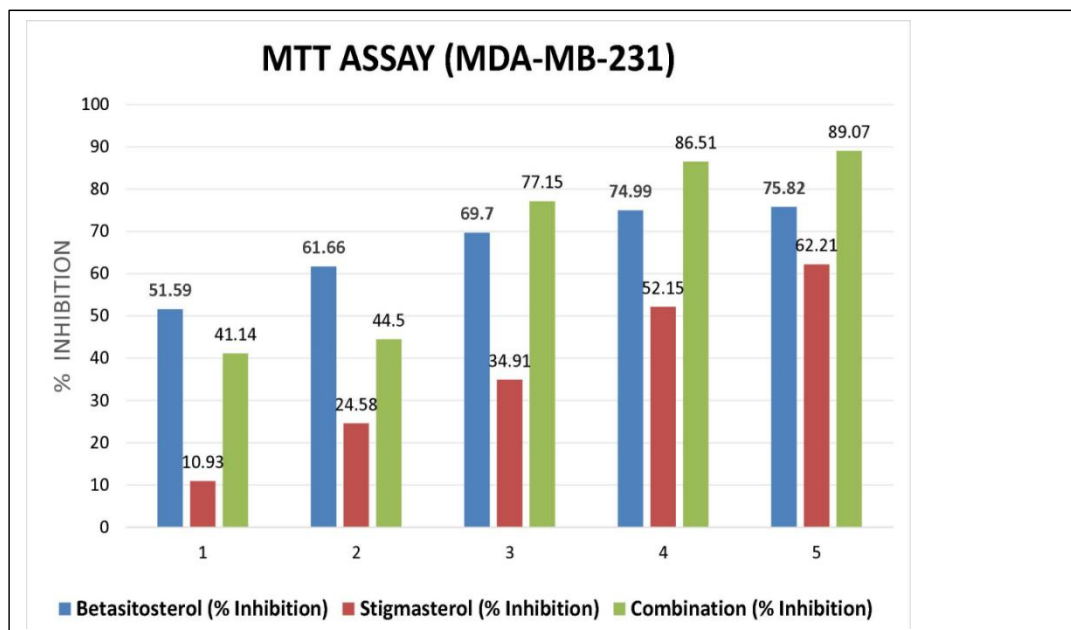


Figure 6.44 Comparative data of MTT assay (MDA-MB-231 cell line)

6.3.2.2 SRB assay of isolated constituents

Beta sitosterol and Stigmasterol and combination of both compounds of different concentration (6.12 µg/ml, 12.5 µg/ml, 25 µg/ml, 50 µg/ml, 100 µg/ml) were investigated for anticancer activity against MCF-7 and MDA-MB-231 cell lines using SRB method.

6.3.2.2.1 SRB assay of isolated constituents using MCF-7 cell line

Table 6.28 SRB assay cell viability of isolated phytoconstituents on MCF-7

Isolated compound	Concentration (µg/ml)	O D	Mean	% Inhibition
Control	-	0.314	0.319	-
		0.326		
		0.317		
		0.21		
	6.12	0.218	0.212	33.44
		0.209		
		0.215		

Beta-Sitosterol	12.5	0.167 0.235	0.206	35.53
	25	0.212 0.201 0.196	0.203	36.36
	50	0.179 0.168 0.182	0.176	44.72
	100	0.078 0.093 0.1	0.090	71.68
Sigmasterol	6.12	0.315 0.211 0.389	0.305	4.39
	12.5	0.217 0.288 0.254	0.253	20.69
	25	0.242 0.189 0.213	0.215	32.71
	50	0.214 0.216 0.209	0.213	33.23
	100	0.163 0.143 0.187	0.164	48.48
Combination of (Beta-sitosterol +Sigmasterol)	6.12	0.179 0.168 0.182	0.176	44.72
	12.5	0.154 0.158 0.168	0.160	49.84

	25	0.135	0.139	56.43
		0.139		
		0.143		
	50	0.124	0.128	59.98
		0.142		
		0.117		
	100	0.065	0.061	80.88
		0.057		
		0.061		

Table. 6.29 Summary of SRB assay percent inhibition against MCF-7

Concentration ($\mu\text{g/ml}$)	Beta-sitosterol (% Inhibition)	Stigmasterol (% Inhibition)	Combination (% Inhibition)
6.12	33.43 ± 0.081	4.38 ± 0.035	44.72 ± 0.030
12.5	35.52 ± 0.035	20.68 ± 0.067	49.84 ± 0.044
25	36.36 ± 0.157	32.70 ± 0.139	56.42 ± 0.046
50	44.72 ± 0.102	33.22 ± 0.015	59.97 ± 0.006
100	71.68 ± 0.143	48.48 ± 0.065	80.88 ± 0.066

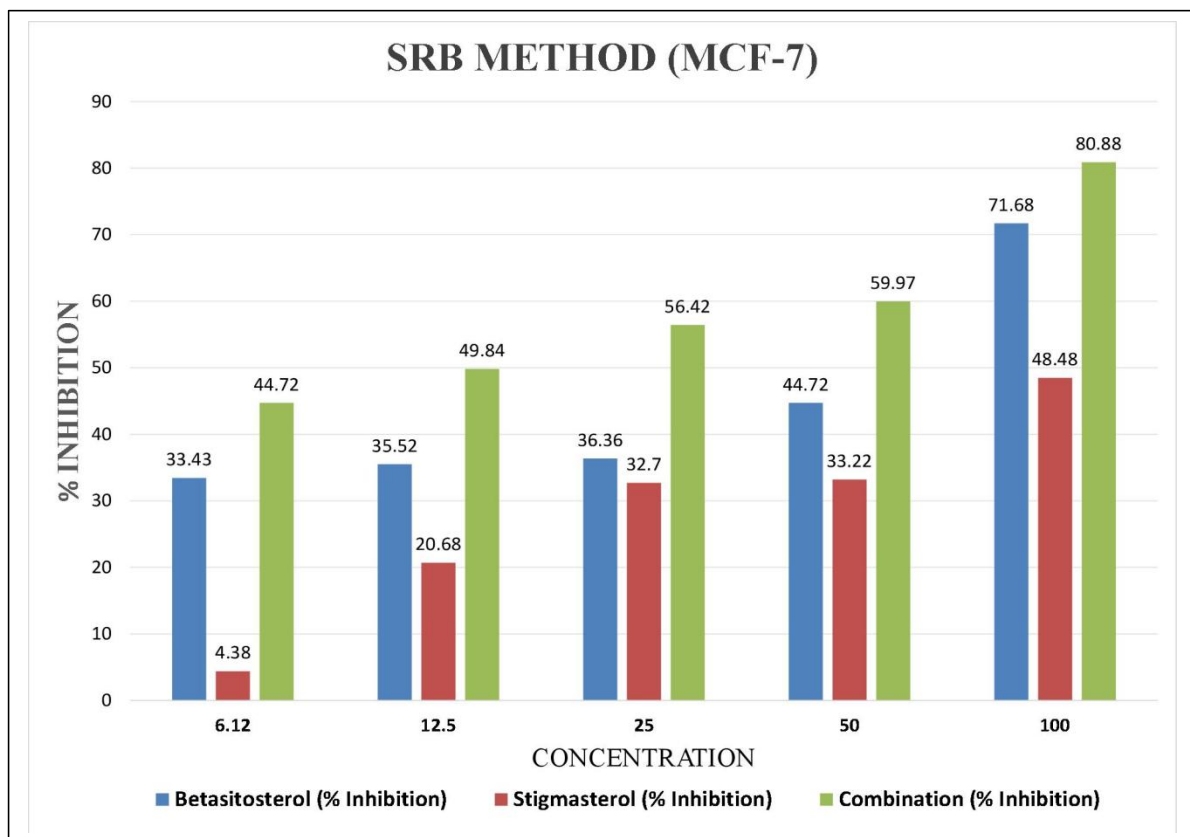


Figure 6.45 Comparative data of SRB method (MCF-7 cell line)

6.3.2.2.2 SRB assay of isolated phytoconstituents using MDA-MB-231 cell line

Table. 6.30 SRB assay cell viability of isolated phytoconstituents on MDA-MB-231

Isolated compound	Concentration (µg/ml)	O D	Mean	% Inhibition
Control	-	0.333	0.325	-
		0.316		
		0.326		
	6.25	0.22 0.216 0.219	0.218	32.82

Beta- sitosterol	12.5	0.213 0.195 0.209	0.205	36.72
	25	0.203 0.192 0.193	0.196	39.69
	50	0.123 0.129 0.12	0.124	61.85
	100	0.087 0.085 0.075	0.082	74.67
Sigmasterol	6.25	0.287 0.29 0.268	0.281	13.33
	12.5	0.274 0.265 0.245	0.261	19.59
	25	0.239 0.265 0.249	0.251	22.77
	50	0.222 0.215 0.21	0.215	33.64
	100	0.193 0.186 0.176	0.185	43.08
	6.25	0.189 0.178 0.186	0.184	43.28

Combination of Beta- sitosterol + Stigmasterol	12.5	0.169	0.162	50.15
		0.165		
		0.152		
	25	0.136	0.136	58.15
		0.142		
		0.13		
	50	0.119	0.120	63.08
		0.132		
		0.109		
	100	0.078	0.070	78.26
		0.045		
		0.089		

Table. 6.31 Summary of SRB assay percent inhibition against MDA-MB-231

Concentration ($\mu\text{g/ml}$)	Beta-sitosterol (% Inhibition)	Stigmasterol (% Inhibition)	Combination (% Inhibition)
6.12	32.82 ± 0.095	13.33 ± 0.038	43.28 ± 0.017
12.5	36.72 ± 0.065	19.59 ± 0.020	50.15 ± 0.038
25	39.69 ± 0.070	22.77 ± 0.017	58.15 ± 0.029
50	61.84 ± 0.044	33.64 ± 0.046	63.08 ± 0.035
100	74.76 ± 0.044	43.08 ± 0.038	78.26 ± 0.029

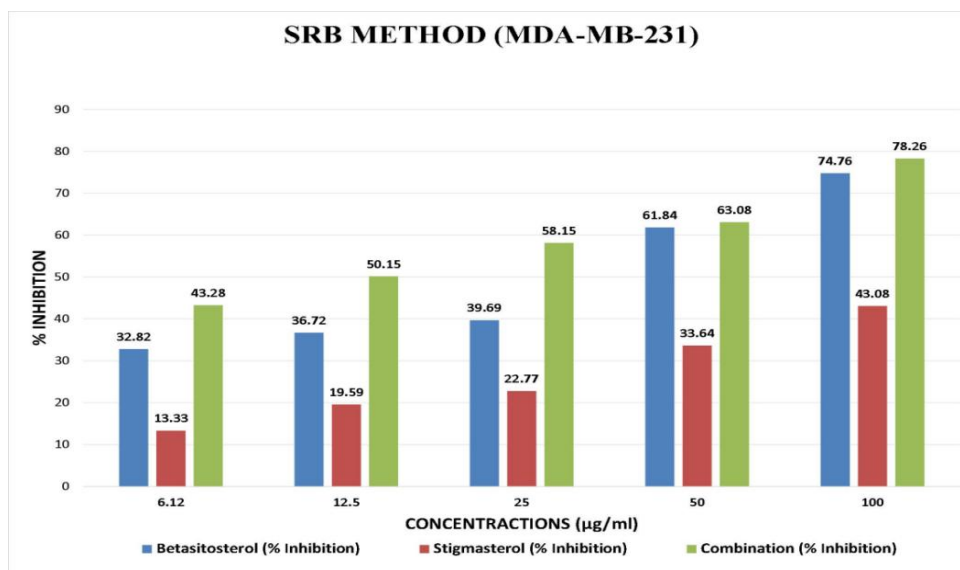


Figure 6.46 Comparative data of SRB method (MDA-MB-231 cell line)

6.3.2.3 Bliss independence for dose response synergism

Bliss independence model is widely used to analyse drug combination data when screening candidate drug combination for observation of the antagonism, additivity and synergistic effect.

6.3.2.3.1 Bliss independence for MTT assay (MCF-7 cell line)

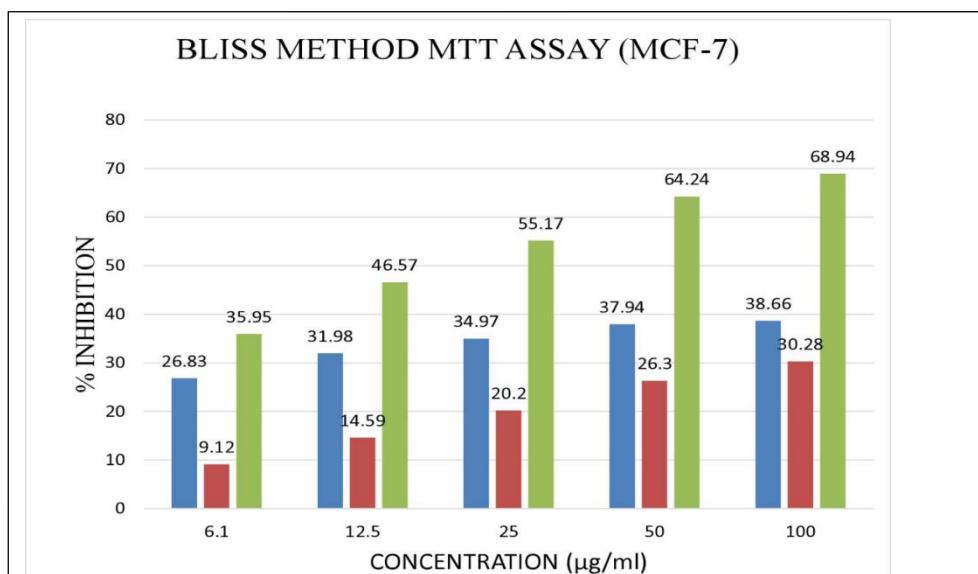


Figure 6.47 Bliss independence for synergism (MTT assay using MCF-7 cell line)

Table. 6.32 Bliss independence expected and observed effect (MTT assay MCF-7)

Concentration (µg/ml)	Expected effect	Observed effect	Combination index (CI)
6.1	35.95	41.52	0.2
12.5	46.57	49.82	0.3
25	55.17	76.8	0.3
50	64.24	86.78	0.4
100	68.94	89.67	0.4

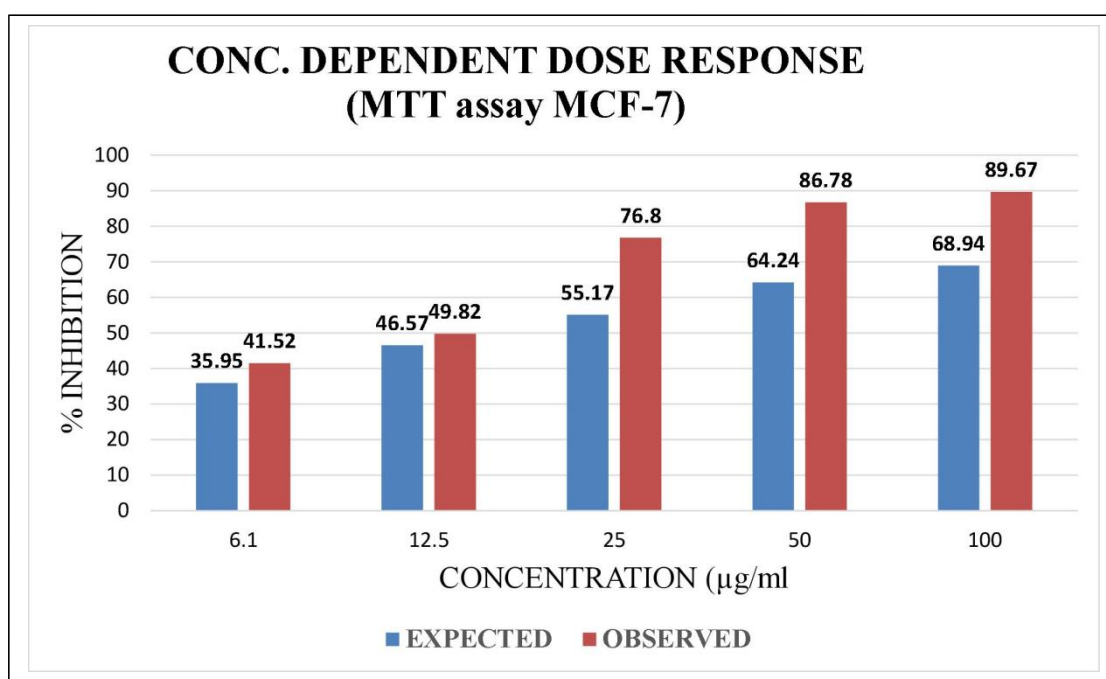


Figure 6.48 Concentration dependent dose response (MTT assay using MCF-7)

6.3.2.3.2 Bliss independence for MTT assay (MDA-MB-231 cell line)

Table. 6.33 Bliss independence expected and observed effect(MTT assay MDA-MB-231)

Concentration (µg/ml)	Expected effect	Observed effect	Combination index (CI)
6.1	36.72	41.14	0.2
12.5	43.12	44.5	0.2
25	52.3	77.15	0.3
50	63.56	86.51	0.3
100	69.01	89.07	0.4

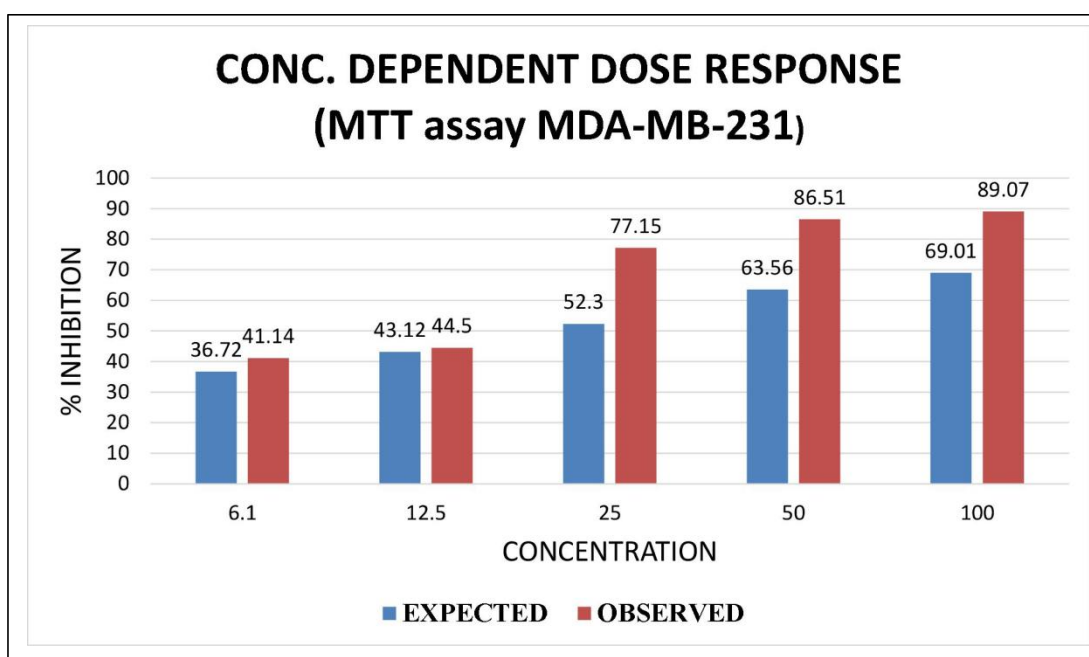


Figure 6.49 Bliss independence for synergism (MTT assay using MDA-MB-231)

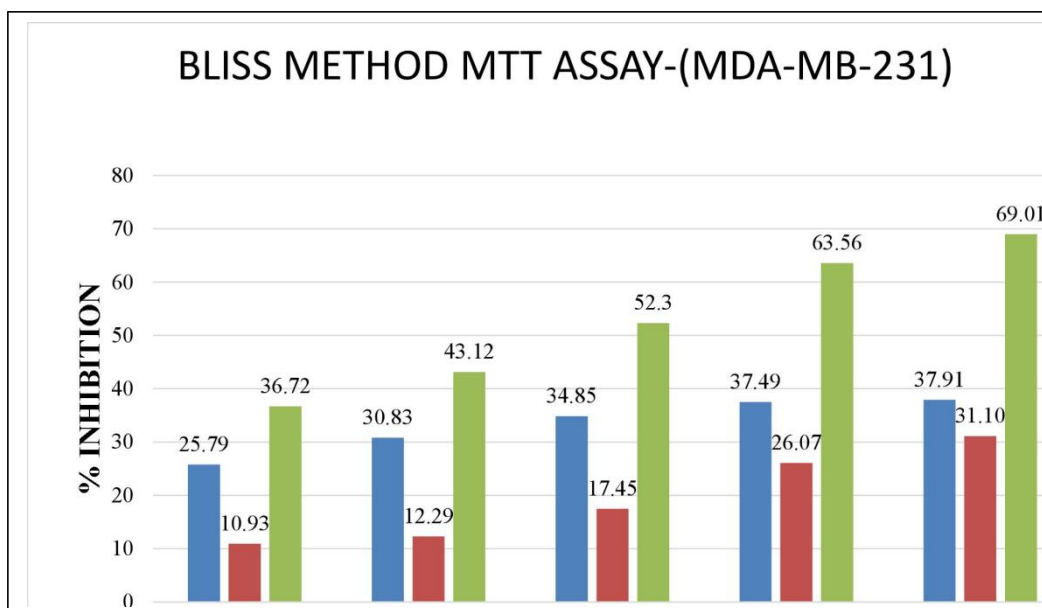


Figure 6.50 Concentration dependent dose response (MTT assay using MDA-MB-231)

6.3.2.3.3 Bliss independence for SRB method (MCF-7 cell line)

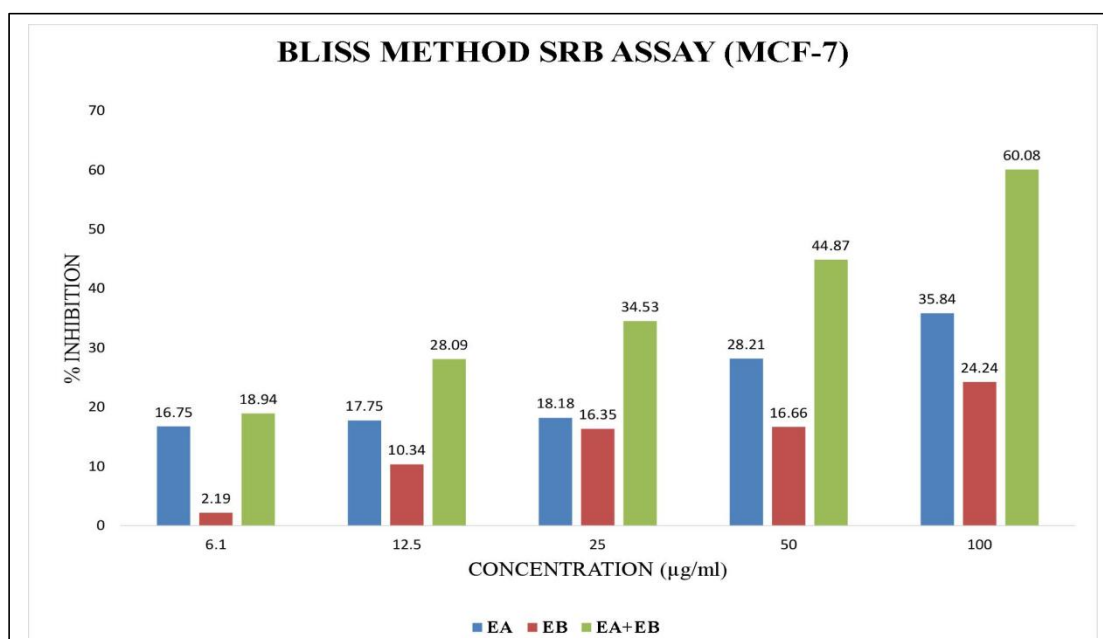


Figure 6.51 Bliss independence for synergism (SRB assay using MCF-7)

Table. 6.34 Bliss independence expected and observed effect (SRB assay MCF-7)

Concentration (µg/ml)	Expected effect	Observed effect	Combination index (CI)
6.1	18.94	44.72	0.05
12.5	28.09	49.84	0.2
25	34.53	56.42	0.3
50	44.87	59.97	0.3
100	60.08	80.88	0.4

6.3.2.3.4 Bliss independence for SRB method (MDA-MB-231 cell line)

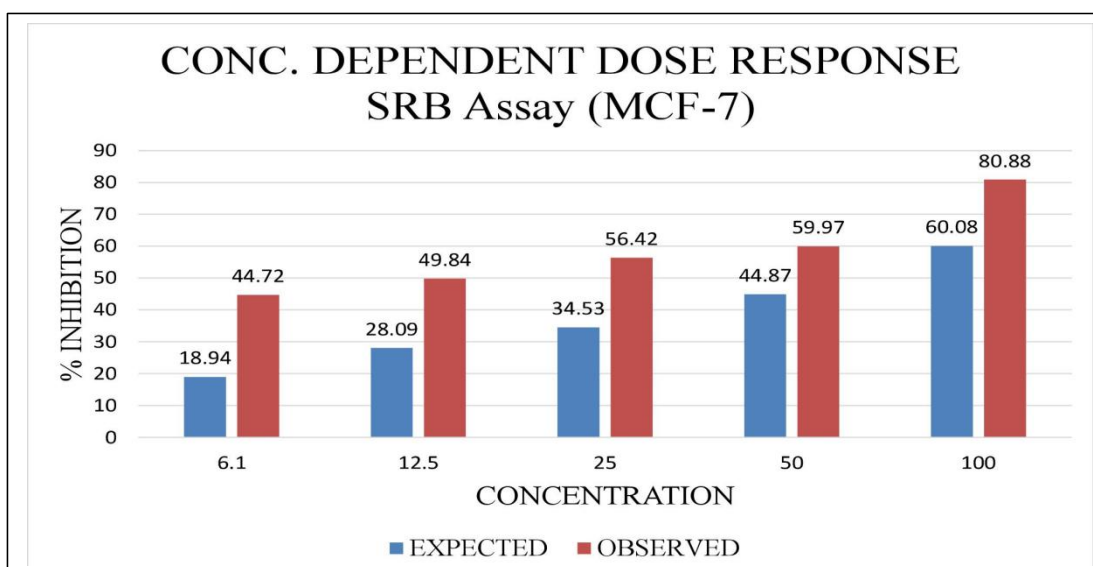


Figure 6.52 Concentration dependent dose response (SRB assay using MCF-7)

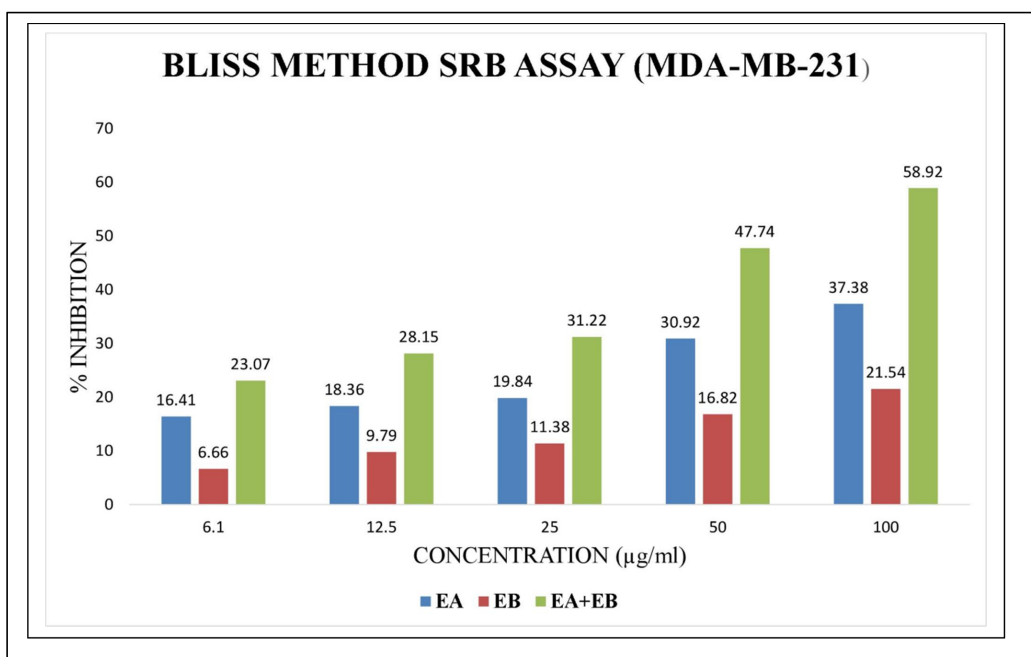


Figure 6.53 Bliss independence for synergism (SRB assay using MDA-MB-231)

Table. 6.35 Bliss independence expected and observed effect (SRB assay MDA-MB-231)

Concentration (µg/ml)	Expected effect	Observed effect	Combination index (CI)
6.1	23.07	43.28	0.2
12.5	28.15	50.15	0.3
25	31.22	58.15	0.3
50	47.74	63.08	0.3
100	58.92	78.26	0.3

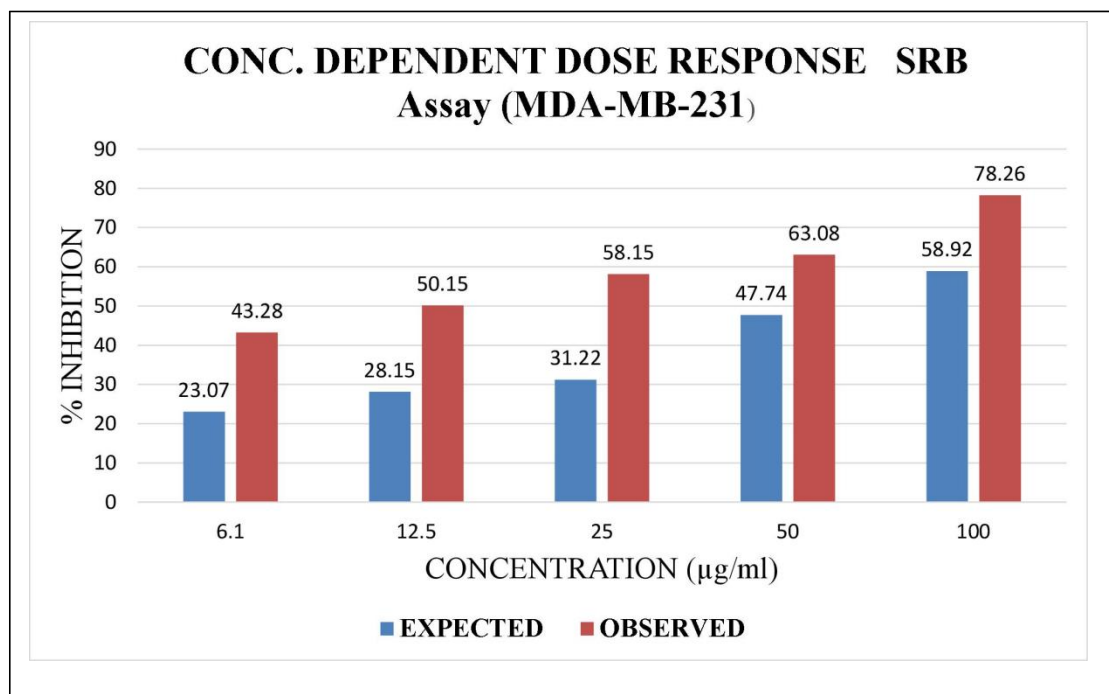


Figure 6.54 Concentration dependent dose response (SRB assay using MDA-MB-231)

From the *in vitro* cell line study it was observed that Beta-sitosterol and Stigmasterol shows good anticancer potential and it shows synergistic effect which is proved by Bliss independence model and dose response depends on concentration.

6.4 Part -IV: Pharmaceutical chemistry approach

6.4.1 Molecular docking study of CES derivatives of Beta-sitosterol and stigmasterol

For synthetic derivative formation from isolated compounds (Beta-sitosterol and stigmasterol) the hypothetical derivatives incorporating different polybasic acids such as maleic anhydride, phthalic anhydride, adipic acid, malonic acid, citric acid etc. were prepared using chemsketch. These prepared CES ester derivatives were screened via *in silico* molecular docking method for analyzing its pharmacological potential. The *in silico* pharmacological potential of synthetic derivatives was screened by using autodock vina, biovia discovery studio and open bable software by using several acids such as maleic anhydride, phthalic anhydride, adipic acid, citric acid and malonic acid. The binding affinities of these derivatives were screened against 3BH5. Amongst them CES derivative of Beta-sitosterol using maleic anhydride shows

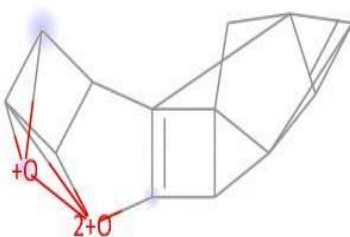

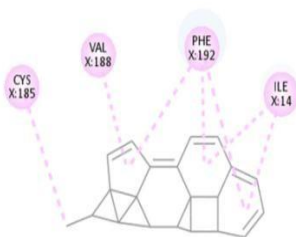
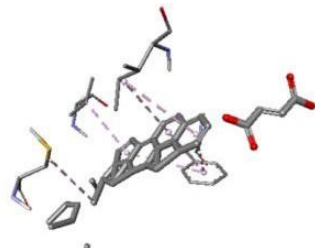
highest binding affinity -18.4 kcal/mol while CES derivative of Stigmasterol using maleic anhydride shows maximum binding affinity -18.6 kcal/mol.

6.4.1.1 Molecular docking for CES derivatives of Beta-sitosterol

Table. 6.36 Binding affinities of Beta-sitosterol derivatives (CES)

Beta-sitosterol CES derivatives	OUTLIGAND MODE (Binding affinity kcal/mol)								
	01	02	03	04	05	06	07	08	09
Adipic acid	-16.8	-16.5	-16.5	-16.2	-16.0	-16.0	-15.9	-15.8	-
Maleic anhydride	-18.4	-18.0	-17.7	-17.6	--17.4	-17.3	-17.1	-16.8	-16.7
Phthalic anhydride	-13.5	-13.2	-13.1	-12.9	-12.0	-11.8	-11.8	-11.7	-11.6
Cirtic acid	-18.0	-18.0	-18.0	-17.8	-	-	-	-	-
Malonic acid	-17.9	-17.4	-17.0	-16.9	-16.9	-16.8	-16.8	-16.5	-16.4

Table. 6.37 2D and 3D interaction of Beta-sitosterol derivatives

Beta-sitosterol CES derivatives	2D INTERACTION	3D INTERACTION
Adipic acid		
Maleic anhydride		

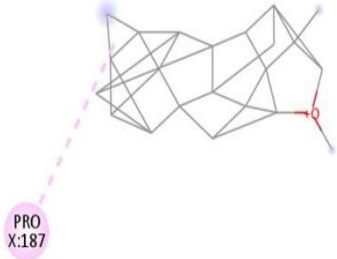
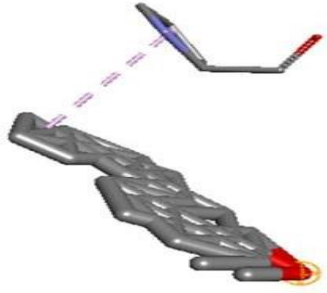
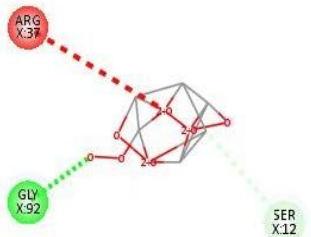
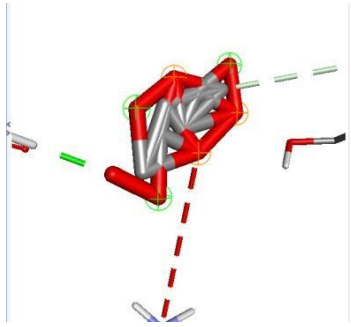
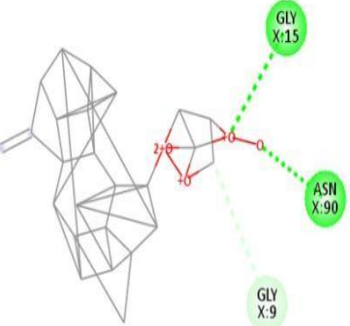
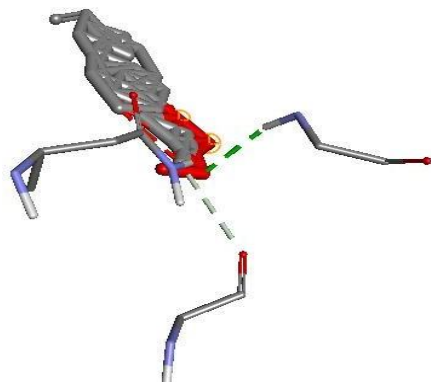
Phthalic anhydride		
Citric acid		
Malonic acid		

Table. 6.38 Amino acid residues and bond interaction of Beta-sitosterol derivatives

Beta-sitosterol CES derivatives	Binding energy (Kcal/mol)	Bond	Amino acid residues
Maleic anhydride	-18.4	Hydrophobic	ILE14 , VAL188 ,CYS185 PHE192,HE192

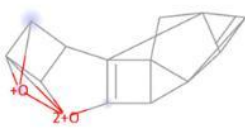

Phthalic anhydride	-13.5	Hydrophobic	PRO187
Citric acid	-18.0	Conventional hydrogen bond	GLY92 ,SER12
Malonic acid	-17.9	Hydrogen bond	GLY15,ASN90 ,GLY9
Adipic acid	-16.8	Unfavorable bump	-

6.4.1.2 Molecular docking for CES derivatives of Stigmasterol

Table. 6.39 Binding affinities of Stigmasterol derivatives (CES)

Stigmasterol CES derivatives	OUTLIGAND MODE (Binding affinity kcal/mol)								
	01	02	03	04	05	06	07	08	09
Adipic acid	-16.8	-16.6	-16.5	-16.2	-16.0	-16.0	-16.0	-15.8	-15.7
Maleic anhydride	-18.6	-18.6	-18.4	-18.3	-18.1	-18.0	-18.0	-18.0	-17.9
Phthalic anhydride	-18.0	-18.0	-17.7	-17.6	-17.5	-17.2	-17.1	-17.0	-16.8
Cirtic acid	-18.4	-18.0	-18.0	-17.8	-17.7	-	-	-	-
Malonic acid	-17.9	-17.4	-17.0	-17.0	-16.9	-16.9	-16.8	-16.8	-16.5

Table. 6.40 2D and 3D interaction of Stigmasterol derivatives

Stigmasterol CES derivatives	2D INTERACTION	3D INTERACTION
Adipic acid		

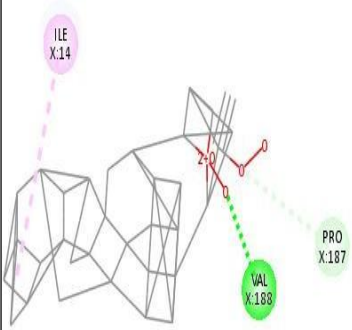
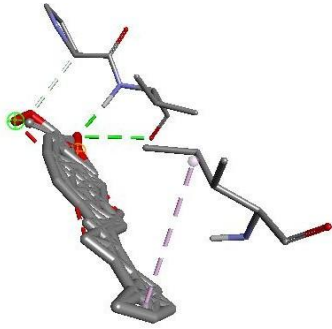
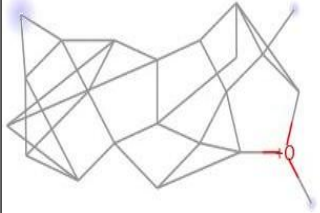
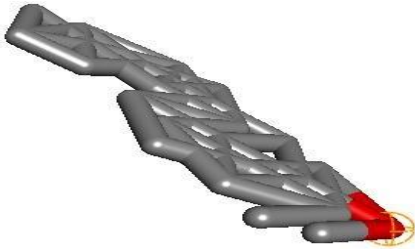
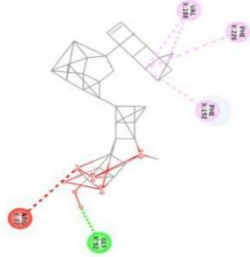
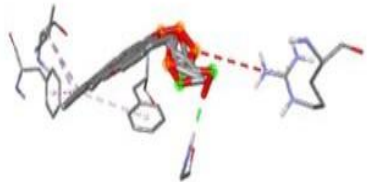
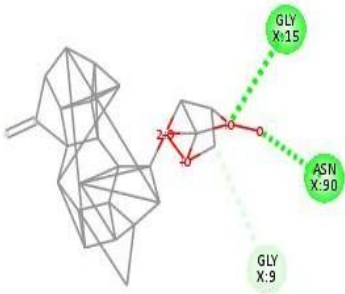
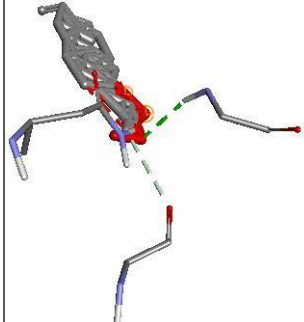
Maleic anhydride		
Phthalic anhydride		
Citric acid		
Malonic acid		

Table. 6.41 Amino acid residues and bond interaction of Stigmasterol derivatives

Stigmasterol CES derivatives	Binding energy (Kcal/mol)	Bond	Amino acid residues
Maleic anhydride	-18.6	Hydrogen bond	GLY15 ,ASN90,HD22 GLY9
Phthalic anhydride	-18.0	Nil	-
Citric acid	-18.4	Hydrogen bond Hydrophobic	LY92 ,VAL188 ,VAL188 PHE192 ,PHE226
Malonic acid	-17.9	Hydrogen bond	GLY15, ASN90:HD22 GLY9
Adipic acid	-16.8	Unfavorable bump	-

6.4.2 Synthetic derivative formation of Beta-sitosterol and stigmasterol

6.4.2.1 Synthetic derivative formation of Beta-sitosterol using Maleic anhydride

After an *in silico* screening of several polybasic acids, it was observed that the maleic anhydride derivative of Beta-sitosterol shows the highest binding affinity. Hence, the synthetic derivative of Beta-sitosterol using Maleic anhydride was prepared, named the CES derivative of Beta-sitosterol.

6.4.2.2 Characterization of CES derivative of Beta-sitosterol (Maleic anhydride)

The characterization of CES derivatives of Beta-sitosterol was carried out using a different spectroscopic methods such as IR, NMR, and mass spectroscopy.

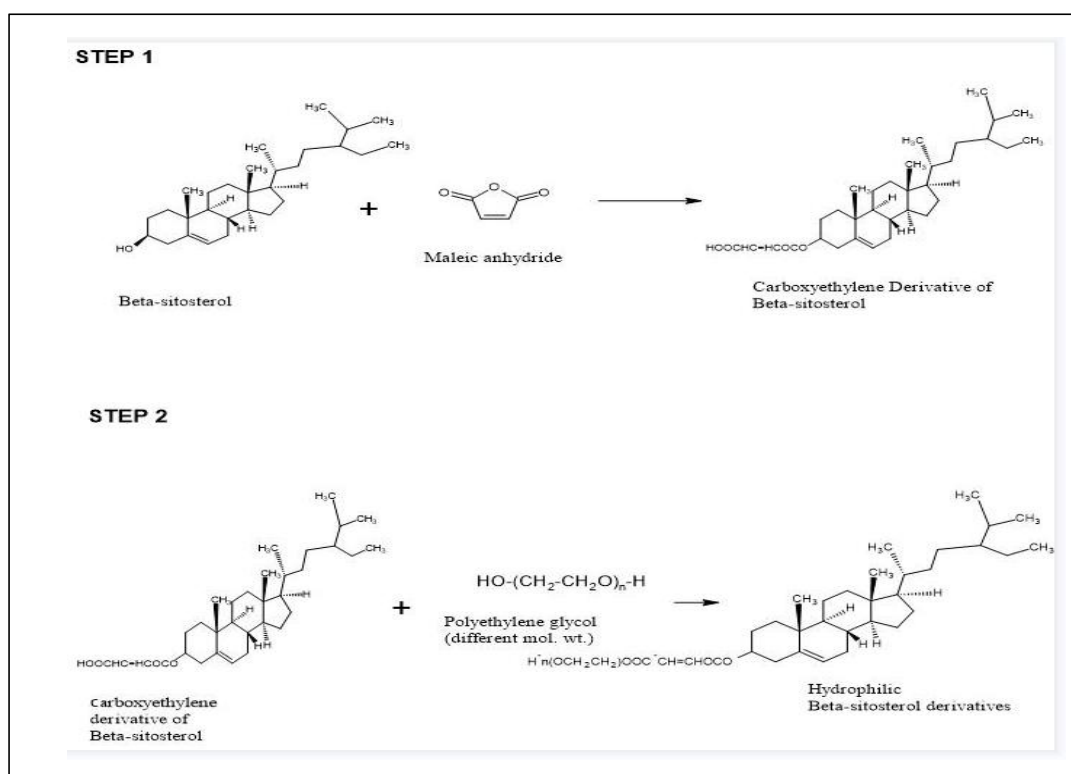


Figure 6.55 Synthetic scheme for Beta-sitosterol derivative using Maleic anhydride

FTIR spectrum of Beta-sitosterol CES derivative

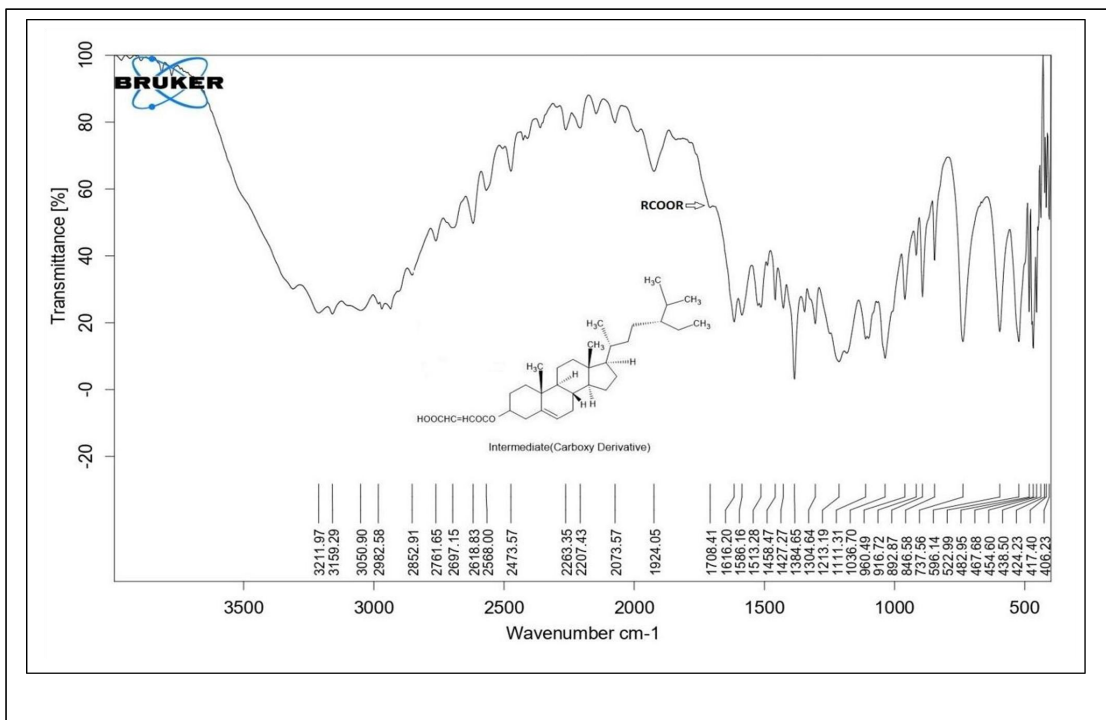


Figure 6.56 FTIR spectrum of Beta-sitosterol CES derivative

Table. 6.42 FTIR interpretation of Beta-sitosterol CES derivative

CES derivatives of Beta-sitosterol(cm^{-1})	Std.value (cm^{-1})	Interpretation
2852.91	2850-2975	Stretching vibration of CH alkane
3050.90	3020-3100	Stretching vibration of CH alkene
1616.20	1600-1680	Stretching vibration of C=C
1427.27	1395-1440	Bending vibration of OH
1384.65	1365-1390	Bending vibration of isopropyl

1036.70, 1111.31, 1213.19	1000-1300	Bending vibration of C-O of alcohol
1427.27 1458.47	1430-1470	Bending vibration of CH ₃
1708.41	1700-1750	Bending vibration of RCOOR

MASS spectrum of CES Beta-sitosterol derivative

The Beta-sitosterol CES derivative (C₃₃H₅₂O₄) usually exhibits a fragmentation pattern with a molecular ion peak at m/z 513. and other characteristic fragments related to ring cleavage at 445, 395, 371, 338, 279, 195, 150, and 122.

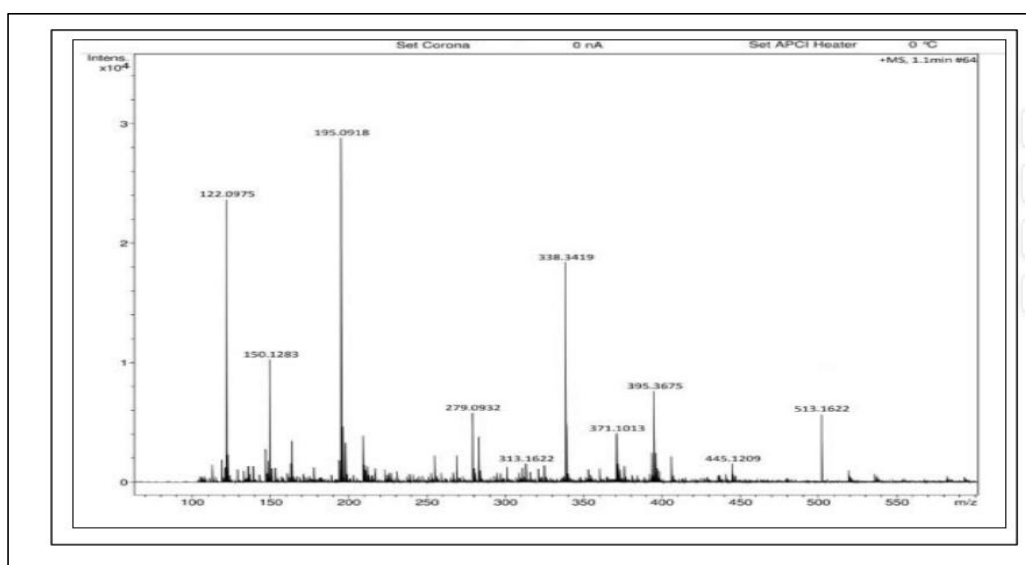


Figure 6.57 MASS spectrum CES derivative of Beta-sitosterol

6.4.2.3 Synthetic derivative formation of stigmasterol using Maleic anhydride

After an *in silico* screen of several polybasic acids, it was observed that the maleic anhydride combine with stigmasterol shows the highest binding affinity. Hence, the chemical derivative of stigmasterol using Maleic anhydride was prepared, named the CES derivative of stigmasterol.

6.4.2.4 Charaterization of CES derivative of stigmasterol (Maleic anhydride)

The characterization of the CES derivative of stigmasterol was carried out using various spectroscopic methods such as IR, NMR, and mass spectroscopy.

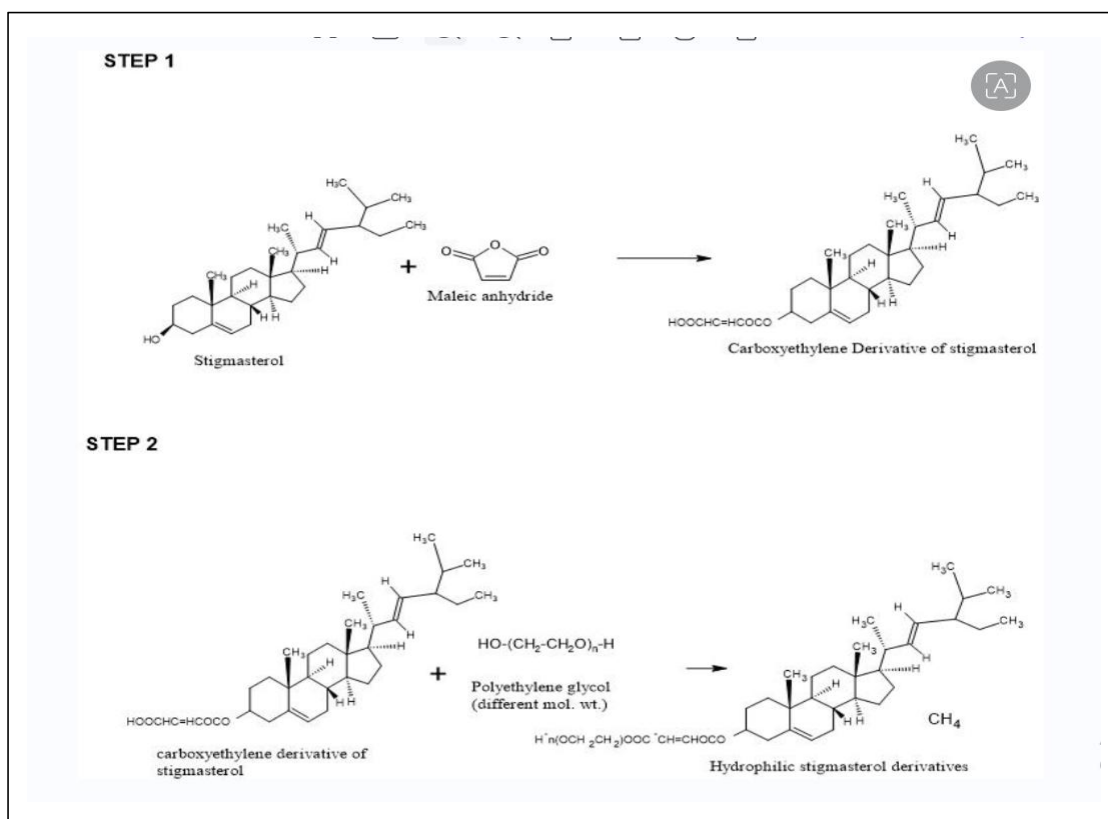


Figure 6.58 Synthetic scheme for stigmasterol derivative using Maleic anhydride

FTIR spectrum of Stigmasterol CES derivative

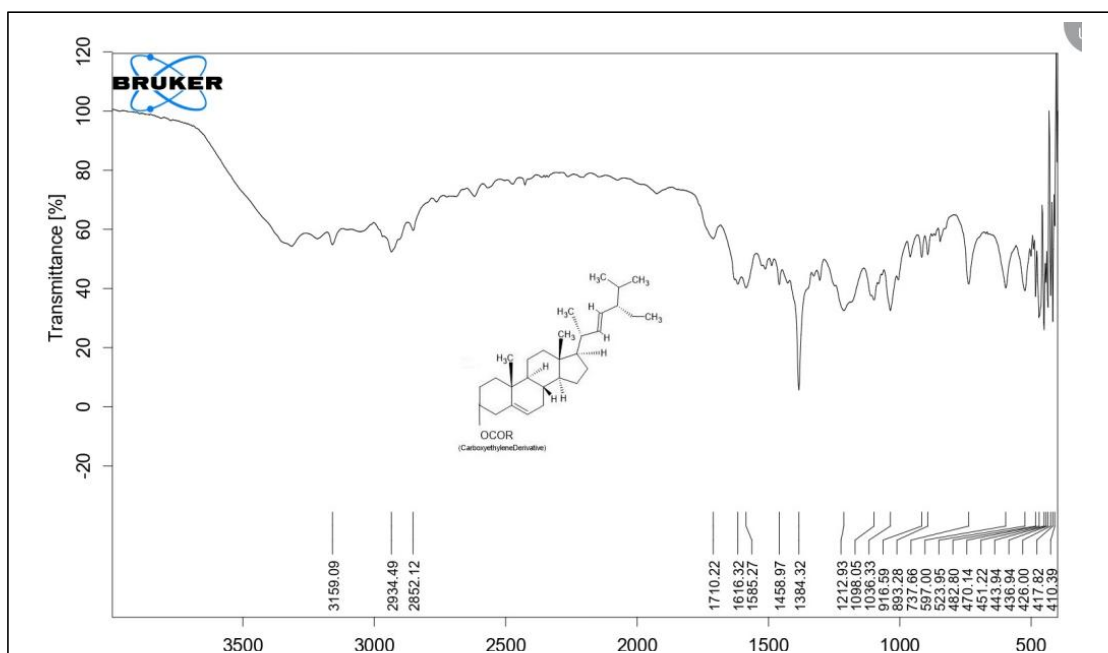


Figure 6.59 FTIR spectrum of Stigmasterol CES derivative

Table. 6.43 FTIR interpretation of Stigmasterol CES derivative

CES derivative of Stigmasterol (cm ⁻¹)	Std.value (cm ⁻¹)	Interpretation
2934.49	2850-2975	Stretching vibration for CH alkane
3159.09	3020-3100	Stretching vibration for CH alkene
1616.12	1600-1680	Stretching vibration for C=C
1384.32	1395-1440	Bending vibration for OH
1036.33,1098.05,1212.93	1000-1300	Bending vibration for C-O of alcohol
1458.97	1430-1470	Bending vibration for CH ₃
1710.22	1710-1750	Bending vibration of RCOOR

MASS spectrum of Stigmasterol CES derivative

The Stigmasterol CES derivative (C₃₃H₅₀O₄) usually exhibits a fragmentation pattern with a molecular ion peak at m/z 511. and other characteristic fragments related to ring cleavage at 445, 397, 338, 283,195,150, and 122.

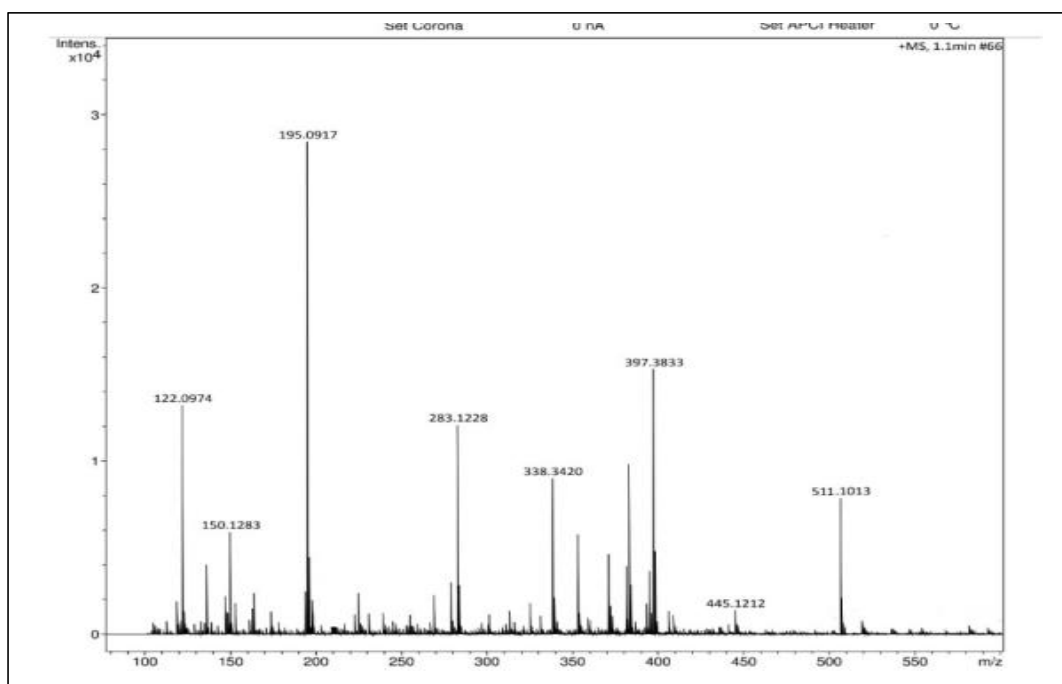


Figure 6.60 MASS spectrum of stigmasterol CES derivative

6.4.3 Hydrophilic derivatives formation of CES Beta-sitosterol and CES stigmasterol

6.4.3.1 Hydrophilic derivatives formation of CES Beta-sitosterol

The hydrophilic derivatives of Beta-sitosterol were prepared using Polyethylene glycol (PEG) of molecular weights 4000, 6000, and 8000, respectively. The confirmation was carried out by using physical methods and IR spectroscopic methods.

Table. 6.44 Physical evaluation of hydrophilic derivatives of Beta-sitosterol

Sr.No	Compound Name	Melting Point (°c)	Solubility
1	Beta-sitosterol HPS-4000	51-55	Soluble in ethanol
2	Beta-sitosterol HPS-6000	55-59	Soluble in isopropyl alcohol
3	Beta-sitosterol HPS-8000	56-62	soluble in ethanol/Slightly soluble in water

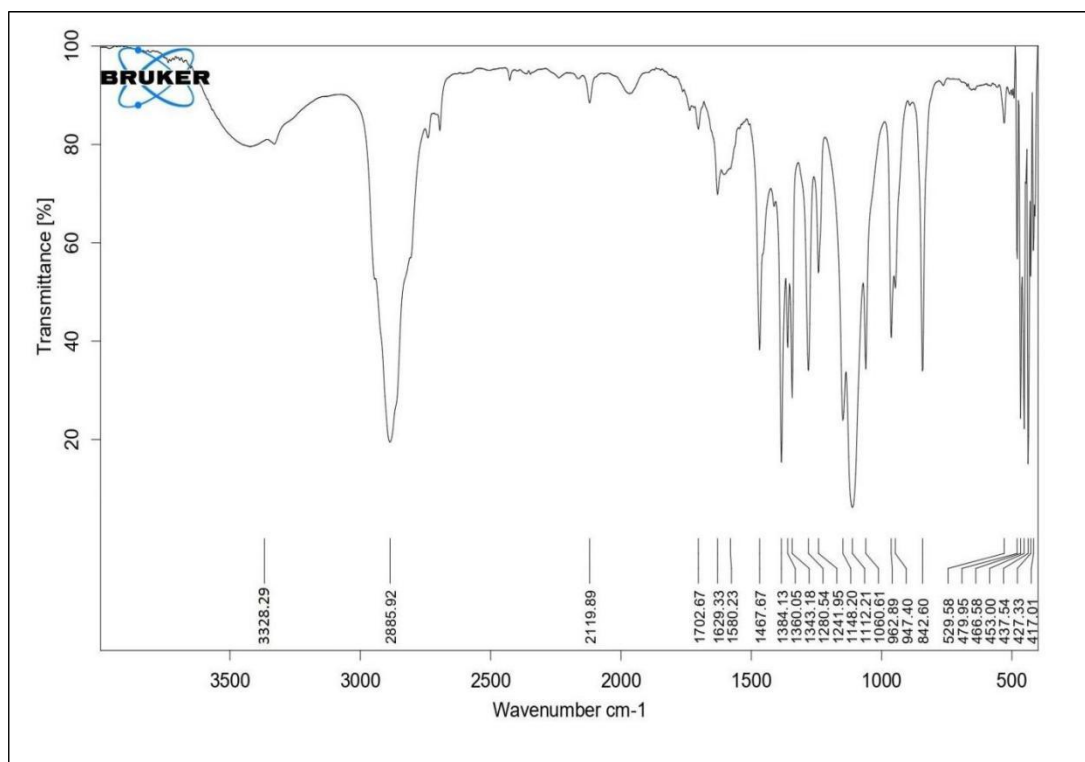


Figure 6.61 FTIR spectrum of hydrophilic derivative of Beta-sitosterol

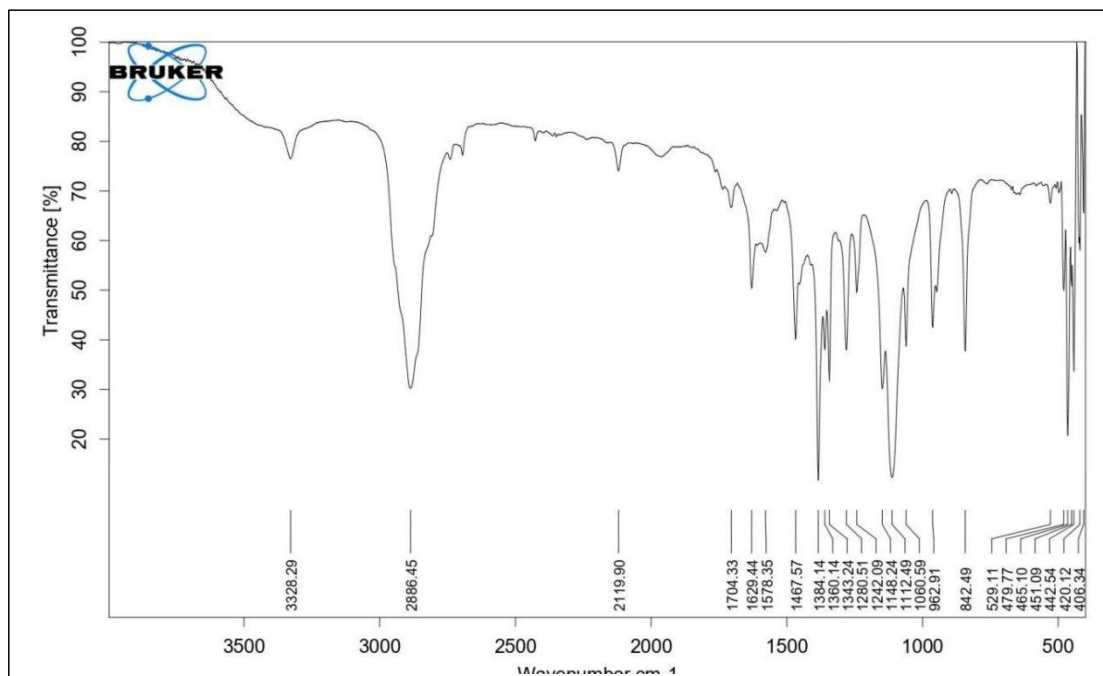


Figure 6.62 FTIR spectrum of hydrophilic derivative of Beta-sitosterol (PEG-6000)

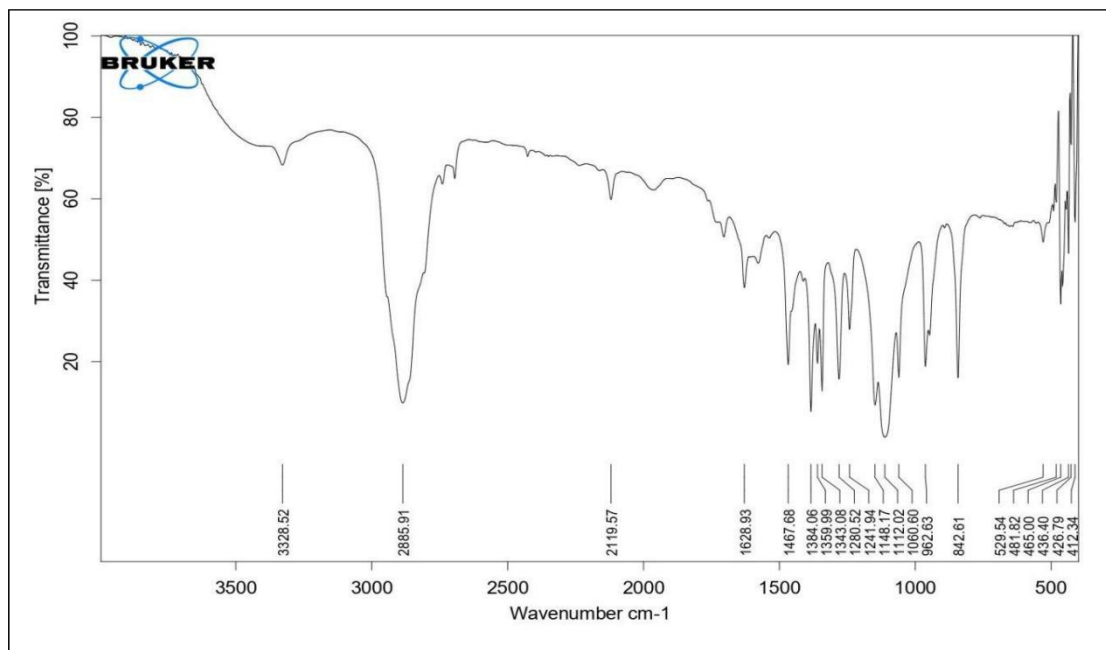


Figure 6.63 FTIR spectrum of hydrophilic derivative of Beta-sitosterol (PEG-8000)

6.4.3.2 Hydrophilic derivatives formation of CES stigmasterol

The hydrophilic derivatives of CES stigmasterol were prepared using Polyethylene glycol (PEG) of molecular weights 4000, 6000, and 8000, respectively. The confirmation was carried out by using physical methods and IR spectroscopic methods.

Table 6.45 Physical evaluation of hydrophilic derivatives of Stigmasterol

Sr.No	Compound Name	Melting point (°c)	Solubility
1	Stigmasterol HPS-4000	51-54	Soluble in ethanol
2	Stigmasterol HPS-6000	56-60	Soluble in isopropyl alcohol
3	Stigmasterol HPS-8000	57-60	Soluble in ethanol Slightly soluble in water

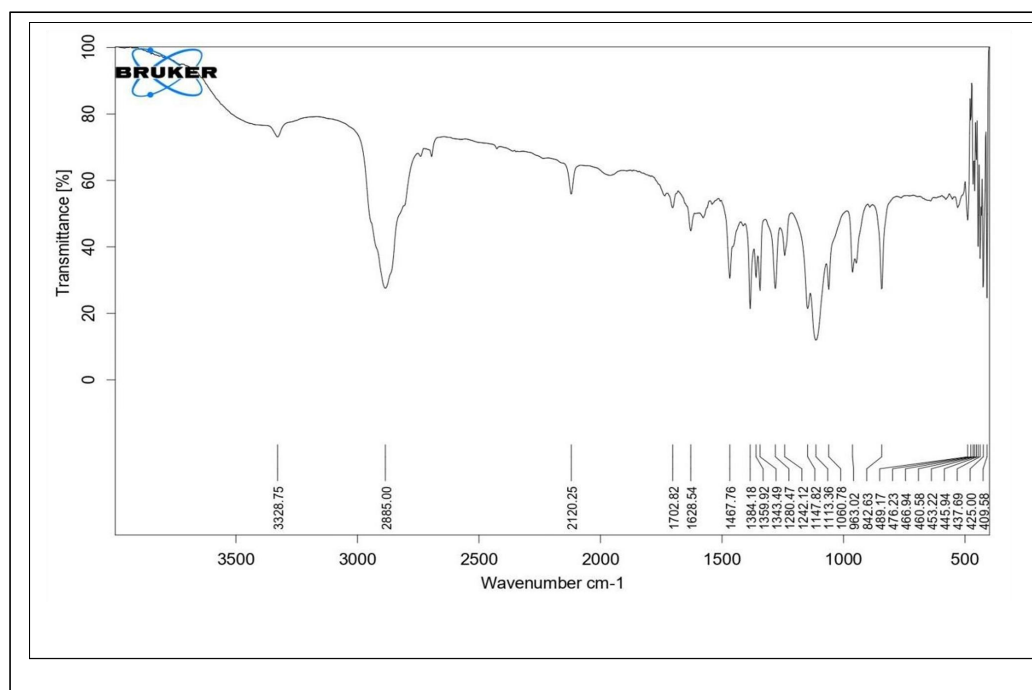


Figure 6.64 FTIR spectrum of hydrophilic derivative of Stigmasterol (PEG-4000)

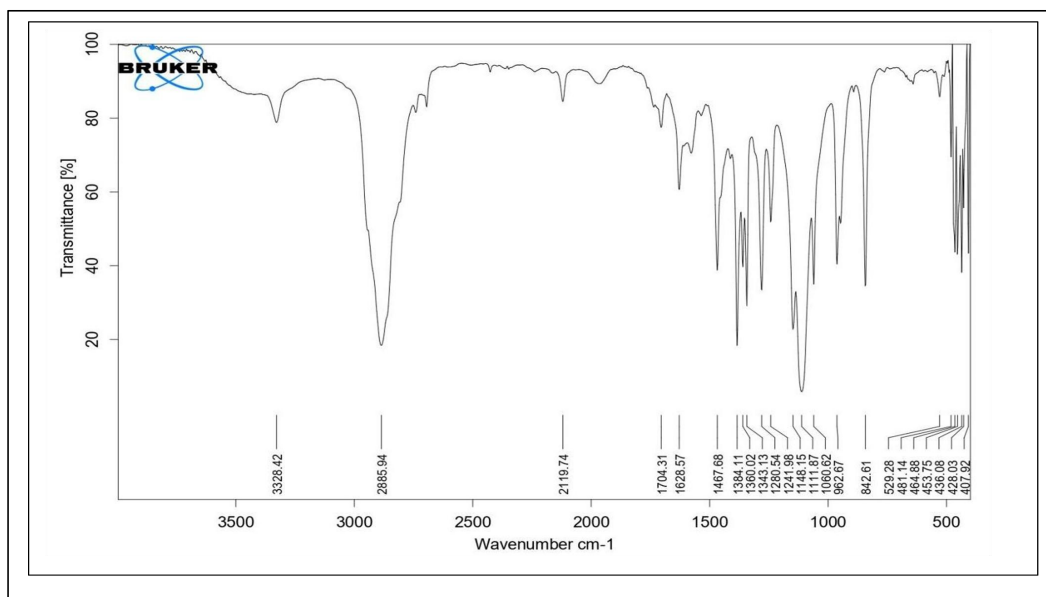


Figure 6.65 FTIR spectrum of hydrophilic derivative of Stigmasterol (PEG-6000)

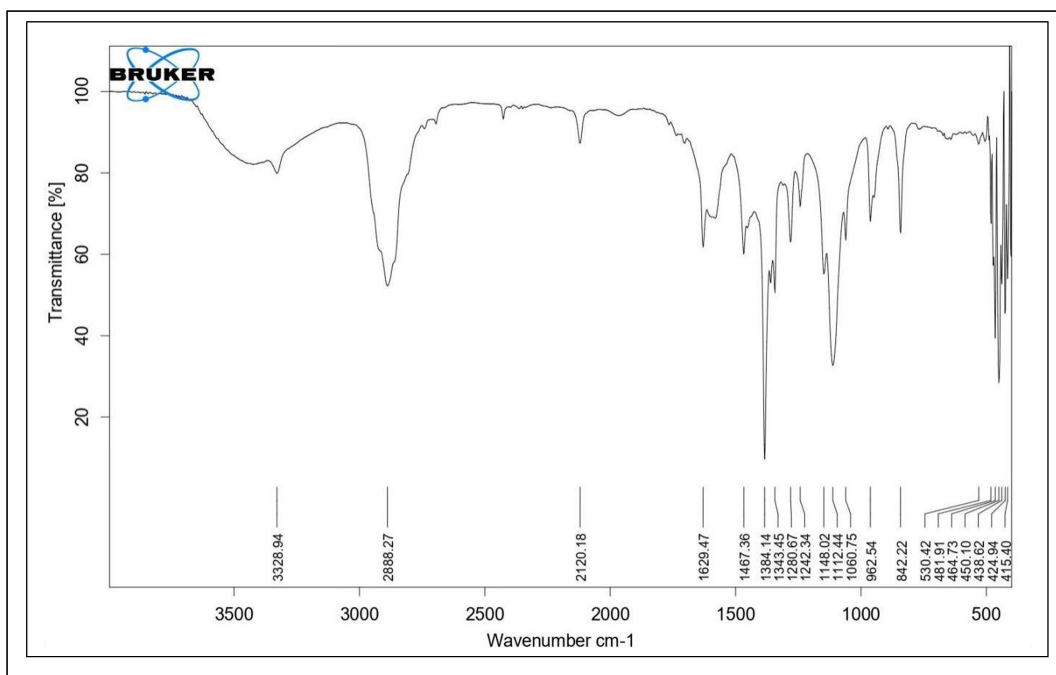


Figure 6.66 FTIR spectrum of hydrophilic derivative of Stigmasterol (PEG-8000)

6.4.4 *In silico* ADME of CES and hydrophilic derivatives

For the estimation of physicochemical parameters of CES and hydrophilic derivatives of Beta-sitosterol and stigmasterol, SwissADME software was employed for physical

and pharmacokinetic screening. The data is described in the table given below..

Table 6.46 Canonical smiles of Beta-sitosterol CES derivatives

Sr. no.	Beta-sitosterol CES derivatives	Canonical smiles
1	Maleic anhydride	<chem>CC[C@@H](C(C)C)CC[C@H]([C@H]1CC[C@@H]2[C@]1(C)CC[C@H]1[C@H]2CC=C2[C@]1(C)CCCC2OC(=O)/C=C/C(=O)O)C</chem>
2	Adipic acid	<chem>C(C)(C)[C@H](CC)CC[C@H]([C@@H]1[C@@]2([C@H]([C@@H]3CC=C4[C@](CCCC4OC(=O)CCCCC(=O)O)([C@H]3CC2)C)CC1)C)C</chem>
3	Citric acid	<chem>C(C)(C)[C@H](CC)CC[C@H]([C@@H]1[C@@]2([C@H]([C@@H]3CC=C4[C@](CCCC4OC(=O)CC(O)(CC(=O)O)C(=O)O)([C@H]3CC2)C)C1)C)C</chem>
4	Malonic acid	<chem>C(C)(C)[C@H](CC)CC[C@H]([C@@H]1[C@@]2([C@H]([C@@H]3CC=C4[C@](CCCC4OC(=O)CC(=O)O)([C@H]3CC2)C)CC1)C)C</chem>
5	Phthalic anhydride	<chem>C(C)(C)[C@H](CC)CC[C@H]([C@@H]1[C@@]2([C@H]([C@@H]3CC=C4[C@](CCCC4OC(=O)c4ccc(cc4)C(=O)O)([C@H]3CC2)C)CC1)C)C</chem>

Table. 6.47 *In silico* physicochemical properties of Beta-sitosterol CES derivatives

Beta-sitosterol CES derivatives	Mol. Formula	Mol. Wt.	No. heavy atoms	No. Arom. heavy atoms	Fraction Csp3	No. rotatable bonds	No. H-bond acceptors	No. H-bond donors	Molar Refractivity
Maleic anhydride	C ₃₃ H ₅₂ O ₄	512.76	37	0	0.82	10	4	1	153.88
Adipic acid	C ₃₅ H ₅₈ O ₄	542.83	39	0	0.89	13	4	1	163.97
Citric acid	C ₃₅ H ₅₆ O ₇	588.81	42	0	0.86	13	7	3	166.94
Malonic acid	C ₃₂ H ₅₂ O ₄	500.75	36	0	0.88	10	4	1	149.54

Phthalic anhydride	C ₃₇ H ₅₄ O ₄	562.82	41	6	0.73	10	4	1	169.83
--------------------	--	--------	----	---	------	----	---	---	--------

Table 6.48 *In silico* lipophilic and hydrophilic properties of Beta-sitosterol CES derivatives

Beta-sitosterol CES derivatives	Lipophilicity (Log P _{o/w})						Hydrophilicity (Log S)		
	iLOGP	XLOGP3	WLOGP	MLOGP	SILICOS-IT	Consensus	ESOL	Ali	SILICOS-IT
Maleic anhydride	4.99	9.73	8.22	6.16	7.18	7.26	Poor	Insoluble	Moderate
Adipic Acid	5.32	10.10	9.22	6.61	8.20	7.89	Poor	Insoluble	Poor
Citric acid	4.32	8.16	7.26	4.89	6.24	6.17	Poor	Insoluble	Moderate
Malonic acid	4.41	9.65	8.05	6.06	6.94	7.02	Poor	Insoluble	Poor
Phthalic anhydride	4.91	11.14	9.59	7.25	8.16	8.21	Poor	Insoluble	Poor

Table 6.49 *In silico* pharmacokinetic profiling of Beta-sitosterol CES derivatives

Beta-sitosterol CES Derivatives	GI absorption	BBB permeability	Metabolism CYP Inhibitors					Membrane Transporters		Lipinski violation
			1A2	2C19	2C9	2D6	3A4	BBB	P-gp Subs	
Maleic anhydride	low	No	No	No	Yes	No	No	No	No	2
Adipic Acid	low	No	No	No	No	No	No	No	No	2
Citric acid	low	No	No	No	No	No	Yes	No	Yes	2
Malonic acid	low	No	No	No	Yes	No	No	No	No	2
Phthalic anhydride	low	No	No	No	No	No	No	No	No	2

Table 6.50 Canonical Smiles of Stigmasterol CES derivatives

Sr. no.	Stigmasterol CES derivatives	Canonical smiles
1	Maleic unhydride	<chem>C(C)(C)C(CC)/C=C/[C@H]([C@@H]1[C@@]2([C@H]([C@@H]3CC=C4[C@](CCCC4OC(=O)/C=C/C(=O)O)([C@H]3CC2)C)CC1)C</chem>
2	Adipic acid	<chem>C(C)(C)C(CC)/C=C/[C@H]([C@@H]1[C@@]2([C@H]([C@@H]3CC=C4[C@](CCCC4OC(=O)CCCC(=O)O)([C@H]3CC2)C)CC1)C</chem>
3	Citric acid	<chem>C(C)(C)C(CC)/C=C/[C@H]([C@@H]1[C@@]2([C@H]([C@@H]3CC=C4[C@](CCCC4OC(=O)CC(O)(CC(=O)O)C(=O)O)([C@H]3CC2)C)CC1)C</chem>
4	Malonic acid	<chem>C(C)(C)C(CC)/C=C/[C@H]([C@@H]1[C@@]2([C@H]([C@@H]3CC=C4[C@](CCCC4OC(=O)CC(=O)O)([C@H]3CC2)C)CC1)C</chem>
5	Phthalic anhydride	<chem>C(C)(C)C(CC)/C=C/[C@H]([C@@H]1[C@@]2([C@H]([C@@H]3CC=C4[C@](CCCC4OC(=O)c4cc(cc4)C(=O)O)([C@H]3CC2)C)CC1)C</chem>

Table 6.51 *In silico* physicochemical properties of Stigmasterol CES derivatives

Stigmasterol CES derivatives	Mol. formula	Mol. Wt.(g/mol)	No. heavy atoms	No. arom. heavy atoms	Fracti on Csp3	No. rotatable bonds	No. H-bond acceptors	No. H-bond donors	Molar Refractivity
Maleic anhydride	C ₃₃ H ₅₀ O ₄	510.75	37	0	0.76	9	4	1	153.40
Adipic acid	C ₃₅ H ₅₆ O ₄	540.82	39	0	0.83	12	4	1	163.49
Citric acid	C ₃₅ H ₅₄ O ₇	586.80	42	0	0.80	12	7	3	166.46
Malonic acid	C ₃₂ H ₅₀ O ₄	498.74	36	0	0.81	9	4	1	149.07
Phthalic anhydride	C ₃₇ H ₅₂ O ₄	560.81	41	6	0.68	9	4	1	169.35

Table 6.52 *In silico* lipophilic and hydrophilic properties of Stigmasterol CES derivatives

Stigmasterol CES derivatives	Lipophilicity (Log P _{O/W})						Hydrophilicity (Log S)		
	iLOGP	XLOGP3	WLOGP	MLOGP	SILICOS-IT	Consensus	ESOL	Ali	SILICOS-IT
Maleic anhydride	4.68	8.95	7.99	6.07	7.00	6.94	Poor	Insoluble	Modestly
Adipic Acid	5.42	9.33	9.00	6.52	8.02	7.66	Poor	Insoluble	Poor
Citric acid	3.67	7.38	7.03	4.81	6.07	5.79	Poor	Poor	Modestly
Malonic acid	4.58	8.88	7.83	5.94	6.76	6.80	Poor	Insoluble	Modestly
Phthalic anhydride	5.50	10.37	9.36	7.17	7.98	8.08	Poor	Insoluble	Poor

Table 6.53 *In silico* pharmacokinetic profiling of Stigmasterol CES derivatives

Stigmasterol CES derivatives	GI absorption	BBB permeability	Metabolism CYP Inhibitors					Membrane Transporters		Lipinski violation
			1A2	2C19	2C9	2D6	3A4	BBB	P-gp Subs	
Maleic anhydride	low	No	No	No	Yes	No	No	No	No	2
Adipic Acid	low	No	No	No	Yes	No	No	No	No	2
Citric acid	low	No	No	No	Yes	No	Yes	No	Yes	2
Malonic acid	low	No	No	No	Yes	No	No	No	No	1
Phthalic anhydride	low	No	No	No	No	No	Yes	No	No	2

Table 6.54 Canonical smiles of hydrophilic Beta-sitosterol derivatives

Hydrophilic Beta-sitosterol derivatives	Canonical smiles
PEG-4	<chem>CCC(CCC(C)C3CCC4C2CC=C1CC(OC(=O)/C=C/C(=O)OCCCCO)CCC1(C)C2CCC34C)C(C)C</chem>
PEG-6	<chem>CCC(CCC(C)C3CCC4C2CC=C1CC(OC(=O)/C=C/C(=O)OCCCCO)CCC1(C)C2CCC34C)C(C)C(C)C</chem>
PEG-8	<chem>CCC(CCC(C)C3CCC4C2CC=C1CC(OC(=O)/C=C/C(=O)OCCCCO)CCC1(C)C2CCC34C)C(C)C(C)C(C)C</chem>

Table 6.55 *In silico* physicochemical properties of hydrophilic Beta-sitosterol derivatives

Hydrophilic Beta-sitosterol derivatives	Mol. Formula	Mol. Wt.(g/mol)	No. heavy atoms	No. arom. heavy atoms	Fraction Csp3	No. rotatable bonds	No. H-bond acceptors	No. H-bond donors	Molar Refractivity
PEG-4	C ₃₇ H ₆₀ O ₅	584.87	42	0	0.84	15	5	1	173.78
PEG-6	C ₃₉ H ₆₄ O ₅	612.92	44	0	0.85	16	5	1	183.39
PEG-8	C ₄₁ H ₆₈ O ₅	640.98	46	0	0.85	17	5	1	193.01

Table 6.56 *In silico* lipophilic and hydrophilic properties of Beta-sitosterol derivatives

Hydrophilic Betasitosterol derivatives	Lipophilicity (Log P _{o/w})						Hydrophilicity (Log S)		
	iLOGP	XLOGP3	WLOGP	MLOGP	SILICOS-IT	Consensus	ESOL	Ali	SILICOS-IT
PEG-4	6.46	10.03	8.45	6.05	8.42	7.88	Poorly	Insoluble	Poorly
PEG-6	6.83	10.83	9.08	6.40	9.10	8.45	Poor	Insoluble	Poorly
PEG-8	6.72	11.62	9.72	6.74	9.78	8.92	Insoluble	Insoluble	Poorly

Table 6.57 *In silico* pharmacokinetic profiling of hydrophilic Beta-sitosterol derivatives

Hydrophilic Betasitosterol derivatives	GI absorption	BBB permeability	Metabolism CYP Inhibitors					Membrane Transporters		Lipinski violation
			1A2	2C19	2C9	2D6	3A4	BBB	P-gp Subs	
PEG-4	low	No	No	No	No	No	No	No	No	2
PEG-6	low	No	No	No	No	No	Yes	No	Yes	2
PEG-8	low	No	No	No	Yes	No	Yes	No	No	2

Table 6.58 Canonical smiles of hydrophilic Stigmasterol derivatives

Hydrophilic Stigmasterol derivatives	Canonical smiles
PEG-4	<chem>CCC(/C=C/C(C)C3CCC4C2CC=C1CC(OC(=O)/C=C/C(=O)OCCCO)CCC1(C)C2CCC34C)C(C)C</chem>

PEG-6	<chem>CCC(/C=C/C(C)C3CCC4C2CC=C1CC(OC(=O)/C=C/C(=O)OCCCCCCO)CCC1(C)C2CCC34C)C(C)C</chem>
PEG-8	<chem>CCC(/C=C/C(C)C3CCC4C2CC=C1CC(OC(=O)/C=C/C(=O)OCCCCCCO)CCC1(C)C2CCC34C)C(C)C</chem>

Table 6.59 *In silico* physicochemical properties of hydrophilic Stigmasterol derivatives

Hydrophilic Stigmasterol derivatives	Mol. formula	Mol. Wt.(g/mol)	No. heavy atoms	No. arom. heavy atoms	Fracti on Csp3	No. rotatable bonds	No. H-bond acceptors	No. H-bond donors	Molar Refractivity
PEG-4	C ₃₇ H ₅₈ O ₅	582.85	42	0	0.78	14	5	1	173.31
PEG-6	C ₃₉ H ₆₂ O ₅	610.91	44	0	0.79	16	5	1	182.92
PEG-8	C ₄₁ H ₆₆ O ₅	638.96	46	0	0.80	18	5	1	192.53

Table 6.60 *In silico* lipophilic and hydrophilic properties of hydrophilic Stigmasterol derivatives

Hydrophilic Stigmasterol derivatives	Lipophilicity (Log P _{o/w})						Hydrophilicity (Log S)		
	iLOGP	XLOGP3	WLOGP	MLOGP	SILICOS-IT	Consensus	ESOL	Ali	SILICOS-IT
PEG-4	6.43	9.26	8.22	5.96	8.24	7.62	Poor	Insoluble	Poor
PEG-6	6.55	9.97	9.00	6.31	9.09	8.19	Poor	Insoluble	Poor
PEG-8	7.23	11.05	9.78	6.65	9.94	8.93	Poor	Insoluble	Poor

Table 6.61 *In silico* pharmacokinetic profiling of hydrophilic Stigmasterol derivatives

Hydrophilic Stigmasterol derivatives	GI absorption	BBB permeability	Metabolism CYP Inhibitors					Membrane Transporters		Lipinski violation
			1A2	2C19	2C9	2D6	3A4	BBB	P-gp Subs	
PEG-4	low	No	No	No	Yes	No	Yes	No	Yes	2
PEG-6	low	No	No	No	Yes	No	Yes	No	Yes	2
PEG-8	low	No	No	No	Yes	No	No	No	Yes	2

6. DISCUSSION

The World Health Organization estimates that cancer is the second leading cause of mortality globally, accounting for around 9.6 million deaths, or one in six deaths. Men are more likely to develop lung, prostate, colorectal, stomach, and liver cancers, whereas women are more likely to develop breast, colorectal, lung, cervical, and thyroid cancers. Given that the most prevalent malignancy in women is breast cancer, 157 out of 185 nations worldwide, 670,000 death worldwide were attributed to breast cancer in 2022 (167). Recent research using traditional medicinal plant knowledge has revealed a variety of terrestrial and marine cancer chemo preventive medicines (168). The current research work emphasized the isolation of phytoconstituents from leaves of *Euphorbia pulcherrima* and seeds of *Ricinus communis* and analyzed their synergistic effect on breast cancer. The selected plants powder were screened for their standardization by using various methods specified in the Ayurvedic Pharmacopoeia of India. In order to separate various phytoconstituents from plants for future investigation into their standardization and pharmacological activity in drug development, crude drug extraction is an essential first step. *Euphorbia pulcherrima* and *Ricinus communis* were extracted using the soxhlet extraction using petroleum ether, ethanol, and water as solvents. Amongst all extracts, petroleum ether extract shows good yield, i.e., 5.3% for *Euphorbia pulcherrima* leaves and 4% for *Ricinus communis* seeds. Although thin layer chromatography makes it possible to separate plant extracts, and used in screening experiments (169). For phytochemical screening, thin layer chromatography of both plants were carried out using pre-coated silica gel slides. In case of petroleum ether extract of *Euphorbia pulcherrima* leaves and *Ricinus communis* seeds solvent system, petroleum ether, ethylacetate, acetonitrile (8.2:1.8:0.1) shows good separation of phytoconstituents when observed under a UV chamber. For quantitative screening of phytoconstituents, column chromatography was employed. For isolation of constituents from *Euphorbia pulcherrima* leaves and *Ricinus communis* seeds the solvent system petroleum ether, ethylacetate, acetonitrile in 8.2:1.8:0.1 via increasing polarity was used, 25 eluents were collected & confirmed using TLC. The spectroscopic approach was utilized to characterize the separated phytoconstituents and confirmed that Beta-sitosterol and stigmasterol were found in *Euphorbia pulcherrima* and *Ricinus communis* petroleum ether extract,

respectively. Further quantification of Beta-sitosterol and stigmasterol in the extract was carried out using HPTLC, where pure compounds serve as standards. Finding suggests that 14.31% of Beta-sitosterol was present in *Euphorbia pulcherrima* extract, while 28.24% of stigmasterol was present in *Ricinus communis*. Molecular docking is a computer based tool to analyze suitable drugs for specific proteins and plays an important role in development of drug. Thus *in silico* approach gains remarkable importance in research and development. In the present study, molecular docking was carried out using two different software naming Schrodinger and Autodock Vina. Molecular docking and MD simulation studies were carried out using Schrodinger upon selected 5 constituents, while PDB ID : 3HB5 is selected as a protein. This protein is a novel inhibitor of the 17 beta-dehydrogenase-1 enzyme. Where rutin shows the uppermost binding affinity -18.61 Kcal/mol, while germanicol shows the lowermost binding affinity -3.12 Kcal/mol againsts protein (PDB ID: 3HB5). Further molecular docking using autodock vina were carried out using nine ligands selected from *Euphorbia pulchirrima* leaves like Beta-sitosterol, germanicol acetate, germanicol, rutin, and kaempferol-3-O-glucoside, while ligands were selected from *Ricinus communis* seeds ricinine, stigmasterol, probucol, and ricinolic acid. Whereas probucol shows the highest binding affinity -9.8 Kcal/mol, while ricinine shows the lowermost binding affinity -5.5 Kcal/mol. In current investigation, RMSD values for the estradiol 17-beta- dehydrogenase -1 enzyme were calculated when it binds with the phytoconstituents. The RMSD values calculated from 1000 trajectories generated during 100 nanoseconds of MD simulations for different complexes. The complex 3HB5, rutin involving demonstrates an ordinary RMSD of 3.43 Å with a standard deviation of 0.39 Å. This suggests a moderate level of structural fluctuation during the MD simulation. The lower standard deviation indicates relatively consistent behaviour across the multiple trajectories, contributing to the stability of the complex. The complex with Kaempferol-3-O-Glucoside shows a somewhat lower average RMSD of 3.28 Å, with a comparatively lower standard deviation of 0.24 Å. These values collectively suggest that these complex experiences less structural deviation during the simulation, show a more stable binding configuration. In case of the stigmasterol complex, it shows an average RMSD of 4.08 Å, the highest among the complexes in the table. The standard deviation of 0.48 Å

suggests a notable degree of structural variability during the MD simulation. This higher RMSD may indicate that the stigmasterol complex experiences more dynamic changes in its structure, potentially affecting its stability. For the Beta-sitosterol complex, the average RMSD is 3.61 Å, with a standard deviation of 0.48 Å. This suggests a moderate level of structural fluctuation, like the rutin complex. The complex's overall stability is aided by the comparable standard deviation, which shows consistent behavior across paths. The germanicol complex has a standard deviation of 0.32 Å and an average RMSD of 3.31 Å. A moderate degree of structural variability during the MD simulation is indicated by these values. The complex's overall stability is enhanced by the reduced standard deviation, which indicates more consistent behavior. During the MD simulations, the RMSD values supply data about the structural stability of the various complexes. Kaempferol-3-O-Glucoside exhibits the lowest average RMSD and standard deviation, indicating a relatively stable binding configuration. Stigmasterol, on the other hand, shows the highest average RMSD, suggesting greater structural variability during the simulation. Rutin, beta-sitosterol, and germanicol complexes fall within a moderate range of structural fluctuation. These findings highlight the varying degrees of stability among the complexes and can guide further investigations into the dynamics and structural changes of these ligand-protein interactions. In evaluating the MD simulations alongside docking scores and binding affinities for the complexes involving rutin, kaempferol-3-O-Glucoside, stigmasterol, beta-sitosterol, and germanicol, key findings emerge. The complex with rutin exhibits a high docking score and specific interactions, yet its MD simulation reveals moderate structural fluctuations, possibly indicating ligand flexibility during binding. In contrast, kaempferol-3-O-Glucoside display a lower docking score but maintains a stable binding configuration with the lowest RMSD, suggesting robust ligand receptor interactions. Stigmasterol demonstrates the highest RMSD, implying greater structural variability during MD simulations. Despite its lower docking score and a broad binding affinity range, the dynamic behavior observed raises questions about the stability of its binding conformation. Beta-sitosterol and germanicol exhibit comparable stability during MD simulations, reflected in their moderate RMSD values. While their docking scores and binding affinities were also moderate, these compounds maintain a relatively

consistent binding configuration, suggesting potential stability in their interactions. Additionally in current research work RMSF values for Estradiol 17-beta-dehydrogenase 1 enzyme were calculated when it binds with the phytoconstituents. RMSF calculated from 1000 trajectories generated during 100 nanoseconds of MD simulations for different complexes. The complex with rutin exhibits an average RMSF of 1.53 Å, with a standard deviation of 0.77 Å. These values recommend that the rutin complex experiences moderate variations in atomic positions during the MD simulations. The standard deviation indicates variability across trajectories, indicating certain regions may undergo more significant fluctuations. The kaempferol-3-O-Glucoside complex display a somewhat higher average RMSF of 1.62 Å, with a standard deviation of 0.63 Å. Despite the slightly higher average RMSF, the lower standard deviation suggests more consistent atomic fluctuations across trajectories, indicating a relatively stable binding configuration. For the stigmasterol complex, the average RMSF is 1.81 Å, with a standard deviation of 0.85 Å. These values suggest notable fluctuations in atomic positions during the MD simulations. The higher standard deviation indicates variability in the extent of fluctuations across different trajectories. The beta-sitosterol complex demonstrates an average RMSF of 1.75 Å, with a standard deviation of 0.73 Å. Like rutin, it experiences moderate fluctuations, with some variability across trajectories as indicated by the standard deviation. The germanicol complex exhibits an average RMSF of 1.57 Å, with a standard deviation of 0.60 Å. These values suggest moderate atomic fluctuations during the MD simulations, with a relatively lower standard deviation, indicating more consistent behaviour across trajectories.

In vitro antioxidant activity has been connected to their ability to treat or prevent the onset of chronic illnesses such as cancer. The DPPH assay, total antioxidant capacity (TAC), total phenolic content, and ferric reducing antioxidant property (FRAP) were used to assess the *in vitro* antioxidant potential of the ethanolic, aqueous, and petroleum ether extracts of *Euphorbia pulcherrima* and *Ricinus communis*. In the case of *Euphorbia pulcherrima*, the DPPH activity ranges between 56.21 ± 0.10 and 86.10 ± 0.15 . The antioxidant activity of all three extracts is higher than 50%. Between 0.50 ± 0.10 mg/g and 0.80 ± 0.15 mg/g, the ferric reducing antioxidant property (FRAP) is taken into consideration. The antioxidant activity of the petroleum ether was high

(90.75± 0.10 mg/g), that of the ethanol extract was low (79.85 ± 0.002 mg/g), and that of the aqueous extract was moderate (52.25± 0.15 mg/g). The petroleum ether extract had a total phenol concentration of 3.85±0.15 mg/g, while the ethanol extract had a phenol level of 2.65±0.10 mg/g.

The DPPH activity of *Ricinus communis* varies from 52.81± 0.015 to 88.50± 0.10. taking into account that ethanolic, aqueous, and petroleum ether extracts all have more than 50% antioxidant activity. The range of the ferric reducing antioxidant property (FRAP) test is 0.57 ±0.010 mg/g to 0.84 ± 0.015 mg/g. The antioxidant activity of petroleum ether was high (92.5 ± 0.05 mg/g), whereas that of ethanol extract was low (79.85 ± 0.002 mg/g) and that of the aqueous extract was moderate (56.5 ± 0.10 mg/g). The petroleum ether extract had a total phenol concentration of 3.95 ± 0.10 mg/g, while the ethanolic extract had a phenol level of 2.95 ± 0.015 mg/g. In relation to gallic acid, the aqueous extract exhibits the lowest total phenol concentration (1.60 ± 0.015 mg/g).

Finding suggests that petroleum ether extract of *Euphorbia pulcherrima* and *Ricinus communis* shows higher antioxidant potential as compared to ethanolic and aqueous extracts. The antioxidant potential of isolated compounds (Beta-sitosterol and stigmasterol) was done by using the DPPH & SOD methods, whereas ascorbic acid serves as the standard. Upon DPPH assay investigation, beta-sitosterol shows 24.38% radical scavenging, while stigmasterol shows 22.28% radical scavenging, and standard (ascorbic acid) shows 57.96% radical scavenging. On the other hand, the SOD method finding clarifies that Beta-sitosterol shows 65.71% radical scavenging while stigmasterol shows 61.94% radical scavenging.

Findings suggest that beta-sitosterol shows higher antioxidant potential as compared to stigmasterol, while ascorbic acid shows the highest antioxidant potential at concentration 1 mg/mL and its percentage radical scavenging activity was plotted in a graph.

In vitro anticancer cell line studies of beta-sitosterol and stigmasterol were carried out using the MDA-MB-231 and MCF-7 cell lines. For estimation of percent inhibition, the MTT assay and SRB method were used. During the investigation of the MTT assay for the MCF-7 cell line, stigmasterol and their combination in a 1:1 ratio were screened between concentrations of 6.12 µg/ml to 100 µg/ml. Beta-sitosterol at 100

µg/ml shows 77.33% inhibition, stigmasterol at 100 µg/ml shows 60.57% inhibition, while a combination of both drugs at 100 µg/ml shows 89.67% inhibition. On the other hand, the MTT assay for the MDA-MB-231 cell line Beta-sitosterol at 100 µg/ml shows 75.82 % inhibition, while at 100 µg/ml shows 62.21% inhibition, while a combination of both drugs at 100 µg/ml shows 89.07% inhibition.

For the SRB assay for the MCF-7 cell line Beta-sitosterol, Stigmasterol and its combination in a 1:1 ratio were screened between concentrations 6.12 µg/ml to 100 µg/ml. Beta-sitosterol at 100 µg/ml shows 71.68% inhibition, stigmasterol at 100 µg/ml shows 48.48% inhibition, while combination of both drugs at 100 µg/ml shows 80.88% inhibition. On the other hand, the SRB assay for MDA-MB-231 cell line, Beta-sitosterol at 100 µg/ml shows 74.76% inhibition, stigmasterol at 100 µg/ml shows 43.08% inhibition while combination of both drugs at 100 µg/ml shows 78.26% inhibition.

For the investigation of synergism between Beta-sitosterol and stigmasterol, a dose-response based bliss independence model was employed for drug combinations i.e., antagonism, additivity, and synergy. According to bliss independence, if the combination index is less than 1, it shows synergism; if it is greater than 1, it shows antagonism, and if it is equal to 1, it shows additive effect. In current research work, the bliss independence model was applied to MTT and SRB assays for both MCF-7 and MDA-MB-231 cell lines. In the case of the MCF-7 cell line, the CI index for the MTT assay is between 0.2 and 0.4 (below 1), while for the SRB assay, the CI index is between 0.05 and 0.4 (below 1). The MTT assay CI index for the MDA-MB-231 cell line ranges from 0.2 to 0.4 (below 1). while for the SRB assay, the CI index is between 0.2 and 0.3 (below 1). Concluding all bliss independence models, it was found that a combination of Beta-sitosterol and stigmasterol in a 1:1 ratio shows synergistic action.

In vitro anticancer cell line study of Beta-sitosterol and stigmasterol were carried out using MCF-7 and MDA-MB-231 cell line. For estimation of percent inhibition MTT assay and SRB method were used. During investigation of MTT assay for (MCF-7 cell line) Beta-sitosterol, stigmasterol and its combination in 1:1 ratio was screened between concentrations 6.12 µg/ml to 100 µg/ml. Beta-sitosterol at 100 µg/ml shows 77.33 % inhibition, stigmasterol at 100 µg/ml shows 60.57 % inhibition while

combination of both drugs at 100 µg/ml shows 89.67 % inhibition. However, the MTT assay for the MDA-MB-231 cell line, Beta-sitosterol at 100 µg/ml shows 75.82 % inhibition, stigmasterol at 100 µg/ml shows 62.21 % inhibition while combination of both drug at 100 µg/ml shows 89.07 percent inhibition.

For SRB assay for MCF-7 cell line, Beta-sitosterol, stigmasterol and its combination in 1:1 ratio was screen between concentrations 6.12 µg/ml to 100 µg/ml. Beta-sitosterol at 100 µg/ml shows 71.68 % inhibition, stigmasterol at 100 µg/ml shows 48.48 % inhibition while combination of both drug at 100 µg/ml shows 80.88 % inhibition. However, the SRB assay for MDA-MB-231 cell line, Beta-sitosterol at 100 µg/ml shows 74.76 % inhibition, stigmasterol at 100 µg/ml shows 43.08 % inhibition while combination of both drug at 100 µg/ml shows 78.26 % inhibition.

In current research work the bliss independence model was applied to MTT and SRB assay for both MCF-7 and MDA- MB-231 cell line. In case of MCF-7 cell line the CI index for MTT assay is in between 0.2 to 0.4 (below 1) while, for SRB assay the CI index is between 0.05-0.4 (below 1). In MDA-MB-231 cell line the CI index for MTT assay is in between 0.2 to 0.4 (below 1) while, for SRB assay the CI index is between 0.2-0.3 (below 1). Concluding all bliss independence models it was found that combination of Beta-sitosterol and stigmasterol in 1:1 ratio shows synergistic action.

For synthetic derivative formation from Beta-sitosterol and stigmasterol, the hypothetical derivatives incorporating maleic anhydride, phthalic anhydride, adipic acid, malonic acid, citric acid, etc. were prepared using chemsketch. These prepared CES ester derivatives were screened via *in silico* molecular docking using autodock vina. Five derivatives from Beta-sitosterol and five derivatives from stigmasterol were screened against 3BH5. Among them, the CES derivative of Beta-sitosterol using maleic anhydride shows the highest binding affinity, -18.4 kcal/mol, while the CES derivative of stigmasterol using maleic anhydride shows the maximum binding affinity, -18.6 kcal/mol. In all acids, the adipic acid derivative of betasitosterol and stigmasterol did not show any kind of interaction.

Later, *in silico* screening of several polybasic acids, the chemical derivatives of Beta-sitosterol and stigmasterol using maleic anhydride were prepared, naming the CES derivative of Beta-sitosterol and stigmasterol, respectively. The characterization

of synthesized derivatives was carried out using spectroscopic methods and found that ester derivatives of Beta-sitosterol and stigmasterol formed successfully. For increasing the polarity of this CES derivative, further treated with polyethylene glycol(PEG) of molecular weight 4000, 6000, and 8000 respectively, and confirmed using Melting point and IR spectroscopic method. Additionally, for the determination of its pharmacokinetics and physicochemical parameters, swiss ADME software was utilized to screen all CES derivatives of Beta-sitosterol and stigmasterol followed by hydrophilic derivatives of Beta-sitosterol and stigmasterol. The hydrophilic derivatives of the most active compound showed prominent result.

Plant phytoconstituents are set to play an increasingly prominent role over synthetic drugs in multiple domains like therapeutics, nutrition, preventive healthcare, and personalized medicine. The focus is shifting towards integrative approaches, hybrid molecules, and smarter delivery systems, backed by technological advancements and sustainable practices. While rigorous research and validation remain essential, the future of plant derived medicines is bright in both global health and industry. The research landscape of plant phytoconstituents versus synthetic drugs has evolved dramatically in recent years, driven by increasing concerns about synthetic drug resistance, side effects, and the growing preference for natural therapeutic alternatives. As researchers with extensive experience in this field, the evidence strongly supports the paradigm shift toward plant based pharmaceuticals and their integration with modern drug development strategies.

CHAPTER – 7

SUMMARY AND CONCLUSION

7. SUMMARY AND CONCLUSION

This section provides an overview of the findings from extensive research. Due to the numerous health benefits associated with both *Euphorbia pulcherrima* leaves and *Ricinus communis* seeds, the current research employs a multidisciplinary approach, focusing on pharmacognostic, phytochemical, molecular docking, pharmacological and pharmaceutical chemistry approaches. In the current research work, the leaves of *Euphorbia pulcherrima* and the seeds of *Ricinus communis* were standardized using several qualitative and quantitative investigation methods as per the official guidelines. The extraction of both plant parts was carried out using Soxhlet extraction techniques, which yielded a maximum amount of extract in petroleum ether. Chromatographic methods including thin layer chromatography and column chromatography were used to further separate the active phytoconstituents from the extracts of *Euphorbia pulcherrima* and *Ricinus communis*.

The findings indicate that several constituents were observed in the extract, among which the sterol group was selected for further evaluation. The isolated phytoconstituents were further characterized using spectroscopic methods such as UV, IR, NMR, and MASS, confirming that Beta-sitosterol from *Euphorbia pulcherrima* and stigmasterol from *Ricinus communis* can be isolated. The quantification of Beta-sitosterol and stigmasterol in the extracts using HPTLC revealed that 14.31% of Beta-sitosterol was present in the *Euphorbia pulcherrima* extract, while 28.24% of stigmasterol was present in the *Ricinus communis* extract.

To claim its anticancer potential, molecular docking studies were performed using the protein PDB ID: 3HB5, and nine ligands were selected based on the phytochemistry of both plants. This protein is a novel inhibitor of the 17-beta-dehydrogenase 1 enzyme. In the current investigation, Schrodinger and AutoDock Vina were the two distinct software programs used for molecular docking. Beta-sitosterol, germanicol acetate, germanicol, rutin, kaempferol-3-O-glucoside, stigmasterol, probucol, and ricinolic acid showed good binding affinity when screened using AutoDock Vina, while ricinine, a toxic substance, showed the lowest binding affinity. Fascinatingly, the results of molecular docking using Schrodinger confirmed that rutin showed excellent binding affinity with the highest docking score and interacted with Phe226, His221, Val188, Asn152, and Ser142 amino acids. MD simulation study was carried

out, and the RMSD and RMSF values were calculated from 1000 trajectories generated during 100 nanoseconds. The findings suggest that kaempferol-3-O-glucoside and germanicol show relatively stable configurations, whereas stigmasterol exhibits higher flexibility. Rutin and Beta-sitosterol fall within a moderate range.

For the ethanolic, aqueous, and petroleum ether extracts of *Euphorbia pulcherrima* and *Ricinus communis*, the total antioxidant capacity (TAC), ferric-reducing antioxidant property (FRAP), and total phenolic content, DPPH assay were examined using an in vitro antioxidant model. Ascorbic acid was used as a standard in the DPPH assay. For the DPPH assay, the concentration range varied from 20 to 100 mg/mL.

The FRAP method used a concentration of 500 μ L, while the total antioxidant capacity was measured at a concentration of 100 mg/mL. The results suggest that as compared to the ethanolic and aqueous extracts, the petroleum ether extracts of *Ricinus communis* and *Euphorbia pulcherrima* exhibit more antioxidant potential. The petroleum ether extracts of *Euphorbia pulcherrima* and *Ricinus communis* exhibit greater antioxidant responses. Additionally, the antioxidant potential of the isolated compounds was evaluated using the DPPH and SOD methods, where ascorbic acid served as the standard. The findings suggest that Beta-sitosterol exhibits higher antioxidant potential compared to stigmasterol. Using MCF-7 and MDA-MB-231 cell lines, the *in vitro* anticancer potential of Beta-sitosterol, stigmasterol, and their combination (ratio 1:1) was investigated.

The MTT and SRB assays were used to estimate the percentage inhibition. The concentration ranges used for this screening were 6.12 μ g/mL to 100 μ g/mL. Beta-sitosterol showed a high percentage inhibition compared to stigmasterol for both cell lines. Conversely, at a dosage of 100 μ g/mL, their combination had the highest percentage inhibition.

For the examination of synergistic action between Beta-sitosterol and stigmasterol, a dose dependent Bliss independence model was employed. which includes antagonist, additive, and synergy. According to this model, the combination index (CI) should be less than 1 to confirm synergism. This model was applied to MTT and SRB assays for SRB assays is less than one, confirming the synergistic potential of Beta-sitosterol and stigmasterol at a 1:1 ratio. Before proceeding with synthetic derivative formation

of Beta-sitosterol and stigmasterol by using different polybasic acids like maleic anhydride, adipic acid, citric acid, malonic acid, and phthalic anhydride. They were screened hypothetically for *in silico* interactions with 3BH5 protein. Based on docking results good binding interaction showed with maleic anhydride, These hypothetically produced CES derivatives were screened for their physicochemical evaluation via SwissADME. Then derivative of Beta-sitosterol and stigmasterol by using maleic anhydride was synthesised named as CES. These synthesized CES derivative was further characterized by using spectroscopic methods. Additionally, the CES derivative was subsequently treated with polyethylene glycol (PEG) with molecular weights of 4000, 6000, and 8000 respectively, to increase the polarity of the CES derivative. The confirmation of hydrophilic derivatives of CES were determined by using both physical and Infrared spectroscopy methods. Furthermore, SwissADME was utilized for estimating the physicochemical parameters of the hydrophilic CES derivatives of Betasitosterol and stigmaserol.

CONCLUSION

In conclusion, both petroleum ether extracts of *Euphorbia pulcherrima* (leaves) and *Ricinus communis* (seeds) show numerous phytoconstituents, while with the Soxhlet extraction method. Several active phytoconstituents were identified using the chromatographic technique. Out of them, Beta-sitosterol and stigmasterol were isolated, characterized and quantify by HPTLC, confirms that 14.31% of Beta-sitosterol and 28.24% stigmasterol were present in *Euphorbia pulcherrima* and *Ricinus communis*, respectively. From *in silico* prediction, we can conclude that rutin show excellent interaction with 17 beta-dehydrogenase 1 enzyme inhibitor when docked using Schrodinger. On the other hand ligands selected from both plants screened for *in silico* studies result showed that probucol shows the highest binding interaction, while Beta-sitosterol, germanicol acetate, rutin, kaempferol-3-O-glucoside, stigmasterol, and ricinolic acid shows good binding interactions, while germanicol and ricinine show weak interactions by using autodock vina. The RMSD and RMSF values give visual image into the flexibility of various complexes during MD simulations. Kaempferol-3-O-Glucoside and germanicol complexes demonstrate relatively stable binding configurations, while stigmasterol exhibits higher flexibility. rutin and Beta-sitosterol fall within a moderate range hence these Beta-sitosterol and stigmasterols are selected for further screening of their *in vitro* breast cancer potential. Considering *in vitro* anti-oxidant activity, both extracts and isolated phytoconstituents show good antioxidant potential, and from the results it was concluded that the petroleum ether extract of *Euphorbia pulcherrima* and *Ricinus communis* shows highest antioxidant potential when compaired to ethanolic and aqueous extracts. Additionally, Beta-sitosterol shows higher antioxidant potential as compared to stigmasterol. The pharmacological evaluation of Beta-sitosterol, stigmasterol, and its combination in a 1:1 ratio for its *in vitro* breast cancer potential was carried out using the MDA-MB-231 and MCF-7 cell lines. Findings suggested that at 100 µg/ml it shows the highest percent inhibition. This screening is done by MTT assay and SRB assay. Moreover, synergism between Beta-sitosterol, and stigmasterol was investigated using the dose dependent Bliss independence model,

and the finding concludes that Beta-sitosterol, and stigmasterol in combination 1:1 ratio show remarkable anti cancer potential. From a synthetic chemistry approach, it was concluded that the maleic anhydride CES derivative of Beta-sitosterol and stigmasterol shows the highest binding affinity. Hence, CES derivatives using maleic anhydride were synthesized and further with PEG of molecular weight 4000, 6000, and 8000 derivatives prepared to increase the hydrophilicity of CES. Finding confirms that hydrophilic CES derivatives increase solubility. Concluding the investigation, it was revealed that both Beta-sitosterol and stigmasterol exhibit significant anticancer potential. Furthermore, when these compounds are combined, synergistic effect is shown and from *in silico* studies confirms that derivatives also shows good physicochemical and pharmacokinetic properties.

It could possibly be possible to conduct an *in vitro* cell line study to evaluate the produced molecule for its potential to treat breast cancer, taking into account the future prospects of this field of research. Furthermore, it may be feasible to conduct *in vivo* screening for anticancer properties of Beta-sitosterol, stigmasterol, and their combination at different concentrations. Potential anticancer properties of the substances Beta-sitosterol and stigmasterol could be explored through *in silico*, *in vitro* and *in vivo* investigations for various types of cancer. It may be possible to further develop the formulation by combining Beta-sitosterol and stigmasterol and conducting pharmacological screening.

Future research in breast cancer will increasingly blend plant phytoconstituents with conventional therapies to maximize efficacy, minimize side effects, and develop personalized, targeted, and sustainable medical specialty treatments. Progress in nanotechnology, genomics, and regulatory science will drive these innovations from the lab to real patient impact. Consider the research aspects examine the potential synergistic effects of combining sterol phytoconstituents with chemotherapy, hormone therapy, or targeted therapy to enhance treatment efficacy and reduce side effects. Conduct *in vivo* studies and clinical trials to evaluate the efficacy and safety of sterol phytoconstituents in breast cancer patients.

CHAPTER – 8

BIBLIOGRAPHY

8. Bibliography

1. Siegel, R. L.; Miller, K.D.; Wagle, N. S.; Jemal A. Cancer statistics. *A Cancer Journal of Clinicians*. 2023, 73 (1), 17-48.
2. Kumar , R.; Saha, P.; Nyarko, R. O.; Lokare, P.; Boateng A.; Kahwa, I.; Boateng, P.; Asum C.; Impact of Covid-19 in Management of Lung Cancer Disease. A Review, *Asian Journal of Pharmaceutical Research and Development*. 2022, 10 (3), 57-64.
3. Thomas, N. S.; Laura, M .S.; A review of Cancer as a metabolic disease. *Seyfried and Shelton Nutrition & Metabolism* . 2010, 7 (7), 1-22.
4. Fidler, I. J. The pathogenesis of cancer metastasis the seed and soil hypothesis revisited. *National Rev. Cancer*. 2003, 3, 453–458.
5. Tarin, D. Cell and tissue interactions in carcinogenesis and metastasis and their clinical significance. *Semin Cancer Biololgy*. 2011, 21, 72–82.
6. Clarke Brian Blackadar. Historical review of the causes of cancer. *World Journal of Clinical Oncology*. 2016 , 7 (1), 54-86.
7. Kaur, B.; Kumar, S.; Kumar, B.. Recent advancements in optical biosensors for cancer detection, *Biosensors and Bioelectronics* . 2022, 197, 113805.
8. World Health Organization (2023 February).
9. Cooper, G. M.; *The Cell A Molecular Approach*. 2nd edition. Sunderland (MA) Sinauer Associates, *The Development and Causes of Cancer*. 2000, Available from: <https://www.ncbi.nlm.nih.gov/books/NBK9963>
10. Green, D. R.; Llambi ,F. Cell Death Signaling. *Cold Spring Harb Perspect Biology*. 2015, 1, 7 (12). doi: 10.1101/cshperspect.a006080. PMID: 26626938; PMCID: PM C4665079.
11. Maumy, L.; Harrissart, G.; Dewaele, P.; Aljaber, A.; Bonneau, C.; Rouzier, R.; Eliès, A. Impact of nutrition on breast cancer mortality and risk of recurrence. A review of the evidence. *Bull Cancer* . 2020, 107, 61–71.
12. Menon, G.; Alkabban, M.; Ferguson, T. Breast Cancer. In *Stat Pearls Internet*. Treasure Island FL Stat Pearls Publishing. 2024.
13. Łukasiewicz, S.; Czezelewski, M.; Forma, A.; Baj, J.; Sitarz, R.; Stanisławek,

- A. Breast Cancer Epidemiology, Risk Factors, Classification, Prognostic Markers, and Current Treatment Strategies - An Updated Review *Cancers* . 2021, 13 (17) , 4287.
14. Traves, K.P .; Cokenakes, S. E. Breast cancer treatment. *American family physician*. 2021 , 104 (2), 171-8.
 15. Grattan, B. J. Plant Sterols as Anticancer Nutrients. Evidence for Their Role in Breast Cancer Nutrients. 2013, 5 (2), 359-387. <https://doi.org/10.3390/nu5020359>.
 16. Pillow, P. C.; Jakovljevic, J.; Bondy, M. L.; Singletary, S.E.; Li, D.; Chang, S. Effect of dietary intake of phytoestrogens on estrogen receptor status in premenopausal women with breast cancer *Nutrition Cancer* . 2005, 51, 162–169.
 17. Zhang, X.; Wang, J.; Zhu, L.; Wang, X.; Meng, F.; Xia, L.; Zhang, H. Advances in Stigmasterol on its anti-tumor effect and mechanism of action. *Frontiers in oncology*. 2022 , 12, 1101289.
 18. Collins, A. R. Antioxidant intervention as a route to cancer prevention. *European Journal of Cancer*. 2005, 41(13), 1923-30.
 19. Yoshida, Y.; Niki, E. Antioxidant effects of phytosterol and its components. *Journal of nutritional science and vitaminology*. 2003, 49 (4), 277-80.
 20. Vargo, G. T.; Rosen, J. M. Modelling breast cancer one size does not fit all. *National Reviews Cancer*. 2007, 7 (9), 659-72. doi: 10.1038/nrc2193. PMID: 17721431.
 21. Van Staveren, W. C.; Solís, D.Y.; Hébrant, A.; Detours, V.; Dumont, J.E.; Maenhaut, C. Human cancer cell lines Experimental models for cancer cells in situ *Dietary Guidelines for Americans*. US Department of Health and Human Services Washington, DC, USA, 2005.
 22. Touillaud ,: For cancer stem cells, *Journal Biochimica et Biophysica Acta*. 2009, (2), 92-103. doi: 10.1016/j.bbcan.2008.12.004. PMID: 19167460.
 23. Nakatsu, N.; Yoshida, Y.; Yamazaki, K.; Nakamura, T.; Dan, S.; Fukui, Y.; Yamori, T. Chemosensitivity profile of cancer cell lines and identification of genes determining chemosensitivity by an integrated bioinformatical approach using cDNA arrays. *Molecular Cancer Therapy*. 2005, 4 (3), 399-412.

24. Ferreira, D.; Adega, F.; Chaves, R. The Importance of Cancer Cell Lines as *in vitro* Models in Cancer Methyloome Analysis and Anticancer Drugs Testing Internet. Oncogenomics and Cancer Proteomics Novel Approaches in Biomarkers Discovery and Therapeutic Targets in Cancer. 2013. Available from: <http://dx.doi.org/10.5772/53110>
25. Moreno, S.; Perno, C.F.; Mallon, P.W.; Behrens, G.; Corbeau, P.; Routy, J.P.; Darcis, G. Two-drug vs. three-drug combinations for HIV-1 do we have enough data to make the switch HIV medicine. 2019 , 2-12.
26. Roell, K. R.; Reif, D. M.; Motsinger, A. A. An introduction to terminology and methodology of chemical synergy perspectives from across disciplines. Frontiers in pharmacology. 2017 , 8, 158.
27. Duarte, D.; Vale, N. Evaluation of synergism in drug combinations and reference models for future orientations in oncology. Current Research in Pharmacology and Drug Discovery. 2022 , 3, 100-110.
28. Olounlad, A. P.; Azando, E. V.; Hounzangb, A.; Sylvie .M.; Attakpa ,Y. A review of the ethnomedical uses phytochemistry and pharmacology of the Euphorbia genus. Pharma Innovation. 2017, 6 (1), 34-39.
29. Aljohani, A.; Fahad, A.; Abdur, R.; Essam, M. ; Umer, R. *In Vivo* Anti-Inflammatory, Analgesic, Sedative, and Muscle Relaxant Activities and Molecular Docking Analysis of Phytochemicals from *Euphorbia pulcherrima* . Hindawi Evidence Based Complementary and Alternative Medicine. 2022 , Article ID 7495867, 9 pages <https://doi.org/10.1155/2022/7495867>.
30. Sharif, H. B.; Mukhtar, M. D.; Mustapha, Y.; Baba, G.; Lawal, A. O. Acute and subchronic toxicity profile of *Euphorbia pulcherrima* methanol extract on Wistar albino rats. Advances in Pharmaceutics. 2015, (1), 539-646.
31. Vilperte, V.; Lucaciu, C. R.; Halbwirth, H. Hybrid de novo transcriptome assembly of poinsettia *Euphorbia pulcherrima* Willd. Ex Klotsch bracts. BioMed Central Genomics . 2019, 20, 900. <https://doi.org/10.1186/s12864-019-6247-3>.
32. Krenzelok, E. P.; Jacobsen, T. D.; Aronis, J. M. Poinsettia exposures have good outcomes just as we thought. The American Journal of Emergency Medicine. 1996,14

(7), 671–674. doi:10.1016/S0735-6757(96)90086-8

33. The Plant List (2022). Version 1.1. Available at: <http://www.theplantlist.org/> (Accessed march).

34. Khan, M. H.; Rauf, A.; Khan, I.; Akram, M.; Mabkhot, Y.N. Chemical composition antileishmanial and antifungal profile of fixed oil of *Euphorbia pulcherrima*. Zeitschrift fur Arznei und Gewurzpflanzen. 2019, 23, 138-42.

35. Yu, C. X.; Wang, R.Y.; Qi, F.M.; Su, P. J.; Yu, Y.F.; Li, B.; Zhao, Y.; Zhi, D. J.; Zhang, Z.X.; Fei, D.Q.; Eupulcherol, A triterpenoid with a new carbon skeleton from *Euphorbia pulcherrima* and its anti-Alzheimer's disease bioactivity. Organic & Biomolecular Chemistry. 2020, 18(1), 76-80.

36. Basnett.; Pradhan.; Das.; Sharma.; Mohanty.; *Euphorbia, Pulcherrima*. A Scientific Update International Journal of Biology, Pharmacy and Allied Sciences . 2024, 13 (5), 2233-2243.

37. Rauf, A.; Raza, M.; Humayun, Khan M.; Hemeg, H. A.; Awthan, Y.S.; Bahattab, O.; Bawazeer, S.; Naz, S.; Basoglu, F.; Saleem, M.; Khan, M. *In vitro* and in silico studies on clinically important enzymes inhibitory activities of flavonoids isolated from *Euphorbia pulcherrima*. Annals of Medicine. 2022, 54 (1), 495-506.

38. David, D. B.; Peter, D. A.; Stephen R. W.; Paul, M. Sterols and triterpenols in latex and cultured tissues of *Euphorbia pulcherrima*, Phytochemistry. 1982, 21 (5), 1115-1118.

39. Karla, E.; González, R.; Marcos S.; María, T. B.; Colinas, L. M.; Rosario, G. M.; María, E.; Diana ,G. Polyphenols in five varieties of *Euphorbia pulcherrima* native to Mexico Revista Mexicana Ciencias Agrícolas . 2022, 13 , 3 .

40. Conover, C. A.; Vines, H. M.; Free Amino Acid Responses of *Euphorbia pulcherrima* Willd. Eckespoint D-7 to Fertilization, Chlormequat Levels and Tissue. Journal of American. Society for Hotriculture Science. 1972 , 97 (2), 255-257.

41. Aljohani, A.S.; Alhumaydhi, F. A.; Rauf, A.; Hamad, E. M.; Rashid, U. *In vivo* Anti-Inflammatory Analgesic, Sedative, Muscle Relaxant Activities and Molecular Docking Analysis of Phytochemicals from *Euphorbia pulcherrima*. Evidence based

Complement Alternative Medicine. 2022, 7495867.

42. Mavundza, E. J.; Street, R. ; Baijnath, H. A review of the ethnomedicinal, pharmacology, cytotoxicity and phytochemistry of the genus *Euphorbia* in southern Africa, South African Journal of Botany. 2022, 144, 403-418.
43. Kemboi, D.; Peter, X.; Langat, M.; Tembu, J. A Review of the Ethnomedicinal Uses Biological Activities, and Triterpenoids of *Euphorbia* Species. Molecules. 2020, 25 (17), 4019. doi: 10.3390/molecules25174019.
44. Bussell, G. Get Ready for Holiday Flowers. Southern Living How To Make Poinsettia Turn Red Mexico, 2009, 44 (12), 88.
45. Hafeez, N.; Phytochemical and Pharmacological Studies on *Euphorbia pulcherrima*. A Review . Phytopharmacology Research Journal. 2023, 2 (3), 13-6.
46. Rauf, A.; Muhammad, N.; . Phytochemical and pharmacological evaluation of aerial parts of *Euphorbia pulcherrima* L. Wudpecker Journal of Pharmacy and Pharmacology. 2013, 2, 15-20.
47. Kong, L.Y.; Min, Z. D. Studies on the chemical constituents of stem and leaf of common poinsettia (*Euphorbia pulcherrima*), Chinese Traditional Herbal Drugs. 1996, 08, 453–456.
48. Anjani, K. A re-evaluation of castor (*Ricinus communis* L.) as a crop plant. Perspectives in Agriculture, Veterinary Science, Nutrition and Natural Resources, 2014, 9 (1), 1-21.
49. Naik, S. N.; Saxena, D. K.; Dole, B. R.; Khare, S. K.; Potential and perspective of castor biorefinery waste biorefinery , USA, Elsevier, 2018, 623-656.
50. Yeboah, A.; Ying, S.; Lu, J.; Xie, Y.; Amoanimaa-Dede, H.; Boateng, K.G.; Chen, M.; Yin, X. Castor oil *Ricinus communis* a review on the chemical composition and physicochemical properties. Food Science and Technology. 2020 , 41, 399-413.
51. Chouhan, H. S.; Swarnakar, G.; Jogpal, B. Medicinal properties of *Ricinus communis*: A review. International Journal of Pharmaceutical Sciences and Research. 2021, 12(7), 3632-42.
52. Alirezalu, A.; Hesari, J.; Emami, S. Physiological and medicinal properties of

castor oil. In book, Recent Progress in Medicinal Plants, 2011, 11, 323-337.

53. USDA National Plant Database. 2006. <https://plants.usda.gov/home>.

54. Abomughaid, M. M.; Teibo, J.O.; Akinfe, O. A.; Adewolu, A. M.; Teibo, T. K.; Afifi, M.; Farga, A. M.; kuraishy, H.M.; Gareeb, A.I.; Alexiou, A.; Papadakis, M. A phytochemical and pharmacological review of *Ricinus communis* L. Discover Applied Sciences. 2024 , 6 (6), 315.

55. Rana, M.; Dhamija, H.; Prashar, B.; Sharma, S. *Ricinus communis* La review. International Journal of Pharmaceutical Sciences and Research. 2012 , 4 (4) , 1706-11.

56. Nadkarni K. M. Indian Materia Medica, Volume One, 2nd edition . 1927, 1, 1065-1070.

57. Marwat, S.; Rehman, F.; Khan, E. A.; Baloch, M.; Sadiq, M.; Khan,U.; Dr. Imdad, J. S; Adaf, S. *Ricinus cmmunis* . Ethnomedicinal uses and pharmacological activities. Pakistan Journal of Pharmaceutical Sciences. 2017, 30, 1815-1827.

58. Waseem, M. A.; Nahid, H. H.; Jamal ,S.M.; Sabir, S. M.; Al-Garni, Meshaal, J. S.; Saleh, A. K. Therapeutic role of *Ricinus communis* L. and its bioactive compounds in disease prevention and treatment. Asian Pacific Journal of Tropical Medicine. 2018 11(3), 177-185.

59. Huguet ,T. T.; New world material medica in Spanish renaissance medicine from scholarly reception to practical impact. Medicine History. 2001, 45, 359–76.

60. Pole, S. Ayurvedic Medicines. The principles of Traditional Practice. Singing Dragon UK. 2012, 153.

61. Malcolm J. Thompson.; William S. Bowers. Lupeol and 30- norlupan-3 β -ol-20-one from the coating of the castor bean *Ricinus communis* L phytochemistry. 1968, 7, 845-847.

62. Zhao, Y.; Sam, K.; Gang, L.; Tianwen, C. β -Sitosterol inhibits cell growth and induces apoptosis in SGC-7901 Human Stomach Cancer Cells Journal of Agricultural and Food Chemistry. 2009, 57 (12), 5211-5218.

63. Rajavel, T.; Packiyaraj, P.; Suryanarayanan, V. et al. β -Sitosterol targets Trx/Trx1 reductase to induce apoptosis in A549 cells via ROS mediated mitochondrial

dysregulation and p53 activation. Scientific Report. 2018, 8, 2071
<https://doi.org/10.1038/s41598-018-20311-6>.

64. Chevuru, S.; Reddy S.; Dr. Priyadharshini, R.; Dr. Jayaraman, S.; Dr. Palati S. Chemopreventive Anticancer Activity Of Beta Sitosterol In Human Prostate Cancer Cells Pc-3 And Emt-Mediated Signaling Regulation An *in Vitro* Study. Journal of Pharmaceutical Negative Results . 2022, 1514-1521.

65. Sinha, R.; Winer, A. G.; Chevinsky, M.; Jakubowski, C.; Chen, Y. B.; Dong, Y.; Hakimi, A. Analysis of renal cancer cell lines from two major resources enables genomics-guided cell line selection. Nature communications. 2017, 8 (1), 15165.

66. Sharmila, R.; Sindhu G. Evaluate the antigenotoxicity and anticancer role of β -sitosterol by determining oxidative DNA damage and the expression of phosphorylated mitogenactivated protein kinases, c-fos, c-jun, and endothelial growth factor receptor. Pharmacognosy Magazine . 2017, 13, 95-101.

67. Elshaer, M.; Gravante, G.; Kosmin, M.; Riaz, A.; and Al-Bahrani, A. A systematic review of the prognostic value of lymph node ratio number of positive nodes and total nodes examined in pancreatic ductal adenocarcinoma. The Annals of The Royal College of Surgeons of England. 2017, 99, 101–106.

68. Chou, T. C. Drug combination studies and their synergy quantification using the Chou-Talalay method. Cancer Research. 2010, 70, 440–446. doi: 10.1158/0008-5472.CAN-09-1947.

69. Omar, H. A.; Tolba, M. F.; Hung, J. H.; Al-Tel, T. H. OSU-2S Sorafenib Synergistic antitumor combination against hepatocellular carcinoma the role of PKC δ /p53. Frontiers Pharmacology. 2016, 7, 463.

70. Cao, Z.; Wang, X.; Lu, L.; Xu, J.; Li, X.; Zhang, G.; Ma, Z.; Shi, A.; Wang, Y.; Song, Y. β -Sitosterol and Gemcitabine Exhibit Synergistic Anti-pancreatic Cancer Activity by Modulating Apoptosis and Inhibiting Epithelial–Mesenchymal Transition by Deactivating Akt/GSK-3 β Signaling. Frontiers Pharmacology. 2019, 9, 1525. doi: 10.3389/fphar.2018.01525.

71. Ferlay, J.; Shin, H.; Bray, F.; Forman, D.; Mathers, C.; Parkin, D. Estimates of

worldwide burden of cancer in 2008. *International Journal Cancer* . 2010, 127, 2893–2917.

72. American Cancer Society Cancer Facts and Figures 2010. Atlanta American Cancer Society . 2010, 1–62.

73. Vundru, S. S.; Kale, R. K.; Singh, R. P. β -Sitosterol induces G1 arrest and causes depolarization of mitochondrial membrane potential in breast carcinoma MDA-MB-231 cells. *BMC Complement Alternative Medicine*. 2013, 13, 280. doi: 10.1186/1472-6882-13-280. PMID: 24160369; PMCID: PMC3819702.

74. Behrens, J. The role of the Wnt signalling pathway in colorectal tumorigenesis. *Journal of Biochemical Society Transactions*. 2005, 33, 672-675.

75. Baskar, A. A.; Ignacimuthu, S.; Paulraj, G. M.; Numair, K. S. Chemopreventive potential of beta-Sitosterol in experimental colon cancer model an *in vitro* and *in vivo* study. *BMC Complement Alternative Medicine*. 2010 , 10, 24. doi: 10.1186/1472-6882-10-24. PMID: 20525330; PMCID: PMC2887773.

76. Ebell, M. H.; Culp, M. B.; Radke, T. J. A Systematic Review of Symptoms for the Diagnosis of Ovarian Cancer. *American Journal of Preventive Medicine* . 2016, 50 (3), 384-394.

77. Bae, H.; Park, S.; Ham, J.; Song, J.; Hong, T.; Choi, J.; Song, G.; Lim, W. ER-Mitochondria Calcium Flux by β -Sitosterol Promotes Cell Death in Ovarian Cancer. 2021, 10 (10), 1583. <https://doi.org/10.3390/antiox10101583>.

78. Cheng, D.; Guo, Z.; Zhang, S. Effect of β -sitosterol on the expression of HPV E6 and p53 in cervical carcinoma cells. *Contemporary Oncology Współczesna Onkologia*. 2015, 19 (1), 36-42. <https://doi.org/10.5114/wo.2015.50011>.

79. Kaur, N.; Chaudhary, J.; Jain, A.; Kishore, L. Stigmasterol: a comprehensive review. *International Journal of Pharmaceutical Sciences and Research*. 2011, 2 (9), 2259.

80. Bakrim, S.; Benkhaira, N.; Bourais, I.; Benali, T.; Lee, L-H.; El Omari, N.; Sheikh, R.A, Goh,K.W.; Ming, L.C.; Bouyahya, A. Health benefits and pharmacological Properties of Stigmasterol. *Antioxidants*. 2022, 11(10), 1912. <https://doi.org/10.3390/antiox11101912>.

81. Dube, N. P.; Tembu, V. J.; Nyemba, G. R. *In vitro* cytotoxic effect of stigmasterol derivatives against breast cancer cells. BMC Complement Medicinal Therapy. 2023, 23, 316 . <https://doi.org/10.1186/s12906-023-04137-y>.
82. Wang, W. L.; Chen, S. M.; Lee, Y. C.; Chang, W.W. Stigmasterol inhibits cancer stem cell activity in endometrial cancer by repressing IGF1R/mTOR/AKT pathway. Journal of Functional Foods. 2022 , 99, 105338.
83. Zhao, J. Q.; Hao, Y.Y.; Gong, T.T.; Wei, Y.F.; Zheng, G.; Du, Z. D.; Zou, B. J.; Yan, S.; Liu, F.H.; Gao ,S.; Wu, Q. J.; Zhao, Y. H. Phytosterol intake and overall survival in newly diagnosed ovarian cancer patients. An ambispective cohort study. Frontier Nutrition. 2022, 9, 974367. doi: 10.3389/fnut.
84. Doubeni, C. A.; Doubeni, A. R.; Myers, A. E. Diagnosis and management of ovarian cancer. American Family Physicians. 2016, 93, 937–44.
85. Bae, H.; Song, G.; Lim, W. Stigmasterol Causes Ovarian Cancer Cell Apoptosis by Inducing Endoplasmic Reticulum and Mitochondrial Dysfunction. Pharmaceutics 2020, 12, 488. <https://doi.org/10.3390/pharmaceutics12060488>.
86. Rizwan, A.; Haq Nawaz, B.;Muhammad, M.; Farooq, A. Centum of Valuable Plant Bioactives. 2021, 213-22. <https://doi.org/10.1016/B978-0-12-822923-1.00019-4>.
87. Kim, Y. S.; Li, X. F.; Kang, K. H.; Ryu, B.; Kim, S. K. Stigmasterol isolated from marine microalgae *Navicula incerta* induces apoptosis in human hepatoma HepG2 cells. Biochemistry and Molecular Biology. 2014, 47(8), 433-8. doi: 10.5483/bmbrep.2014.47.8.153. PMID: 24286323; PMCID: PMC4206714.
88. Tabassum, A.; jameela, M.; jat, R. Chemopreventive effect of acetohexamide and stigmasterol against uvb- induced skin cancer. Frontier Journal of Pharmaceutical Sciences and Research. 2019, 2, 47-51.
89. Han, N.R.; Park, H.J.; Ko, S.G.; Moon, P.D. Stigmasterol exerts an anti-melanoma property through down-regulation of Reactive Oxygen Species and Programmed cell death Ligand 1 in melanoma cells. Antioxidants. 2024, 13 (3), 380. <https://doi.org/10.3390/antiox13030380>.

90. Li, K.; Yuan, D.; Yan, R.; Meng, L.; Zhang, Y.; Zhu, K. Stigmasterol exhibits potent antitumor effects in human gastric cancer cells mediated via inhibition of cell migration cell cycle arrest mitochondrial mediated apoptosis and inhibition of JAK/STAT signalling pathway. *Journal of the Balkan Union of Oncology* . 2018, 23 (5), 1420-1425. PMID: 30570868.
91. Tao, S.; Li, Z.; Y, W.; Pei, H.; Xiao, N.; Zhao, M. L.; Hong-Xiang, L. Steroids from *Commiphora mukul* display antiproliferative effect against human prostate cancer PC3 cells via induction of apoptosis, *Bioorganic & Medicinal Chemistry Letters*. 2012, 22 , (14), 4801- 4806.
92. Singla, A. K.; Pathak, K. Anti-inflammatory studies on *Euphorbia prostrata*. *Journal of Ethnopharmacology* . 1989, 27, 55-61.
93. Lanhers, M. C.; Fleurentin, J.; Dorfman, P.; Mortier, F.; Pelt, J.M. Analgesic, antipyretic and anti-inflammatory properties of *Euphorbia hirta*. *Planta Medicine* . 1991, 57, 225-31.
94. Singh, K. K.; Rauniar, G. P.; Sangraula, H. Experimental study of neuro pharmacological profile of *Euphorbia pulcherrima* in mice and rats. *Journal of Neuro science Rural Practice*. 2012, 3 (3), 311-9. doi: 10.4103/0976-3147.102612. PMID: 23188984; PMCID: PMC3505323.
95. Yakubu, A. I.; Dauda, M. *In vitro* antimicrobial activity of some phytochemical fractions of *Euphorbia pulcherrima* L. (*Poinsettia*). *Journal of medicinal plant research*. 2011, 5, 2470-2475.
96. Abdur R .; Naveed, M. Phytochemical and pharmacological evaluation of aerial parts of *Euphorbia pulcherrima* L. *Wudpecker Journal of Pharmacy and Pharmacology*. 2013, 2 (2), 015-020.
97. Basnett, A.; Pradhan, S.; Das, R.; Sharma, C. To investigate phytochemical parameter Pharmacognostical evaluation pharmacological anti-bacterial activity of the extract of *Euphorbia pulcherrima*. *Journal of Drug Delivery and Therapeutics*. 2023, 13 (8), 60-67.
98. Goel, A.; Kanika, S. Effect of *Euphorbia pulcherrima* Leaf and Inflorescence

Extract on Various Cytomorphological Parameters of *Aspergillus fumigatus*. World Academy of Science, Engineering and Technology International Journal of Biotechnology and Bioengineering. 2013, 7 (9), 859-862.

99. Lutsyk, M. D.; Lutsyk, A. D.; Kipiani, E. K.; Krupko, A. E. The toxicity and antitumor activity of three individual fractions of lectins from *Ricinus communis* seeds. Neoplasma. 1977, 24, 341.

100. Final report on the safety assessment of *Ricinus communis* (castor) seed oil, hydrogenated castor oil, glyceryl ricinoleate, glyceryl ricinoleate SE, ricinoleic acid, potassium ricinoleate, sodium ricinoleate, zinc ricinoleate, cetyl ricinoleate, ethyl ricinoleate, glycol ricinoleate, isopropyl ricinoleate, methyl ricinoleate, and octyldodecyl ricinoleate. International Journal of Toxicology. 2007, 26 (S-3), 31–77. doi:10.1080/10915810701663150.

101. Vieira, C.; Evangelista, S.; Cirillo, R.; Lippi, A.; Maggi, C.; Manzini, S. Effect of ricinoleic acid in acute and subchronic experimental models of inflammation. Mediators Inflammation. 2000, 9, 223–8.

102. Pingale, S. S. Hepato suppression by *Ricinus communis* against CCl₄ induced liver toxicity in rat. Journal of Pharmaceutical Research. 2010, 3, 39–42.

103. Nemudzivhadi, V.; Masoko, P. *In vitro* assessment of cytotoxicity antioxidant and anti-inflammatory activities of *Ricinus communis* Euphorbiaceae leaf extracts. Evidence Based Complement Alternative Medicine 2014, 1–8. doi: <http://dx.doi.org/10.1155/2014/625961>.

104. Al-Mamun, M. A.; Akter, Z.; Uddin, M. J. Characterization and evaluation of antibacterial and antiproliferative activities of crude protein extracts isolated from the seed of *Ricinus communis* in Bangladesh. BMC Complement Alternative Medicine. 2016, 16, 211. <https://doi.org/10.1186/s12906-016-1185-y>.

105. Singh, R. K.; Gupta, M. K.; Katiyar, D.; Srivastava, A.; & Singh, P. *In-vitro* antioxidant activity of the successive extracts of *Ricinus communis* stems. International Journal of Pharmaceutical Sciences and Research. 2010, 1 (8), 100-103.

106. Siegel, R. L. Colorectal cancer statistics . A cancer journal for clinicians 67, ,

2017, 47, 177–193.

107. Prakash, E.; Gupta, D. K. *In Vitro* Study of Extracts of *Ricinus communis* Linn on Human Cancer Cell lines. *Journal of Medical Sciences and Public Health*. 2014, 2, 15–20 .

108. Jena, J. ; Gupta, A. K. *Ricinus communis* Linn: A Phytopharmacological Review. *International Journal of Pharmacy and Pharmaceutical Sciences* . 2012, 4, 25–29.

109. Majumder, M.; Debnath, S.; Gajbhiye, R. L. *Ricinus communis* L. fruit extract inhibits migration/invasion, induces apoptosis in breast cancer cells and arrests tumor progression *in vivo*. *Science Report* . 2019, 14493. <https://doi.org/10.1038/s41598-019-50769-x>.

110. Lamba, S.S.; Buch, K.Y.; Lewis, H.; Lamba, J. Phytochemicals as potential hypoglycemic agents. *Studies in Natural Products Chemistry*. 2000, 21, 457–495.

111. Poonam, S.; Prachi, A.; Y. Krishna, M.; Vibha ,T. Antidiabetic activity of 50% ethanolic extract of *Ricinus communis* and its purified fractions, *Food and Chemical Toxicology*. 2008, 46, (11), 3458-3466. <https://doi.org/10.1016/j.fct.2008.08.020> .

112. Sandhyakumary, K.; Bobby. R. G.; Indira, M. Antifertility effects of *Ricinus communis* Linn on rats. *Phytotherapy Research*. 2003, 17, 508-511.

113. Loweinstein, D. H. Seizures and epilepsy. In *Harrison's principles of internal medicine*. New York, McGraw Hill Medical Publishing Division. 2005, 2357-2372.

114. Tripathi, A. C.; Gupta, R.; Saraf, S. K.; Phytochemical investigation characterization and anticonvulsant activity of *Ricinus communis* seeds in mice. *Natural Product Research* . 2011, 25 (S19), 1881-84.

115. Ladda, P. L. Screening of *Ricinus communis* Linn. leaves for anticonvulsant and analgesic activity. *Asian Journal Pharmaceutical Clinical Research* . 2014, 7(3), 110-4.

116. Rachhadiya, R. M.; Kabra, M. P.; Shete, R.V. Evaluation of antiulcer activity of castor oil in rats. *International Journal of Research in Ayurveda & Pharmacy*. 2011, 2 (4), 1349-1353.

117. Prasad, M. K.; Rachhadiya, R. M.; Shete, R.V. Pharmacological investigation on the wound healing effects of castor oil in rats. *International Journal of Universal*

Pharmacy and Life sciences. 2011, 1 (1), 21- 28.

118. Miller, K. D.; Ortiz, A. P.; Pinheiro, P. S.; Bandi, P.; Minihan, A.; Fuchs, H. E. Cancer Statistics for the US Hispanic Latino Population . A Cancer Journal Clinicians . 2021,71 (6), 466 - 487. doi: 10.3322/caac. 21695.

119. Dent, R.; Trudeau, M.; Pritchard, K.; Hanna, W.; Kahn, H.; Sawka ,C.A. Triple-Negative Breast Cancer Clinical Features and Patterns of Recurrence. Clinical Cancer Research . 2007, 13, 4429–34. doi: 10.1158/1078-0432.CCR-06-3045.

120. Wang, K.; Hu, Y.; Han, L.; Zhao, S.; Song, C.; Sun, S.; Hui, Y.; Jiang , N.; X, Ling z.; Zhao, Z. *Salvia chinensis* Benth Inhibits Triple-Negative Breast Cancer Progression by Inducing the DNA Damage Pathway. Frontiers in Oncology. 2022, 12. 882784. 10.3389/fonc.2022.882784.

121. Cao, Z. Q.; Wang, X. X.; Lu, L.; Xu, J.W.; Li ,X.B.; Zhang, G. R.; Ma, Z. J.; Shi, A. C.; Wang, Y.; Song, Y. J. β -Sitosterol and gemcitabine exhibit synergistic anti-pancreatic Cancer activity by modulating apoptosis and inhibiting epithelial–mesenchymal transition by deactivating Akt/GSK-3 β signaling. Frontiers in pharmacology. 2019 , 9, 1525.

122. Antoniou, G.; Kountourakis, P.; Papadimitriou, K.; Vassiliou, V.; Papamichael, D. Adjuvant therapy for resectable pancreatic adenocarcinoma: review of the current treatment approaches and future directions. Cancer Treatment. 2014, 40, 78–85. doi: 10.1016/j.ctrv.2013.05.008 .

123. Dela Cruz, C. S.; Tanoue, L. T. Matthay, R. A. Lung cancer: epidemiology, etiology, and prevention. Clinics in Chest Medicine. 2011, 32, 605–644.

124. Rajavel, T.; Mohankumar, R.; Archunan, G. Beta sitosterol and Daucosterol (phytosterols identified in *Grewia tiliaefolia*) perturbs cell cycle and induces apoptotic cell death in A549 cells. Science Report. 2017, 7, 3418 . <https://doi.org/10.1038/s41598-017-03511-4>.

125. Dias, B. G.; Banerjee, S. B.; Goodman, J. V.; Ressler, K. J. Towards new approaches to disorders of fear and anxiety. Current Opinion in Neurobiology. 2013, 23, 346–352.

126. Vanmierlo, T.; Bogie, J.; Mailleux, J.; Vanmol, J.; Lutjohann, D.; Mulder, M.; Hendriks, J.J. Plant sterols: Friend or foe in CNS disorders *Progress in Lipid Research*. 2015, 58, 26–39.
127. Panayotis, N.; Freund, P. A.; Marvaldi, L.; Shalit, T.; Brandis, A.; Mehlman, T.; Tsoory, M. M.; Fainzilber, M. β -sitosterol reduces anxiety and synergizes with established anxiolytic drugs in mice. *Cell Reports Medicine*. 2021, 2 (5), 100281.
128. Worthington, R. J.; Melander, C. Combination approaches to combat multidrug-resistant bacteria, *Trends Biotechnology*. 2013, 31, 177–184.
129. Wright, G. D.; Antibiotic adjuvants rescuing antibiotics from resistance. *Trends Microbiology*. 2016, 24, 862–871.
130. Tong, W. Y.; Muhammad, A. K.; Nur Amiera, S.; Leong, C. R.; Darah, I.; Wen-Nee, T. Stigmasterol, An adjuvant for beta lactam antibiotics against beta-lactamase positive clinical isolates, *Steroids*, 2017, 128, 68-71. ISSN 0039-128 <https://doi.org/10.1016/j.>
131. Li, R.; Bu, L.; Cai, L. Cuproptosis lipoylated TCA cycle proteins-mediated novel cell death pathway. *Signal Transduct Target therapy*. 2022, 7 (1), 158.
132. Wang, Y.; Yuxiao, M.; Tan, J. Stigmasterol and barasertib target cuproptosis-related prognostic model for the synergistic treatment of breast cancer. 2023, 10, 21203.
133. Wang, Y. Preparation and identification of an anti-idiotypic antibody antagonist (FG8) for EGFR that shows potential activity against liver cancer cells. *Biotechnology Letters*. 2021, (43), 369-382.
134. Hussein, H. A.; Khaphi, F. L. The apoptotic activity of curcumin against oral cancer cells without affecting normal cells in comparison to paclitaxel activity. *Applied Biochemistry and Biotechnology*. 2023, 1-15.
135. Hussein, H. A.; Khaphi, F. L.; Jassem, R. M. Enhancing the effectiveness of paclitaxel with stigmasterol bioactive compounds for cancer treatment. *International Journal of Innovative Research and Scientific Studies*. 2024, 30,7(3), 1227-34.
136. Elshamy, A.; Omran, G.; Abdalhaseeb, M.; Houssen, M. Chemotherapeutic Effect of Stigmasterol in Sorafenib Treated Breast Cancer Cell Lines vsia Modulation of

NF- κ B and ERK Signaling Pathways. Egyptian Journal of Chemistry. 2024, 67 (3), 227-234. doi: 10.21608/ejchem.2023.204388.7825.

137. Pezzani, R.; Salehi, B.; Vitalini, S.; Iriti, M.; Zuñiga, F. A.; Sharifi-Rad, J.; Martorell, M.; Martins, N. Synergistic Effects of Plant Derivatives and Conventional Chemotherapeutic Agents: An Update on the Cancer Perspective *Medicina* 2019, 55, 110. <https://doi.org/10.3390/medicina55040110>.

138. Aljarba, N. H.; Ali, H.; Alkahtani, S. Synergistic Dose Permutation of Isolated Alkaloid and Sterol for Anticancer Effect on Young Swiss Albino Mice. *Drug Design, Development and Therapy*. 2021, 15, 4043–4052.

<https://doi.org/10.2147/DDDT.S322769>.

139. THE AYURVEDIC PHARMACOPOEIA OF INDIA, Government of India, Ministry of Health and Family Welfare, Department of AYUSH, Published by, The Controller of Publication. First edition 2007, 2 (2), 140-143.

140. Pulok, K.; Mukherjee. *Quality Control and Evaluation of Herbal Drugs, Evaluating Natural Products and Traditional Medicine*. Elsevier. 2019.

141. K.R. Khandelwal. *Practical Pharmacognosy Techniques and Experiments*. Nirali Prakashan. 2006, 15th edition.

142. Zengin, G.; Uysal, A.; Aktumsek, A. *Euphorbia denticulata* Lam. A promising source of phyto-pharmaceuticals for the development of novel functional formulations. *Biomedicine and Pharmacotherapy*. 2017, 87, 27-36.

143. Mazumdar, M.; Fournier, D.; Zhu, D. W.; Cadot, C. ; Poirier, D.; Lin, S. X. Binary and ternary crystal structure analyses of a novel inhibitor with 17 β -HSD type 1. A lead compound for breast cancer therapy. *Biochemical Journal*. 2009, 424, 357-66.

144. Madhavi, G.; Adzhigirey, M.; Day, T.; Annabhimoju, R.; Sherman, W. Protein and ligand preparation Parameters, protocols, and influence on virtual screening enrichments. *Journal of computer aided molecular design* . 2013, 27 (3), 221-34. .

145. Oboyle, N, M.; Banck, M.; James, C. A.; Morley, .; Vandermeersch, T.; Hutchison, G. R. Open Babel. An open chemical toolbox. *J Chem inform*. 2011, 3.

146. William, L.; Jorgensen, J.; Tirado-Rives. The OPLS Potential Functions for

Proteins. Energy Minimizations for Crystals of Cyclic Peptides and Crambin. Journal of Americal Chemical Society. 1988, 110.

147. Rarey, M.; Kramer, .; Lengauer, T.; Klebe, G. A Fast Flexible Docking Method using an Incremental Construction Algorithm. 1996, 261.

148. Lokhande, K.; Doiphode, S.; Vyas, R.; Swamy. K. Molecular docking and simulation studies on SARS-CoV-2 Mpro reveals Mitoxantrone, Leucovorin, Birinapant, and Dynasore as potent drugs against COVID-19. Journal of Biomolecular Structuctral Dynamics . 2021, 39, 7294-305.

149. Schneider, N.; Lange, G.; Hindle, S.; Klein, R.; Rarey, M. A consistent description of HYdrogen bond and dehydration energies in protein-ligand complexes: Methods behind the HYDE scoring function. Journal of Computer Aided Molecular Design. 2013, 27, 15–29.

150. Lokhande, K. B.; Kale, A.; Shahakar, B.; Shrivastava, A.; Nawani, N.; Swamy, K. V.; Singh, A.; Pawar, S. V. Terpenoid phytochemicals from mangrove plant *Xylocarpus moluccensis* as possible inhibitors against SARS-CoV-2: *In silico* strategy. Computational biology and chemistry. 2023, 106, 107912. <https://doi.org/10.1016/j.compbiolchem.2023.107912>.

151. Kevin, J. B.; Edmond, C.; Huafeng, X.; Ron, O. D.; Michael, P. E.; Brent, A.; Gregersen, John, L. K.; Istvan, K. Scalable Algorithms for Molecular Dynamics Simulations on Commodity Clusters. Proceedings of the ACM/IEEE Conference on Super computing (SC06). Tampa, Florida. 2006, 11-17.

152. Bhimanwar, R. S.; Lokhande, K. B.; Shrivastava, A.; Singh, A.; Chitlange, S. S.; Mittal, A. Identification of potential drug candidates as TGR5 agonist to combat type II diabetes using *in silico* docking and molecular dynamics simulation studies. Journal of biomolecular structure & dynamics. 2023, 41(22), 13314–1333.

153. More, P.; Lokhande, K. B.; Swamy, K. V.; Nagar, S.; Baheti, A. GC-MS profiling of *Bauhinia variegata* major phytoconstituents with computational identification of potential lead inhibitors of SARS-CoV-2 Mpro. Computers in biology and medicine. 2022, 147, 105679. <https://doi.org/10.1016/j.compbimed.2022.105679>
154. Shrivastava, A.; Mathur, K.; Verma, R. K.; Jayadev, S. K.; Vyas, D. K.; Singh, A. Molecular dynamics study of tropical calcific pancreatitis (TCP) associated calcium-sensing receptor single nucleotide variation. Frontiers in Molecular biological sciences, 2022, 9, 982831.
155. Basma, A. A.; Zakaria, Z.; Latha , L.Y.; Sasidharan, S. Antioxidant activity and phytochemical screening of the methanol extracts of *Euphorbia hirta* L. Asian Pacific Journal of Tropical Medicine. 2011, 4, 386–390. [https://doi.org/10.1016/S1995-7645\(11\)60109-0](https://doi.org/10.1016/S1995-7645(11)60109-0) .
156. Bautista-Hernández, I.; Aranda-Ledesma, N. E.; Rojas, R. Antioxidant activity of polyphenolic compounds obtained from *Euphorbia antisiphilitica* by-products. Heliyon . 2021, 7. <https://doi.org/10.1016/j.heliyon.2021.06734>.
157. Mohamad, M.; Ismail, Y. A Study on Antioxidant Properties of *Eurycoma Longifolia* (Tongkat Ali). Journal of Pharmaceutical Negative Results. 2022, 13, 146–149. <https://doi.org/10.47750/pnr.2022.13.S07.022>.
158. Salunke, M.; Wakure , B.; Wakte, P, A comparative analysis of antioxidant activity and total phenolic content of four seaweeds collected from southcoast of India. International Journal of Botany Studies. 2021, 7, 32-38.
159. Hyland, K.; Voisin, E.; Banoun, H.; Auclair, C. Superoxide dismutase assay using alkaline dimethylsulfoxide as superoxide anion-generating system. Analytical biochemistry. 1983, 135(2), 280-7.
160. Kavitha, V.; Mohamed Ali, S. Studies on Phytochemical screening and antioxidant activity of *Chromolaena odorata* and *Annona squamosa*. International journal of innovative research in science Engineering and technology. 2013, 2 (12), 7315-7321.

161. Liocher, S. I.; Fridovich, I.; The Effects of Superoxide Dismutase on H₂O₂ Formation. *Free radical biology & medicine*. 2007, 42, 1465-1469.
162. Sawant,V. J.; Bamane, S. R. ; Shejwal, R. V.; Patil, S. B.Comparison of drug delivery potentials of surface functionalized cobalt and zinc ferrite nanohybrids for curcumin in to MCF-7 breast cancer cells. *Journal of Magnetism and Magnetic Materials* . 2016,417, 222-229.
163. Manikyam, H.; Joshi, S. K.; Vakadi, S.; Patil, S. B. Anticancer activity of novel terpenoid saponin of *Psidium guajava* on MCF-7 cancer cell line using DAPI and MTT assays, *African Journal of Pharmacy and Pharmacology* . 2021,15 (12) , 206- 211.
164. Sadeghi-aliabadi, H.; Minaian, M.; Dabestan, A. Cytotoxic evaluation of doxorubicin in combination with simvastatin against human cancer cells. *Research in Pharmaceutical Sciences*. 2010, 5 (2), 127-133.
165. Diana, H.; Duarte, N. Evaluation of synergism in drug combinations and reference models for future orientations in oncology. *Current Research in Pharmacology and Drug Discovery*. 2022, 3, 100110.
166. Chung, D.W.; Choi, Y.T. Synthesis and Solubility of Hydrophilic Derivatives of β - Sitosterol. *Journal of Industrial and Engineering Chemistry*. 2007, 13, 367-372.
167. Chaudhary, P.; Janmeda,P.; Pareek, A.; Chuturgoon, A.; Sharma, R. Etiology of lung carcinoma and treatment through medicinal plants, marine plants and green synthesized nanoparticles. A comprehensive review. *Biomedicine & Pharmacotherapy*. 2024, 173.
168. Waksmundzka-Hajnos, M.; Hawrył, M.; Hawrył, A.; Józwiak, G. Thin Layer Chromatography in Phytochemical Analysis. *Handbook of Bioanalytics*. Springer Cham. 2022, 1-31. https://doi.org/10.1007/978-3-030-63957-0_24-1.
169. Victor, R.; Preedy, P.;Vinood P. Medicinal plants, antioxidant potential, and cancer. *Cancer (Second Edition)* Academic Press. 2021, 349-357.
170. Bao,X.; Zhang,Y.; Zhang ,H.; Xia, L. Molecular Mechanism of β -Sitosterol and its Derivatives in Tumor Progression. *Front Oncol*. 2022, 12, 926975.



भारत सरकार / GOVERNMENT OF INDIA
पर्यावरण, वन एवं जल वायु परिवर्तन मंत्रालय
MINISTRY OF ENVIRONMENT, FORESTS & CLIMATE CHANGE
भारतीय वनस्पति सर्वेक्षण / BOTANICAL SURVEY OF INDIA
पश्चिमी क्षेत्रीय केंद्र / WESTERN REGIONAL CENTRE
७ कोरेगांव मार्ग, पुणे / 7- KOREGAON ROAD, PUNE- 411001



Tel.: 020-29707072, 020-29707078 Fax : 020-29707039 : e-mail : bsiwrcpune@gmail.com

नं./No.BSI/WRC/Iden. Cer./2022/0802220002464

दिनांक/ Date : 08.02.2022

प्रमाणपत्र/CERTIFICATE

यह प्रमाणित किया जाता है कि/This is to certify that Mrs. Prashali Gorakh Shinde, Assistant Professor from College of Pharmacy, Akluj, Tal. Malshiras Dist. Solapur के द्वारा प्रस्तुत किया गया नमूना/किये गये नमूने, हमारे विशेषज्ञ एवं वैज्ञानिक द्वारा निम्नलिखित अनुसार पहचाना गया/पहचाने गये है।/the specimen/specimens submitted by aforesaid is/are identified and authenticated by our expert's & Scientist as :

नमूना संख्या Specimen No.	वनस्पति का नाम Plant Name	वानस्पतिक कुल Family
PGSEP3	Euphorbia pulcherrima Willd. ex Klotzsch	Euphorbiaceae

Handwritten signature and date: 08/02/2022

(डी. एल. शिरोडकर / D.L. Shirodkar)

वानस्पतिज्ञ/Botanist

भावस, पक्षेकें, पुणे / BSI, WRC, Pune-1

D. L. SHIRODKAR
BOTANIST

Botanical Survey of India
Western Regional Centre

7, Koregaon Park, Pune- 411001.



भारत सरकार / GOVERNMENT OF INDIA
पर्यावरण, वन एवं जल वायु परिवर्तन मंत्रालय
MINISTRY OF ENVIRONMENT, FORESTS & CLIMATE CHANGE
भारतीय वनस्पति सर्वेक्षण / BOTANICAL SURVEY OF INDIA
पश्चिमी क्षेत्रीय केंद्र / WESTERN REGIONAL CENTRE
७ कोरेगांव मार्ग, पुणे / 7- KOREGAON ROAD, PUNE- 411001



Tel.: 020-29707072, 020-29707078 Fax : 020-29707039 : e-mail : bsiwrcpune@gmail.com

नं./No.BSI/WRC/Iden. Cer./2022/2901220010676- (2)

दिनांक/ Date : 31.01.2022

प्रमाणपत्र/CERTIFICATE

यह प्रमाणित किया जाता है कि/This is to certify that Mrs. Prashali Gorakh Shinde, Assistant Professor from College of Pharmacy, Akluj, Tal. Malshiras Dist. Solapur के द्वारा प्रस्तुत किया गया नमूना/किये गये नमूने, हमारे विशेषज्ञ एवं वैज्ञानिक द्वारा निम्नलिखित अनुसार पहचाना गया/पहचाने गये है।/the specimen/specimens submitted by aforesaid is/are identified and authenticated by our expert's & Scientist as :

नमूना संख्या Specimen No.	वनस्पति का नाम Plant Name	वानस्पतिक कुल Family
RCPGS2	Ricinus communis L.	Euphorbiaceae

Prashali S.
31.01.2022

(डी.एल. शिरोडकर / D.L. Shiroadkar)

वानस्पतिज्ञ / Botanist

भवन, पक्षेकें, पुणे / BSI, WRC, Pune-1

D. L. SHIRODKAR
BOTANIST

Botanical Survey of India
Western Regional Centre
7, Koregaon Park, Pune- 411001.



BIOCYTE

INSTITUTE OF RESEARCH & DEVELOPMENT

Flat No.11, Shri-Ram Residency, Near Bypass Road,
Kalanagar, Sangli, Maharashtra – 416416

Mob.9595753875, 9226765719

E-mail-biocyte@sangli@gmail.com

Certificate

BiRD/99/01/24-25

Date: 10/03/2025

TO WHOM SO EVER IT MAY CONCERN

This is to grant permission to **Ms. Shinde Prashali Gorakh**, Ph.D. Scholar, School of Pharmaceutical Sciences , Lovely Professional University, Punjab, under the guidance of Professor Dr. Gurdeep Singh & Assistant Professor Dr. Deepak Kardile, to conduct the part of research work from her research entitled “**Synergistic anticancer potential of isolated phytoconstituents from *Euphorbia pulcherrima* and *Ricinus communis* (Euphorbiaceae) against breast cancer .**” The research work was completed at the Biocyte Institute of Research & Development in Sangli. This NOC is applicable only until the end of the study duration.



Managing Director